

**When to Refresh a Functional Representation:  
Online Monitoring of Structural Change in  
Functional Time Series**

Jiajing Sun, Meiting Zhu, Wolfgang Karl Härdle, Oliver Linton and Zhuo Lin

*University of Chinese Academy of Sciences, Xiamen University,*

*Bucharest University of Economic Studies, University of Cambridge*

*and Chinese Academy of Sciences*

**Supplementary Material**

This online Supplement accompanies the manuscript and follows the notation, abbreviations, and conventions of the main paper; abbreviations such as DGP, BB, FPCA, HAC, LRV, KS, weighted-CvM, SN, SSMS, and RSMS are used without redefinition. Section S1 gives the proofs of the main results and related theoretical material, including the open-end extensions, fixed alternatives, local power, and contaminated-training results. Section S2 reports the simulated critical values for the main KS and weighted-CvM monitoring statistics, for both finite horizons and the open-end case. Section S3 gives the broader BB, fIID, and fMA(1) simulation results for the main monitoring statistics, including additional rejection-rate panels, HAC kernel and bandwidth sensitivity, the RSMS off-diagonal diagnostic, average-detection-delay curves, localized-break settings, and contaminated-training checks. Section S4 defines supplementary CUSUM and MOSUM monitoring statistics and reports their simulated critical values and sim-

ulation comparisons after the same FPCA compression. Section S5 reports additional empirical checks for the S&P 500 application, including a three-dimensional return-surface view, retained-dimension robustness, alternative training-sample lengths, and supplementary signal dates.

The replication code and the tables and figures used in the paper are available at <https://github.com/Jiajing-Sun/functional-representation-monitoring>. The repository contains R scripts for the main simulations, critical-value simulations, contaminated-training study, supplementary CUSUM and MOSUM comparisons, and the empirical analysis. The licensed TickData input used in the empirical application is documented there but is not redistributed.

## S1 Proofs of the Main Results and Additional Theory

### S1.1 Notation and Main Results Referenced in the Proofs

The proofs below use the assumptions and finite-horizon results from the main paper: Definition 1, Assumptions 1–3, Assumptions 5–7, Assumptions 8–10, Theorems 1–4, Theorems 5–6, and Proposition 7.

This subsection also records the open-end assumptions and limit results used for the  $T = \infty$  critical values.

**Assumption S1.1** (Open-end monitoring-score approximation). *Let*

*$t_{m,k} = k/(m + k)$  and define*

$$Z_m(t_{m,k}) = \frac{m}{m+k} \frac{S_m(k)}{\sqrt{m}}, \quad k \geq 1,$$

with  $Z_m(0) = 0$  and linear interpolation between consecutive grid points on  $[0, 1)$ . Assume that  $Z_m$  admits a continuous extension to  $t = 1$ , and define

$$Z_m(1) := \lim_{k \rightarrow \infty} Z_m(t_{m,k}).$$

For the boundary exponent  $\gamma \in [0, 1/2)$  used in the KS statistic, there exists a standard  $K$ -dimensional Brownian motion  $Z_K$  on  $[0, 1]$ , independent of the training-sample Brownian bridge  $B_K^0$ , such that

$$\sup_{0 < t \leq 1} \frac{\|Z_m(t) - \Sigma_K^{1/2} Z_K(t)\|}{t^\gamma} = o_p(1).$$

**Assumption S1.2** (Open-end weighted-CvM weights). *The open-end weight  $w : [0, \infty) \rightarrow [0, \infty)$  is locally bounded and locally Riemann integrable, satisfies*

$$\int_0^\infty w(s) ds < \infty,$$

*and its Riemann sums have negligible tails:*

$$\lim_{L \rightarrow \infty} \limsup_{m \rightarrow \infty} \frac{1}{m} \sum_{j > mL} w(j/m) = 0.$$

**Theorem S1.1** (Open-end KS null limits). *Suppose Assumptions 1–3 and S1.1 hold. Let  $Z_K$  be a standard  $K$ -dimensional Brownian motion on  $[0, 1]$ ,*

independent of the training-sample Brownian bridge  $B_K^0$ . If Assumption 5 also holds, then, for  $\gamma \in [0, 1/2)$ ,

$$\sup_{k \geq 1} \mathcal{M}_m^H(k) \Rightarrow \sup_{0 < t \leq 1} \frac{Z_K(t)^\top Z_K(t)}{t^{2\gamma}}.$$

Under Assumptions 1–3 and S1.1,

$$\sup_{k \geq 1} \mathcal{M}_m^S(k) \Rightarrow \sup_{0 < t \leq 1} \frac{Z_K(t)^\top V_K^{-1} Z_K(t)}{t^{2\gamma}}.$$

If Assumption 6 also holds, then

$$\sup_{k \geq 1} \mathcal{M}_m^R(k) \Rightarrow \sup_{0 < t \leq 1} \frac{Z_K(t)^\top R_K^{-2} Z_K(t)}{t^{2\gamma}}.$$

**Theorem S1.2** (Open-end weighted-CvM null limits). *Suppose Assumption S1.2 and the corresponding assumptions of Theorem S1.1 hold. Then*

$$\sup_{k \geq 1} \mathcal{I}_m^H(k) \Rightarrow \int_0^\infty w(s) \frac{U_K(s)^\top U_K(s)}{(1+s)^2} ds,$$

$$\sup_{k \geq 1} \mathcal{I}_m^S(k) \Rightarrow \int_0^\infty w(s) \frac{U_K(s)^\top V_K^{-1} U_K(s)}{(1+s)^2} ds,$$

and, under Assumption 6,

$$\sup_{k \geq 1} \mathcal{I}_m^R(k) \Rightarrow \int_0^\infty w(s) \frac{U_K(s)^\top R_K^{-2} U_K(s)}{(1+s)^2} ds.$$

Equivalently, with  $t = s/(1 + s)$ , the open-end limit has the form

$$\int_0^1 \frac{w\{t/(1-t)\}}{(1-t)^2} Z_K(t)^\top A Z_K(t) dt,$$

where  $A = I_K, V_K^{-1}, R_K^{-2}$  for HAC, SSMS, and RSMS, respectively.

For the local-power proof, the local alternatives satisfy  $\Delta_m = \Delta_0/\sqrt{m}$ , for a fixed  $\Delta_0 \in \mathbb{H}$ , equivalently  $\delta_{m,K} = \delta_K/\sqrt{m}$ , for a fixed nonzero  $\delta_K \in \mathbb{R}^K$ . For Proposition 7, write the two restrictions on training-sample contamination as

$$\sup_{0 \leq r \leq 1} \left\| m^{-1/2} \sum_{t=1}^{\lfloor mr \rfloor} d_{t,m} \right\| \rightarrow 0, \quad (\text{S1.1})$$

$$\frac{1}{m} \sum_{t=1}^m \|d_{t,m}\|^2 \rightarrow 0. \quad (\text{S1.2})$$

## S1.2 Preliminary lemmas for the null limits

The lemmas in this subsection are used in the HAC, SSMS, and RSMS null proofs. Throughout, let

$$G_m^{(0)}(r) = \frac{1}{\sqrt{m}} \sum_{t=1}^{\lfloor mr \rfloor} a_t^{(0)}, \quad r \geq 0.$$

By Brownian scaling, Assumption 3 can be written equivalently as follows:  
after possibly redefining  $B_K$  on the same probability space,

$$\sup_{0 \leq r \leq 1+T} \left\| G_m^{(0)}(r) - \Sigma_K^{1/2} B_K(r) \right\| = o_p(1), \quad (\text{S1.3})$$

for every fixed finite  $T > 0$ . We also write

$$U_m(s) = \frac{1}{\sqrt{m}} S_m(\lfloor ms \rfloor), \quad s \geq 0,$$

and use the same symbol  $B_K^0(r) = B_K(r) - rB_K(1)$  for the standard  $K$ -dimensional Brownian bridge on  $[0, 1]$ .

**Lemma S1.3** (Null partial-sum limit for the monitoring process). *Suppose Assumptions 1–3 hold. Then, for every fixed  $T < \infty$ ,*

$$\sup_{0 \leq s \leq T} \left\| U_m(s) - \Sigma_K^{1/2} U_K(s) \right\| = o_p(1),$$

where  $U_K(s) = B_K(1+s) - (1+s)B_K(1)$ .

*Proof.* Let  $k = \lfloor ms \rfloor$ . By the monitoring contrast approximation in (3.3),

$$\sup_{0 \leq s \leq T} \left\| U_m(s) - \left\{ G_m^{(0)} \left( 1 + \frac{k}{m} \right) - G_m^{(0)}(1) - \frac{k}{m} G_m^{(0)}(1) \right\} \right\| = o_p(1).$$

Combining this display with (S1.3), and using  $|k/m - s| \leq m^{-1}$  together

with the almost sure uniform continuity of the Brownian motion on compact intervals, gives

$$\sup_{0 \leq s \leq T} \left\| U_m(s) - [\Sigma_K^{1/2} B_K(1+s) - (1+s)\Sigma_K^{1/2} B_K(1)] \right\| = o_p(1),$$

which proves the claim. The term involving  $G_m^{(0)}(1)$  is the non-negligible training-mean contribution, not a negligible estimation error.  $\square$

**Lemma S1.4** (Training self-normalizer limit for SSMS). *Suppose Assumptions 1–3 hold. Then*

$$D_m \Rightarrow \Sigma_K^{1/2} V_K \Sigma_K^{1/2}.$$

*Proof.* For  $0 \leq r \leq 1$ , define the training partial-sum bridge process

$$H_m(r) = \frac{1}{\sqrt{m}} \sum_{t=1}^{\lfloor mr \rfloor} z_t.$$

By the training contrast approximation in (3.2),

$$\sup_{0 \leq r \leq 1} \left\| H_m(r) - \left\{ G_m^{(0)}(r) - \frac{\lfloor mr \rfloor}{m} G_m^{(0)}(1) \right\} \right\| = o_p(1).$$

Combining this display with (S1.3) at  $T = 0$ , and using again that

$\lfloor mr \rfloor / m - r = o(1)$  uniformly on  $[0, 1]$ , we obtain

$$\sup_{0 \leq r \leq 1} \left\| H_m(r) - \Sigma_K^{1/2} (B_K(r) - rB_K(1)) \right\| = o_p(1).$$

That is,

$$\sup_{0 \leq r \leq 1} \|H_m(r) - \Sigma_K^{1/2} B_K^0(r)\| = o_p(1). \quad (\text{S1.4})$$

Next, write  $P_t = \sum_{j=1}^t z_j$ . Since  $H_m(r)$  is piecewise constant on  $[(t-1)/m, t/m)$ ,

$$\int_0^1 H_m(r) H_m(r)^\top dr = \frac{1}{m} \sum_{t=1}^m \frac{P_t}{\sqrt{m}} \frac{P_t^\top}{\sqrt{m}} = \frac{1}{m^2} \sum_{t=1}^m P_t P_t^\top = D_m.$$

Therefore, (S1.4) and the continuous mapping theorem, applied to the continuous map  $f \mapsto \int_0^1 f(r) f(r)^\top dr$ ,

$$D_m \Rightarrow \int_0^1 \Sigma_K^{1/2} B_K^0(r) B_K^0(r)^\top \Sigma_K^{1/2} dr = \Sigma_K^{1/2} V_K \Sigma_K^{1/2}.$$

□

**Lemma S1.5** (Training self-normalizer limit for RSMS). *Suppose Assumptions 1–3 and 6 hold. Then*

$$\tilde{R}_m \Rightarrow \Sigma_{K, \text{diag}}^{1/2} R_K.$$

*Proof.* Let  $H_m(r)$  be as in Lemma S1.4. By Assumption 6,

$$\begin{aligned} \sup_{0 \leq r \leq 1} \left\| \widehat{W}_m H_m(r) - W_0 \Sigma_K^{1/2} B_K^0(r) \right\| &\leq \|\widehat{W}_m - W_0\| \sup_{0 \leq r \leq 1} \|H_m(r)\| \\ &\quad + \|W_0\| \sup_{0 \leq r \leq 1} \|H_m(r) - \Sigma_K^{1/2} B_K^0(r)\| \\ &= o_p(1). \end{aligned}$$

The first term is  $o_p(1)$  because  $\widehat{W}_m = W_0 + o_p(1)$  and the bridge process  $H_m$  is tight in  $\ell^\infty([0, 1]; \mathbb{R}^K)$ ; the second term is  $o_p(1)$  by (S1.4). Since  $W_0 \Sigma_K W_0^\top = \Sigma_{K, \text{diag}}$  is diagonal and positive definite, the Gaussian process  $W_0 \Sigma_K^{1/2} B_K^0(\cdot)$  has the same law as  $\Sigma_{K, \text{diag}}^{1/2} B_K^0(\cdot)$  after a harmless relabeling of the standard Brownian bridge coordinates.

For each coordinate  $\ell$ , the range map

$$f \mapsto \sup_{0 \leq r \leq 1} f(r) - \inf_{0 \leq r \leq 1} f(r)$$

is continuous on  $C([0, 1])$ . The definition of  $\widetilde{B}_{m, \ell}(t)$  implies that  $m^{-1/2} \widetilde{B}_{m, \ell}(\lfloor mr \rfloor)$  is exactly the  $\ell$ th coordinate of  $\widehat{W}_m H_m(r)$  up to an  $o(m^{-1})$  discretization error. Hence, applying the coordinatewise range map and using continuous mapping,

$$\widetilde{R}_{m, \ell} \Rightarrow \Sigma_{K, \text{diag}, \ell \ell}^{1/2} \left( \sup_{0 \leq r \leq 1} B_{K, \ell}^0(r) - \inf_{0 \leq r \leq 1} B_{K, \ell}^0(r) \right),$$

for each  $\ell = 1, \dots, K$ . Stacking the coordinates gives the stated diagonal-matrix limit. □

### S1.3 Proof of Theorem 1 for the HAC KS statistic

Fix a finite horizon  $T < \infty$  and write  $k_m(s) = \lfloor ms \rfloor$ . By the definition of the training-centered monitoring sum and the high-level contrast approximation (3.3), the feasible statistic has the same first-order path as the population-centered contrast

$$\sum_{t=m+1}^{m+k_m(s)} a_t^{(0)} - \frac{k_m(s)}{m} \sum_{t=1}^m a_t^{(0)}.$$

Combining this approximation with the strong approximation (3.1) yields

$$\sup_{0 \leq s \leq T} \left\| \frac{1}{\sqrt{m}} S_m \{k_m(s)\} - \Sigma_K^{1/2} U_K(s) \right\| = o_p(1), \quad (\text{S1.5})$$

where, as in the main text,

$$U_K(s) = B_K(1+s) - (1+s)B_K(1), \quad s \geq 0,$$

with  $B_K$  a standard  $K$ -dimensional Brownian motion. In particular, each sample path of  $s \mapsto U_K(s)$  is continuous on compact intervals.

Next, Assumption 5 implies

$$\widehat{\Gamma}_m^{-1} = \Sigma_K^{-1} + o_p(1)$$

in operator norm. Therefore,

$$\begin{aligned} & \sup_{0 \leq s \leq T} \left| \frac{S_m\{k_m(s)\}^\top \widehat{\Gamma}_m^{-1} S_m\{k_m(s)\}}{m} - U_K(s)^\top U_K(s) \right| \\ & \leq \sup_{0 \leq s \leq T} \left| \frac{S_m\{k_m(s)\}^\top \widehat{\Gamma}_m^{-1} S_m\{k_m(s)\}}{m} - U_K(s)^\top \Sigma_K^{1/2} \widehat{\Gamma}_m^{-1} \Sigma_K^{1/2} U_K(s) \right| \\ & \quad + \sup_{0 \leq s \leq T} \left| U_K(s)^\top \Sigma_K^{1/2} \widehat{\Gamma}_m^{-1} \Sigma_K^{1/2} U_K(s) - U_K(s)^\top U_K(s) \right| \\ & \leq \sup_{0 \leq s \leq T} \left\| \frac{1}{\sqrt{m}} S_m\{k_m(s)\} - \Sigma_K^{1/2} U_K(s) \right\| \left\{ \begin{array}{l} \sup_{0 \leq s \leq T} \left\| \widehat{\Gamma}_m^{-1} \frac{1}{\sqrt{m}} S_m\{k_m(s)\} \right\| \\ + \sup_{0 \leq s \leq T} \left\| \widehat{\Gamma}_m^{-1} \Sigma_K^{1/2} U_K(s) \right\| \end{array} \right\} \\ & \quad + \sup_{0 \leq s \leq T} \|U_K(s)\|^2 \left\| \Sigma_K^{1/2} \widehat{\Gamma}_m^{-1} \Sigma_K^{1/2} - I_K \right\| = o_p(1), \end{aligned}$$

because the bracketed term is stochastically bounded on every compact interval by (S1.5), the continuity of  $U_K$ , and the consistency of  $\widehat{\Gamma}_m^{-1}$ .

Hence,

$$\sup_{0 \leq s \leq T} \left| \frac{S_m\{k_m(s)\}^\top \widehat{\Gamma}_m^{-1} S_m\{k_m(s)\}}{m} - U_K(s)^\top U_K(s) \right| = o_p(1).$$

Since  $s \mapsto (1+s)^{-2} \{s/(1+s)\}^{-2\gamma}$  is continuous and bounded on every

interval  $[\varepsilon, T]$  with  $\varepsilon > 0$ , we obtain

$$\sup_{\varepsilon \leq s \leq T} \left| \mathcal{M}_m^H\{k_m(s)\} - \frac{U_K(s)^\top U_K(s)}{(1+s)^2 \left(\frac{s}{1+s}\right)^{2\gamma}} \right| = o_p(1).$$

The convergence above first yields the required result on every interval  $[\varepsilon, T]$ , where  $\varepsilon > 0$ . By Assumption 4, the contribution from  $0 < s \leq \varepsilon$  is asymptotically negligible. Letting  $\varepsilon \downarrow 0$  therefore gives

$$\sup_{1 \leq k \leq \lfloor mT \rfloor} \mathcal{M}_m^H(k) \Rightarrow \sup_{0 < s \leq T} \frac{U_K(s)^\top U_K(s)}{(1+s)^2 \left(\frac{s}{1+s}\right)^{2\gamma}}.$$

#### S1.4 Proof of Theorem 2 for Shao's KS statistic

*Proof.* Fix  $T < \infty$ . By Lemma S1.3,

$$\sup_{0 \leq s \leq T} \left\| \frac{1}{\sqrt{m}} S_m(\lfloor ms \rfloor) - \Sigma_K^{1/2} U_K(s) \right\| = o_p(1),$$

and by Lemma S1.4,  $D_m \Rightarrow \Sigma_K^{1/2} V_K \Sigma_K^{1/2}$ . Since  $V_K$  is almost surely positive definite, matrix inversion is continuous at the limit, so

$$D_m^{-1} \Rightarrow \Sigma_K^{-1/2} V_K^{-1} \Sigma_K^{-1/2}.$$

Therefore, uniformly on  $s \in [0, T]$ ,

$$\frac{1}{m} S_m(\lfloor ms \rfloor)^\top D_m^{-1} S_m(\lfloor ms \rfloor) \Rightarrow U_K(s)^\top V_K^{-1} U_K(s),$$

again by continuous mapping. After division by the deterministic boundary, the convergence first holds uniformly on every interval  $[\varepsilon, T]$ , where  $\varepsilon > 0$ . By Assumption 4, applied with  $A_m = D_m^{-1}$ , the contribution from  $0 < s \leq \varepsilon$  is asymptotically negligible. Letting  $\varepsilon \downarrow 0$  gives

$$\sup_{1 \leq k \leq \lfloor mT \rfloor} \mathcal{M}_m^S(k) \Rightarrow \sup_{0 < s \leq T} \frac{U_K(s)^\top V_K^{-1} U_K(s)}{(1+s)^2 \left(\frac{s}{1+s}\right)^{2\gamma}},$$

which proves (3.5). □

### S1.5 Proof of Theorem 3 for the adjusted-range-based KS statistic

*Proof.* The convergence of  $\tilde{R}_m$  is Lemma S1.5. For the monitoring numerator, combine Lemma S1.3 with Assumption 6:

$$\begin{aligned} \sup_{0 \leq s \leq T} \left\| \frac{1}{\sqrt{m}} \tilde{S}_m(\lfloor ms \rfloor) - W_0 \Sigma_K^{1/2} U_K(s) \right\| &\leq \|\widehat{W}_m - W_0\| \sup_{0 \leq s \leq T} \|U_m(s)\| \\ &\quad + \|W_0\| \sup_{0 \leq s \leq T} \|U_m(s) - \Sigma_K^{1/2} U_K(s)\| \\ &= o_p(1). \end{aligned}$$

As in Lemma S1.5, the limit process has the same law as  $\Sigma_{K,\text{diag}}^{1/2} U_K(s)$ . Since  $R_K$  is diagonal with strictly positive entries almost surely, the map

$$(x, A) \mapsto x^\top A^{-2} x$$

is continuous at  $(\Sigma_{K,\text{diag}}^{1/2} U_K(s), \Sigma_{K,\text{diag}}^{1/2} R_K)$ . Hence, uniformly on compact  $s$ -intervals,

$$\frac{1}{m} \tilde{S}_m(\lfloor ms \rfloor)^\top \tilde{R}_m^{-2} \tilde{S}_m(\lfloor ms \rfloor) \Rightarrow U_K(s)^\top R_K^{-2} U_K(s).$$

After division by the deterministic boundary, the convergence first holds uniformly on every interval  $[\varepsilon, T]$ . By Assumption 4, applied to  $\tilde{S}_m(k)$  with  $A_m = \tilde{R}_m^{-2}$ , the contribution from  $0 < s \leq \varepsilon$  is asymptotically negligible. Letting  $\varepsilon \downarrow 0$  yields (3.6). The asymptotic-size statement follows by taking critical values from the finite-horizon limiting pivotal law.  $\square$

## S1.6 Proof of Theorem 4 for weighted-CvM statistics

### HAC part

We again begin with a fixed finite horizon  $T < \infty$ . Set

$$g_{\text{H}}(s) = \frac{U_K(s)^\top U_K(s)}{(1+s)^2}, \quad 0 \leq s \leq T.$$

By Theorem 1 with  $\gamma = 0$ , the proof above actually yields the stronger uniform approximation

$$\sup_{0 \leq s \leq T} \left| \mathcal{M}_m^{\text{H}}\{k_m(s)\} \Big|_{\gamma=0} - g_{\text{H}}(s) \right| = o_p(1). \quad (\text{S1.6})$$

Because  $g_{\text{H}}$  has almost surely continuous sample paths on  $[0, T]$  and Assumption 7 states that  $w$  is bounded and Riemann integrable, standard Riemann-sum approximation gives, almost surely,

$$\sup_{0 \leq s \leq T} \left| \frac{1}{m} \sum_{j=1}^{k_m(s)} w(j/m) g_{\text{H}}(j/m) - \int_0^s w(u) g_{\text{H}}(u) du \right| \rightarrow 0. \quad (\text{S1.7})$$

Now decompose

$$\begin{aligned} & \sup_{0 \leq s \leq T} \left| \mathcal{I}_m^{\text{H}}\{k_m(s)\} - \int_0^s w(u) g_{\text{H}}(u) du \right| \\ & \leq \frac{1}{m} \sum_{j=1}^{\lfloor mT \rfloor} |w(j/m)| \sup_{0 \leq r \leq T} \left| \mathcal{M}_m^{\text{H}}\{k_m(r)\} \Big|_{\gamma=0} - g_{\text{H}}(r) \right| \\ & \quad + \sup_{0 \leq s \leq T} \left| \frac{1}{m} \sum_{j=1}^{k_m(s)} w(j/m) g_{\text{H}}(j/m) - \int_0^s w(u) g_{\text{H}}(u) du \right|. \end{aligned}$$

The first term is  $o_p(1)$  by boundedness of  $w$  and (S1.6); the second term converges to zero by (S1.7). Consequently,

$$\sup_{0 \leq s \leq T} \left| \mathcal{I}_m^{\text{H}}\{k_m(s)\} - \int_0^s w(u) g_{\text{H}}(u) du \right| = o_p(1),$$

and the continuous-mapping theorem yields the finite-horizon limit

$$\sup_{1 \leq k \leq \lfloor mT \rfloor} \mathcal{I}_m^H(k) \Rightarrow \sup_{0 < s \leq T} \int_0^s w(u) \frac{U_K(u)^\top U_K(u)}{(1+u)^2} du.$$

□

**SSMS part**

*Proof.* For  $0 \leq s \leq T$ , write

$$J_m^S(s) = \frac{1}{m} \sum_{j=1}^{\lfloor ms \rfloor} w(j/m) \frac{S_m(j)^\top D_m^{-1} S_m(j)}{m(1+j/m)^2}.$$

By the proof of Theorem 2,

$$\sup_{0 \leq u \leq T} \left| \frac{1}{m} S_m(\lfloor mu \rfloor)^\top D_m^{-1} S_m(\lfloor mu \rfloor) - U_K(u)^\top V_K^{-1} U_K(u) \right| = o_p(1).$$

Since  $w$  is bounded and Riemann integrable, standard Riemann-sum arguments give

$$\sup_{0 \leq s \leq T} \left| J_m^S(s) - \int_0^s w(u) \frac{U_K(u)^\top V_K^{-1} U_K(u)}{(1+u)^2} du \right| = o_p(1).$$

The map  $f \mapsto \sup_{0 \leq s \leq T} f(s)$  is continuous at continuous functions, so the stated finite-horizon supremum limit follows.

□

**RSMS part**

*Proof.* For  $0 \leq s \leq T$ , write

$$J_m^R(s) = \frac{1}{m} \sum_{j=1}^{\lfloor ms \rfloor} w(j/m) \frac{\tilde{S}_m(j)^\top \tilde{R}_m^{-2} \tilde{S}_m(j)}{m(1+j/m)^2}.$$

By the proof of Theorem 3,

$$\sup_{0 \leq u \leq T} \left| \frac{1}{m} \tilde{S}_m(\lfloor mu \rfloor)^\top \tilde{R}_m^{-2} \tilde{S}_m(\lfloor mu \rfloor) - U_K(u)^\top R_K^{-2} U_K(u) \right| = o_p(1).$$

Since  $w$  is bounded and Riemann integrable, standard Riemann-sum arguments give

$$\sup_{0 \leq s \leq T} \left| J_m^R(s) - \int_0^s w(u) \frac{U_K(u)^\top R_K^{-2} U_K(u)}{(1+u)^2} du \right| = o_p(1).$$

The map  $f \mapsto \sup_{0 \leq s \leq T} f(s)$  is continuous at continuous functions, so the stated finite-horizon supremum limit follows.

□

### S1.7 Open-end KS and weighted-CvM arguments

The open-end argument uses the compactification  $t = s/(1 + s)$ . For  $0 \leq t < 1$ , set

$$Z_K(t) = (1 - t)B_K\left(\frac{1}{1 - t}\right) - B_K(1), \quad Z_K(1) = -B_K(1).$$

Since  $B_K(r)/r \rightarrow 0$  almost surely as  $r \rightarrow \infty$ , the process is continuous at  $t = 1$ . If  $0 \leq t \leq u < 1$ , direct covariance calculation gives

$$\text{Cov}\{Z_K(t), Z_K(u)\} = tI_K,$$

and, for  $0 \leq r \leq 1$ ,

$$\text{Cov}\{Z_K(t), B_K(r) - rB_K(1)\} = 0.$$

Thus  $Z_K$  is a standard  $K$ -dimensional Brownian motion on  $[0, 1]$ , independent of the training-sample Brownian bridge  $B_K^0$ .

The training-centered monitoring limit satisfies

$$\frac{U_K(s)}{1 + s} = Z_K\left(\frac{s}{1 + s}\right), \quad g_\gamma(s) = (1 + s) \left(\frac{s}{1 + s}\right)^\gamma,$$

and hence

$$\frac{U_K(s)}{g_\gamma(s)} = \frac{Z_K(t)}{t^\gamma}, \quad t = \frac{s}{1+s}.$$

The endpoint  $t = 1$  is nonzero in general: it equals  $Z_K(1) = -B_K(1)$ . Near  $t = 0$ ,  $\gamma < 1/2$  and the Brownian path imply  $Z_K(t)/t^\gamma \rightarrow 0$  almost surely. Assumption S1.1 therefore gives the weighted uniform approximation needed for the continuous-mapping theorem on the compact interval  $[0, 1]$ . Combining this approximation with Assumption 5 yields the HAC part of Theorem S1.1; replacing the HAC inverse by the limits  $V_K^{-1}$  and  $R_K^{-2}$  of the training-sample self-normalizers gives the SSMS and RSMS parts.

For the weighted-CvM statistics, the same compactification gives

$$\int_0^\infty w(s) \frac{U_K(s)^\top A U_K(s)}{(1+s)^2} ds = \int_0^1 \frac{w\{t/(1-t)\}}{(1-t)^2} Z_K(t)^\top A Z_K(t) dt,$$

where  $A = I_K, V_K^{-1}, R_K^{-2}$ . Assumption S1.2 controls the tail of the Riemann sums and makes the integral finite under the null. On every compact interval  $[0, L]$ , the finite-horizon weighted-CvM argument applies; the negligible-tail condition then lets  $L \rightarrow \infty$ . This proves Theorem S1.2.  $\square$

## S1.8 Fixed alternatives, local power, and training contamination

**Drift decomposition.**

**Lemma S1.6** (Monitoring partial sums under fixed and local alternatives).

Suppose Assumptions 1–3 hold for the baseline no-change process, and Assumptions 8–10 hold. Let  $\kappa_m = k_m^\dagger/m$ . Then, for each fixed  $T < \infty$ ,

$$\sup_{0 \leq s \leq T} \left\| \frac{1}{\sqrt{m}} S_m(\lfloor ms \rfloor) - \Sigma_K^{1/2} U_K(s) - \sqrt{m} (s - \kappa_m)_+ \delta_{m,K} \right\| = o_p(1).$$

Under the local alternative  $\sqrt{m} \delta_{m,K} \rightarrow \delta_K$  and  $\kappa_m \rightarrow \kappa \in [0, T)$ , this becomes

$$\sup_{0 \leq s \leq T} \left\| \frac{1}{\sqrt{m}} S_m(\lfloor ms \rfloor) - \Sigma_K^{1/2} U_K(s) - (s - \kappa)_+ \delta_K \right\| = o_p(1).$$

*Proof.* We decompose the observed monitoring-score process into a baseline no-change component and a deterministic post-change drift. Specifically, for  $1 \leq j \leq \lfloor mT \rfloor$ , write

$$z_{m+j} = z_{m+j}^{(0)} + \mathbf{1}\{j > k_m^\dagger\} (\delta_{m,K} + \rho_{j,m}),$$

where  $z_{m+j}^{(0)}$  denotes the training-centered monitoring score that would be observed under the baseline no-change regime,  $\delta_{m,K}$  is the retained-score mean shift, and  $\rho_{j,m}$  is a uniformly negligible remainder.

Importantly,  $z_{m+j}^{(0)}$  is not conditionally centered given the training sample. It retains the training-mean contribution generated by centering all

monitoring scores using the fixed training-sample mean. Consequently, Assumption 8 requires the baseline monitoring-score partial sums to satisfy

$$\sup_{0 \leq s \leq T} \left\| \frac{1}{\sqrt{m}} \sum_{j=1}^{\lfloor ms \rfloor} z_{m+j}^{(0)} - \Sigma_K^{1/2} U_K(s) \right\| = o_p(1),$$

where

$$U_K(s) = B_K(1+s) - (1+s)B_K(1)$$

contains the non-negligible training-mean contribution.

By the baseline no-change monitoring-score approximation in Assumption 8,

$$\sup_{0 \leq s \leq T} \left\| \frac{1}{\sqrt{m}} \sum_{j=1}^{\lfloor ms \rfloor} z_{m+j}^{(0)} - \Sigma_K^{1/2} U_K(s) \right\| = o_p(1).$$

The remainder term satisfies

$$\sup_{\substack{1 \leq j \leq \lfloor mT \rfloor \\ j > k_m^\dagger}} \|\rho_{j,m}\| = o(m^{-1/2}).$$

Therefore, uniformly for  $s \in [0, T]$ ,

$$\frac{1}{\sqrt{m}} \sum_{j=k_m^\dagger+1}^{\lfloor ms \rfloor} \rho_{j,m} = o(1).$$

Hence, uniformly for  $s \in [0, T]$ ,

$$\begin{aligned} \frac{1}{\sqrt{m}} S_m(\lfloor ms \rfloor) &= \frac{1}{\sqrt{m}} \sum_{j=1}^{\lfloor ms \rfloor} z_{m+j}^{(0)} + \frac{(\lfloor ms \rfloor - k_m^\dagger)_+}{\sqrt{m}} \delta_{m,K} \\ &\quad + \frac{1}{\sqrt{m}} \sum_{j=k_m^\dagger+1}^{\lfloor ms \rfloor} \rho_{j,m}. \end{aligned}$$

Since

$$\sup_{0 \leq s \leq T} \left| \frac{\lfloor ms \rfloor}{m} - s \right| \leq \frac{1}{m},$$

it follows that

$$\sup_{0 \leq s \leq T} \left\| \frac{(\lfloor ms \rfloor - k_m^\dagger)_+}{\sqrt{m}} \delta_{m,K} - \sqrt{m} (s - \kappa_m)_+ \delta_{m,K} \right\| = o(1).$$

Combining the above displays yields

$$\sup_{0 \leq s \leq T} \left\| \frac{1}{\sqrt{m}} S_m(\lfloor ms \rfloor) - \Sigma_K^{1/2} U_K(s) - \sqrt{m} (s - \kappa_m)_+ \delta_{m,K} \right\| = o_p(1), \quad \kappa_m = \frac{k_m^\dagger}{m}.$$

Adding the stochastic and deterministic parts, we obtain

$$\sup_{0 \leq s \leq T} \left\| \frac{1}{\sqrt{m}} S_m(\lfloor ms \rfloor) - \Sigma_K^{1/2} U_K(s) - \sqrt{m} (s - \kappa_m)_+ \delta_{m,K} \right\| = o_p(1).$$

Under  $\sqrt{m} \delta_{m,K} \rightarrow \delta_K$  and  $\kappa_m \rightarrow \kappa \in [0, T)$ ,

$$\sqrt{m} (s - \kappa_m)_+ \delta_{m,K} = (s - \kappa_m)_+ (\sqrt{m} \delta_{m,K}) \rightarrow (s - \kappa)_+ \delta_K,$$

uniformly on  $[0, T]$ . The result follows by a standard continuous mapping argument. □

**Proof of Theorem 5**

*Proof. KS statistics.* We first consider the finite-horizon case  $T < \infty$ .

By Assumption 9, choose any  $s_0 \in (\kappa, T)$ . Then Lemma S1.6 implies

$$\frac{1}{\sqrt{m}} S_m(\lfloor ms_0 \rfloor) = \Sigma_K^{1/2} U_K(s_0) + \sqrt{m} (s_0 - \kappa_m)_+ \delta_{m,K} + o_p(1).$$

Since  $s_0 > \kappa$  and  $\kappa_m \rightarrow \kappa$ , we have  $(s_0 - \kappa_m)_+ \geq c_0 > 0$  for all sufficiently large  $m$ . Moreover,  $\delta_{m,K} \rightarrow \delta_K \neq 0$ , so

$$\left\| \sqrt{m} (s_0 - \kappa_m)_+ \delta_{m,K} \right\| \rightarrow \infty.$$

Because  $\Sigma_K^{1/2} U_K(s_0) = O_p(1)$ , it follows that

$$\left\| \frac{1}{\sqrt{m}} S_m(\lfloor ms_0 \rfloor) \right\| \xrightarrow{P} \infty, \quad \text{hence} \quad \frac{\|S_m(\lfloor ms_0 \rfloor)\|^2}{m} \xrightarrow{P} \infty.$$

We next control the lower tail of the self-normalizers. By Lemma S1.4,

$$D_m^{-1} \Rightarrow \Sigma_K^{-1/2} V_K^{-1} \Sigma_K^{-1/2},$$

where the limit is almost surely positive definite. Similarly, by Lemma S1.5,

$$\tilde{R}_m^{-2} \Rightarrow (\Sigma_{K,\text{diag}}^{1/2} R_K)^{-2},$$

where the limit has strictly positive diagonal entries almost surely. Therefore, for every  $\varepsilon > 0$ , there exists  $c_\varepsilon > 0$  such that, with probability at least  $1 - \varepsilon$  for all sufficiently large  $m$ ,

$$\lambda_{\min}(D_m^{-1}) \geq c_\varepsilon, \quad \lambda_{\min}(\tilde{R}_m^{-2}) \geq c_\varepsilon.$$

Fix  $s_0$ . The boundary denominator in both KS statistics evaluated at  $k = \lfloor ms_0 \rfloor$  is a finite positive constant multiple of  $m$ . On the event above, the quadratic forms are bounded below by  $c_\varepsilon$  times the squared Euclidean norm. Therefore,

$$\mathcal{M}_m^S(\lfloor ms_0 \rfloor) \geq c_{\varepsilon,1} \frac{\|S_m(\lfloor ms_0 \rfloor)\|^2}{m},$$

for some constant  $c_{\varepsilon,1} > 0$  on an event with probability at least  $1 - \varepsilon$  for all

large  $m$ . Since  $\varepsilon$  is arbitrary,

$$\mathcal{M}_m^S(\lfloor ms_0 \rfloor) \xrightarrow{P} \infty.$$

For RSMS,  $\tilde{S}_m(k) = \widehat{W}_m S_m(k)$ . Since  $\widehat{W}_m = W_0 + o_p(1)$  and  $W_0$  is nonsingular, there exists  $c_W > 0$  such that

$$\sigma_{\min}(\widehat{W}_m) \geq c_W$$

with probability tending to one. Therefore,

$$\|\tilde{S}_m(\lfloor ms_0 \rfloor)\|^2 \geq c_W^2 \|S_m(\lfloor ms_0 \rfloor)\|^2$$

with probability tending to one. Combining this bound with the lower-tail bound for  $\tilde{R}_m^{-2}$  gives

$$\mathcal{M}_m^R(\lfloor ms_0 \rfloor) \xrightarrow{P} \infty.$$

Since the KS monitoring statistics take the supremum over  $1 \leq k \leq \lfloor mT \rfloor$ , we conclude that

$$\mathbb{P}(\mathcal{T}_m^S \leq \lfloor mT \rfloor \mid H_a) \rightarrow 1, \quad \mathbb{P}(\mathcal{T}_m^R \leq \lfloor mT \rfloor \mid H_a) \rightarrow 1.$$

**Weighted-CvM statistics.** We first consider the finite-horizon case  $T <$

$\infty$ .

By Assumption 9, choose an interval  $J = [s_1, s_2] \subset (\kappa, T)$  such that

$$\int_J w(s) ds > 0.$$

By Lemma S1.6, uniformly for  $s \in J$ ,

$$\frac{1}{\sqrt{m}} S_m(\lfloor ms \rfloor) = \Sigma_K^{1/2} U_K(s) + \sqrt{m} (s - \kappa_m)_+ \delta_{m,K} + o_p(1).$$

Since  $s \geq s_1 > \kappa$  and  $\kappa_m \rightarrow \kappa$ , there exists  $c_0 > 0$  such that  $(s - \kappa_m)_+ \geq c_0$  for all  $s \in J$  and all sufficiently large  $m$ . Moreover,  $\delta_{m,K} \rightarrow \delta_K \neq 0$ , so

$$\inf_{s \in J} \left\| \frac{1}{\sqrt{m}} S_m(\lfloor ms \rfloor) \right\| \xrightarrow{P} \infty.$$

Hence

$$\inf_{s \in J} \frac{\|S_m(\lfloor ms \rfloor)\|^2}{m} \xrightarrow{P} \infty.$$

By the same eigenvalue lower-tail argument used for the KS statistics above, for every  $\varepsilon > 0$  there exists  $c_\varepsilon > 0$  such that, with probability at least  $1 - \varepsilon$  for all sufficiently large  $m$ ,

$$\lambda_{\min}(D_m^{-1}) \geq c_\varepsilon, \quad \lambda_{\min}(\tilde{R}_m^{-2}) \geq c_\varepsilon.$$

Since the boundary denominator is bounded above by a finite constant multiple of  $m$  uniformly on  $J$ , the SSMS quadratic form is bounded below by a positive multiple of  $\|S_m(\lfloor ms \rfloor)\|^2/m$  on this event. For RSMS,  $\widehat{W}_m = W_0 + o_p(1)$  and nonsingularity of  $W_0$  imply that  $\sigma_{\min}(\widehat{W}_m)$  is bounded away from zero with probability tending to one. Hence the RSMS quadratic form is also bounded below by a positive multiple of  $\|S_m(\lfloor ms \rfloor)\|^2/m$ . Therefore,

$$\inf_{s \in J} \mathcal{M}_m^S(\lfloor ms \rfloor) \xrightarrow{P} \infty, \quad \inf_{s \in J} \mathcal{M}_m^R(\lfloor ms \rfloor) \xrightarrow{P} \infty.$$

We now pass to the weighted-CvM statistics. Since  $w$  is nonnegative and Riemann integrable and  $\int_J w(s) ds > 0$ , the corresponding Riemann sums satisfy

$$\frac{1}{m} \sum_{\substack{1 \leq j \leq \lfloor mT \rfloor \\ j/m \in J}} w(j/m) \longrightarrow \int_J w(s) ds > 0.$$

For  $k = \lfloor mT \rfloor$ ,

$$\mathcal{I}_m^S(k) \geq \left\{ \inf_{s \in J} \mathcal{M}_m^S(\lfloor ms \rfloor) \right\} \frac{1}{m} \sum_{\substack{1 \leq j \leq \lfloor mT \rfloor \\ j/m \in J}} w(j/m).$$

The first factor diverges in probability and the second factor converges to

a strictly positive constant. Hence,

$$\mathcal{I}_m^S(\lfloor mT \rfloor) \xrightarrow{P} \infty.$$

The same argument, with  $\mathcal{M}_m^R$  in place of  $\mathcal{M}_m^S$ , gives

$$\mathcal{I}_m^R(\lfloor mT \rfloor) \xrightarrow{P} \infty.$$

Hence both weighted-CvM stopping times are consistent on  $[0, \lfloor mT \rfloor]$ :

$$\mathbb{P}(\mathcal{T}_{m,\text{CvM}}^S \leq \lfloor mT \rfloor \mid H_a) \rightarrow 1, \quad \mathbb{P}(\mathcal{T}_{m,\text{CvM}}^R \leq \lfloor mT \rfloor \mid H_a) \rightarrow 1.$$

This is the asserted finite-horizon consistency result. □

### Proof of Theorem 6

*Proof. KS statistics.* We first establish the joint weak convergence of the monitoring partial-sum process and the training self-normalizers under the local alternative.

Define

$$X_m(s) := \frac{1}{\sqrt{m}} S_m(\lfloor ms \rfloor), \quad s \in [0, T].$$

By Lemma S1.6, under the local alternative,

$$\sup_{0 \leq s \leq T} \left\| X_m(s) - \Sigma_K^{1/2} U_K(s) - (s - \kappa)_+ \delta_K \right\| = o_p(1).$$

Hence

$$X_m(\cdot) \Rightarrow X(\cdot) \quad \text{in } \ell^\infty([0, T]),$$

where

$$X(s) = \Sigma_K^{1/2} U_K(s) + (s - \kappa)_+ \delta_K.$$

For the standardized local-power limits below, write

$$\eta_S := \Sigma_K^{-1/2} \delta_K, \quad \eta_R := \Sigma_{K, \text{diag}}^{-1/2} W_0 \delta_K.$$

Since both  $D_m$  and  $\tilde{R}_m$  are constructed solely from the training sample, their limits are unchanged under the local alternative. In particular,

$$D_m \Rightarrow \Sigma_K^{1/2} V_K \Sigma_K^{1/2}, \quad \tilde{R}_m \Rightarrow \Sigma_{K, \text{diag}}^{1/2} R_K.$$

Because the limits are almost surely positive definite (or have strictly positive diagonal entries), it follows that

$$D_m^{-1} \Rightarrow \Sigma_K^{-1/2} V_K^{-1} \Sigma_K^{-1/2}, \quad \tilde{R}_m^{-2} \Rightarrow (\Sigma_{K, \text{diag}}^{1/2} R_K)^{-2}.$$

Consider the quadratic form

$$Q_m^S(s) := X_m(s)^\top D_m^{-1} X_m(s).$$

By joint convergence and the continuous mapping theorem,

$$Q_m^S(\cdot) \Rightarrow Q^S(\cdot) \quad \text{in } \ell^\infty([0, T]),$$

where

$$\begin{aligned} Q^S(s) &= X(s)^\top \Sigma_K^{-1/2} V_K^{-1} \Sigma_K^{-1/2} X(s) \\ &= (U_K(s) + (s - \kappa)_+ \eta_S)^\top V_K^{-1} (U_K(s) + (s - \kappa)_+ \eta_S), \end{aligned}$$

where  $\eta_S$  is the SSMS-standardized retained-score drift.

Dividing by the deterministic boundary

$$g_\gamma(s)^2 = (1 + s)^2 \left( \frac{s}{1 + s} \right)^{2\gamma}.$$

The convergence after division by  $g_\gamma(s)^2$  first holds on every interval  $[\varepsilon, T]$ .

The small-time contribution is controlled by Assumption 4. If  $\kappa > 0$ , the local drift is absent near the origin; if  $\kappa = 0$ , its contribution divided by

$g_\gamma(s)$  vanishes as  $s \downarrow 0$ , because  $\gamma < 1/2$ . Letting  $\varepsilon \downarrow 0$ , we obtain

$$\sup_{0 < s \leq T} \frac{Q_m^S(s)}{g_\gamma(s)^2} \Rightarrow \sup_{0 < s \leq T} \frac{(U_K(s) + (s - \kappa)_+ \eta_S)^\top V_K^{-1} (U_K(s) + (s - \kappa)_+ \eta_S)}{g_\gamma(s)^2}.$$

Define the whitened partial sums

$$\tilde{X}_m(s) := \frac{1}{\sqrt{m}} \tilde{S}_m(\lfloor ms \rfloor) = \widehat{W}_m X_m(s), \quad \widehat{W}_m = W_0 + o_p(1).$$

Then

$$\tilde{X}_m(\cdot) \Rightarrow \tilde{X}(\cdot) \quad \text{in } \ell^\infty([0, T]),$$

where

$$\tilde{X}(s) = W_0 \Sigma_K^{1/2} U_K(s) + (s - \kappa)_+ W_0 \delta_K.$$

Define

$$O := \Sigma_{K, \text{diag}}^{-1/2} W_0 \Sigma_K^{1/2}.$$

Since

$$OO^\top = \Sigma_{K, \text{diag}}^{-1/2} W_0 \Sigma_K W_0^\top \Sigma_{K, \text{diag}}^{-1/2} = I_K,$$

the matrix  $O$  is orthogonal. Therefore,

$$\tilde{X}(s) = \Sigma_{K, \text{diag}}^{1/2} \{OU_K(s) + (s - \kappa)_+ \eta_R\},$$

where

$$\eta_{\mathbb{R}} := \Sigma_{K, \text{diag}}^{-1/2} W_0 \delta_K.$$

Define

$$R_{K,O} = \text{diag}(R_{K,O,1}, \dots, R_{K,O,K}),$$

where

$$R_{K,O,\ell} = \sup_{0 \leq r \leq 1} \{OB_K^0(r)\}_\ell - \inf_{0 \leq r \leq 1} \{OB_K^0(r)\}_\ell, \quad \ell = 1, \dots, K.$$

Consider

$$Q_m^{\mathbb{R}}(s) := \tilde{X}_m(s)^\top \tilde{R}_m^{-2} \tilde{X}_m(s).$$

Jointly with  $\tilde{X}_m$ , the rotated training-sample self-normalizer satisfies

$$\tilde{R}_m \Rightarrow \Sigma_{K, \text{diag}}^{1/2} R_{K,O}.$$

Therefore, by joint convergence and the continuous mapping theorem,

$$Q_m^{\mathbb{R}}(\cdot) \Rightarrow Q^{\mathbb{R}}(\cdot),$$

where

$$Q^{\mathbb{R}}(s) = (OU_K(s) + (s - \kappa)_+ \eta_{\mathbb{R}})^\top R_{K,O}^{-2} (OU_K(s) + (s - \kappa)_+ \eta_{\mathbb{R}}).$$

Applying the same argument first on  $[\varepsilon, T]$ , controlling the small-time contribution by Assumption 4, and then letting  $\varepsilon \downarrow 0$ , yields

$$\sup_{0 < s \leq T} \frac{Q_m^R(s)}{g_\gamma(s)^2} \Rightarrow \sup_{0 < s \leq T} \frac{(OU_K(s) + (s - \kappa)_+ \eta_R)^\top R_{K,O}^{-2} (OU_K(s) + (s - \kappa)_+ \eta_R)}{g_\gamma(s)^2}.$$

Combining the above displays proves the stated local-power limits for both KS-type monitoring statistics.

**Weighted-CvM statistics.** We prove the weighted-CvM local-power limits by first establishing process convergence and then applying the integrated functionals.

Define the partial-sum process

$$X_m(s) := \frac{1}{\sqrt{m}} S_m(\lfloor ms \rfloor), \quad s \in [0, T].$$

By Lemma S1.6 under the local alternative,

$$\sup_{0 \leq s \leq T} \|X_m(s) - \Sigma_K^{1/2} U_K(s) - (s - \kappa)_+ \delta_K\| = o_p(1),$$

so that

$$X_m(\cdot) \Rightarrow X(\cdot) := \Sigma_K^{1/2} U_K(\cdot) + (\cdot - \kappa)_+ \delta_K \quad \text{in } \ell^\infty([0, T]).$$

As in the KS local-power proof, the training-based self-normalizers satisfy

$$D_m \Rightarrow \Sigma_K^{1/2} V_K \Sigma_K^{1/2}, \quad \tilde{R}_m \Rightarrow \Sigma_{K,\text{diag}}^{1/2} R_K,$$

and the inverses exist almost surely:

$$D_m^{-1} \Rightarrow \Sigma_K^{-1/2} V_K^{-1} \Sigma_K^{-1/2}, \quad \tilde{R}_m^{-2} \Rightarrow (\Sigma_{K,\text{diag}}^{1/2} R_K)^{-2}.$$

For the SSMS (Shao-style) weighted-CvM case, define

$$h_m^{\text{S}}(u) := \frac{X_m(u)^\top D_m^{-1} X_m(u)}{(1+u)^2} w(u), \quad u \in [0, T].$$

Similarly, for RSMS define

$$h_m^{\text{R}}(u) := \frac{\tilde{X}_m(u)^\top \tilde{R}_m^{-2} \tilde{X}_m(u)}{(1+u)^2} w(u),$$

where  $\tilde{X}_m(u) = \widehat{W}_m X_m(u) = W_0 X_m(u) + o_p(1)$ .

Under the local alternative the drift is  $O_p(1)$ , so the weighted-CvM statistic has a nondegenerate integral limit rather than a divergence argument. By the joint convergence above and the continuous mapping theorem, the SSMS integrand converges to the corresponding quadratic limit. Since  $w$  is bounded and Riemann integrable on  $[0, T]$ , the Riemann sums defining

the weighted-CvM statistic converge to the same integral functional. Hence

$$\mathcal{I}_m^S(\lfloor mT \rfloor) \Rightarrow \int_0^T \frac{(U_K(u) + (u - \kappa)_+ \eta_S)^\top V_K^{-1} (U_K(u) + (u - \kappa)_+ \eta_S)}{(1 + u)^2} w(u) du.$$

The same argument applies to RSMS, using  $\tilde{X}_m$  and  $\tilde{R}_m$ :

$$\mathcal{I}_m^R(\lfloor mT \rfloor) \Rightarrow \int_0^T \frac{(U_K(u) + (u - \kappa)_+ \eta_R)^\top R_K^{-2} (U_K(u) + (u - \kappa)_+ \eta_R)}{(1 + u)^2} w(u) du.$$

Combining the above steps proves the stated local-power limits for both SSMS and RSMS weighted-CvM cases.  $\square$

**Proof of Proposition 7**

*Proof.* We compare the contaminated and uncontaminated training self-normalizers through the corresponding training-bridge processes.

Define

$$C_m(r) = \frac{1}{\sqrt{m}} \sum_{t=1}^{\lfloor mr \rfloor} d_{t,m}, \quad 0 \leq r \leq 1.$$

By (S1.1),

$$\sup_{0 \leq r \leq 1} \|C_m(r)\| \rightarrow 0.$$

Let

$$\bar{C}_m(r) := C_m(r) - rC_m(1)$$

be the corresponding bridge version. Then

$$\sup_{0 \leq r \leq 1} \|\bar{C}_m(r)\| \leq 2 \sup_{0 \leq r \leq 1} \|C_m(r)\| = o(1).$$

Let  $\bar{H}_m^{(0)}(r)$  denote the clean training bridge and  $\bar{H}_m(r)$  the contaminated one. Then

$$\bar{H}_m(r) = \bar{H}_m^{(0)}(r) + \bar{C}_m(r).$$

Recall

$$D_m = \int_0^1 \bar{H}_m(r) \bar{H}_m(r)^\top dr, \quad D_m^{(0)} = \int_0^1 \bar{H}_m^{(0)}(r) \bar{H}_m^{(0)}(r)^\top dr.$$

Then

$$\|D_m - D_m^{(0)}\| \leq 2 \sup_{0 \leq r \leq 1} \|\bar{C}_m(r)\| \int_0^1 \|\bar{H}_m^{(0)}(r)\| dr + \int_0^1 \|\bar{C}_m(r)\|^2 dr.$$

Under the null assumptions, the clean bridge satisfies

$$\sup_{0 \leq r \leq 1} \|\bar{H}_m^{(0)}(r)\| = O_p(1),$$

so that

$$\int_0^1 \|\bar{H}_m^{(0)}(r)\| dr = O_p(1).$$

Together with  $\sup_r \|\bar{C}_m(r)\| = o(1)$ , we obtain

$$\|D_m - D_m^{(0)}\| = o_p(1).$$

Hence  $D_m$  has the same weak limit as  $D_m^{(0)}$ .

Let  $\hat{\Sigma}_m$  and  $\hat{\Sigma}_m^{(0)}$  denote the (training-sample) covariance matrices constructed from  $z_t$  and  $z_t^{(0)}$ , respectively. Writing

$$z_t = z_t^{(0)} + d_{t,m},$$

we have

$$\hat{\Sigma}_m - \hat{\Sigma}_m^{(0)} = \frac{1}{m} \sum_{t=1}^m \left( z_t^{(0)} d_{t,m}^\top + d_{t,m} z_t^{(0)\top} + d_{t,m} d_{t,m}^\top \right).$$

Each term is  $o_p(1)$ . Indeed,

$$\left\| \frac{1}{m} \sum_{t=1}^m z_t^{(0)} d_{t,m}^\top \right\| \leq \left( \frac{1}{m} \sum_{t=1}^m \|z_t^{(0)}\|^2 \right)^{1/2} \left( \frac{1}{m} \sum_{t=1}^m \|d_{t,m}\|^2 \right)^{1/2} = o_p(1),$$

by (S1.2) and bounded second moments of  $z_t^{(0)}$ , which follow from Assumption 1. The same bound holds for the transpose term, and

$$\left\| \frac{1}{m} \sum_{t=1}^m d_{t,m} d_{t,m}^\top \right\| \leq \frac{1}{m} \sum_{t=1}^m \|d_{t,m}\|^2 \rightarrow 0.$$

Hence

$$\|\widehat{\Sigma}_m - \widehat{\Sigma}_m^{(0)}\| = o_p(1).$$

Let

$$\widehat{\Sigma}_m = \widehat{L}_m \widehat{\Lambda}_m \widehat{L}_m^\top, \quad \widehat{\Sigma}_m^{(0)} = \widehat{L}_m^{(0)} \widehat{\Lambda}_m^{(0)} \{\widehat{L}_m^{(0)}\}^\top$$

be the corresponding  $LDL^\top$  (square-root-free Cholesky) decompositions, where the  $L$  matrices are unit lower triangular and the  $\Lambda$  matrices are diagonal. The RSMS whitening matrices are

$$\widehat{W}_m = (\widehat{\Lambda}_m + \rho I_K)^{-1/2} \widehat{L}_m^{-1}, \quad \widehat{W}_m^{(0)} = (\widehat{\Lambda}_m^{(0)} + \rho I_K)^{-1/2} \{\widehat{L}_m^{(0)}\}^{-1},$$

with the same small ridge  $\rho > 0$  used in the main text. Since the ridge-regularized  $LDL^\top$ -based whitening map is continuous at the limiting positive-definite training covariance, it follows that

$$\|\widehat{W}_m - \widehat{W}_m^{(0)}\| = o_p(1).$$

Let  $\widetilde{H}_m(r) = \widehat{W}_m \bar{H}_m(r)$  and  $\widetilde{H}_m^{(0)}(r)$  the corresponding clean version.

Then

$$\begin{aligned} \sup_{0 \leq r \leq 1} \|\tilde{H}_m(r) - \tilde{H}_m^{(0)}(r)\| &\leq \|\widehat{W}_m - \widehat{W}_m^{(0)}\| \sup_r \|\bar{H}_m^{(0)}(r)\| \\ &\quad + \|\widehat{W}_m\| \sup_r \|\bar{C}_m(r)\| \\ &= o_p(1). \end{aligned}$$

For each coordinate  $\ell$ ,

$$|\tilde{R}_{m,\ell} - \tilde{R}_{m,\ell}^{(0)}| \leq 2 \sup_{0 \leq r \leq 1} |\tilde{H}_{m,\ell}(r) - \tilde{H}_{m,\ell}^{(0)}(r)| = o_p(1),$$

so that

$$\|\tilde{R}_m - \tilde{R}_m^{(0)}\| = o_p(1).$$

Since the uncontaminated self-normalizers satisfy

$$D_m^{(0)} \Rightarrow \Sigma_K^{1/2} V_K \Sigma_K^{1/2}, \quad \tilde{R}_m^{(0)} \Rightarrow \Sigma_{K,\text{diag}}^{1/2} R_K,$$

Slutsky's theorem gives the same weak limits for the contaminated versions. Consequently, training contamination satisfying (S1.1)–(S1.2) does not affect the asymptotic limits of the SSMS and RSMS training-sample self-normalizers.  $\square$

The simulation results in Appendix S3 are related to the mechanism in Shao and Zhang (2010). In their in-sample structural-break problem,

the naive KS statistic with Shao-type SN can lose power as the break magnitude increases because the SN denominator increases much faster than the numerator. Their one-change-point  $G_n$  statistic recomputes the self-normalizer at each time point, using forward recursive sums before that point and backward recursive sums after it. At the true break, the normalizer is insensitive to the jump magnitude while the numerator grows with the jump. In the present online setting, when the training sample is mildly contaminated, the Shao-type self-normalizer can be inflated before online monitoring begins; this is consistent with the more conservative SSMS behavior relative to the adjusted-range KS statistic in the contaminated-training experiments.

## **S2 Critical Values for the Main Monitoring Statistics**

### **S2.1 KS-type critical values for the main monitoring statistics**

The tables in this subsection give the simulated asymptotic critical values used for the HAC, SSMS, and RSMS KS and weighted-CvM statistics studied in the paper. In this appendix,  $q$  denotes the retained score dimension used in the Monte Carlo simulation; it plays the same role as the retained dimension  $K$  in the main text. The finite-horizon critical values are sim-

ulated from the null limiting distributions in main-paper Theorems 1–4. For  $T = \infty$ , the simulations use the open-end limiting distributions in Theorems S1.1 and S1.2; in those distributions, the endpoint  $t = 1$  is the compactified limit corresponding to  $s \rightarrow \infty$ . Thus the  $T = \infty$  critical values are simulated directly from the open-end limit, rather than obtained by extending the finite-horizon table. We report the  $(1 - \alpha)$  quantiles for  $\alpha \in \{0.01, 0.05, 0.10\}$ , for  $q = 1, \dots, 30$ , and for monitoring horizons  $T \in \{1, 2, 5, 10, \infty\}$ .

For the finite-horizon tables we use 10,000 Monte Carlo replications and an equispaced monitoring grid with  $k_{\max} = 10,000$ . Equivalently,  $(m, k_{\max}) = (10,000, 10,000)$  for  $T = 1$ ,  $(5,000, 10,000)$  for  $T = 2$ ,  $(2,000, 10,000)$  for  $T = 5$ , and  $(1,000, 10,000)$  for  $T = 10$ . For the open-end case  $T = \infty$  we use 5,000 replications, a training-grid size of 1,500, and a monitoring-grid size of 2,000. KS-type critical values are simulated separately for  $\gamma \in \{0, 0.15\}$ .

For weighted-CvM monitoring, the finite-horizon weight families are  $w_U(\tau) \equiv 1$ ,  $w_E(\tau) = 2(1 - \tau)$ ,  $w_M(\tau) = 6\tau(1 - \tau)$ , and  $w_L(\tau) = 2\tau$ , with  $\tau = s/T \in [0, 1]$ . For  $T = \infty$ , the open-end weight families are the

corresponding integrable transforms

$$w_{\text{U}}^{(\infty)}(s) = (1 + s)^{-2}, \quad w_{\text{E}}^{(\infty)}(s) = 2(1 + s)^{-3},$$
$$w_{\text{L}}^{(\infty)}(s) = 2s(1 + s)^{-3}, \quad w_{\text{M}}^{(\infty)}(s) = 6s(1 + s)^{-4}.$$

Because the open-end weight functions differ from their finite-horizon counterparts, the  $T = \infty$  weighted-CvM critical values are tabulated separately below.

## S2. CRITICAL VALUES FOR THE MAIN MONITORING STATISTICS

Table S2.1: HAC-based KS critical values,  $\gamma \in \{0, 0.15\}$ .

<b>Panel A: <math>\gamma = 0</math></b>															
$q$	$T = 1$			$T = 2$			$T = 5$			$T = 10$			$T = \infty$		
	1%	5%	10%	1%	5%	10%	1%	5%	10%	1%	5%	10%	1%	5%	10%
1	3.9165	2.4638	1.9074	5.1167	3.3587	2.5763	6.6189	4.1600	3.1816	6.9506	4.5649	3.5275	7.7217	4.9810	3.7354
2	5.1650	3.5348	2.8360	6.9980	4.7851	3.8584	8.8075	6.0808	4.9146	9.3589	6.5205	5.2501	10.6646	7.2973	5.8309
3	6.3502	4.4882	3.7145	8.3057	5.9864	4.9409	10.6997	7.6264	6.3363	11.2575	8.2352	6.8232	12.0984	9.1139	7.3877
4	7.2800	5.3317	4.4769	9.6935	7.1473	5.9770	12.4051	9.1166	7.6445	12.9705	9.6894	8.2500	14.1622	10.7620	9.1383
5	8.2352	6.1943	5.2203	10.8042	8.1159	6.9574	13.8135	10.3743	8.8019	14.6628	11.1940	9.4870	16.6063	12.4190	10.5778
6	9.0621	6.9491	5.9908	11.9446	9.2206	7.8495	14.9734	11.6488	9.9790	16.2748	12.6258	10.8103	18.3877	13.9167	12.0261
7	9.8088	7.7497	6.7933	13.0853	10.2902	8.8353	16.5477	12.9102	11.1528	17.7634	13.8892	12.1731	20.1286	15.4400	13.4043
8	10.6302	8.4933	7.3577	14.4959	11.1777	9.7465	17.6810	14.2167	12.3416	19.4714	15.5136	13.4006	21.6675	16.8700	14.7134
9	11.4194	9.1882	8.0483	15.5305	12.1540	10.7083	18.8247	15.3794	13.5568	20.7915	16.8077	14.5665	23.0941	18.2438	16.0530
10	11.9812	9.8899	8.7086	16.4273	13.1058	11.5882	20.2020	16.4256	14.6223	22.2157	18.0832	15.9718	24.5858	19.7413	17.4323
11	12.9339	10.6040	9.3961	17.4693	14.0228	12.4950	21.4094	17.6082	15.6243	23.3449	19.2924	17.1696	26.5872	21.2689	18.7966
12	13.4066	11.2975	10.0597	18.5000	15.0080	13.3334	22.5344	18.7070	16.7715	25.0058	20.4956	18.3441	27.6926	22.5636	20.1763
13	14.4767	11.9092	10.6966	19.4247	15.7809	14.1583	24.0265	19.8457	17.8869	26.2564	21.7203	19.4438	29.1485	23.8334	21.4350
14	15.2545	12.5741	11.3335	20.3576	16.6829	14.9594	25.6181	20.9366	18.9397	27.6108	22.9538	20.5120	30.5517	25.2699	22.7152
15	15.9730	13.2275	11.9371	21.3417	17.5552	15.7616	26.8177	22.0158	19.9115	28.7268	24.1145	21.6961	32.1247	26.3680	24.0043
16	16.5959	13.9007	12.5390	22.2445	18.3484	16.6090	27.8040	23.1958	20.8505	30.0021	25.2639	22.7452	33.6657	27.8473	25.2291
17	17.3157	14.4770	13.1658	23.2906	19.2354	17.4336	28.9174	24.3713	21.8969	31.6418	26.4064	23.8325	34.8885	29.0907	26.2699
18	18.0312	15.1440	13.7949	24.1923	20.1794	18.2673	30.2988	25.5006	22.9251	32.7704	27.5316	24.9845	36.5816	30.5574	27.6006
19	18.7647	15.7675	14.3695	25.1724	21.1290	19.0178	31.3668	26.6268	23.9203	34.3034	28.6670	26.1728	37.9106	31.6034	28.8983
20	19.5840	16.5049	14.9349	26.1099	21.8728	19.8483	32.6615	27.6417	24.9839	34.9211	29.8893	27.2647	38.9938	32.8988	30.1165
21	20.1890	17.1071	15.5122	27.0624	22.6967	20.6121	34.1407	28.7245	26.0431	36.1194	31.1448	28.3349	39.7329	34.2170	31.4332
22	20.9138	17.7392	16.1207	28.1909	23.5432	21.4599	35.2646	29.7485	27.0129	37.6193	32.1711	29.4610	41.9966	35.5385	32.4846
23	21.5572	18.3137	16.7342	29.0695	24.4089	22.1844	36.2011	30.6596	27.9173	38.6714	33.3596	30.5907	43.1869	36.7927	33.4982
24	22.2252	18.8893	17.3389	29.7447	25.1843	22.9814	37.3487	31.7956	29.0344	40.2079	34.3842	31.5245	44.4702	38.1606	35.0129
25	22.9069	19.4798	17.9786	30.6000	26.0551	23.7933	39.0262	32.9224	30.0193	41.5158	35.5017	32.7336	45.7994	39.3917	36.2743
26	23.5805	20.1765	18.5763	31.0550	26.9211	24.6143	40.0112	34.0088	30.9837	42.8607	36.6799	33.7596	47.1647	40.5951	37.3299
27	24.2166	20.7817	19.1459	32.5543	27.7576	25.3901	41.0258	34.8869	32.0601	43.9352	37.9387	34.8892	48.5438	42.0201	38.5500
28	24.7299	21.4228	19.7727	33.4694	28.5070	26.1540	41.9292	35.9235	32.9718	45.1663	38.9538	36.0755	49.7556	43.2809	39.7681
29	25.2904	22.1140	20.4016	34.4282	29.2318	27.0708	43.1476	36.8880	33.9980	46.6898	40.1232	37.0587	51.3841	44.3442	40.9725
30	26.1526	22.7242	20.9197	35.2741	30.0622	27.8702	44.3233	37.7368	34.9428	47.7244	41.3730	38.1012	53.0971	45.6625	42.1675

<b>Panel B: <math>\gamma = 0.15</math></b>															
$q$	$T = 1$			$T = 2$			$T = 5$			$T = 10$			$T = \infty$		
	1%	5%	10%	1%	5%	10%	1%	5%	10%	1%	5%	10%	1%	5%	10%
1	5.0511	3.2005	2.5259	5.9565	4.0305	3.1412	7.2502	4.6674	3.6250	7.4945	4.9677	3.9276	8.0512	5.2155	4.0513
2	6.5890	4.5749	3.7300	8.1939	5.6989	4.5842	9.6754	6.7058	5.4670	9.9093	7.0318	5.7342	10.9328	7.6551	6.2084
3	8.1030	5.7772	4.8070	9.6758	7.0612	5.8880	11.5867	8.3413	7.0020	11.9009	8.8087	7.3800	12.5293	9.4708	7.7958
4	9.2200	6.8193	5.7122	11.2133	8.3350	7.0413	13.4047	9.9483	8.3835	13.7183	10.3650	8.8350	14.6264	11.2358	9.4970
5	10.3577	7.8953	6.6997	12.5777	9.4402	8.1329	14.9716	11.3100	9.6501	15.3281	11.8392	10.1552	17.0396	12.7503	11.0411
6	11.4091	8.8268	7.6134	13.7154	10.6885	9.2026	16.2390	12.6503	10.9452	17.2136	13.3647	11.4862	18.7742	14.4259	12.4814
7	12.2924	9.8471	8.4997	14.9838	11.8958	10.3292	17.7755	14.0364	12.1507	18.6503	14.6883	12.9105	20.5883	15.9315	13.8447
8	13.0557	10.7494	9.2842	16.7632	12.9383	11.3411	18.8941	15.3851	13.4120	20.3864	16.3060	14.1823	22.0356	17.3764	15.2092
9	14.3824	11.5710	10.1979	17.8241	14.0318	12.4223	20.1444	16.6530	14.7283	21.8225	17.7085	15.4052	23.5056	18.8326	16.5441
10	15.1248	12.4247	11.0319	18.9270	15.0766	13.4315	21.7176	17.7661	15.8383	23.1979	19.1585	16.7592	25.0348	20.2912	17.8917
11	16.1957	13.3143	11.8400	19.9710	16.1517	14.4656	23.1042	18.9478	16.9312	24.5832	20.3843	18.0884	26.7492	21.7365	19.2282
12	16.9030	14.1925	12.6654	21.1253	17.2900	15.4153	24.2363	20.1276	18.1161	26.2684	21.5357	19.3204	28.1955	23.0316	20.5984
13	18.0661	14.9296	13.4724	22.2425	18.1184	16.3270	25.6122	21.3439	19.3292	27.3723	22.7619	20.4448	29.6885	24.5460	21.9701
14	19.0618	15.7477	14.2661	23.1954	19.1844	17.2335	27.5509	22.5507	20.4059	29.0053	24.1236	21.6167	30.9235	25.7568	23.2896
15	19.9799	16.6092	15.0107	24.2642	20.1654	18.1786	28.6811	23.7210	21.4625	30.0748	25.2447	22.7789	32.7522	26.9483	24.5594
16	20.7228	17.3749	15.7453	25.3328	21.1185	19.1263	29.7031	24.9349	22.4706	31.4188	26.4784	23.8538	34.1950	28.4050	25.8229
17	21.6572	18.1248	16.4904	26.7621	22.1035	20.0931	31.0072	26.2035	23.5694	32.9377	27.6595	25.0407	35.4122	29.7699	27.0152
18	22.4561	18.9866	17.3073	27.6118	23.1229	21.0390	32.3672	27.2819	24.6822	34.1960	28.7744	26.1917	37.1591	31.0751	28.1147
19	23.3261	19.7257	17.9747	29.0261	24.1759	21.8991	33.6099	28.5118	25.7607	35.7183	30.0573	27.4003	38.3157	32.2248	29.5757
20	24.4241	20.5420	18.6911	29.9998	25.0521	22.7545	34.8413	29.5728	26.8710	36.3956	31.3161	28.5186	39.6786	33.4758	30.7393
21	25.0323	21.3854	19.3951	31.0106	26.0286	23.6710	36.3675	30.6953	27.9642	37.5258	32.4699	29.6594	40.8392	34.6774	31.8880
22	25.9747	22.1772	20.1660	32.2299	27.0250	24.6030	37.5610	31.8127	28.9886	39.0208	33.6069	30.8095	42.4707	35.9304	32.9986
23	26.8880	22.8517	20.9028	33.1768	27.9054	25.4212	38.6467	32.8742	29.9730	40.0804	34.8001	31.9209	43.8227	37.1649	34.1296
24	27.6318	23.5794	21.7097	34.1468	28.9039	26.3628	39.7671	34.0348	31.0366	41.6720	35.9679	32.9436	44.8795	38.6333	35.5061
25	28.3743	24.3030	22.4241	35.0738	29.8896	27.3088	41.5395	35.1767	32.0712	43.0732	37.0332	34.1552	46.7543	40.0239	36.6689
26	29.3686	25.1283	23.2174	36.1363	30.8184	28.1673	42.5769	36.3665	33.1454	44.5817	38.2019	35.3281	47.9762	41.2072	37.8311
27	30.1185	25.9028	23.9269	37.2078	31.7042	29.0777	43.6716	37.2637	34.2787	45.5400	39.6262	36.3749	49.3000	42.5251	39.0027
28	30.8880	26.7273	24.6646	38.2298	32.6031	29.9502	44.7629	38.3377	35.2737	46.8647	40.6390	37.5727	50.1712	43.7331	40.2833
29	31.5278	27.4628	25.4576	39.3722	33.4695	30.9309	45.9732	39.3522	36.3553	48.4603	41.8839	38.6274	51.7131	44.8402	41

Table S2.2: Shao’s KS critical values,  $\gamma \in \{0, 0.15\}$ .

Panel A: $\gamma = 0$															
$q$	$T = 1$			$T = 2$			$T = 5$			$T = 10$			$T = \infty$		
	1%	5%	10%	1%	5%	10%	1%	5%	10%	1%	5%	10%	1%	5%	10%
1	61.1692	32.6251	22.1281	92.7874	45.7831	31.0813	104.0601	54.1614	37.3774	119.9345	60.9035	41.2306	125.4659	64.5525	44.4808
2	119.4341	66.6268	48.4224	158.7733	92.3532	67.5270	202.3803	112.2517	83.8161	219.0175	125.6359	91.8423	261.5101	141.1637	103.7501
3	181.2722	109.6751	83.2873	242.0474	149.5751	111.5425	308.2206	180.1181	141.8459	325.2595	201.8591	152.5928	376.6135	233.8170	169.2561
4	254.3359	159.2767	124.5910	333.0036	209.7493	164.8924	430.7384	271.4087	211.6499	442.7788	285.1651	225.4431	525.1386	326.6511	254.3761
5	333.6036	218.9016	170.3278	439.5197	281.5632	224.7465	551.6765	356.8651	284.8150	593.0173	391.9126	308.7508	650.7221	444.1149	346.7081
6	420.8112	281.7607	225.4792	563.4592	367.8338	296.4000	678.3653	465.0149	372.5796	737.2354	506.4300	405.3321	849.0542	559.8871	450.1861
7	509.8984	349.5790	284.7962	665.2405	449.7303	371.6401	825.4440	572.9039	460.7480	889.4025	627.2455	510.8433	985.1820	693.7892	561.4010
8	600.8422	424.0187	347.2166	823.4706	541.8922	451.1452	995.5738	706.8816	577.0918	1071.9876	759.2283	633.0944	1215.8908	832.1987	696.2941
9	708.3027	501.7141	419.0791	950.1474	651.7608	542.3977	1146.7474	839.2525	694.7893	1240.2189	897.2161	745.1696	1395.4808	984.6237	816.6248
10	815.8082	588.2900	487.5641	1093.0744	774.2187	636.4519	1335.4390	968.6122	818.2561	1463.6146	1060.7384	888.3466	1599.2867	1155.6190	975.3942
11	936.6075	680.2968	571.3882	1237.7515	895.4571	744.1251	1512.6099	1108.1201	930.4989	1731.1296	1228.3537	1033.6505	1828.4641	1332.4542	1141.1152
12	1078.3735	785.4602	655.1589	1383.4676	1029.5505	864.1793	1720.3287	1268.0574	1079.2971	1908.7657	1406.0678	1189.2828	2084.6794	1536.8990	1298.7056
13	1192.0652	881.9880	737.5461	1540.9695	1153.4431	975.4980	1943.9309	1472.7226	1219.2463	2145.5753	1582.3514	1343.2807	2316.5352	1726.8888	1490.1331
14	1305.8357	986.1600	841.4380	1683.6918	1310.2011	1105.4554	2200.8896	1620.5728	1378.4790	2380.9803	1745.6154	1519.3211	2590.5686	1983.3621	1675.0935
15	1440.5650	1096.2265	937.6345	1885.1042	1450.5693	1239.1725	2403.0146	1754.6608	1547.4608	2592.5415	1944.6099	1690.4494	2844.6893	2216.4770	1888.2389
16	1588.8528	1222.6830	1043.6280	2083.0129	1611.0943	1380.4009	2628.4532	1989.8111	1710.0985	2837.1231	2170.4070	1874.1388	3094.1528	2462.0611	2111.0245
17	1740.9898	1336.0270	1149.8414	2297.6130	1776.3154	1522.4182	2839.7877	2199.8948	1898.5024	3163.9163	2408.0998	2077.9764	3456.4959	2701.4816	2338.4419
18	1904.4677	1445.6241	1254.4037	2485.9738	1949.8147	1677.9468	3025.1775	2425.8225	2095.5726	3418.4117	2648.0448	2292.7474	3722.1191	2937.2400	2567.4853
19	2060.0817	1573.8105	1365.4704	2719.0099	2099.7656	1840.8980	3309.1749	2629.1756	2283.1628	3725.8226	2894.4674	2504.4408	4048.3437	3183.4355	2806.9759
20	2242.2753	1715.8785	1490.9818	2915.6343	2276.9767	1996.5798	3610.7821	2850.5323	2496.0279	4000.7819	3108.4648	2784.2158	4455.7407	3464.4763	3054.6718
21	2408.3197	1859.0382	1623.0505	3135.4113	2482.1265	2173.0264	3885.3296	3085.5404	2705.3202	4269.3285	3362.3086	2970.8459	4720.9116	3738.0058	3291.1915
22	2573.6919	2006.2190	1754.0165	3409.2860	2667.8433	2350.2945	4209.0712	3331.8715	2945.1695	4580.9780	3666.3464	3205.5722	5151.1737	3987.9878	3522.1715
23	2738.8586	2154.9330	1891.4240	3651.5329	2887.4679	2539.6737	4490.6820	3590.5075	3164.4021	4906.9820	3932.3256	3456.8712	5464.1223	4292.0487	3806.0465
24	2952.7369	2295.5200	2039.5440	3868.0142	3104.7620	2767.6164	4766.6508	3844.9508	3404.8772	5264.6657	4184.5020	3722.9647	5874.2662	4656.9924	4124.8254
25	3192.3592	2476.7382	2185.0977	4116.2899	3334.9770	2929.9831	5188.9935	4128.0711	3643.8833	5616.4482	4495.5461	3964.0276	6287.3729	5083.2619	4417.0096
26	3343.7107	2653.4221	2332.9673	4353.4487	3557.5390	3154.0216	5432.6299	4400.8768	3938.5266	6162.9316	4747.0709	4247.0709	6920.5681	5388.4093	4712.4234
27	3509.6106	2815.1720	2491.4706	4642.3140	3776.8063	3350.4064	5765.3325	4727.2261	4194.0028	6323.3341	5112.5582	4546.8023	7167.2708	5685.9780	4992.6239
28	3695.4519	3006.0717	2650.3850	4928.8719	3991.8131	3553.6359	6179.0277	5011.2881	4452.5425	6720.7909	5450.0132	4836.7497	7582.7178	6029.3121	5342.9233
29	3930.7631	3181.2631	2818.8944	5206.9259	4245.3920	3760.3729	6490.2801	5310.1301	4746.5035	7143.6511	5761.3521	5154.1068	7977.6593	6387.1863	5654.4288
30	4179.1232	3381.8024	3005.6605	5446.0585	4486.4024	3994.7942	6840.4717	5578.8644	5031.0101	7526.3075	6114.3268	5439.4449	8432.4485	6795.1411	5977.7781

Panel B: $\gamma = 0.15$															
$q$	$T = 1$			$T = 2$			$T = 5$			$T = 10$			$T = \infty$		
	1%	5%	10%	1%	5%	10%	1%	5%	10%	1%	5%	10%	1%	5%	10%
1	80.6373	43.7794	30.2145	111.2393	55.5930	39.2312	118.0652	61.7774	45.5973	133.8357	67.6646	47.0643	132.9313	70.0182	49.6262
2	155.9644	88.4734	65.0170	190.4159	110.6272	82.3292	226.6662	125.6977	95.7670	236.0521	137.9002	102.3357	269.9183	152.6976	112.2160
3	234.7844	143.1873	109.9223	283.7873	179.2470	135.3188	343.3063	209.8408	159.9347	346.7075	221.1076	167.2223	387.6207	247.0362	183.1976
4	331.9408	209.9397	164.0974	390.9107	251.5674	199.4518	468.2289	299.9781	238.3644	474.3702	310.9686	246.4827	555.4131	345.0559	270.5515
5	423.2560	282.5173	224.1586	507.4476	338.0549	268.9514	599.8453	398.9634	321.4584	631.2075	422.2422	337.6891	678.7652	461.8259	365.5929
6	544.9044	362.5091	293.9266	649.3046	433.6264	353.2166	747.9191	511.7735	415.0014	778.7681	541.9327	437.8797	874.7009	583.5585	474.8281
7	653.4072	447.6354	369.8239	772.1705	533.9489	433.4068	896.2910	635.4670	511.9839	937.4199	672.0903	553.1520	1027.8484	715.5054	591.3771
8	765.5414	543.1643	447.5760	944.4395	638.2252	534.3406	1073.8771	775.6876	639.3377	1131.6184	815.3475	675.7578	1256.8069	866.6205	674.2726
9	897.8743	643.2743	506.2110	1099.8444	760.5207	638.9628	1252.3459	916.2152	769.4932	1331.5486	957.3771	804.4310	1444.5683	1018.2677	853.2644
10	1029.5507	752.6337	626.3191	1265.1223	902.3553	750.4517	1441.5667	1063.2177	898.7342	1537.8533	1131.3965	952.8426	1621.7093	1197.9021	1011.3611
11	1180.3271	859.3981	729.3032	1426.7519	1044.6491	874.5096	1653.1258	1216.3310	1032.7584	1855.1306	1269.2604	1106.5028	1884.1324	1380.2139	1174.7322
12	1358.5494	995.5157	836.6492	1593.2732	1198.6545	1012.0669	1880.5083	1385.3559	1185.7419	2004.1047	1495.4072	1272.4942	2152.0620	1592.8507	1305.1876
13	1503.2573	1123.2137	942.4581	1786.6591	1343.5831	1143.8422	2107.3624	1585.9755	1337.6818	2259.5199	1681.3533	1433.9955	2394.4747	1787.6019	1531.8185
14	1654.5016	1250.3992	1070.4729	1956.1229	1513.4591	1294.6014	2376.8954	1763.2977	1504.9739	2498.5555	1869.4918	1622.1234	2627.6641	2033.4118	1726.7627
15	1811.4965	1397.7765	1196.9309	2171.4009	1680.2981	1445.7416	2582.1181	1950.8479	1690.1626	2756.8005	2071.0659	1794.3192	2905.7219	2282.1072	1957.3041
16	2000.1267	1542.1482	1323.5951	2417.9925	1867.2886	1608.2019	2800.5887	2166.0762	1862.8415	2995.6494	2302.5955	1991.5766	3173.0783	2537.1315	2182.6336
17	2190.8327	1697.2969	1460.3377	2619.7132	2063.7540	1775.9146	3071.0067	2384.7873	2065.4001	3321.7392	2537.8213	2207.9625	3527.2948	2783.8930	2403.3965
18	2368.7047	1824.6393	1596.9552	2855.8946	2268.6810	1951.8890	3293.4146	2620.5076	2273.4205	3594.2880	2798.2038	2440.5934	3778.5841	3012.0034	2644.8241
19	2581.5872	1994.3592	1735.9489	3122.2621	2445.1955	2140.7186	3526.7440	2832.6416	2493.6904	3926.3969	3042.8787	2647.3386	4128.5405	3254.1744	2891.6626
20	2813.4055	2167.3920	1887.7109	3355.8444	2638.8906	2317.9365	3873.2181	3078.7516	2715.2064	4200.8866	3287.0628	2885.5693	4529.0679	3563.2833	3138.5623
21	3015.8439	2347.3868	2052.7875	3609.2352	2867.5680	2510.6236	4205.2355	3290.9959	2941.8465	4517.0860	3537.3263	3141.9934	4849.1516	3828.1998	3360.5593
22	3207.7061	2527.0895	2221.4767	3902.2199	3084.4156	2717.7748	4560.9620	3585.5011	3187.4872	4789.2693	3861.2863	3381.2506	5225.7731	4096.4627	3613.5303
23	3435.3480	2712.7605	2391.0162	4197.0302	3336.3261	2948.5030	4835.6803	3877.5507	3429.6936	5148.5031	4137.6441	3652.4627	5555.6470	4429.8726	3905.4454
24	3687.2251	2898.2014	2568.8243	4475.1256	3584.8853	3175.5361	5117.7521	4156.0154	3691.6986	5490.1295	4419.1745	3915.1343	6032.1241	4781.4637	4236.7771
25	3994.9820	3115.7284	2751.0815	47											

S2. CRITICAL VALUES FOR THE MAIN MONITORING STATISTICS

Table S2.3: Adjusted-range-based KS critical values,  $\gamma \in \{0, 0.15\}$ .

Panel A: $\gamma = 0$															
$q$	$T = 1$			$T = 2$			$T = 5$			$T = 10$			$T = \infty$		
	1%	5%	10%	1%	5%	10%	1%	5%	10%	1%	5%	10%	1%	5%	10%
1	3.2988	1.9776	1.4677	4.9664	2.7646	2.0450	6.0175	3.4040	2.5237	6.6349	3.8677	2.8589	7.2385	4.0979	3.0114
2	4.6570	2.9023	2.2444	6.2869	3.9917	3.0476	8.5944	5.1567	3.9713	9.3035	5.7407	4.3981	10.3839	6.1835	4.8239
3	5.6294	3.7276	2.9678	7.5426	5.0617	3.9968	10.4356	6.5096	5.1984	11.0964	7.2520	5.7763	11.7054	7.8262	6.1369
4	6.4033	4.4448	3.5920	8.5547	5.9683	4.8378	11.8367	7.7425	6.3118	12.7152	8.6074	6.9629	13.1793	9.3024	7.4727
5	7.1940	5.0681	4.1198	9.8304	6.8265	5.6384	13.0522	8.7800	7.2611	13.9178	9.8392	8.0451	14.8438	10.6066	8.7523
6	7.8635	5.7493	4.7662	10.7627	7.6293	6.3967	14.1093	9.8539	8.1880	15.0962	11.0401	9.1166	16.6299	11.8904	9.9232
7	8.4555	6.3696	5.3404	11.7086	8.4551	7.1239	15.1386	10.9723	9.1093	16.3716	12.1002	10.1587	17.9748	12.9779	11.0493
8	9.0659	6.8574	5.8943	12.3990	9.3162	7.8710	16.0137	12.0800	10.1409	17.5543	13.3147	11.2473	19.4077	14.3306	12.2357
9	9.6277	7.4254	6.4552	13.5541	10.0404	8.6297	16.8762	13.0828	11.0655	18.8738	14.2936	12.3231	20.976	15.4020	13.2357
10	10.3762	7.9710	6.9258	14.3281	10.7594	9.3010	17.7392	14.0159	12.0247	20.4078	15.3237	13.2125	21.5359	16.5164	14.2195
11	11.0179	8.5247	7.4740	15.2458	11.5247	10.0287	18.7926	14.8884	12.8561	21.4748	16.3761	14.2119	23.0880	17.7415	15.2660
12	11.6291	9.0548	7.9543	16.0446	12.2447	10.7100	19.8152	15.6883	13.6233	22.6750	17.1937	15.0931	23.7266	18.7514	16.2950
13	12.2128	9.6147	8.4295	16.7010	12.8655	11.3300	20.9983	16.5729	14.5365	23.4742	18.2020	15.9879	25.0109	19.9786	17.3599
14	12.6987	10.1406	8.8851	17.5710	13.6283	12.0257	22.1706	17.4705	15.4190	24.4092	19.2944	16.8955	26.6556	21.0156	18.4250
15	13.3229	10.6252	9.3873	18.4592	14.3192	12.6283	23.4364	18.4528	16.1255	25.9506	20.2930	17.8383	27.8329	22.1711	19.4049
16	14.0142	11.0836	9.8665	19.0866	14.9762	13.2911	24.2656	19.2620	16.9811	26.8816	21.3250	18.7633	29.2129	23.2770	20.3541
17	14.4260	11.6119	10.3170	20.0238	15.5961	13.9459	25.1517	20.1970	17.8295	28.0240	22.2729	19.7018	30.1352	24.3255	21.4436
18	14.9681	12.1246	10.7608	20.5274	16.2523	14.5548	26.2728	21.1143	18.6942	29.2834	23.0815	20.6134	31.2686	25.1680	22.4942
19	15.4733	12.5470	11.2492	21.3328	16.9426	15.1664	27.1193	21.8671	19.4504	30.4433	24.2123	21.5431	32.3960	26.1717	23.4762
20	16.0081	13.0852	11.7283	21.8279	17.6031	15.7456	28.1664	22.6683	20.1926	31.5104	25.1831	22.3923	33.4884	27.2701	24.4686
21	16.4170	13.5887	12.1802	22.5606	18.2518	16.3651	29.3499	23.5941	20.9833	32.3443	26.1714	23.3412	33.9523	28.1634	25.3890
22	16.9549	14.1243	12.6279	23.7201	18.9155	16.9274	30.2492	24.3295	21.8849	33.1845	26.9296	24.1205	34.8697	29.2101	26.2957
23	17.5595	14.5763	13.0887	24.3915	19.5956	17.5131	31.0713	25.2950	22.6350	34.3182	27.9176	25.1293	36.5807	30.1282	27.2957
24	18.0634	15.0369	13.5703	24.8409	20.2929	18.1931	31.8502	26.0541	23.3429	35.3853	28.8418	25.9403	38.2117	31.5296	28.2152
25	18.4747	15.5255	13.9777	25.5196	20.9957	18.8302	33.0921	26.9705	24.1615	35.9438	29.8695	26.8481	39.7267	32.4299	29.1783
26	19.0916	15.9892	14.4987	26.3285	21.5836	19.4724	34.0969	27.9213	24.9647	37.0199	30.7615	27.6594	40.6342	33.2912	30.2019
27	19.6265	16.4596	14.9179	27.0359	22.3773	20.0577	34.6794	28.6572	25.6813	37.8592	31.5750	28.5776	41.1777	34.4823	31.0638
28	20.2408	16.9603	15.3978	27.6383	22.8642	20.7009	35.2865	29.4771	26.4236	39.0850	32.5295	29.4050	42.0339	35.2205	32.1136
29	20.7620	17.4639	15.8461	28.3412	23.4771	21.3167	36.2939	30.3609	27.3092	39.6562	33.4010	30.3185	43.0128	36.2355	32.9922
30	21.2532	17.9667	16.3455	28.8573	24.1740	21.8855	37.0750	31.1838	27.9827	40.2784	34.3019	31.1865	44.1198	37.0442	34.0259

Panel B: $\gamma = 0.15$															
$q$	$T = 1$			$T = 2$			$T = 5$			$T = 10$			$T = \infty$		
	1%	5%	10%	1%	5%	10%	1%	5%	10%	1%	5%	10%	1%	5%	10%
1	4.3244	2.6330	1.9714	5.9629	3.3439	2.5060	6.5768	3.8332	2.9128	7.1915	4.2959	3.2204	7.5258	4.3650	3.2656
2	5.9340	3.8155	2.9535	7.4451	4.7717	3.7074	9.4392	5.7603	4.4529	10.0916	6.2699	4.8260	10.7415	6.5173	5.0795
3	7.2303	4.8396	3.8722	8.9237	5.9944	4.7651	11.2895	7.2025	5.7992	11.7788	7.8612	6.2562	12.0342	8.1427	6.4853
4	8.2708	5.7120	4.6573	10.1820	7.0556	5.7620	12.9336	8.6217	7.0033	13.4060	9.3034	7.5157	13.7566	9.6336	7.8700
5	9.0602	6.4775	5.3475	11.4241	8.0357	6.6553	14.2514	9.6505	8.0582	14.8383	10.5421	8.7158	15.1457	11.0044	9.1178
6	10.0738	7.3435	6.1179	12.5821	8.9287	7.4882	15.2852	10.7454	9.0567	16.1755	11.8248	9.7834	17.1961	12.3588	10.3230
7	10.8144	8.0594	6.8047	13.4632	9.8787	8.3558	16.4414	11.9596	10.0470	17.4401	12.8468	10.9254	18.2107	13.5800	11.4140
8	11.5196	8.7782	7.5249	14.3743	10.8714	9.1556	17.5654	13.1588	11.1457	18.5884	14.1034	12.0502	19.9241	14.7403	12.5384
9	12.4972	9.4375	8.2226	15.5239	11.7262	10.0572	18.3362	14.2394	12.0844	19.8286	15.1709	13.0526	20.7845	15.8852	13.5763
10	13.0892	10.1150	8.7829	16.4579	12.5180	10.9026	19.1619	15.1807	13.0630	21.1927	16.3443	14.0343	22.0445	17.0179	14.6365
11	13.9651	10.7976	9.4516	17.5575	13.3850	11.6672	20.2387	16.0956	13.9640	22.6796	17.3558	15.0461	23.6600	18.2533	15.7238
12	14.6996	11.4685	10.0694	18.5236	14.1735	12.3990	21.5664	16.9906	14.8511	23.7802	18.1452	16.0318	24.9319	19.1681	16.7166
13	15.3480	12.1051	10.6513	19.2945	14.8272	13.1504	22.5222	17.9229	15.7684	24.7802	19.1774	16.9476	26.3571	20.3746	17.8276
14	15.8659	12.7618	11.2684	20.3694	15.6949	13.9637	24.0117	18.8849	16.6816	25.9064	20.2690	17.8453	27.0353	21.5779	18.8821
15	16.6185	13.3980	11.8478	21.2355	16.5223	14.8277	25.1527	19.9043	17.4565	27.4868	21.3978	18.8381	28.5820	22.7771	19.8373
16	17.4874	13.9384	12.4134	22.0433	17.2857	15.4101	26.1072	20.8627	18.3519	28.0855	22.4582	19.7983	29.7425	23.7084	20.8758
17	18.0016	14.5642	13.0114	22.9091	18.0129	16.1137	26.9731	21.7506	19.3095	29.6106	23.3914	20.7314	30.6424	24.8491	21.9869
18	18.5727	15.2060	13.5855	23.6593	18.8059	16.8211	28.0712	22.6963	20.1360	30.5361	24.4090	21.6759	32.0723	25.6198	22.9758
19	19.2598	15.7167	14.1094	24.4733	19.4984	17.5116	29.0062	23.5358	21.0011	31.9204	25.4639	22.5544	32.6501	26.9658	23.9456
20	20.0548	16.4017	14.7056	24.9933	20.3371	18.1524	30.1105	24.3716	21.8332	32.9917	26.4524	23.5910	33.9545	27.8268	24.9046
21	20.6041	17.0244	15.2777	25.7947	21.0425	18.8430	31.5210	25.3780	22.6362	33.8066	27.4083	24.5562	34.4251	28.7739	25.8755
22	21.3392	17.7254	15.8738	26.9181	21.7641	19.5166	32.3227	26.1896	23.5805	34.9401	28.2401	25.3426	35.7457	29.8528	26.7962
23	22.1043	18.2347	16.4299	27.7746	22.5519	20.1605	33.1442	27.2406	24.4076	36.0018	29.2216	26.3227	36.9344	30.6912	27.8341
24	22.6879	18.8289	16.9860	28.3259	23.2906	20.9065	34.0197	27.9903	25.0764	36.8912	30.1665	27.1862	38.6686	32.1231	28.7821
25	23.1005	19.3962	17.5239	29.3173	24.0250	21.6418	35.2543	28.9243	26.0162	37.6850	31.1713	28.1303	39.9729	33.0785	29.7699
26	23.8819	20.0177	18.1199	30.0834	24.7418	22.4040	36.2641	29.9197	26.8344	38.8014	32.1185	28.9826	41.0100	33.9477	30.7232
27	24.5761	20.5613	18.6836	30.9556	25.5932	23.0415	37.0301	30.8128	27.5793	39.4615	33.0684	29.8385	41.6371	34.9067	31.6626
28	25.3131	21.1662	19.2104	31.6344	26.2043	23.7809	37.6204	31.6661	28.4316	40.7430	34.0098	30.7833	42.7191	35.9296	32.7404
29	26.0812	21.7842	19.7978	32.3767	26.9455	24.4424	38.7631	32.5285	29.3133	41.4506	34.8838	31.7577	43.7716	36.8449	33.6426
30	26.5948	22.3236	20.3982	33.1079	27.7282	25.1395	39.5452	33.3668	30.1345	42.4351	35.9172	32.6332	44.8076	37.7602	34.6580

## S2.2 Weighted-CvM critical values: finite horizons and open-end

Tables S2.4–S2.15 report the finite-horizon weighted-CvM critical values for  $T \in \{1, 2, 5, 10\}$ . The tables are grouped by standardization: the HAC LRV-scaled statistic is reported in Tables S2.4–S2.7, Shao’s self-normalized statistic in Tables S2.8–S2.11, and the adjusted-range self-normalized statistic in Tables S2.12–S2.15. Within each group, the weights are ordered as constant  $w_U$ , early  $w_E$ , mid  $w_M$ , and late  $w_L$ .

Table S2.4: Critical values for the HAC-based weighted-CvM statistic with constant weight  $w_U$  (finite horizons)

$q$	$T = 1$			$T = 2$			$T = 5$			$T = 10$		
	1%	5%	10%	1%	5%	10%	1%	5%	10%	1%	5%	10%
1	1.6960	1.0480	0.7456	5.2909	3.1318	2.2553	19.2019	11.2178	8.2601	46.6112	27.3607	19.7535
2	2.4844	1.6052	1.2728	7.2878	4.8720	3.7884	27.7989	18.2313	14.0803	65.3775	43.0594	33.4170
3	3.0565	2.1598	1.7375	9.0785	6.3513	5.2135	34.4575	23.8690	19.1628	80.4749	56.3726	45.6968
4	3.6539	2.6182	2.1698	10.8505	7.7729	6.4859	41.4783	29.2305	24.0572	94.2015	68.1083	56.7189
5	4.1976	3.1226	2.6033	12.2970	9.0170	7.6594	45.7943	33.7721	28.4452	106.6556	79.8889	66.7835
6	4.5833	3.5503	3.0481	13.6524	10.3224	8.8559	49.9616	38.1380	32.7196	118.9984	91.0674	77.1427
7	5.0439	4.0005	3.4387	15.1902	11.7573	10.0575	55.1662	43.2302	36.9068	130.4290	101.2983	88.2070
8	5.5900	4.4207	3.8608	16.5638	12.9752	11.2956	59.3741	47.8267	41.1998	144.5634	113.3644	98.1623
9	5.9868	4.8230	4.2348	17.7121	14.2067	12.5191	64.1577	52.1923	45.9799	155.3450	124.8153	107.8474
10	6.3642	5.2464	4.6338	19.0778	15.3347	13.7460	69.5748	56.0629	49.6852	167.5947	134.8649	118.3004
11	6.9027	5.6099	5.0135	20.5192	16.6009	14.8875	74.6317	60.1473	53.7032	175.9513	144.9537	129.1720
12	7.3002	6.0296	5.3861	22.0072	17.7505	15.9497	77.6114	64.4973	57.7861	190.3936	155.0308	137.1846
13	7.7214	6.4224	5.7850	23.0529	18.8396	17.0051	82.6473	69.1614	62.1341	200.2017	164.8883	147.2528
14	8.0835	6.7781	6.1463	24.4533	20.0443	18.0161	87.9495	73.3533	65.9490	211.1550	174.7744	156.0209
15	8.5265	7.1809	6.5284	25.6000	21.1929	19.1385	93.6908	77.2028	69.8072	219.5748	184.3939	165.0318
16	8.9555	7.5809	6.9034	26.8002	22.3910	20.2011	97.7925	81.5957	73.5375	233.0729	194.0268	174.2856
17	9.3293	7.9735	7.2373	28.3086	23.5158	21.2811	102.4805	85.3404	77.2314	243.6825	202.6170	183.0413
18	9.7199	8.3824	7.6193	29.3290	24.6334	22.4220	106.1122	89.0277	81.1281	255.2513	211.8956	192.7025
19	10.1221	8.7267	7.9661	30.7345	25.7489	23.4275	110.4534	92.9687	84.9069	266.5498	222.4576	201.2816
20	10.4958	9.1092	8.3460	31.7533	26.9495	24.3855	114.8050	97.4783	88.7604	272.1668	231.5981	210.5035
21	10.8903	9.4928	8.6773	33.1648	28.0124	25.5309	120.2223	101.4092	92.7718	282.7260	240.3301	219.9681
22	11.3323	9.8576	9.0236	34.5887	29.1919	26.5687	124.0055	104.9866	96.1942	294.6833	250.1443	228.5610
23	11.7259	10.2523	9.3717	35.8610	30.1742	27.6169	127.9699	108.8631	99.7714	302.9259	259.3238	237.3703
24	12.3400	10.5800	9.7218	37.0647	31.2188	28.5675	131.8562	113.3189	103.8025	312.9834	268.8917	246.5073
25	12.7120	10.9520	10.1018	38.1656	32.5364	29.7719	136.8574	117.3006	107.4582	323.9573	278.0743	255.4320
26	13.1031	11.3122	10.4615	39.6360	33.4347	30.7920	141.5504	121.3258	110.9874	334.6623	287.8175	264.4713
27	13.4101	11.6618	10.8123	41.0031	34.4596	31.8553	144.1397	124.9288	114.7678	344.4800	297.7210	273.6926
28	13.7328	12.0080	11.1752	41.7746	35.5131	32.8265	149.0367	129.1673	118.5597	353.5288	307.2695	282.7777
29	14.1318	12.3588	11.5256	42.7760	36.6663	33.8328	153.4550	133.2183	122.4179	365.7282	316.4034	291.3118
30	14.6113	12.7318	11.8549	43.8785	37.7479	34.8331	157.0790	136.2402	126.1726	374.9874	325.9334	299.5633

S2. CRITICAL VALUES FOR THE MAIN MONITORING STATISTICS

Table S2.5: Critical values for the HAC-based weighted-CvM statistic with early-emphasis weight  $w_E$  (finite horizons)

$q$	$T = 1$			$T = 2$			$T = 5$			$T = 10$		
	1%	5%	10%	1%	5%	10%	1%	5%	10%	1%	5%	10%
1	1.2192	0.7405	0.5410	4.0197	2.3402	1.7194	16.0750	9.2146	6.7435	39.9036	23.9994	17.2797
2	1.7958	1.1518	0.9308	5.4769	3.6879	2.8936	22.6395	14.8448	11.5819	56.6837	37.1308	29.0188
3	2.2237	1.5633	1.2580	6.7293	4.8505	3.9908	27.8582	19.5533	15.8190	69.5989	49.1834	39.3924
4	2.6537	1.8924	1.5872	8.1442	5.9129	4.9626	33.6579	23.8895	19.8494	81.5291	59.3168	49.4100
5	3.0202	2.2550	1.8841	9.2618	6.9682	5.9130	37.2955	27.6040	23.5836	93.1497	69.4183	58.3645
6	3.3610	2.5651	2.2128	10.4027	7.8600	6.8178	41.3070	31.6841	27.0776	103.0350	79.2385	67.4727
7	3.6568	2.8958	2.5141	11.6598	8.9325	7.7601	45.8131	35.8619	30.7065	113.0859	88.2686	76.7809
8	3.9832	3.1952	2.8076	12.5777	9.9332	8.6770	49.7569	39.4948	34.4583	125.8942	98.6178	85.8613
9	4.3210	3.4886	3.0895	13.4964	10.9189	9.6095	53.0609	43.0742	38.0737	135.6309	108.5553	93.9761
10	4.6535	3.8027	3.3605	14.4266	11.8347	10.5334	57.3236	46.3842	41.3704	145.4421	117.7390	103.5830
11	4.9339	4.0660	3.6413	15.5163	12.7742	11.4407	61.3893	49.8907	44.5641	153.4921	126.4006	112.5897
12	5.2645	4.4005	3.9232	16.5314	13.7019	12.2959	64.5013	53.5484	47.7957	166.5339	134.9630	120.0335
13	5.6452	4.6797	4.2106	17.5861	14.5556	13.1006	68.4037	57.4165	51.5329	173.7953	144.1236	128.5705
14	5.8831	4.9334	4.4946	18.5876	15.4685	13.9166	72.4259	60.7444	54.6246	183.4478	152.7768	136.6744
15	6.1686	5.2176	4.7595	19.5999	16.3691	14.7528	77.5841	64.2340	58.0179	192.1948	161.0245	144.4378
16	6.5015	5.5001	5.0306	20.6027	17.3210	15.6166	80.9692	67.4863	61.2018	202.5761	169.3108	152.4782
17	6.7955	5.7915	5.2807	21.6359	18.1498	16.4968	85.0483	70.8941	64.5001	213.6273	177.2790	160.4313
18	7.0948	6.0688	5.5516	22.5602	19.0115	17.3287	88.8029	73.7283	67.6662	222.7658	185.3057	168.5977
19	7.3711	6.3592	5.8140	23.4963	19.9203	18.0638	92.3589	77.0404	70.8124	233.6218	194.1095	176.5424
20	7.6944	6.6261	6.0799	24.3767	20.7245	18.8752	94.7282	80.5855	74.0362	240.9454	202.5345	184.7182
21	8.0134	6.9246	6.3363	25.5422	21.6067	19.7162	98.7709	83.9996	77.0336	249.1763	210.9672	193.0828
22	8.3223	7.1710	6.6012	26.3514	22.5130	20.5396	102.1337	87.2661	80.0578	256.4225	219.5883	200.1342
23	8.6210	7.4787	6.8718	27.3468	23.3070	21.3468	105.2286	90.5216	83.1701	265.0596	226.8272	207.8732
24	8.9102	7.7359	7.1278	28.0999	24.1573	22.1015	109.0344	93.9779	86.3029	272.8470	235.1320	216.0387
25	9.2058	8.0064	7.4066	29.2403	25.0882	22.9486	112.6024	96.9678	89.3041	281.5303	243.3813	224.2300
26	9.5046	8.2583	7.6674	30.0794	25.9191	23.8301	116.8122	100.8456	92.2796	291.5452	252.1437	231.8273
27	9.8223	8.4931	7.9391	31.1674	26.7175	24.5567	119.8435	103.6554	95.4375	301.1944	260.3065	240.0835
28	10.0261	8.7656	8.1898	31.9054	27.5558	25.3398	123.1191	107.0375	98.7326	308.8145	268.8306	247.8969
29	10.3080	9.0555	8.4484	32.8313	28.3513	26.1214	126.0853	110.4834	102.0022	317.9655	277.3184	255.3976
30	10.5844	9.3240	8.7011	33.7913	29.1044	26.9488	130.7101	112.8583	105.1345	327.3901	285.2664	262.9072

Table S2.6: Critical values for the HAC-based weighted-CvM statistic with mid-emphasis weight  $w_M$  (finite horizons)

$q$	$T = 1$			$T = 2$			$T = 5$			$T = 10$		
	1%	5%	10%	1%	5%	10%	1%	5%	10%	1%	5%	10%
1	1.8063	1.1015	0.7814	5.7036	3.3482	2.3796	21.0436	12.0204	8.8287	49.5154	29.3929	21.1769
2	2.6191	1.6711	1.3377	7.6800	5.1522	4.0257	29.8619	19.4638	14.9808	69.0281	45.9483	35.6150
3	3.2424	2.2452	1.8135	9.5218	6.7261	5.4952	36.7157	25.4906	20.3920	85.8761	59.9074	48.6993
4	3.9111	2.7320	2.2700	11.4903	8.2254	6.8325	44.0579	31.0645	25.5497	100.0279	71.9600	60.1244
5	4.4001	3.2659	2.7122	12.9903	9.5528	8.0458	49.0016	35.9859	30.2586	112.5031	85.3085	70.8554
6	4.8262	3.7008	3.1616	14.5413	10.9407	9.3190	53.4979	40.7657	34.6755	126.1940	96.6664	81.7020
7	5.2863	4.1751	3.5970	16.2208	12.3400	10.6502	58.6463	46.2703	39.1120	138.7533	107.4887	93.0602
8	5.8430	4.6151	4.0151	17.3372	13.7390	11.9252	64.0755	51.0758	43.9319	152.8198	120.3206	103.9907
9	6.2613	5.0261	4.4088	18.7378	15.0253	13.1939	67.6374	55.5029	48.8210	164.9284	131.8574	114.1388
10	6.6769	5.4518	4.8193	19.9923	16.2241	14.4518	74.4318	59.6481	52.8738	178.1170	143.8361	125.4705
11	7.1731	5.8266	5.2269	21.6780	17.5237	15.6832	79.1260	63.9435	56.9772	187.6522	153.9911	136.4495
12	7.7200	6.2888	5.5922	22.9639	18.7649	16.7830	82.8137	68.3803	61.3719	201.6373	164.2858	145.3038
13	8.0549	6.6973	6.0172	24.1717	19.8932	17.8910	88.4413	73.3469	65.7643	212.9384	174.7560	155.4711
14	8.4280	7.1048	6.3986	25.7374	21.1492	19.0309	93.6921	78.0443	69.8407	223.0472	184.9494	165.1783
15	8.8645	7.4989	6.7871	26.9150	22.3903	20.1359	99.2482	82.1727	74.2100	233.6511	194.8016	174.4850
16	9.3129	7.9098	7.1749	28.4099	23.6716	21.3024	104.6163	86.7640	78.1119	245.5874	205.5529	184.3553
17	9.7050	8.3007	7.5395	29.7061	24.8446	22.4465	109.1978	90.4179	81.8016	259.0577	214.5703	193.3649
18	10.1310	8.7124	7.9093	30.9015	25.9298	23.5626	113.1200	94.5706	85.8887	270.4070	224.2537	203.7240
19	10.5361	9.0909	8.2763	32.3384	27.1607	24.6451	117.6387	98.7274	90.0375	282.8830	234.6394	212.5454
20	11.0727	9.4534	8.6804	33.5299	28.3785	25.6747	121.9458	103.0815	94.1476	289.6066	245.1158	222.0526
21	11.4511	9.8719	9.0470	34.9857	29.4526	26.8051	127.8854	107.3761	98.2220	300.7001	253.9637	232.6945
22	11.8565	10.2415	9.3579	36.4987	30.6653	27.9574	131.8544	111.2485	101.9097	312.3907	264.4604	241.5430
23	12.3137	10.6204	9.7531	38.2248	31.7200	29.0799	135.8975	115.2210	105.8520	319.1070	274.3772	250.8082
24	12.7879	10.9713	10.1439	38.8099	32.8894	30.0957	140.2653	120.1743	109.9110	331.3096	283.6432	260.4574
25	13.1962	11.3615	10.4960	40.0981	34.0903	31.1949	145.3924	124.1763	113.7062	343.2697	293.7369	269.7030
26	13.5943	11.7685	10.8647	41.4282	35.1995	32.3760	150.0272	128.5351	117.5080	354.8113	303.9042	279.4784
27	13.9783	12.1110	11.2391	43.1384	36.1717	33.4175	152.8286	132.4589	121.4180	364.3697	315.0985	288.9121
28	14.3219	12.5079	11.6398	44.2592	37.3613	34.4351	156.1148	137.0999	125.5618	372.7630	325.0530	298.6524
29	14.6933	12.8533	11.9591	45.1009	38.5915	35.6128	161.4069	141.1116	129.5487	385.8067	335.0554	306.8060
30	15.2231	13.2557	12.3350	46.3099	39.7374	36.5957	166.7279	144.5102	133.4827	396.9077	344.2572	316.0773

Table S2.7: Critical values for the HAC-based weighted-CvM statistic with late-emphasis weight  $w_L$  (finite horizons)

$q$	$T = 1$			$T = 2$			$T = 5$			$T = 10$		
	1%	5%	10%	1%	5%	10%	1%	5%	10%	1%	5%	10%
1	2.2934	1.3570	0.9620	6.6669	3.9841	2.8549	23.4731	13.5437	9.7924	53.9103	31.8687	22.4503
2	3.2264	2.0891	1.6421	9.3114	6.2153	4.7271	33.3258	21.7730	16.6329	73.7900	48.8597	37.7733
3	4.0141	2.8061	2.2483	11.5234	7.9438	6.5354	40.9963	28.2156	22.6934	92.2121	64.4741	52.5535
4	4.7700	3.3893	2.8164	13.8292	9.7516	8.0678	49.1695	34.8703	28.4213	106.7332	77.7500	64.5238
5	5.4378	4.0255	3.3773	15.5664	11.3308	9.5434	54.8483	40.1843	33.6154	121.6277	90.7412	75.6551
6	6.0131	4.5835	3.9061	17.2717	12.9805	11.0123	59.5766	45.3087	38.5462	137.1826	104.0906	87.6250
7	6.5304	5.1702	4.4226	19.1654	14.6440	12.5135	65.9061	51.4295	43.6282	150.3090	115.1968	99.7253
8	7.2403	5.7305	4.9597	20.8088	16.2320	13.9950	70.3894	56.7136	48.6672	165.3039	128.8752	111.3411
9	7.8021	6.2210	5.4342	22.5974	17.6946	15.5594	75.7899	61.8234	53.9314	176.3462	141.5027	122.3210
10	8.2959	6.7411	5.9508	23.9214	19.1853	17.0428	82.1082	66.4739	58.4679	190.9429	152.8564	134.0551
11	8.8869	7.2525	6.4181	25.8712	20.6296	18.4850	87.7889	71.1564	63.2394	200.4666	164.3224	145.4962
12	9.4591	7.7805	6.9311	27.4985	22.1327	19.7631	91.7888	76.2652	68.1939	215.6312	175.9513	155.9150
13	9.9893	8.2654	7.4316	29.0853	23.4220	21.0484	98.2506	81.3756	72.8412	228.1591	187.1553	166.4027
14	10.4556	8.7228	7.9013	30.4182	24.9350	22.3220	104.7380	86.0647	77.5721	241.1447	197.6257	176.3844
15	11.0414	9.1933	8.3644	31.7906	26.2654	23.6384	111.1179	90.9028	81.8620	250.2702	208.6413	186.2727
16	11.6442	9.7541	8.7962	33.3621	27.7844	25.0334	115.8938	96.0139	86.3550	263.8148	219.4579	196.7698
17	12.0794	10.2392	9.7622	35.0694	29.2605	26.3233	119.7222	100.7191	90.5288	278.1513	229.6343	206.9043
18	12.6764	10.7372	9.7622	36.9603	30.4594	27.7438	125.7666	105.4225	95.1611	288.8160	239.9142	217.2726
19	13.0844	11.1780	10.1884	38.5463	31.9242	28.9319	130.3971	110.1563	99.4233	302.4748	251.4603	227.5711
20	13.6525	11.6460	10.6544	39.9418	33.2673	30.2514	136.5086	115.2936	104.0086	308.8759	262.4163	237.5777
21	14.0257	12.1165	11.0772	41.5201	34.7735	31.5348	142.1714	119.7810	108.6357	321.6399	272.9193	248.0689
22	14.5954	12.6374	11.5313	43.1213	36.0914	32.8719	146.6871	124.0936	112.5918	332.8375	282.3154	258.1854
23	15.1355	13.1136	11.9722	44.5099	37.2496	34.1316	152.0822	128.3937	117.0067	343.1852	293.3896	268.2598
24	15.7986	13.5516	12.4058	46.2113	38.5757	35.3978	156.0863	133.0797	121.6031	354.1950	303.6887	277.8898
25	16.2481	13.9874	12.8076	47.7519	40.1780	36.7641	162.1958	137.9750	126.1155	369.6201	313.9714	288.1802
26	16.7507	14.4591	13.3119	49.2557	41.4303	37.9465	167.5649	142.9235	130.4430	378.2936	325.2935	298.8492
27	17.3055	14.9546	13.7951	50.6886	42.7639	39.2278	172.3485	147.1986	134.8695	389.8020	336.3106	308.7037
28	17.7292	15.3891	14.2464	51.9893	44.0678	40.3871	177.0198	152.4403	138.8028	399.8909	346.0520	319.1126
29	18.1707	15.8623	14.6902	53.4092	45.4348	41.7789	182.0505	156.4115	143.4405	415.0933	357.1894	328.3010
30	18.6879	16.3135	15.1299	54.4428	46.6384	43.1031	186.5293	160.4513	147.7215	424.8049	368.4499	337.4196

Table S2.8: Critical values for Shao's weighted-CvM monitoring statistic with continuous weight  $w_U$  (finite horizons)

$q$	$T = 1$			$T = 2$			$T = 5$			$T = 10$		
	1%	5%	10%	1%	5%	10%	1%	5%	10%	1%	5%	10%
1	25.1787	12.5029	7.9185	88.3514	39.1943	24.9710	290.2010	133.2044	87.9144	722.4899	334.9389	208.3654
2	51.6565	27.7471	19.4559	158.1567	85.4599	59.2487	582.2854	303.8736	214.9945	1437.7488	735.9279	509.1786
3	83.0245	47.9904	35.2954	249.5730	145.4453	108.1767	913.5161	531.6512	385.1494	2131.6794	1275.9526	923.4322
4	119.3649	71.8261	55.2264	346.0680	209.9903	163.8360	1314.2138	794.8150	607.0206	2988.7799	1860.7905	1418.5974
5	157.7500	99.5366	77.7858	454.5008	291.6908	225.9867	1706.5185	1082.4026	836.9489	4009.2306	2573.8962	2000.7612
6	204.3046	133.2533	104.3398	598.5928	388.4008	303.8792	2133.3333	1403.4899	1115.7604	5048.2195	3403.4731	2659.5303
7	246.5066	167.0723	134.6135	741.7790	478.2706	391.1156	2598.8544	1765.2266	1406.0634	6185.2204	4224.2513	3462.6412
8	296.3544	206.1778	167.3510	881.3248	586.9918	481.6610	3185.5627	2231.0768	1778.2125	7493.3719	5202.5585	4252.7760
9	351.8885	245.5151	204.7129	1038.4555	718.1264	585.8998	3674.5341	2659.9456	2184.4025	8818.5949	6221.3013	5094.5698
10	398.4795	290.3037	241.8703	1211.4355	849.2733	700.7324	4338.5499	3129.8811	2587.3937	10613.1343	7416.4530	6123.3072
11	463.6889	337.0401	284.1419	1373.1119	999.2581	824.1313	4945.1707	3587.9928	3001.9367	12296.8159	8674.4888	7190.5437
12	544.0471	391.0655	327.4868	1572.7822	1149.4101	966.2315	5694.2297	4121.4235	3482.7542	14104.1110	10019.1729	8348.6236
13	599.4159	443.8659	372.5661	1744.6130	1296.8513	1105.3207	6432.3877	4717.0791	3966.1836	15613.7527	11366.3056	9573.0029
14	665.5590	499.5399	424.4802	1944.3885	1481.9312	1254.6811	7283.2287	5306.9697	4508.0875	17399.4930	12675.5553	10790.3249
15	743.4741	559.1577	480.7939	2171.7976	1655.6291	1419.8855	7994.4816	5968.3423	5086.5440	19133.1294	14140.4481	12200.4726
16	820.2692	620.6611	537.9972	2432.2385	1845.7820	1581.7896	8697.5018	6608.7148	5655.5051	20860.5859	15849.3181	13538.8454
17	904.8805	687.7182	593.7108	2668.9092	2056.2269	1759.1164	9584.8990	7380.7775	6316.6378	23519.1857	17635.1432	15125.0489
18	961.6967	752.6380	653.8087	2911.4815	2260.2597	1945.4456	10331.2392	8093.2343	6961.1189	25137.0655	19524.2180	16768.6582
19	1049.9920	825.7800	717.8776	3145.9654	2465.2062	2141.8016	11236.2009	8839.2463	7660.2145	27864.3144	21305.1236	18533.9630
20	1160.4210	907.4284	783.5138	3443.1841	2685.3756	2328.2079	12307.4487	9623.4239	8426.4351	29683.6438	23094.9165	20240.1722
21	1238.8708	980.3827	855.8546	3676.7510	2912.8127	2548.1259	13219.0436	10402.7110	9193.2586	31889.9009	25176.0282	21980.3479
22	1333.7062	1056.0809	926.5483	3995.5330	3171.6896	2771.2697	14352.6606	11309.6593	9996.2238	34104.2089	27153.9281	23915.6217
23	1430.1192	1149.4608	1007.4998	4321.5616	3417.0115	3003.4004	15227.1866	12189.8976	10816.4793	37039.1662	29289.9166	25785.0533
24	1544.2892	1223.9648	1089.2142	4669.9825	3671.4260	3250.4558	16198.0195	13126.2519	11641.3134	39402.1642	31613.4644	27744.2763
25	1676.7584	1319.3314	1177.8558	4952.1386	3952.4218	3499.9130	17625.5148	14062.3783	12536.6648	42333.4800	33980.9601	29812.4167
26	1777.4455	1412.2047	1261.3379	5193.7854	4259.7441	3752.1679	18632.8991	15170.8467	13416.5094	44969.8663	36065.9322	31980.6496
27	1877.4992	1503.8363	1343.8394	5552.8185	4521.2474	4003.4747	19802.7581	16222.2168	14572.3969	47597.9259	38565.9775	34032.2942
28	1993.7326	1605.3137	1436.2223	5933.0283	4825.0386	4276.6628	20920.7451	17330.1635	15437.7361	50526.3040	41051.2235	36480.4644
29	2093.2370	1711.6554	1536.1259	6224.0978	5130.4449	4556.8498	22091.5361	18306.9721	16378.8356	54237.5871	43648.4801	38949.4330
30	2229.7183	1820.4135	1632.1307	6547.9335	5405.6322	4841.2404	23301.7891	19396.0795	17396.6775	57205.2243	46574.2825	41219.3910

## S2. CRITICAL VALUES FOR THE MAIN MONITORING STATISTICS

Table S2.9: Critical values for Shao's weighted-CvM monitoring statistic with early-emphasis weight  $w_E$  (finite horizons)

$q$	$T = 1$			$T = 2$			$T = 5$			$T = 10$		
	1%	5%	10%	1%	5%	10%	1%	5%	10%	1%	5%	10%
1	18.9131	8.9443	5.7859	65.2316	30.1833	19.0369	237.5465	109.8950	72.1173	640.3386	289.9202	180.9359
2	37.0987	20.2177	14.2148	118.0147	64.8041	45.4503	481.1592	251.3356	177.2258	1217.9112	642.9064	442.7249
3	59.2203	34.7583	25.7371	182.1012	110.9831	81.9072	762.4484	436.7132	319.5783	1850.2559	1105.2586	803.2231
4	86.1335	52.1512	39.8361	257.0540	161.3944	125.3847	1054.3716	653.7932	503.3134	2562.1232	1619.0398	1237.0987
5	113.5807	72.0515	56.0866	344.4084	224.3509	173.5554	1383.0460	885.9828	687.9552	3428.0985	2254.7395	1748.0725
6	146.6892	95.8111	75.4696	439.7839	295.8736	234.1969	1712.7307	1158.8206	921.9033	4342.5394	2951.3499	2322.5160
7	175.9844	121.0322	97.4323	547.3524	368.3386	300.8411	2150.2515	1451.9543	1170.5323	5332.1972	3683.9931	3018.6108
8	210.6467	148.6479	121.8692	662.2947	454.4704	372.2980	2628.3677	1831.2054	1482.0507	6563.2323	4546.9110	3718.2667
9	253.3188	176.8895	148.5896	770.9687	544.6192	453.6766	3088.5188	2175.8779	1797.2182	7692.9950	5415.2196	4491.3228
10	300.1362	208.3337	175.9188	901.7763	648.2598	540.9221	3576.9857	2578.2137	2136.8863	9101.0593	6475.9422	5348.6879
11	334.2693	243.3004	204.9850	1042.2521	755.6428	639.8606	4055.4193	2971.0279	2500.2087	10708.7431	7568.5614	6286.3708
12	384.7264	284.0115	237.1678	1183.0632	868.5733	738.8513	4622.9427	3423.5479	2895.5395	11904.8072	8753.9192	7289.5281
13	429.7548	320.5724	269.5754	1332.1794	988.5281	848.8979	5245.9878	3883.2001	3311.6588	13424.7110	9927.7928	8359.5058
14	479.2769	361.4804	308.1624	1482.7007	1130.8738	965.6713	5924.8815	4390.6733	3744.7017	14976.8651	11092.4272	9483.8122
15	545.0421	404.0674	348.1219	1649.9627	1263.9508	1086.6405	6555.1542	4892.1041	4222.8211	16635.9210	12443.3353	10700.3798
16	598.8620	450.0360	390.0749	1831.0493	1420.7381	1218.1012	7142.0046	5464.6131	4695.8288	18296.2474	13863.1426	11884.2625
17	649.2598	498.4333	432.3674	2039.4327	1569.4445	1357.2669	7947.5048	6035.9383	5245.7838	20212.3058	15364.7006	13294.9175
18	695.0904	549.6933	477.8139	2215.3934	1734.9239	1497.9636	8586.0665	6651.3285	5799.1052	21871.7951	17030.9304	14704.5006
19	755.2052	596.6466	525.2958	2436.0076	1882.5079	1649.5120	9253.1450	7260.4403	6345.0420	24012.7597	18623.3181	16177.7755
20	826.8163	655.1061	574.8353	2642.4908	2042.6437	1797.7600	10066.8697	7959.7115	6973.4504	25814.2077	20237.2654	17695.0937
21	893.4681	707.8706	623.2843	2841.8224	2232.1834	1963.0238	10777.2126	8660.6636	7609.4226	27777.5939	22051.0516	19219.6899
22	963.3048	763.8052	674.5128	3072.7015	2416.9376	2143.2900	11949.7703	9354.8838	8279.9069	29526.5387	23868.3072	20915.1239
23	1033.9496	833.0295	736.3221	3358.3372	2614.1345	2312.9514	12665.4673	10077.7115	9008.2781	31276.1491	25634.5379	22588.8291
24	1101.6848	900.6409	791.7251	3557.0064	2824.8364	2501.2765	13548.4419	10884.3782	9687.4894	34265.4063	27496.0009	24360.3121
25	1198.5416	963.8532	856.0493	3818.4137	3030.2595	2687.7963	14342.2113	11678.3254	10418.3450	36804.2045	29490.5294	26232.8195
26	1276.0735	1034.0678	918.1680	4026.5147	3261.1661	2887.2296	15398.8308	12523.9525	11162.4836	39371.2797	31481.8516	28104.0774
27	1352.0313	1095.6115	985.1701	4289.5395	3479.9918	3094.6809	16189.7799	13405.1159	11918.0935	41578.8369	33784.7980	30027.4986
28	1443.2080	1167.6979	1056.2711	4620.3654	3720.2779	3304.7605	17195.1828	14266.0866	12779.3761	44094.0558	35930.1954	32068.9765
29	1522.8396	1249.7234	1121.4631	4835.9155	3968.6117	3505.2489	18380.3852	15138.9415	13614.4758	46578.3398	38292.4245	33999.0965
30	1609.9258	1327.5016	1192.3173	5096.2372	4181.0337	3727.7887	19121.1174	16099.5349	14509.1757	49965.7189	40570.2467	36049.0768

Table S2.10: Critical values for Shao's weighted-CvM monitoring statistic with mid-emphasis weight  $w_M$  (finite horizons)

$q$	$T = 1$			$T = 2$			$T = 5$			$T = 10$		
	1%	5%	10%	1%	5%	10%	1%	5%	10%	1%	5%	10%
1	27.0106	13.1323	8.2730	93.7480	41.9797	26.1080	304.1985	141.0836	93.4979	778.4444	351.4437	220.9312
2	54.7679	29.2247	20.4025	166.0945	89.4392	62.5631	626.5279	327.0643	228.7589	1518.7224	780.6651	545.8102
3	87.0119	50.1813	36.9780	259.6576	155.6551	113.6488	990.2896	565.1303	411.3483	2258.5777	1352.6477	980.7336
4	127.8533	74.5724	57.4301	365.0855	222.1233	172.2424	1394.6352	849.3789	645.3214	3215.6925	1986.0754	1499.0434
5	168.1530	104.2323	80.5942	484.7519	312.2772	238.2533	1816.9926	1148.2554	893.1420	4299.2876	2742.0228	2114.9388
6	208.5351	138.9034	109.2224	632.5749	410.5787	320.9629	2259.2549	1497.8991	1185.5873	5349.2286	3598.5800	2816.4765
7	257.3287	174.8934	140.6534	782.1573	507.4389	414.9461	2774.6442	1872.2223	1496.8358	6614.8093	4484.3147	3670.0999
8	309.9056	214.5020	175.1742	927.5401	622.1522	509.7179	3403.5980	2367.4666	1886.9035	8038.3026	5527.4061	4506.7057
9	366.2978	258.0047	212.6047	1101.9336	754.8763	619.3678	3956.0650	2829.2543	2312.0796	9374.8226	6645.8148	5397.3860
10	422.7189	301.6661	252.4527	1289.9707	896.5953	742.2571	4657.8390	3323.8328	2753.7539	11143.7987	7867.2113	6481.7362
11	489.1423	352.3938	295.7547	1455.7612	1054.2368	872.2152	5243.2825	3817.0318	3189.4154	13113.3807	9247.5016	7605.6758
12	566.7586	408.6013	340.4264	1646.9336	1208.4964	1015.6840	6003.8533	4390.0899	3687.1176	14869.8903	10604.5052	8807.8716
13	629.5683	462.9687	385.8035	1856.6348	1370.6478	1163.2973	6838.6898	5020.2900	4230.1823	16593.5649	12019.4997	10147.5518
14	695.6048	521.2612	443.7600	2054.2804	1557.3079	1321.1475	7783.8444	5630.0438	4786.2734	18514.0631	13434.1406	11425.8046
15	776.8749	582.8361	500.3907	2286.2918	1748.1401	1495.9646	8544.5514	6332.8239	5391.1470	20319.9098	15074.3212	12877.3900
16	859.9452	646.8361	559.6154	2552.9635	1949.3593	1667.9466	9280.4095	7022.7683	6020.5657	22185.3192	16745.5228	14332.0960
17	945.2074	715.8138	619.9132	2851.6260	2162.1991	1854.6010	10294.4442	7857.9888	6681.8020	25102.4354	18695.4589	15993.5172
18	1008.9397	786.5252	681.5639	3083.9342	2372.0443	2045.9214	11026.0707	8594.8987	7358.4109	26657.9162	20745.9798	17767.8069
19	1097.4223	861.6694	746.2183	3360.3471	2593.4459	2260.7045	11871.2710	9399.7608	8111.3999	29598.6708	22675.2054	19624.2596
20	1200.6410	948.2061	814.5170	3648.4569	2841.6496	2454.0643	12905.8793	10241.1660	8930.9842	31671.7700	24476.3953	21446.7104
21	1294.1990	1015.5383	886.9218	3907.1547	3084.1469	2683.1554	14051.6162	11071.4971	9754.6042	33996.3018	26576.1563	23311.7492
22	1399.2856	1102.0957	964.7701	4206.8825	3335.4917	2910.8454	15277.9720	11989.1662	10596.8328	36153.6275	28754.6092	25278.1443
23	1490.7043	1194.7937	1049.3870	4611.7440	3600.3339	3159.2890	16271.7073	12949.6301	11469.1125	39362.1330	31026.6213	27315.5346
24	1605.2423	1282.9514	1132.7514	4951.7164	3872.0906	3416.2084	17336.9091	13939.1276	12336.0260	41832.9266	33511.1923	29332.8475
25	1749.6529	1372.6800	1221.5188	5274.0120	4170.4085	3688.5921	18611.1974	14994.3785	13294.4357	44860.7320	35955.8989	31508.7775
26	1854.1275	1478.7054	1307.2515	5652.8606	4502.6506	3950.5772	19760.4332	16165.5768	14158.2007	47521.0209	38242.1204	33778.5042
27	1961.8357	1565.2354	1399.0061	5876.7031	4758.5623	4126.6173	20918.2622	17213.0190	15228.7341	50421.4240	40800.4748	36129.7441
28	2084.8592	1670.7940	1499.5120	6354.5986	5102.5621	4527.1216	22170.0757	18368.4168	16333.8956	53613.2041	43479.1864	38583.1250
29	2194.5910	1786.0967	1599.9661	6631.3243	5424.4941	4797.7534	23517.0635	19471.9445	17391.8962	57520.6839	46158.7578	41154.3210
30	2320.0622	1907.8847	1698.2377	6989.9868	5709.0730	5093.2808	24712.1650	20528.4627	18458.2515	60631.8741	49199.2510	43594.5527

Table S2.11: Critical values for Shao's weighted-CvM monitoring statistic with late-emphasis weight  $w_L$  (finite horizons)

$q$	$T = 1$			$T = 2$			$T = 5$			$T = 10$		
	1%	5%	10%	1%	5%	10%	1%	5%	10%	1%	5%	10%
1	33.7636	16.2105	10.2239	112.0662	48.9726	31.1526	338.4742	158.7171	104.0058	817.1289	378.5401	238.5833
2	68.4557	36.0373	24.9193	201.0839	107.5438	74.1073	709.4964	362.3468	261.1663	1617.4787	835.6276	587.7489
3	107.8351	61.6007	45.3687	315.6997	183.3633	139.8367	1102.4806	635.0525	459.9874	2476.2351	1460.9649	1055.4127
4	154.9494	92.9272	71.5535	436.1953	263.4707	204.6669	1552.4721	950.5141	720.0137	3409.4261	2124.0279	1595.6745
5	205.3631	129.8696	100.3541	581.6431	363.8766	281.6984	2023.5885	1279.6091	998.6418	4643.0534	2923.1193	2252.5003
6	269.8338	172.0949	134.9208	757.8165	489.9222	379.2847	2577.5867	1668.2181	1319.2269	5855.7727	3851.5773	3019.1163
7	322.0518	217.1403	173.9445	935.9640	600.1630	487.3578	3119.4672	2099.5540	1659.0193	7079.2723	4840.4352	3885.5955
8	387.0094	267.5227	216.0045	1131.0773	729.8286	601.7455	3765.1013	2656.0079	2088.7906	8465.0849	5953.4716	4817.6240
9	455.8819	317.2195	263.0288	1329.1746	896.1441	729.1089	4371.9000	3154.6666	2589.6897	10109.8045	7119.7305	5783.2673
10	530.0376	376.8869	311.0424	1527.7640	1067.4549	868.8111	5157.5523	3688.3864	3067.1385	12143.2621	8465.2705	6937.6965
11	610.0399	438.8705	366.2392	1745.5562	1257.2235	1024.4787	5906.3040	4208.2158	3559.8889	14045.6068	9860.2544	8171.2071
12	706.9328	507.6909	424.0341	1990.3716	1443.5508	1205.3370	6771.0688	4888.2148	4095.6115	15987.7224	11423.0238	9488.6838
13	782.7144	574.5701	480.3178	2208.3188	1642.6510	1371.3631	7661.3915	5632.5522	4657.5921	17879.0212	12888.8636	10233.5453
14	870.6448	648.5751	546.9034	2467.8951	1852.4065	1556.8116	8664.8876	6250.7024	5308.4726	19933.8086	14363.9955	12333.1370
15	958.9822	722.4739	618.6082	2745.3826	2064.0892	1763.2763	9597.9330	7044.6872	5984.0910	21823.5892	16138.9575	13767.0037
16	1069.8752	804.5131	692.2843	3042.6770	2301.6803	1961.7289	10433.2849	7839.7488	6650.4828	23835.5467	17947.2945	15371.8751
17	1172.4140	886.1426	765.3864	3371.2110	2562.3275	2177.7815	11294.3193	8746.5504	7456.4278	26582.8877	19995.0026	17054.5807
18	1267.9725	974.4269	842.0919	3614.3321	2814.8798	2414.3250	12131.6317	9602.8054	8233.7579	28731.6764	22218.7649	19041.3783
19	1377.5486	1066.3692	921.4740	3947.2977	3076.2774	2650.2449	13233.7490	10464.8913	9052.4990	31787.7766	24248.1275	20897.2840
20	1517.6901	1165.0923	1007.4840	4271.1789	3361.0615	2884.1385	14611.6793	11391.0780	9930.9166	33910.6863	26153.1460	22890.2963
21	1607.2289	1261.0876	1100.9041	4593.9639	3643.1481	3164.6539	15666.0515	12337.7450	10854.5960	36273.3817	28365.8254	24861.9362
22	1735.0897	1360.7076	1191.7432	4948.4021	3939.1468	3435.7093	16956.7940	13370.0503	11735.7253	39067.0280	30739.6274	27011.3365
23	1867.0433	1474.2631	1296.6791	5399.1804	4256.0714	3724.1197	17978.8747	14451.0955	12704.5857	42186.2822	33186.8753	29245.3170
24	2017.6376	1576.8917	1401.1569	5739.7927	4577.8191	4047.2447	19429.5133	15484.5461	13716.0025	45051.2829	35781.3828	31307.7600
25	2177.1012	1691.9752	1509.1632	6155.9623	4936.3968	4332.8852	20862.3220	16619.6127	14704.7182	48198.9075	38447.5634	33650.3131
26	2307.8484	1815.0991	1607.9973	6507.8931	5273.2381	4651.0873	22120.3422	17871.3925	15767.4451	50900.1545	40911.6702	36088.1604
27	2436.1339	1927.9344	1726.7885	6936.8136	5619.7450	4954.0752	23590.0956	19148.2209	16967.1479	54283.0337	43709.0999	38711.2042
28	2576.5471	2055.2343	1841.7758	7362.3287	5998.6604	5285.8493	24875.3475	20386.5471	18125.6397	57784.0028	46722.1328	41310.0588
29	2712.3641	2196.0105	1967.8070	7791.7898	6350.3924	5641.3715	26409.3184	21578.8708	19271.4667	61852.1937	49573.3335	44054.5855
30	2898.6494	2331.0269	2093.3287	8172.8224	6714.3363	5996.4537	27808.9556	22867.1427	20494.8760	65126.8982	52808.0487	46790.2271

Table S2.12: Critical values for adjusted-range-based weighted-CvM monitoring statistic with constant weight  $w_U$  (finite horizons)

$q$	$T = 1$			$T = 2$			$T = 5$			$T = 10$		
	1%	5%	10%	1%	5%	10%	1%	5%	10%	1%	5%	10%
1	1.4623	0.8018	0.5562	4.8670	2.5306	1.7226	17.5642	8.9962	6.1456	44.1475	22.6566	15.2064
2	2.1375	1.3096	0.9753	6.5042	3.8894	2.9348	26.4564	14.9591	10.8025	62.0631	35.6922	26.8907
3	2.6239	1.7259	1.3555	7.8961	5.1636	4.0824	31.6206	19.8576	15.2806	75.5687	47.9293	37.3223
4	3.0845	2.1051	1.7087	9.3629	6.3387	5.1063	38.3305	24.1519	19.4312	87.9698	58.1192	46.2969
5	3.5264	2.4966	2.0179	10.8588	7.4003	6.0721	42.0484	27.9924	22.9018	97.3453	67.7572	55.3203
6	4.0285	2.8583	2.3697	12.1519	8.5124	6.9943	45.3714	31.6871	26.2691	107.6149	77.3910	63.3462
7	4.2933	3.1872	2.6969	13.0431	9.4736	7.9600	49.0256	35.8175	29.7952	117.5842	86.3264	71.4699
8	4.6457	3.5135	3.0047	14.1364	10.5786	8.9165	53.4420	39.4278	33.4320	128.8038	95.9252	80.6100
9	5.0701	3.8738	3.3249	15.2756	11.5881	9.9214	56.7363	43.1497	36.7465	138.9117	104.3635	88.8379
10	5.4483	4.1636	3.6064	16.2288	12.4572	10.8066	60.1731	46.7809	40.0270	149.8798	112.7705	96.5598
11	5.7285	4.4713	3.8973	17.3831	13.4484	11.6883	64.0751	49.9609	43.0865	159.0541	120.7604	104.2054
12	6.1032	4.8013	4.1825	18.4678	14.3609	12.5889	67.6353	53.0402	46.6201	169.1021	127.6170	111.8956
13	6.4238	5.0979	4.4943	19.8570	15.1482	13.4115	71.1791	56.3071	49.6357	177.9390	135.7321	119.1431
14	6.8129	5.3933	4.7595	20.9091	16.1427	14.2905	76.4283	59.5414	52.7557	187.0524	143.5523	126.6028
15	7.0510	5.6909	5.0586	22.0186	17.0398	15.1689	80.9109	63.0470	55.3293	195.6156	152.9565	135.1550
16	7.4344	5.9880	5.3472	22.8534	17.9233	15.9656	84.5760	66.5262	58.5011	204.2303	161.8311	141.3506
17	7.7264	6.2727	5.5988	23.6149	18.8937	16.8465	87.7188	69.4676	61.5224	211.7427	169.1825	149.1691
18	8.0504	6.5459	5.8844	24.4092	19.7320	17.5926	91.1799	72.6231	64.4897	225.6425	176.9788	156.8254
19	8.3646	6.8118	6.1494	25.4224	20.5318	18.4526	95.2340	75.6867	67.7915	233.1688	185.0158	163.9759
20	8.7152	7.1207	6.4250	26.4008	21.4174	19.1917	97.6384	79.2082	70.9009	243.4086	192.6648	172.2160
21	9.0242	7.3905	6.7128	27.3344	22.2711	20.0274	101.8809	82.5867	73.8458	248.4137	200.6564	179.1289
22	9.2974	7.6823	6.9992	28.3747	23.1268	20.8073	105.4281	85.5123	76.7718	256.9164	206.7903	185.8962
23	9.6819	7.9552	7.2406	29.4424	23.9922	21.5949	109.0545	88.7964	79.6160	262.4073	215.0754	193.9792
24	10.0071	8.2391	7.4858	30.1968	24.8500	22.4593	112.5387	91.7047	82.6713	270.7259	222.9838	200.4105
25	10.2678	8.4987	7.7626	31.1700	25.8226	23.2576	115.5604	95.2152	85.5825	278.4777	230.3002	207.6011
26	10.5367	8.8210	8.0229	32.0201	26.6174	24.0821	119.1954	98.5045	88.4980	286.0579	238.3722	214.9580
27	10.9515	9.1189	8.2484	33.0816	27.5459	24.9168	121.4997	101.3325	91.4398	292.2653	245.2751	221.8505
28	11.2118	9.4079	8.5573	33.8786	28.3340	25.7054	124.1094	104.3253	94.3882	301.8209	253.8964	229.0477
29	11.5218	9.6907	8.8264	34.6944	29.1826	26.4498	127.4799	108.1058	97.5470	309.2330	260.1844	237.1744
30	11.8284	9.9889	9.1264	35.7894	29.9306	27.3593	130.1394	111.0984	100.2582	315.7228	267.1261	243.4430

S2. CRITICAL VALUES FOR THE MAIN MONITORING STATISTICS

Table S2.13: Critical values for adjusted-range-based weighted-CvM monitoring statistic with early-emphasis weight  $w_E$  (finite horizons)

$q$	$T = 1$			$T = 2$			$T = 5$			$T = 10$		
	1%	5%	10%	1%	5%	10%	1%	5%	10%	1%	5%	10%
1	1.0641	0.5856	0.4007	3.6476	1.9146	1.3366	14.1514	7.3999	5.0723	36.8705	19.5431	13.2380
2	1.5096	0.9383	0.7095	4.8775	2.9568	2.2369	21.5692	12.1275	8.9868	54.4912	31.6399	23.5060
3	1.8600	1.2475	0.9931	6.0165	3.9535	3.1332	26.4686	16.2049	12.5833	64.6249	41.7961	32.6321
4	2.2696	1.5412	1.2397	7.2847	4.9004	3.9134	31.0082	20.1391	15.9884	75.6926	50.3603	40.5038
5	2.5711	1.8033	1.4782	8.2157	5.6865	4.6799	35.0106	23.0929	19.0075	84.3379	59.0409	48.2473
6	2.9005	2.0769	1.7258	9.1541	6.5456	5.4204	37.8906	26.1258	21.9177	94.2018	67.5548	55.5487
7	3.1416	2.3053	1.9678	9.8361	7.2866	6.1451	40.9774	29.5865	24.8116	103.3628	75.0444	62.8009
8	3.3969	2.5476	2.1953	10.7780	8.1331	6.9093	44.6442	32.6809	27.6891	111.9719	83.5325	70.3893
9	3.6559	2.8280	2.4237	11.4832	8.9399	7.6340	47.2233	35.5671	30.4485	119.8454	91.4318	77.7256
10	3.9680	3.0682	2.6217	12.3668	9.6199	8.3304	50.6064	38.7156	33.1013	128.9554	98.7753	84.8174
11	4.1973	3.2544	2.8369	13.1952	10.3455	9.0129	53.1531	41.4918	35.8991	138.5189	105.5428	91.7400
12	4.4373	3.4803	3.0530	14.0326	11.0697	9.7167	56.8502	43.8663	38.7338	146.1773	111.8180	97.9234
13	4.6933	3.6982	3.2674	14.8470	11.7377	10.3619	60.2192	46.7598	41.1346	153.9698	119.3078	104.6964
14	4.8934	3.9218	3.4715	15.7730	12.4326	10.9996	63.5149	49.5581	43.7763	162.3114	126.2293	110.7653
15	5.0872	4.1385	3.6851	16.5856	13.1256	11.6585	67.1188	52.2048	46.1309	170.6170	133.7270	117.7387
16	5.3045	4.3679	3.8834	17.1327	13.9165	12.3078	69.7276	55.0319	48.6838	177.4258	141.5227	123.9572
17	5.5909	4.5646	4.0959	18.0227	14.6070	13.0373	71.8209	57.8212	51.2823	183.9752	147.6600	130.9545
18	5.7848	4.7972	4.2965	18.6716	15.1911	13.5897	75.4744	60.2457	53.7050	195.6413	154.6460	137.2371
19	6.0697	4.9845	4.4966	19.4327	15.8556	14.2306	78.4207	62.9179	56.3840	203.9696	162.1690	144.1949
20	6.3658	5.2052	4.6988	20.0390	16.5169	14.8865	81.3763	65.7286	59.0772	211.4944	168.2932	150.8603
21	6.5437	5.3903	4.8971	20.8569	17.2286	15.4725	83.8789	68.4630	61.4419	217.1810	175.8372	156.8992
22	6.7638	5.6119	5.1196	21.6264	17.8499	16.1229	86.8996	71.2014	63.8093	225.3769	181.9074	163.5078
23	7.0347	5.8135	5.3080	22.4103	18.5417	16.7203	89.4311	73.8873	66.3551	230.7919	188.3848	169.2164
24	7.2730	6.0075	5.4884	22.9500	19.1529	17.3527	92.4109	76.1262	68.7952	237.3825	194.9852	175.3619
25	7.4515	6.2137	5.6845	23.7753	19.9107	17.9927	95.7134	78.7791	71.3447	243.0296	201.2614	181.9573
26	7.6901	6.3989	5.8926	24.2935	20.4859	18.6144	98.4566	81.8954	73.6667	249.5096	208.1439	188.0586
27	7.9506	6.6257	6.0771	25.1222	21.2421	19.2400	100.7310	84.1821	76.1006	255.6058	215.1200	194.2344
28	8.1560	6.8446	6.2712	25.9268	21.7987	19.8578	102.7512	86.5579	78.8526	263.6204	222.5008	200.5525
29	8.3673	7.0645	6.4752	26.6138	22.5584	20.4783	105.7207	89.3881	81.3790	269.8499	227.5613	207.9493
30	8.5754	7.2885	6.6932	27.2322	23.1053	21.1372	108.1385	91.9366	83.5763	276.7686	234.4851	213.9208

Table S2.14: Critical values for adjusted-range-based weighted-CvM monitoring statistic with mid-emphasis weight  $w_M$  (finite horizons)

$q$	$T = 1$			$T = 2$			$T = 5$			$T = 10$		
	1%	5%	10%	1%	5%	10%	1%	5%	10%	1%	5%	10%
1	1.5730	0.8466	0.5785	5.1486	2.6867	1.8414	18.5620	9.6392	6.5282	46.7456	24.0873	16.2128
2	2.2363	1.3663	1.0193	6.9427	4.1401	3.0889	27.8083	15.9487	11.4564	66.1485	38.2347	28.6653
3	2.7233	1.8150	1.4109	8.4448	5.4726	4.3136	34.8606	21.1554	16.3172	80.6648	50.8669	39.4862
4	3.2878	2.2183	1.7957	10.1531	6.7129	5.3995	40.6062	25.8969	20.5661	93.8223	61.7812	49.1595
5	3.7371	2.5946	2.1110	11.4401	7.8330	6.3793	44.8526	29.8219	24.2093	102.2203	72.2265	58.5582
6	4.1817	2.9851	2.4745	12.8928	9.0104	7.3668	48.6863	33.7844	27.9883	113.9252	82.0921	67.0390
7	4.5475	3.3508	2.8089	13.8782	10.0464	8.3728	52.6776	38.0105	31.6320	125.9178	91.3581	75.6368
8	4.9173	3.6851	3.1384	15.0423	11.2298	9.3864	57.0158	41.8711	35.5103	137.5149	101.3689	85.1057
9	5.2722	4.0438	3.4498	16.0670	12.2495	10.4555	60.8304	45.8679	39.0299	147.0509	110.5794	94.0455
10	5.6656	4.3579	3.7580	17.1304	13.1933	11.3858	65.0481	49.5877	42.4003	159.4359	119.3137	101.9201
11	6.0420	4.6850	4.0457	18.4507	14.1464	12.2982	68.5163	53.2242	45.7333	168.5981	128.0295	110.1552
12	6.3920	5.0200	4.3547	19.2174	15.1127	13.2726	72.3648	56.3754	49.3875	178.9653	135.3508	118.4586
13	6.7031	5.3155	4.6694	20.7751	16.0038	14.1002	77.0092	59.6727	52.6938	188.3712	144.1074	125.8999
14	7.0958	5.6277	4.9738	21.9241	17.0514	15.0329	81.5040	63.2509	55.9335	198.2042	151.8669	133.9260
15	7.4104	5.9472	5.2657	22.9563	17.9462	15.9337	85.6216	67.0857	58.7171	207.6575	161.9153	142.3834
16	7.6876	6.2181	5.5637	24.0164	18.9450	16.8222	89.5932	70.5327	62.0289	215.0817	170.8613	149.6140
17	8.0269	6.5356	5.8277	24.8985	19.9569	17.7633	93.1845	73.5471	65.1766	224.1697	178.7701	158.1860
18	8.3151	6.8271	6.1395	25.7842	20.8371	18.5456	97.4314	76.9585	68.4104	238.0673	187.4529	165.8122
19	8.7666	7.1028	6.3992	26.8055	21.6939	19.3783	100.3164	80.5066	71.7488	246.5407	195.4336	173.3090
20	9.1342	7.3930	6.6977	27.7239	22.5609	20.1636	103.7755	83.9837	75.0472	257.8651	204.1225	181.9299
21	9.4918	7.6987	6.9877	28.5401	23.4644	21.0646	107.7639	87.4935	78.2294	262.6331	212.2175	189.0672
22	9.8038	7.9954	7.2744	30.0972	24.4296	21.9075	111.4032	90.8281	81.4744	270.8273	218.9241	196.2799
23	10.1056	8.3005	7.5277	31.0301	25.2834	22.7212	116.2186	93.9701	84.6311	279.3609	228.0453	204.1278
24	10.4431	8.5768	7.8040	31.7507	26.2508	23.5747	118.9657	97.1638	87.6506	287.3540	235.4258	211.1092
25	10.6996	8.8491	8.0460	32.9572	27.2024	24.5197	122.9572	100.5504	90.6959	294.9024	243.6891	219.0611
26	10.9414	9.1346	8.3416	33.8909	27.9958	25.3666	126.0380	104.2386	93.8488	303.6844	251.6200	226.4267
27	11.3882	9.4545	8.5917	34.7434	28.9397	26.1999	129.3280	107.2427	96.7183	309.5098	258.9096	234.6547
28	11.6508	9.7471	8.8859	35.6687	29.7525	26.9502	132.6532	110.8291	99.9151	319.7393	267.6180	241.5584
29	11.9405	10.0658	9.1706	36.4611	30.6902	27.8305	135.3868	114.3142	103.3609	328.3776	274.7251	249.8276
30	12.3167	10.3850	9.4902	37.5840	31.4982	28.7038	138.9136	117.5172	106.0231	334.6058	281.7136	256.4223

Table S2.15: Critical values for adjusted-range-based weighted-CvM monitoring statistic with late-emphasis weight  $w_L$  (finite horizons)

$q$	$T = 1$			$T = 2$			$T = 5$			$T = 10$		
	1%	5%	10%	1%	5%	10%	1%	5%	10%	1%	5%	10%
1	1.9354	1.0451	0.7147	6.2928	3.1725	2.1893	21.0638	10.6075	7.4056	50.7720	25.9696	17.4384
2	2.7173	1.6837	1.2478	8.2691	4.9323	3.6971	30.9635	17.8133	12.9212	71.7260	40.9492	30.6523
3	3.4996	2.2377	1.7633	10.0629	6.5157	5.0976	37.8943	23.5560	18.0795	87.7520	54.8296	42.5105
4	4.0280	2.7275	2.2004	11.9124	7.9686	6.3275	45.1252	28.6291	22.9128	102.4461	65.9982	52.9656
5	4.6222	3.2109	2.5980	13.6676	9.2641	7.5262	49.5247	33.0804	26.9227	111.1385	77.3266	62.5001
6	5.2073	3.6643	3.0403	15.1776	10.5189	8.7123	53.9524	37.7287	30.9665	123.6190	87.9857	71.6270
7	5.6186	4.1328	3.4630	16.5473	11.8393	9.8944	59.1249	42.3040	35.0631	134.9550	97.9146	81.0022
8	6.0135	4.5478	3.8593	18.1455	13.1953	10.9948	63.3720	46.4717	39.3202	147.4992	108.7306	90.7657
9	6.5959	4.9543	4.2711	19.2933	14.3577	12.2708	66.6979	51.4071	43.3816	159.2226	118.4241	100.4854
10	7.1255	5.3533	4.6431	20.5704	15.5355	13.3264	72.0304	55.4805	47.1320	171.1700	127.1010	109.0732
11	7.5059	5.7457	4.9842	22.0168	16.7482	14.4989	75.9039	59.0114	50.9342	180.1211	136.8534	117.3921
12	7.8774	6.1916	5.3764	23.6630	17.8860	15.6117	80.3551	62.7816	54.7777	191.8227	144.5502	126.4287
13	8.3391	6.5704	5.7378	24.9894	18.8685	16.5822	84.9113	66.5877	58.2746	201.7046	154.4400	134.4924
14	8.7004	6.9127	6.1200	26.3216	20.1477	17.6449	90.5205	70.4072	62.0321	211.3803	163.5445	142.8227
15	9.1334	7.2886	6.4938	27.4887	21.1673	18.7041	95.3673	74.4221	65.2250	224.4436	173.0167	151.7172
16	9.6179	7.6688	6.8268	28.5498	22.2405	19.8539	99.9463	78.2611	68.9797	231.9098	182.7023	160.1251
17	10.0667	8.0669	7.1753	29.3851	23.3444	20.9080	103.4834	82.0045	72.5523	241.4961	191.5249	168.4698
18	10.4198	8.4129	7.5311	30.4484	24.3770	21.8434	107.7019	85.9032	75.7243	253.9219	200.0764	176.7562
19	10.8534	8.7207	7.8552	31.9703	25.3969	22.7769	112.4756	89.7837	79.5254	265.2436	209.0057	185.2441
20	11.2550	9.1251	8.2090	33.1339	26.4945	23.7940	115.9980	93.2123	83.2115	275.0266	218.2251	193.3725
21	11.6390	9.5136	8.5801	34.4061	27.6324	24.7669	120.5999	97.3159	86.4952	282.2595	226.7707	202.2585
22	12.0743	9.8743	8.9345	35.7887	28.7298	25.7442	125.3520	100.5280	90.0088	287.5223	235.1231	209.7407
23	12.5079	10.1606	9.2668	37.0728	29.6625	26.6889	128.9119	104.8566	93.5291	298.0133	243.7660	218.5486
24	12.8549	10.5217	9.5745	37.7792	30.7411	27.6838	132.5497	108.0000	97.0143	308.1733	251.6091	226.0934
25	13.1913	10.9093	9.8997	39.1122	31.8591	28.7944	136.3902	112.2762	100.5570	316.6831	261.0852	234.4080
26	13.6058	11.3054	10.2250	40.0899	32.9608	29.7948	141.2958	116.2037	104.0589	326.2442	269.9610	242.1733
27	14.0361	11.6465	10.5720	41.2357	33.9758	30.8129	144.1169	119.6847	107.1740	331.8384	277.4246	250.2757
28	14.4415	12.0460	10.9248	42.2787	34.9352	31.7185	147.2789	123.2547	110.6481	340.7754	286.7320	258.6892
29	14.7757	12.4253	11.2885	43.3959	35.9923	32.7016	150.6924	126.9730	114.1451	349.2574	294.0102	266.6014
30	15.2123	12.7599	11.6596	44.4231	37.1102	33.6348	154.3945	130.4724	117.3366	357.3896	301.9425	274.1303

**Open-end weighted-CvM critical values.** Tables S2.16–S2.18 report the  $T = \infty$  weighted-CvM critical values for the HAC LRV-standardized, Shao self-normalized, and adjusted-range self-normalized statistics. Each table reports the four integrable open-end weights  $w_U^{(\infty)}$ ,  $w_E^{(\infty)}$ ,  $w_M^{(\infty)}$ , and  $w_L^{(\infty)}$  in separate columns.

S2. CRITICAL VALUES FOR THE MAIN MONITORING STATISTICS

Table S2.16: Open-end critical values for the HAC-based weighted-CvM statistic under the four integrable  $T = \infty$  weight families.

$q$	$w_U^{(\infty)}(s) = (1+s)^{-2}$			$w_E^{(\infty)}(s) = 2(1+s)^{-3}$			$w_M^{(\infty)}(s) = 6s(1+s)^{-4}$			$w_L^{(\infty)}(s) = 2s(1+s)^{-3}$		
	1%	5%	10%	1%	5%	10%	1%	5%	10%	1%	5%	10%
1	2.8218	1.6816	1.1893	1.7465	1.0690	0.7754	2.7948	1.6765	1.2054	3.9517	2.3375	1.6277
2	3.8661	2.6492	2.0730	2.4994	1.6936	1.3435	3.9075	2.6665	2.0929	5.4895	3.6475	2.8677
3	4.7438	3.4707	2.8062	3.0914	2.2471	1.8384	4.7408	3.4823	2.8395	6.6033	4.8056	3.8575
4	5.6617	4.2277	3.5571	3.6612	2.7692	2.3141	5.7294	4.3179	3.5634	7.7174	5.7980	4.8665
5	6.5634	5.0067	4.2546	4.2475	3.2172	2.7684	6.8228	5.0274	4.2760	9.1539	6.8394	5.8233
6	7.4044	5.7140	4.9032	4.7721	3.7065	3.1859	7.4893	5.7453	4.9161	10.1214	7.8456	6.7479
7	8.2489	6.3879	5.5874	5.3126	4.1366	3.6305	8.2807	6.3755	5.5739	11.3196	8.7548	7.6385
8	9.1961	7.0274	6.2030	5.8424	4.6425	4.0225	9.3045	7.1076	6.2377	12.5313	9.6440	8.3990
9	9.7820	7.7672	6.8349	6.3199	5.0899	4.4745	9.8725	7.8211	6.8953	13.5142	10.6027	9.2810
10	10.5261	8.4225	7.5006	6.8140	5.5055	4.8930	10.6252	8.4389	7.4890	14.3497	11.5013	10.1207
11	11.2093	9.0942	8.1389	7.3837	5.9366	5.3017	11.4568	9.1251	8.1201	15.3100	12.4664	11.0247
12	11.8563	9.7465	8.7033	7.7518	6.3844	5.6862	11.9408	9.7995	8.7112	16.2210	13.3535	11.8924
13	12.6528	10.4032	9.3113	8.2640	6.7683	6.0603	12.8386	10.4630	9.3364	17.2106	14.1518	12.7099
14	13.4196	10.9823	9.9289	8.8004	7.1968	6.4702	13.5701	11.1117	9.9317	18.1680	14.9644	13.5823
15	13.9147	11.6261	10.4919	9.1932	7.6001	6.8604	14.2886	11.7444	10.5020	19.2193	15.7964	14.3084
16	14.6423	12.2959	11.0482	9.5350	8.0142	7.2490	14.8497	12.3078	11.0472	20.0935	16.6999	15.0791
17	15.4364	12.9738	11.6926	9.9993	8.5056	7.6419	15.6422	13.0648	11.7901	20.9666	17.7471	15.8832
18	15.8932	13.6771	12.3425	10.3987	8.9260	8.0837	16.2463	13.7183	12.3719	21.8093	18.6426	16.7554
19	16.4925	14.2333	12.9314	10.9100	9.2750	8.4536	16.8889	14.3407	13.0140	22.8144	19.4086	17.5928
20	17.1686	14.9190	13.6043	11.3355	9.6791	8.8433	17.4655	14.9216	13.5645	23.7426	20.2826	18.3864
21	17.8504	15.4116	14.1307	11.7614	10.0888	9.2496	18.0575	15.5465	14.1584	24.5947	20.9565	19.2069
22	18.4988	16.0858	14.6991	12.1471	10.4778	9.6192	18.7104	16.1400	14.7491	25.3472	21.7656	19.9551
23	19.2540	16.6435	15.2737	12.5561	10.8754	10.0862	19.5224	16.7412	15.3958	26.3077	22.5514	20.6877
24	19.7758	17.2562	15.9515	12.9215	11.3027	10.4326	19.9771	17.2781	15.9536	27.1635	23.5008	21.5481
25	20.3573	17.8172	16.4793	13.3719	11.6915	10.7950	20.5021	17.9432	16.5462	27.9939	24.1998	22.2525
26	20.8892	18.4892	17.0999	13.7091	12.1185	11.2082	21.0819	18.5738	17.1240	28.6460	25.1369	23.0811
27	21.6090	19.0010	17.6229	14.0753	12.4922	11.5744	21.8653	19.1058	17.6725	29.6424	25.7427	23.7758
28	22.3606	19.6785	18.2271	14.5633	12.9011	11.9406	22.4749	19.7178	18.3065	30.3776	26.5787	24.6704
29	23.0065	20.2499	18.7513	14.9186	13.2893	12.3302	22.9707	20.3028	18.7903	31.5277	27.3842	25.4480
30	23.6373	20.8251	19.3722	15.2812	13.6154	12.6897	23.6057	20.9113	19.4050	32.3712	28.1564	26.2221

Table S2.17: Open-end critical values for Shao's weighted-CvM monitoring statistic under the four integrable  $T = \infty$  weight families.

$q$	$w_U^{(\infty)}(s) = (1+s)^{-2}$			$w_E^{(\infty)}(s) = 2(1+s)^{-3}$			$w_M^{(\infty)}(s) = 6s(1+s)^{-4}$			$w_L^{(\infty)}(s) = 2s(1+s)^{-3}$		
	1%	5%	10%	1%	5%	10%	1%	5%	10%	1%	5%	10%
1	42.4159	19.8843	13.1092	26.0184	13.4348	8.6484	41.7000	20.4947	13.2513	59.3773	27.8926	17.6705
2	88.6399	48.1260	33.7097	54.3223	30.9304	21.8578	88.0895	48.6739	34.1810	124.2380	65.1754	46.1851
3	137.5507	80.6765	58.7472	87.3064	51.8967	38.1850	140.3254	80.7163	58.9344	191.7427	111.2566	80.2326
4	191.5978	118.5771	90.8627	124.2334	76.1727	58.9495	195.0658	119.3381	90.7811	267.1565	163.4403	123.9469
5	247.1246	161.5934	126.3236	159.8381	103.0773	82.4628	249.0163	161.8147	125.7512	341.7733	222.8658	172.6373
6	316.2960	211.1834	166.6664	203.5526	134.6427	109.9879	319.0085	212.9001	169.1581	433.5342	292.6044	229.1879
7	378.5054	268.1155	218.4565	248.6092	171.9174	140.6078	380.9389	268.5270	219.8273	518.1109	364.8773	296.4171
8	465.1004	326.1476	271.3062	302.3648	210.7402	173.1947	475.6063	328.2749	270.8991	633.4926	445.0069	370.5277
9	537.2390	384.8940	323.1449	354.3670	251.0677	210.3698	556.6147	391.1481	323.5293	748.0445	531.6786	442.8302
10	624.8775	464.4722	389.7794	409.6664	300.5116	252.2226	636.9470	463.6542	390.2865	864.9371	636.9200	535.0725
11	735.5217	532.5103	458.3086	492.9083	350.5660	295.9062	767.3438	533.8455	457.2546	1021.2217	736.7769	623.3962
12	836.1931	614.0084	526.7669	548.3901	401.2343	346.8381	850.8276	622.6778	528.5497	1161.7038	843.0840	722.0253
13	954.7262	712.5228	598.6636	621.2937	459.6508	392.6875	958.2617	717.9465	603.6165	1305.4496	965.0027	819.8557
14	1049.1870	809.4000	684.6354	679.4587	517.5343	446.3739	1074.4036	812.7401	684.0422	1441.8694	1104.8918	937.8712
15	1148.1865	906.6276	771.8571	750.1414	585.7255	505.0765	1166.3467	904.2841	774.9447	1570.0926	1243.0369	1061.7533
16	1278.7052	1008.2271	872.4938	835.0023	650.2946	567.8242	1302.7252	1005.8972	877.8731	1794.5589	1390.0257	1204.7344
17	1443.1355	1109.0048	974.5863	933.9666	727.7104	628.2769	1461.9520	1113.0939	968.8586	1966.1036	1527.7562	1333.4319
18	1546.2052	1233.8737	1080.0934	995.9189	805.8031	699.3986	1569.1495	1236.9003	1072.2308	2158.1794	1690.5222	1471.6161
19	1729.6241	1339.2489	1189.4484	1104.0551	879.5584	773.2121	1720.0093	1353.6000	1185.6043	2360.3852	1828.1172	1615.9153
20	1873.0807	1468.8329	1299.3279	1216.9456	966.9096	849.4226	1883.9342	1477.2447	1299.5249	2558.1095	2014.1112	1775.3608
21	2042.5828	1588.8844	1407.8119	1306.5022	1034.6029	919.1783	2054.4772	1594.0082	1402.8289	2825.4616	2162.0452	1911.5474
22	2248.8565	1709.2557	1515.2998	1421.1503	1124.7568	997.8653	2235.1223	1722.4220	1525.9687	3048.0676	2324.0968	2064.6617
23	2370.7454	1849.7183	1641.7399	1523.5821	1206.0740	1077.4986	2404.1206	1854.5615	1649.7017	3220.2729	2530.6621	2229.9406
24	2540.9655	1987.5982	1791.0635	1644.2272	1300.1120	1167.6404	2565.9676	1998.1310	1791.9132	3480.1078	2722.4536	2428.9253
25	2689.3920	2152.7375	1921.2049	1755.1061	1399.7293	1260.8332	2744.3353	2162.6083	1929.8213	3703.8551	2949.6542	2615.7145
26	2860.7551	2294.1583	2056.5068	1869.2028	1500.3561	1350.1898	2890.5880	2293.1910	2055.3648	3912.9617	3141.1299	2795.7525
27	3040.0058	2451.5960	2169.4245	1994.8783	1589.3187	1436.5287	3072.9196	2457.0155	2196.0522	4181.0444	3330.0783	2945.3613
28	3204.5619	2617.0523	2331.7148	2113.2060	1694.3629	1535.6452	3276.8740	2629.8160	2336.8147	4399.2628	3569.1923	3155.4040
29	3391.9169	2786.0529	2483.5590	2227.3471	1808.2800	1625.6865	3441.1319	2786.0257	2490.0976	4660.1591	3778.5850	3351.4244
30	3637.3849	2953.4415	2653.3988	2397.3209	1926.0396	1729.7176	3685.0309	2978.5337	2659.6405	4935.5578	4023.3638	3579.8171

Table S2.18: Open-end critical values for the adjusted-range weighted-CvM monitoring statistic under the four integrable  $T = \infty$  weight families.

$q$	$w_U^{(\infty)}(s) = (1+s)^{-2}$			$w_E^{(\infty)}(s) = 2(1+s)^{-3}$			$w_M^{(\infty)}(s) = 6s(1+s)^{-4}$			$w_L^{(\infty)}(s) = 2s(1+s)^{-3}$		
	1%	5%	10%	1%	5%	10%	1%	5%	10%	1%	5%	10%
1	2.5030	1.3310	0.9218	1.5851	0.8627	0.5990	2.5855	1.3450	0.9298	3.5187	1.8328	1.2595
2	3.6343	2.1894	1.6481	2.2847	1.3841	1.0883	3.7004	2.2134	1.6585	5.0474	3.0344	2.2357
3	4.3941	2.9135	2.2971	2.7476	1.8500	1.5019	4.3680	2.8813	2.3240	6.0555	3.9688	3.1385
4	5.0376	3.5478	2.8716	3.2656	2.2629	1.8830	5.0821	3.5305	2.8958	7.1333	4.8846	3.9400
5	5.7726	4.1191	3.4191	3.7062	2.6348	2.2206	5.8916	4.0994	3.4212	7.9501	5.6872	4.7000
6	6.4526	4.7227	3.9676	4.2427	3.0297	2.5585	6.5254	4.7226	3.9720	8.9413	6.5245	5.4306
7	7.0795	5.2814	4.4868	4.6828	3.4373	2.9110	7.2427	5.3415	4.4762	10.1653	7.2311	6.1598
8	7.8645	5.8883	5.0141	5.1186	3.8181	3.2729	7.7919	5.9232	5.0215	10.7691	8.0276	6.8151
9	8.5262	6.3867	5.4966	5.5742	4.1403	3.6063	8.5794	6.3789	5.5133	11.6368	8.7846	7.4206
10	9.0912	6.9482	5.9723	5.8589	4.4759	3.9083	9.0344	6.9236	6.0099	12.2842	9.4373	8.1108
11	9.6674	7.4332	6.4652	6.2724	4.8879	4.2186	9.6468	7.4981	6.4377	13.3428	10.1295	8.7839
12	10.0832	7.9845	6.9460	6.6016	5.2143	4.5584	10.1820	7.9759	6.9696	13.9939	10.8616	9.4362
13	10.9208	8.4341	7.4508	7.1429	5.5728	4.8941	11.1181	8.5129	7.4502	15.0514	11.4058	10.1252
14	11.5419	8.9937	7.9384	7.5263	5.9118	5.2213	11.7425	9.0089	7.9787	15.8802	12.3007	10.8151
15	12.1489	9.5409	8.4294	7.8884	6.2112	5.5418	12.3776	9.5350	8.4687	16.5793	12.9381	11.3669
16	12.5341	10.0680	8.8744	8.1739	6.5144	5.8480	12.8191	10.0262	8.9442	17.2858	13.7653	12.0421
17	12.9065	10.6046	9.4104	8.4443	6.8842	6.2088	13.1203	10.6120	9.4596	17.6689	14.4541	12.7184
18	13.5386	11.0320	9.9551	8.8137	7.1874	6.5177	13.6468	11.0549	9.9406	18.3331	15.0992	13.4446
19	14.0594	11.5869	10.3945	9.2234	7.5514	6.8043	14.0993	11.6115	10.4278	19.2300	15.7184	14.0759
20	14.6081	12.0706	10.9196	9.5466	7.9106	7.1214	14.7687	12.1495	10.8810	19.9669	16.3929	14.7490
21	15.2432	12.4996	11.3482	9.8371	8.2024	7.4161	15.2954	12.5626	11.3412	20.5789	17.0051	15.3870
22	15.5992	13.1127	11.8652	10.1666	8.5835	7.7509	15.6919	13.1784	11.8891	21.0415	17.7457	16.0109
23	16.0157	13.5255	12.2841	10.5328	8.8558	8.0703	16.3538	13.6409	12.3508	21.8640	18.3843	16.6484
24	16.5749	14.0733	12.7360	10.7926	9.1792	8.3415	16.7263	14.1580	12.7623	22.4613	19.1007	17.2102
25	16.9311	14.5137	13.1778	11.1864	9.5066	8.6341	17.2730	14.5478	13.2208	23.2561	19.6786	17.8987
26	17.5105	15.0198	13.6583	11.6576	9.8245	8.9707	17.7571	15.0500	13.7273	24.0830	20.4600	18.4402
27	18.0900	15.4991	14.0977	11.9712	10.1042	9.2762	18.3611	15.4951	14.1561	24.8918	21.0514	19.0816
28	18.6220	15.9312	14.5522	12.3134	10.4508	9.6019	18.9153	16.0788	14.6386	25.4458	21.7227	19.7108
29	19.0106	16.3828	15.0377	12.5966	10.7180	9.8968	19.3338	16.4781	15.1083	26.1727	22.2713	20.3182
30	19.5021	16.8888	15.4459	12.9622	11.0081	10.1487	19.7998	16.9995	15.5107	26.9010	22.9931	20.8468

### S3 Supplementary Simulation Results

Table S3.1: Main simulation summary for the default KS statistics and the retained weighted-CvM diagnostic.

Method	Null MAD	Level shift SAP	Smooth change SAP	Overall SAP
RSMS KS ( $\gamma = 0$ )	3.7	87.8	54.2	71.0
SSMS KS ( $\gamma = 0$ )	0.7	82.3	47.1	64.7
HAC KS ( $\gamma = 0$ )	4.7	91.0	60.3	75.7
RSMS CvM-Late	3.4	86.0	42.4	64.2
SSMS CvM-Late	0.6	81.0	36.9	59.0
HAC CvM-Late	4.0	89.0	47.7	68.3

Note: Entries average over the available null designs (BB, fIID, and fMA(1)) and, for SAP, over DGPs, monitoring horizons, and break locations in the level-shift and smooth-change designs. MAD denotes mean absolute deviation of empirical size from the 5% nominal level; CvM-Late uses the late-emphasis weight  $w_L$ .

This section gives the broader simulation results for the KS and weighted-CvM monitoring statistics. The main paper reports compact summary tables and uses fMA(1) display figures; here the BB, fIID, and fMA(1) results are shown separately. The DGPs, training-sample FPCA score construction, horizons, and break grids are the same as in the paper’s simulation section. In all simulation tables and figures, FPCA is estimated on the training sample, the retained score dimension is selected by the 95% FVE criterion, and the resulting score stream is used for HAC, SSMS, and RSMS. Monte Carlo rejection rates use 1000 replications per simulation setting. The critical values used in this section are those in Appendix S2; they are based on 10,000 Brownian replications for finite horizons and 5,000 replications for the open-end entries.

The simulations use a 21-dimensional cubic B-spline representation on

$[0, 1]$ , evaluate curves on a 301-point grid, and estimate FPCA from the training sample. The spline innovations use independent Gaussian coefficients with standard deviation  $1/j$  in the  $j$ th basis direction. In the fMA(1) DGP, the random coefficient operator is normalized to spectral norm 0.7. The default HAC bandwidth is  $L = \lfloor 4(m/100)^{2/9} \rfloor$ , with a Bartlett kernel unless a sensitivity table states otherwise; matrix inversions use ridge  $10^{-10}$  and adjusted ranges use floor  $10^{-8}$ . Main finite-horizon critical values use 10,000 Brownian replications on  $q = 1, \dots, 30$ ,  $T \in \{1, 2, 5, 10\}$ , and a monitoring grid of 10,000 points.

### **S3.1 Additional rejection-rate results for the level-shift and smooth-change settings**

The main text reports fMA(1) display figures and DGP-averaged summary tables. The figures below keep the BB, fIID, and fMA(1) results separate for the level-shift and smooth-change settings. The KS panels give raw rejection rates and SAP for each DGP. For weighted-CvM, the late-emphasis weight  $w_L$  is shown first across the three DGPs because it is the weighted-CvM entry used in the main summary table. The following panels then compare all four weights separately for BB, fIID, and fMA(1).

**KS raw rejection rates and SAP across DGPs**

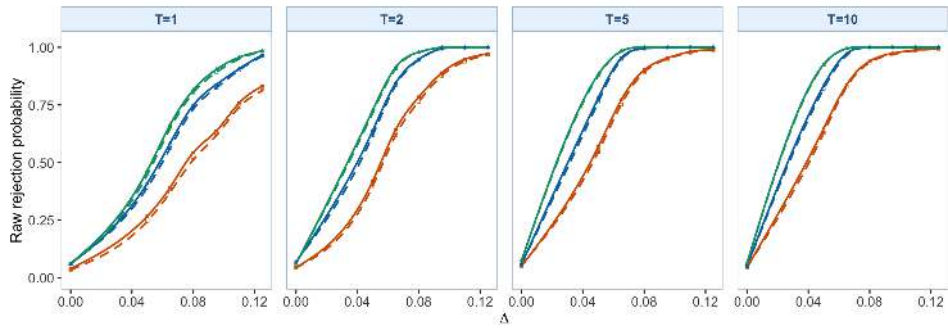
Figures S3.1–S3.4 show the DGP-specific results behind the main-paper summary table. HAC often has the highest raw rejection rates, but the points at  $\Delta = 0$  also show its larger empirical size. After size adjustment, RSMS remains above SSMS over much of the break grid for IID and fMA(1). The BB panels are lower-signal settings, so all three standardizations have lower rejection rates.

**Weighted-CvM SAP across DGPs**

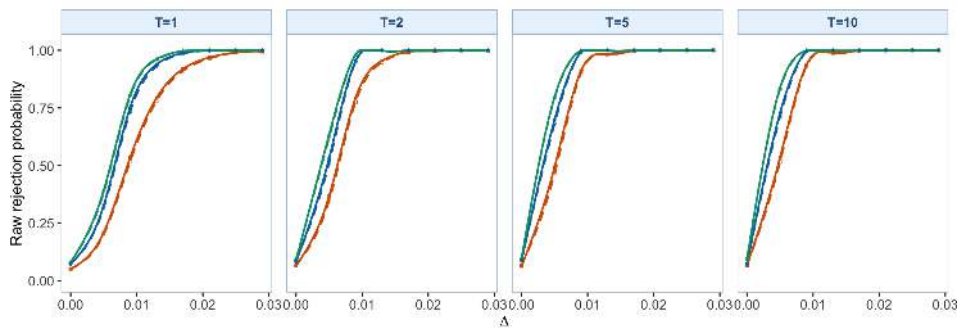
The late-emphasis weighted-CvM panels provide the closest weighted-CvM analogue to the main KS comparison. The ordering is similar: after empirical size adjustment, RSMS is usually above SSMS, while HAC can have higher raw rejection rates but is more sensitive to empirical size distortion and kernel and bandwidth choices.

**Weighted-CvM weight comparisons across DGPs**

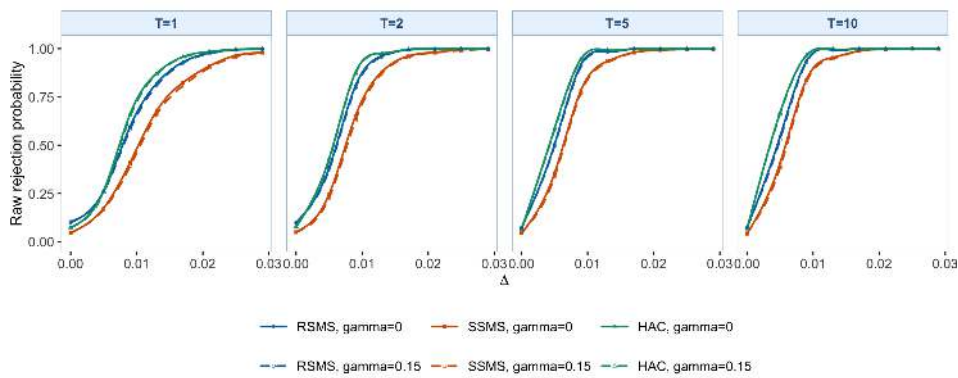
Figures S3.7–S3.12 show the weighted-CvM weight comparison behind the main summary table. The early-emphasis weight reacts to the start of the monitoring path, while the late and uniform weights put more mass on accumulated post-break movement. In the smooth-change setting, where



(a) BB errors.



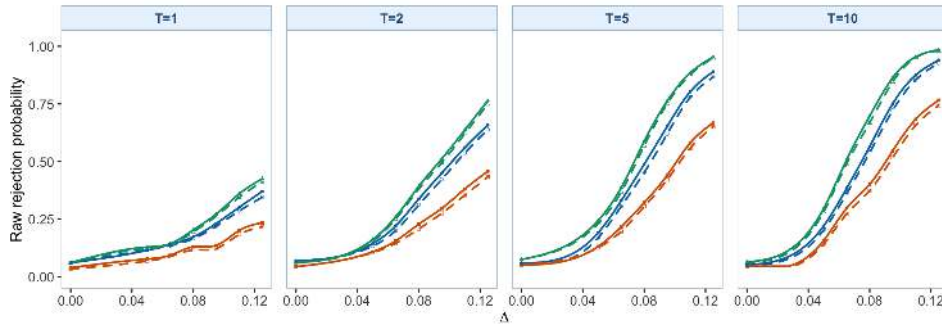
(b) IID errors.



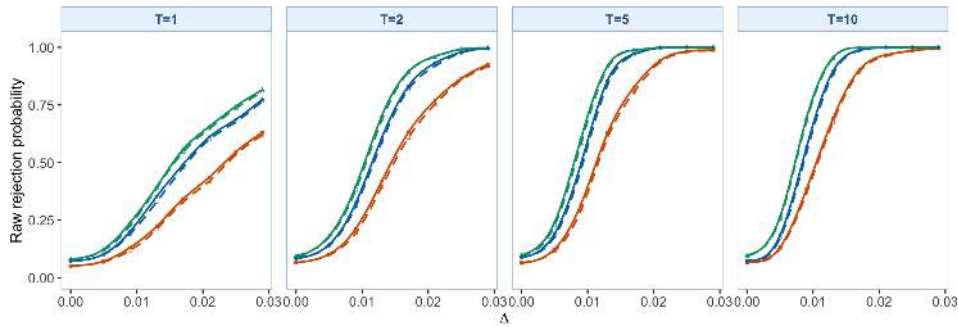
(c) fMA(1) errors.

Figure S3.1: Raw rejection curves for the main KS statistics under the level-shift setting. Each subfigure fixes one DGP, and the four internal columns correspond to  $T = 1, 2, 5, 10$ . The point where each curve meets the vertical axis is the empirical size under the null. The legend below the final subfigure identifies the six method-boundary combinations.

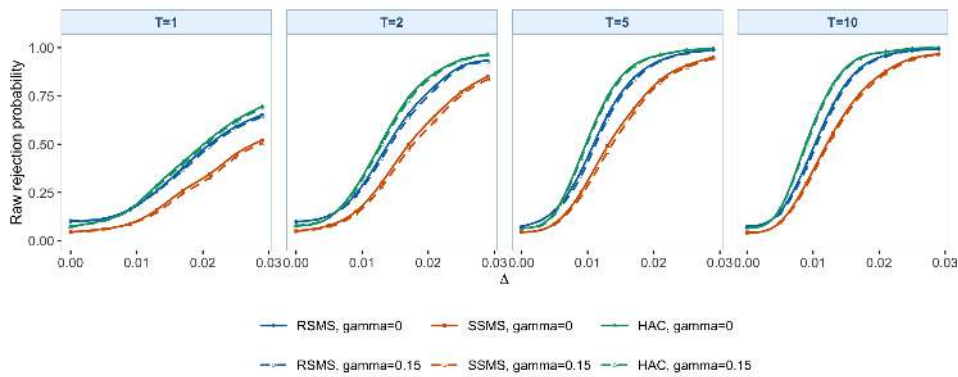
S3. SUPPLEMENTARY SIMULATION RESULTS



(a) BB errors.

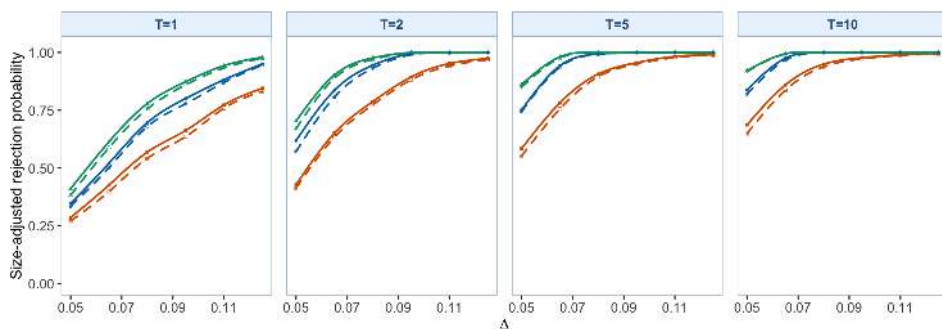


(b) IID errors.

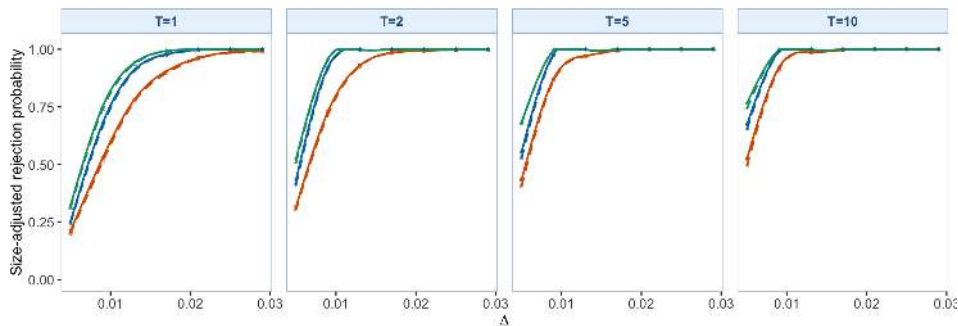


(c) fMA(1) errors.

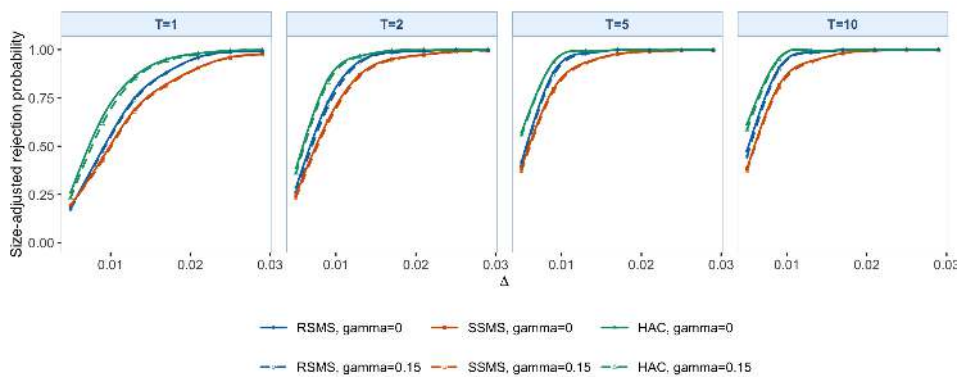
Figure S3.2: Raw rejection curves for the main KS statistics under the smooth-change setting. Each subfigure fixes one DGP, and the four internal columns correspond to  $T = 1, 2, 5, 10$ . The point where each curve meets the vertical axis is the empirical size under the null. The legend below the final subfigure identifies the six method-boundary combinations.



(a) BB errors.



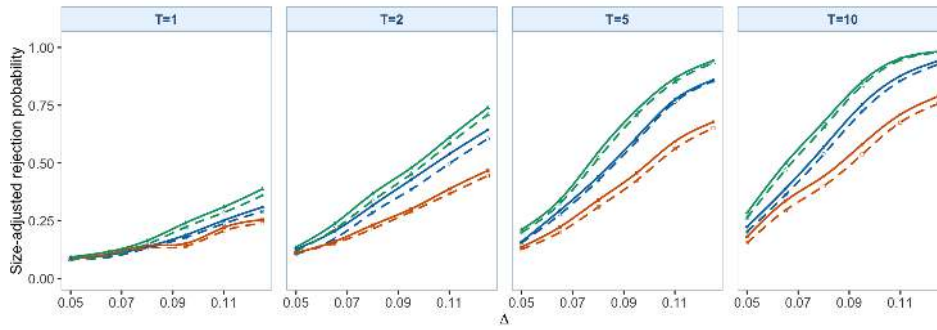
(b) IID errors.



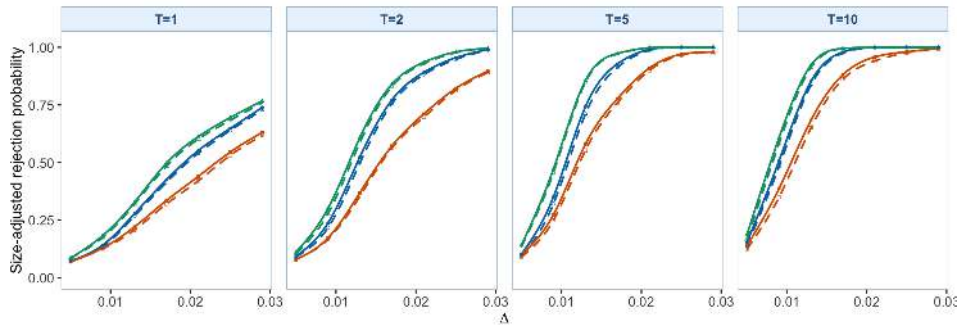
(c) fMA(1) errors.

Figure S3.3: KS SAP curves for the main KS statistics under the level-shift setting. Each subfigure fixes one DGP, and the four internal columns correspond to  $T = 1, 2, 5, 10$ . The empirical-size adjustment is computed separately for each simulation setting.

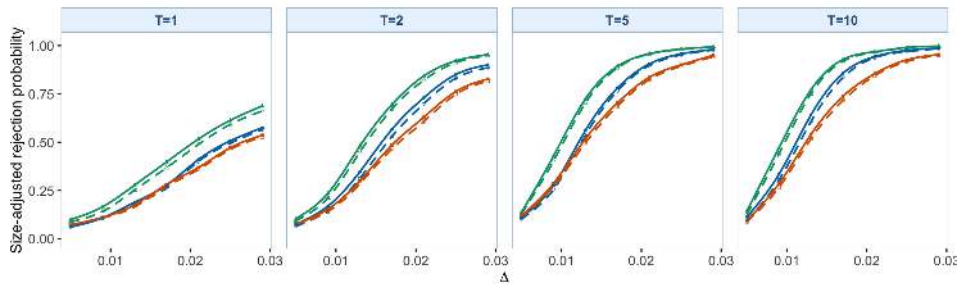
S3. SUPPLEMENTARY SIMULATION RESULTS



(a) BB errors.



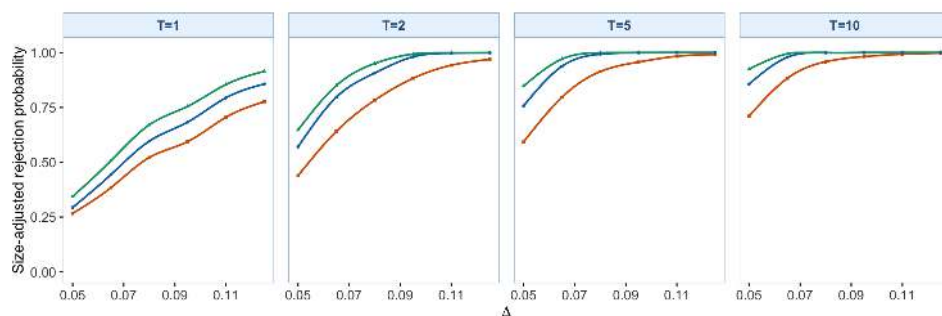
(b) IID errors.



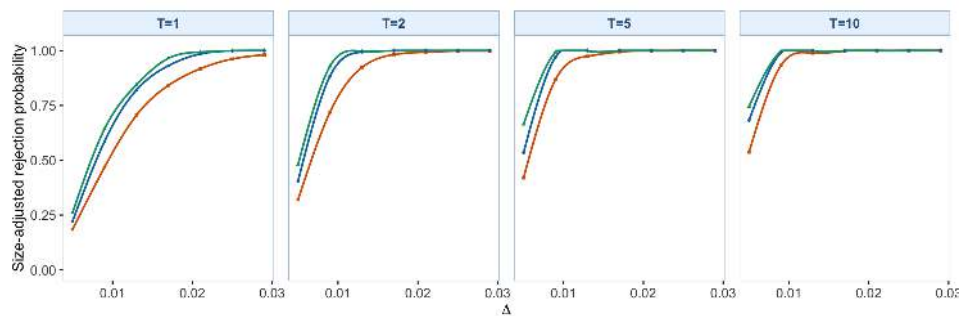
— RSMS, gamma=0    — SSMS, gamma=0    — HAC, gamma=0  
 - - RSMS, gamma=0.15    - - SSMS, gamma=0.15    - - HAC, gamma=0.15

(c) fMA(1) errors.

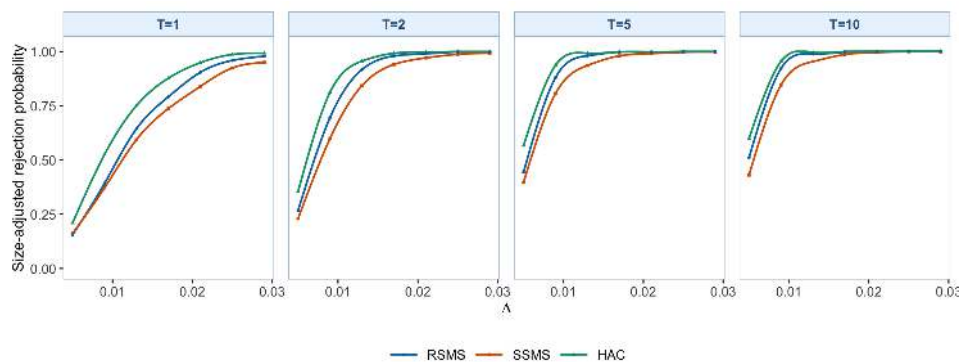
Figure S3.4: KS SAP curves for the main KS statistics under the smooth-change setting. Each subfigure fixes one DGP, and the four internal columns correspond to  $T = 1, 2, 5, 10$ . The empirical-size adjustment is computed separately for each simulation setting.



(a) BB errors.



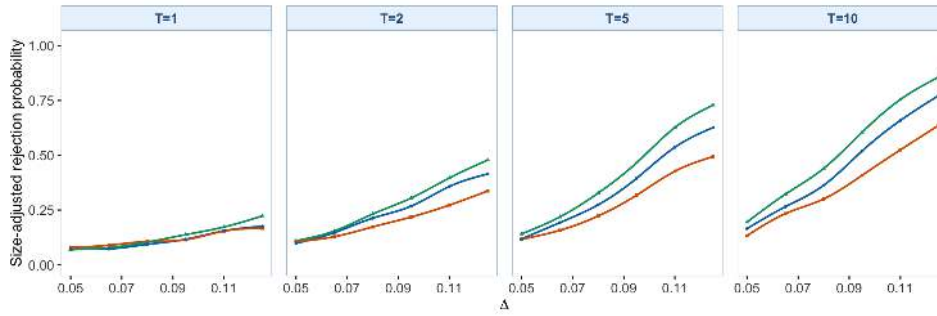
(b) IID errors.



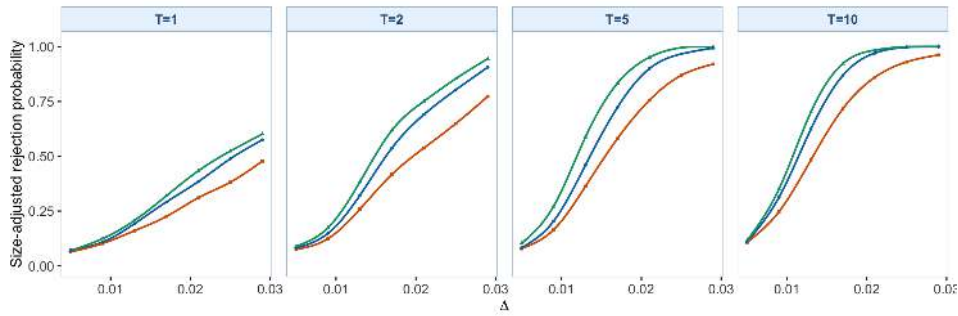
(c) fMA(1) errors.

Figure S3.5: Late-emphasis weighted-CvM SAP curves under the level-shift setting. Each subfigure fixes one DGP, and the four internal columns correspond to  $T = 1, 2, 5, 10$ . The legend below the final subfigure identifies RSMS, SSMS, and HAC.

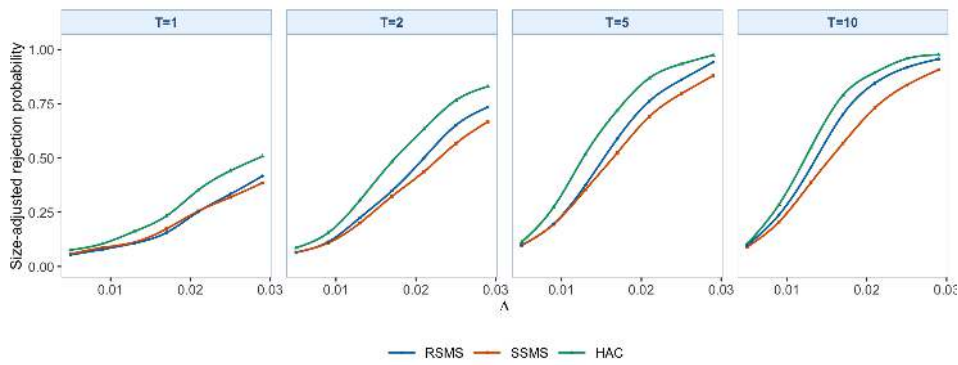
S3. SUPPLEMENTARY SIMULATION RESULTS



(a) BB errors.

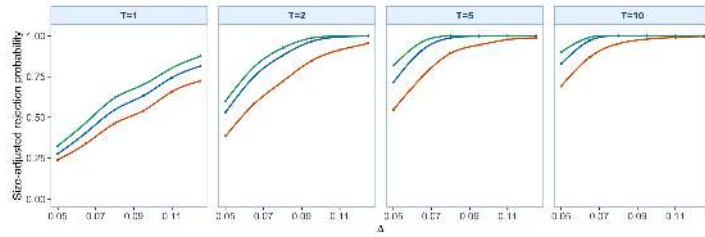


(b) IID errors.

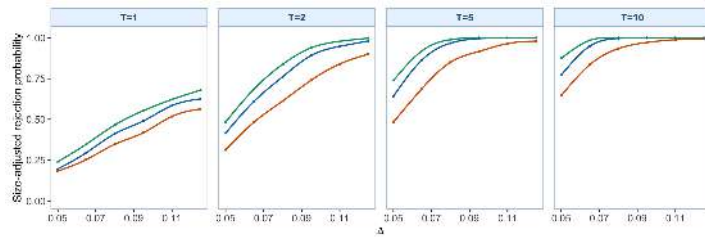


(c) fMA(1) errors.

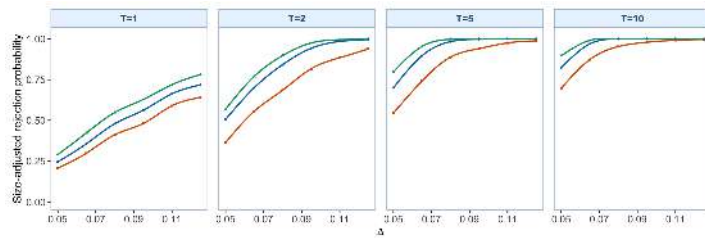
Figure S3.6: Late-emphasis weighted-CvM SAP curves under the smooth-change setting. Each subfigure fixes one DGP, and the four internal columns correspond to  $T = 1, 2, 5, 10$ . The legend below the final subfigure identifies RSMS, SSMS, and HAC.



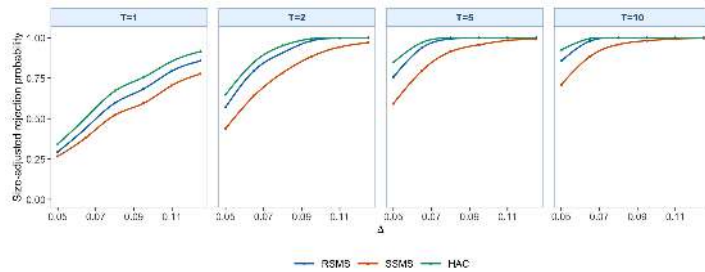
(a) Uniform weight  $w_U$ .



(b) Early-emphasis weight  $w_E$ .



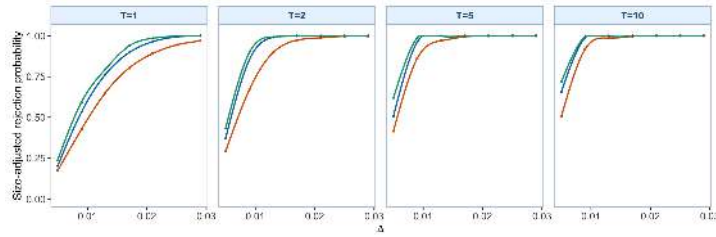
(c) Mid-emphasis weight  $w_M$ .



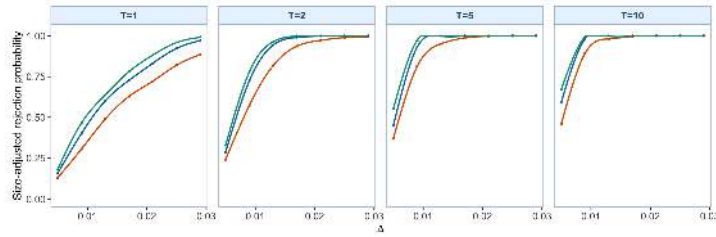
(d) Late-emphasis weight  $w_L$ .

Figure S3.7: Weighted-CvM SAP curves for the level-shift setting under the BB DGP. Each subfigure uses BB errors, and the four internal columns correspond to  $T = 1, 2, 5, 10$ . The legend below the final subfigure identifies RSMS, SSMS, and HAC.

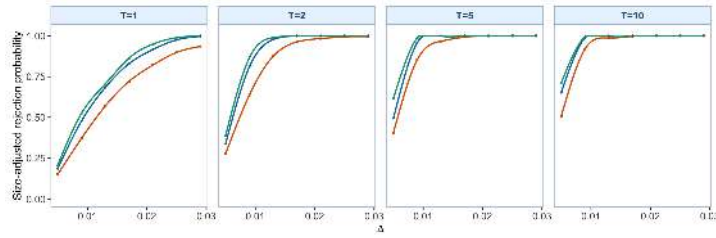
### S3. SUPPLEMENTARY SIMULATION RESULTS



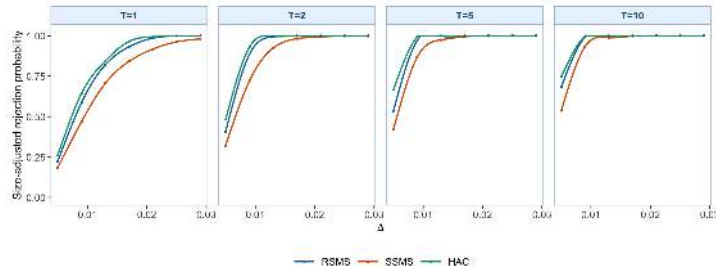
(a) Uniform weight  $w_U$ .



(b) Early-emphasis weight  $w_E$ .



(c) Mid-emphasis weight  $w_M$ .



(d) Late-emphasis weight  $w_L$ .

Figure S3.8: Weighted-CvM SAP curves for the level-shift setting under the IID DGP. Each subfigure uses IID errors, and the four internal columns correspond to  $T = 1, 2, 5, 10$ . The legend below the final subfigure identifies RSMS, SSMS, and HAC.

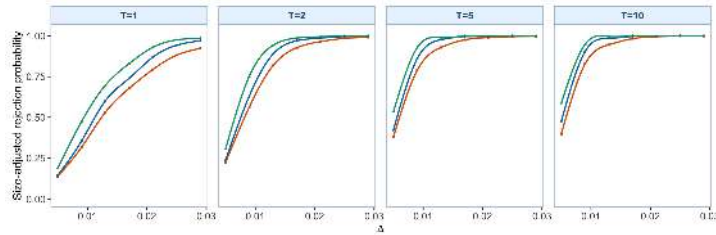
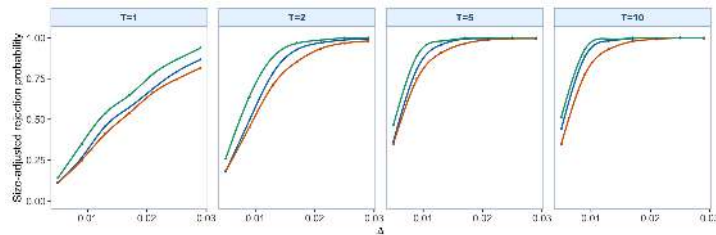
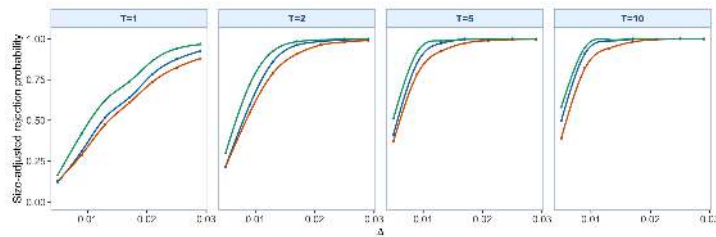
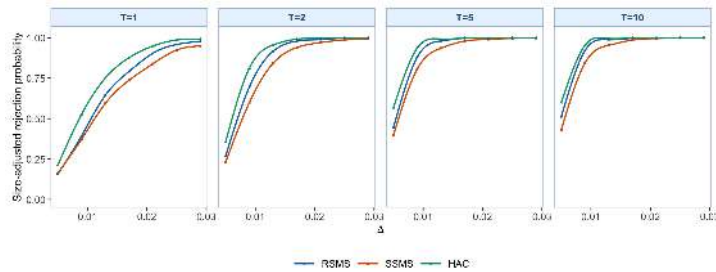
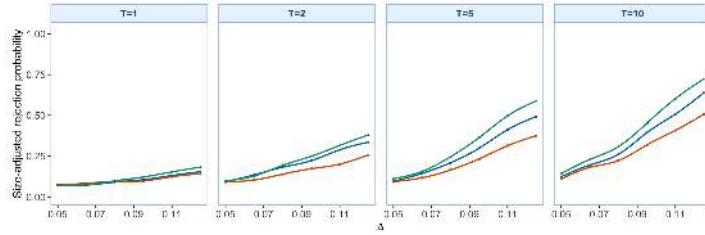
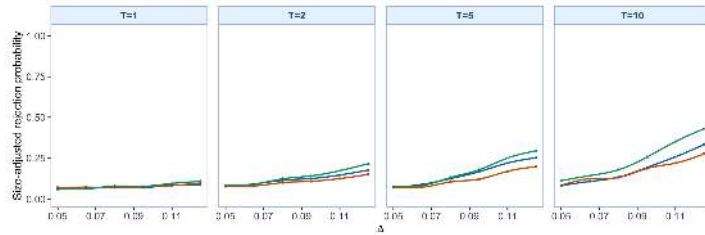
(a) Uniform weight  $w_U$ .(b) Early-emphasis weight  $w_E$ .(c) Mid-emphasis weight  $w_M$ .(d) Late-emphasis weight  $w_L$ .

Figure S3.9: Weighted-CvM SAP curves for the level-shift setting under the fMA(1) DGP. Each subfigure uses fMA(1) errors, and the four internal columns correspond to  $T = 1, 2, 5, 10$ . The legend below the final subfigure identifies RSMS, SSMS, and HAC.

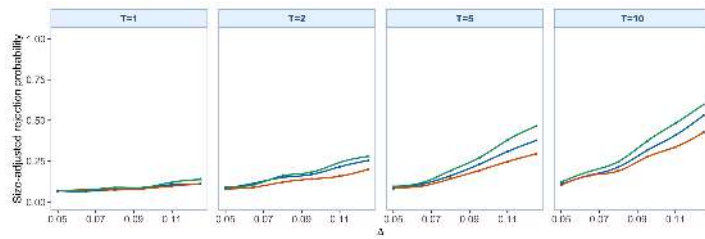
### S3. SUPPLEMENTARY SIMULATION RESULTS



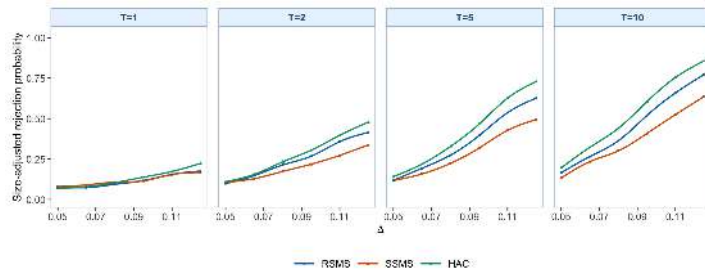
(a) Uniform weight  $w_U$ .



(b) Early-emphasis weight  $w_E$ .

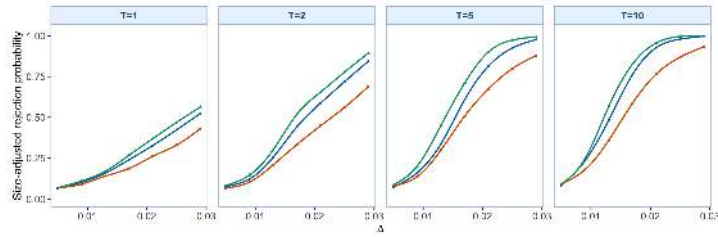


(c) Mid-emphasis weight  $w_M$ .

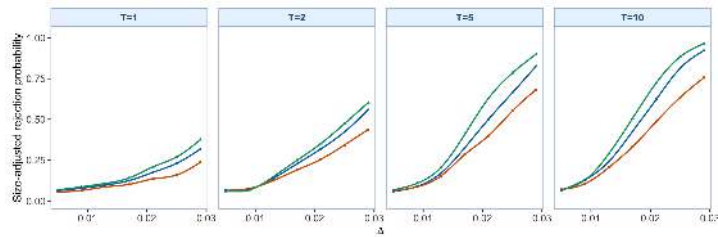


(d) Late-emphasis weight  $w_L$ .

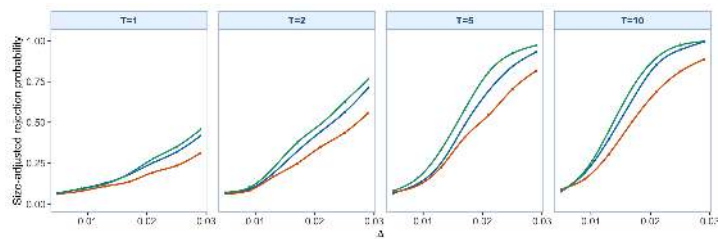
Figure S3.10: Weighted-CvM SAP curves for the smooth-change setting under the BB DGP. Each subfigure uses BB errors, and the four internal columns correspond to  $T = 1, 2, 5, 10$ . The legend below the final subfigure identifies RSMS, SSMS, and HAC.



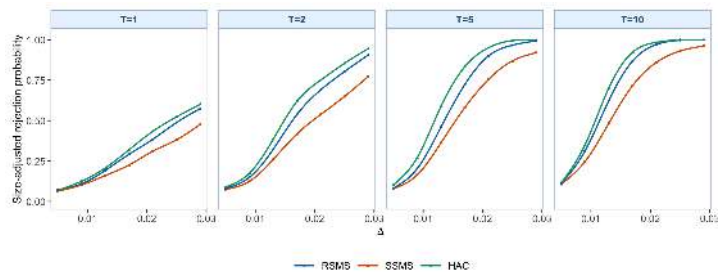
(a) Uniform weight  $w_U$ .



(b) Early-emphasis weight  $w_E$ .



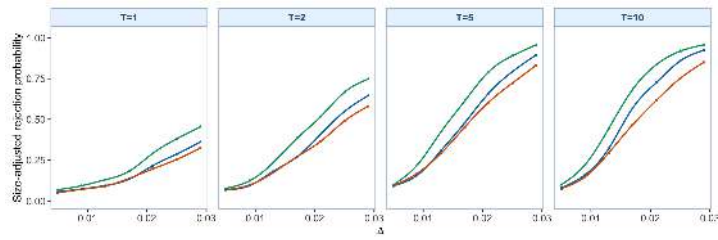
(c) Mid-emphasis weight  $w_M$ .



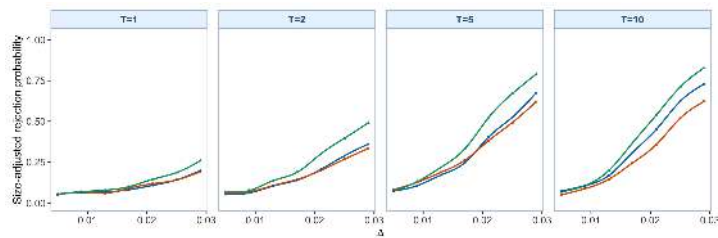
(d) Late-emphasis weight  $w_L$ .

Figure S3.11: Weighted-CvM SAP curves for the smooth-change setting under the IID DGP. Each subfigure uses IID errors, and the four internal columns correspond to  $T = 1, 2, 5, 10$ . The legend below the final subfigure identifies RSMS, SSMS, and HAC.

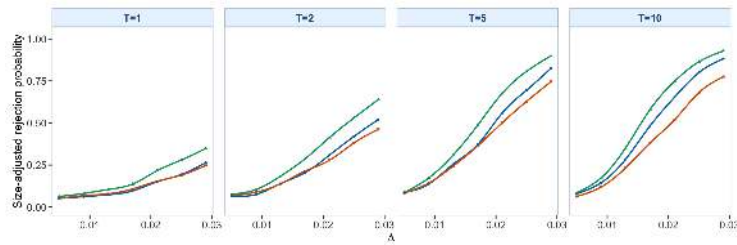
### S3. SUPPLEMENTARY SIMULATION RESULTS



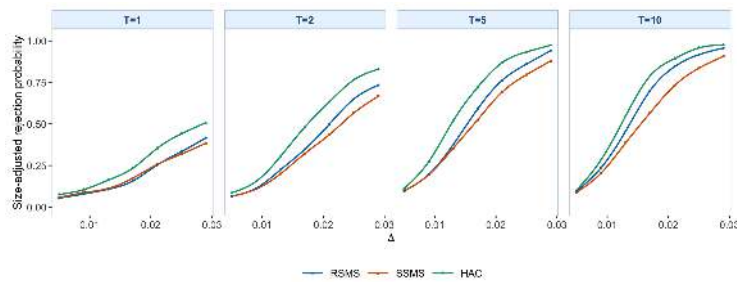
(a) Uniform weight  $w_U$ .



(b) Early-emphasis weight  $w_E$ .



(c) Mid-emphasis weight  $w_M$ .



(d) Late-emphasis weight  $w_L$ .

Figure S3.12: Weighted-CvM SAP curves for the smooth-change setting under the fMA(1) DGP. Each subfigure uses fMA(1) errors, and the four internal columns correspond to  $T = 1, 2, 5, 10$ . The legend below the final subfigure identifies RSMS, SSMS, and HAC.

the break builds gradually, this difference is especially visible.

### **S3.2 HAC kernel and bandwidth sensitivity under the fMA(1) setting**

This subsection varies the kernel and bandwidth in the HAC LRV estimator for the KS monitoring statistic. The fMA(1) DGP is the dependent setting used in the main paper and is the setting in which these choices matter most. HAC estimators require a kernel, a bandwidth, and sometimes prewhitening (Andrews, 1991; Andrews and Monahan, 1992). In finite samples, the resulting null rejection and stopping behavior can change with those choices, especially under realistic dependence (Den Haan and Levin, 1997; Müller, 2007; Hong et al., 2024). The comparison is therefore used to document implementation sensitivity rather than to select a single HAC specification.

Figure S3.13 and Table S3.2 report empirical size, raw power, SAP, and ADD under these kernel and bandwidth choices. Empirical size ranges from 8.0% to 13.0% when  $\gamma = 0$  and from 8.7% to 14.0% when  $\gamma = 0.15$ ; by comparison, SSMS stays close to the nominal level and RSMS is less size-distorted than several HAC specifications. Some kernel and bandwidth choices give higher raw power and shorter stopping delays, but they also reject more often under the null. Once each statistic is compared using its own empirical-size adjustment, the spread in SAP narrows. The self-normalized statistics avoid kernel and bandwidth choices and still give comparable em-

pirical size, SAP, and ADD in this simulation setting.

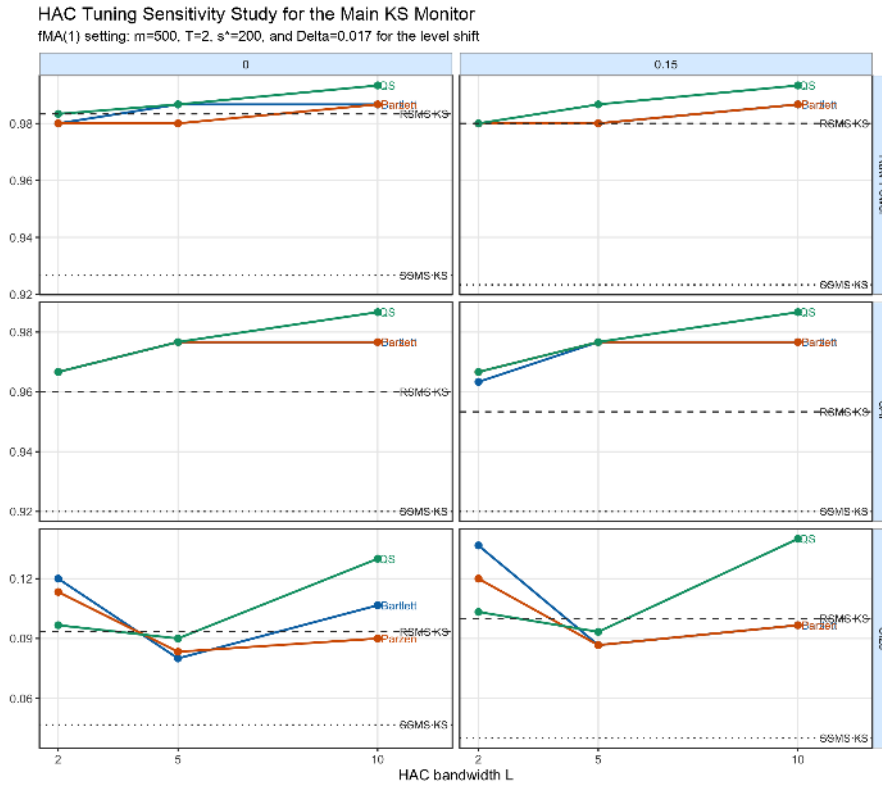


Figure S3.13: HAC kernel and bandwidth sensitivity for the main KS statistic under the fMA(1) DGP. The figure fixes the fMA(1) DGP with  $m = 500$ ,  $T = 2$ , and  $s^* = 200$ . The raw-power and SAP panels use the level-shift alternative with  $\Delta = 0.017$ , while the size panels use  $\Delta = 0$ . The legend below the figure identifies the HAC kernel lines and the two horizontal reference lines.

### S3. SUPPLEMENTARY SIMULATION RESULTS

Table S3.2: HAC kernel and bandwidth sensitivity for the main KS statistic under the fMA(1) DGP. Entries report empirical size, raw power, SAP, and ADD; size and power entries are percentages.

Method	Size	Level Raw	Level SAP	Level ADD	Smooth Raw	Smooth SAP	Smooth ADD
<b>Panel A: <math>\gamma = 0</math></b>							
RSMS KS	9.3	98.3	96.0	237.4	48.3	37.0	592.0
SSMS KS	4.7	92.7	92.0	282.8	34.0	34.7	597.9
HAC Bartlett (L=2)	12.0	98.0	96.7	212.6	57.3	39.0	592.5
HAC Bartlett (L=5, default)	8.0	98.7	97.7	209.2	59.0	49.0	608.6
HAC Bartlett (L=10)	10.7	98.7	97.7	196.6	62.0	48.7	597.9
HAC Parzen (L=2)	11.3	98.0	96.7	213.2	56.7	39.7	593.3
HAC Parzen (L=5, default)	8.3	98.0	97.7	209.6	59.0	48.0	611.5
HAC Parzen (L=10)	9.0	98.7	97.7	199.1	60.3	48.3	594.0
HAC quadratic spectral (QS) (L=2)	9.7	98.3	96.7	215.2	57.7	43.7	601.4
HAC QS (L=5, default)	9.0	98.7	97.7	201.2	59.3	50.7	594.2
HAC QS (L=10)	13.0	99.3	98.7	185.1	65.0	50.3	579.8
<b>Panel B: <math>\gamma = 0.15</math></b>							
RSMS KS	10.0	98.0	95.3	223.9	45.7	36.3	571.7
SSMS KS	4.0	92.3	92.0	274.9	33.0	34.7	582.5
HAC Bartlett (L=2)	13.7	98.0	96.3	198.6	55.7	37.3	582.5
HAC Bartlett (L=5, default)	8.7	98.0	97.7	191.8	58.3	47.7	605.2
HAC Bartlett (L=10)	9.7	98.7	97.7	182.5	61.0	48.3	587.9
HAC Parzen (L=2)	12.0	98.0	96.7	199.5	56.0	40.0	590.7
HAC Parzen (L=5, default)	8.7	98.0	97.7	195.9	56.3	44.7	600.6
HAC Parzen (L=10)	9.7	98.7	97.7	184.6	59.0	46.7	589.9
HAC QS (L=2)	10.3	98.0	96.7	198.7	57.0	41.7	590.0
HAC QS (L=5, default)	9.3	98.7	97.7	187.2	58.3	48.3	590.6
HAC QS (L=10)	14.0	99.3	98.7	171.9	63.7	48.3	566.1

Note: The study adopts the fMA(1) setting used in the paper: fMA(1) errors,  $m = 500$ ,  $T = 2$ ,  $s^* = 200$ , and 95% FVE FPCA compression. Empirical size is evaluated at nominal 5% under  $\Delta = 0$ . “Level” denotes the level-shift setting and “Smooth” denotes the smooth-change setting; both use  $\Delta = 0.017$ . Raw power uses the asymptotic 5% critical value. SAP denotes size-adjusted power based on each method’s empirical 95th percentile under the null. ADD is the mean post-break stopping delay among asymptotic rejections. The HAC rows use kernel-specific long-run covariance estimators with bandwidth  $L$ ; the default Bartlett bandwidth for  $m = 500$  is  $L = 5$ .

### S3.3 Finite-sample RSMS off-diagonal diagnostic

The adjusted-range self-normalizer is constructed after lag-0 whitening and applies coordinatewise adjusted-range SN. Under serial dependence, lag-0 whitening need not make the long-run covariance exactly diagonal. The main paper therefore uses the finite-sample diagnostic

$$\Delta_m^{\text{off}} = \frac{\|\text{offdiag}(\widehat{W}_m \widehat{\Gamma}_m \widehat{W}_m^\top)\|_F}{\|\widehat{W}_m \widehat{\Gamma}_m \widehat{W}_m^\top\|_F}.$$

Table S3.3 reports this diagnostic for the fMA(1) simulation setting and for the empirical S&P 500 score dimensions. The values are not close to zero, so the paper treats approximate diagonalization as a condition to check rather than as an automatic consequence of whitening. In these checks, however, the off-diagonal component remains a minority share of the transformed HAC covariance norm. The diagnostic should therefore be read as support for the reported RSMS implementation, not as a claim that lag-0 covariance estimates the long-run covariance. Lag-0 whitening fixes a stable training-sample coordinate system before the coordinatewise adjusted ranges are formed. Coordinatewise scales are absorbed by those ranges; the relevant check is whether the transformed long-run covariance is close enough to diagonal. HAC-whitened RSMS can be used as a sensitivity check, but

### S3. SUPPLEMENTARY SIMULATION RESULTS

making it the default would reintroduce the kernel and bandwidth choices that SN is intended to avoid.

Table S3.3: Finite-sample off-diagonal diagnostic for the RSMS approximate-diagonalization condition.

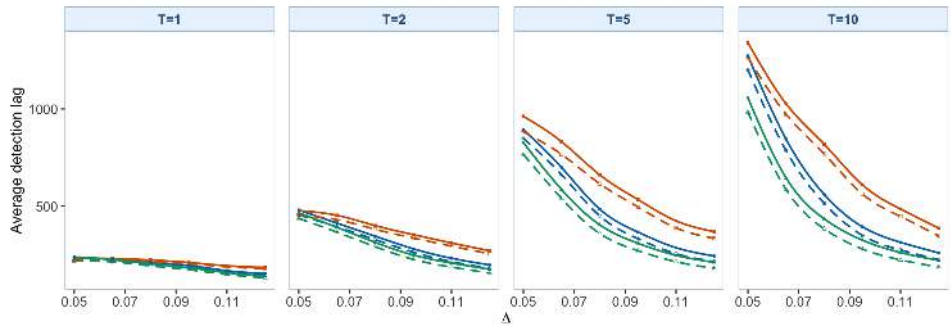
Design	Replications	$K$ summary	Mean $\Delta_m^{\text{off}}$	Median	90th pct.	Empirical $\Delta_m^{\text{off}}$
<b>Panel A:</b> fMA(1) simulation setting fMA(1), $m = 500$ , $T = 2$ , 95% FVE	1000	7.83	0.174	0.174	0.203	–
<b>Panel B:</b> empirical S&P 500 training sample						
$K = 3$ , $m = 50$	–	3	–	–	–	0.249
$K = 4$ , $m = 50$	–	4	–	–	–	0.230
$K = 5$ , $m = 50$	–	5	–	–	–	0.240

Note: The simulation row uses the fMA(1) setting with fMA(1) errors, a clean training sample, the 301-point grid representation, 95% FVE score selection, and the default Bartlett HAC covariance. The  $K$  entry in Panel A is the mean selected score dimension; the median selected dimension is 8, with selected  $K \in \{7, 8, 9\}$  across the 1000 replications. The empirical rows use the October 21–December 31, 2019 training sample and retained score dimensions  $K = 3, 4, 5$ . The diagnostic is a finite-sample check on the size of off-diagonal dependence after lag-0 whitening; it is not a proof of the main-paper approximate-diagonalization assumption.

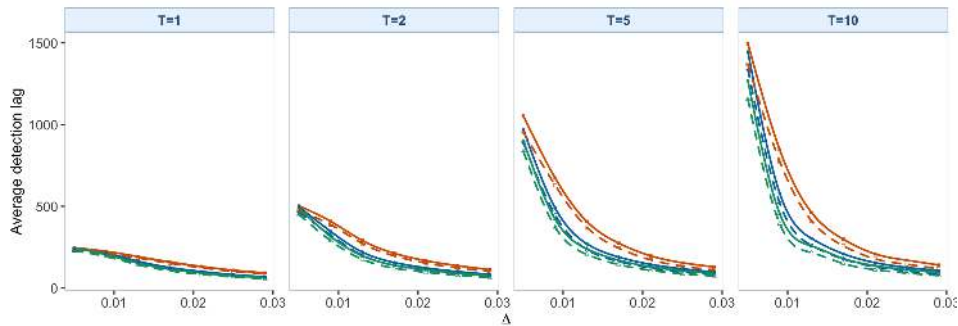
#### S3.4 ADD curves for the level-shift and smooth-change settings

Figures S3.14 and S3.15 report ADD for the main KS statistics under the level-shift and smooth-change settings, respectively. Figures S3.16 and S3.17 give the same ADD comparison for the late-weighted weighted-CvM statistic. Figures S3.18–S3.20 and Figures S3.21–S3.23 then compare the four weighted-CvM weights separately for each DGP.

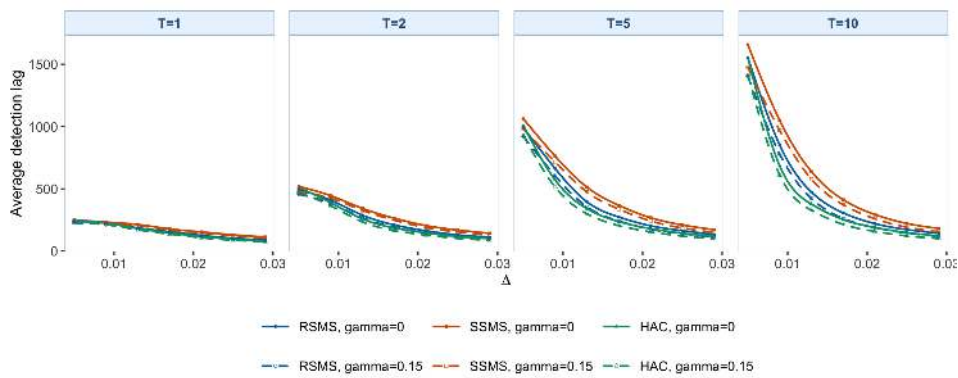
The ADD figures show how the rejection-rate comparisons translate into stopping delays. Within the self-normalized statistics, RSMS usually stops earlier than SSMS. HAC sometimes has shorter delays, but those entries should be read together with its empirical size under the null. For



(a) BB DGP.



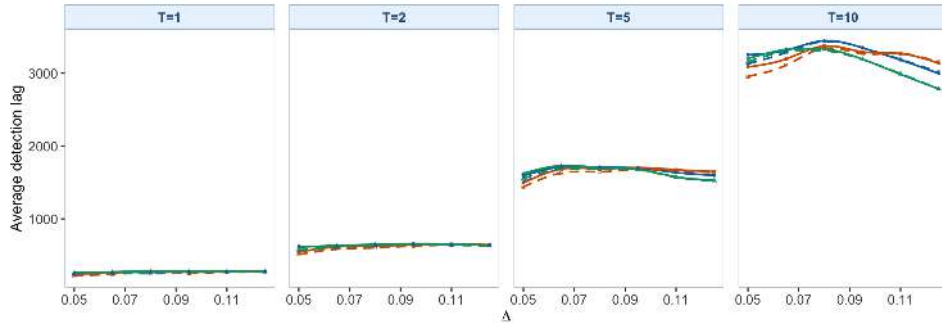
(b) IID DGP.



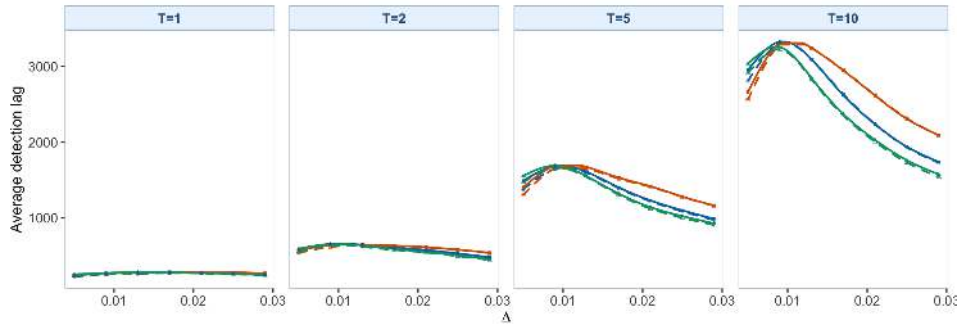
(c) fMA(1) DGP.

Figure S3.14: KS ADD curves for the level-shift setting. Lower curves indicate earlier post-break stopping, and the four internal columns in each subfigure correspond to  $T = 1, 2, 5, 10$ . The legend below the final subfigure identifies the six method-boundary combinations.

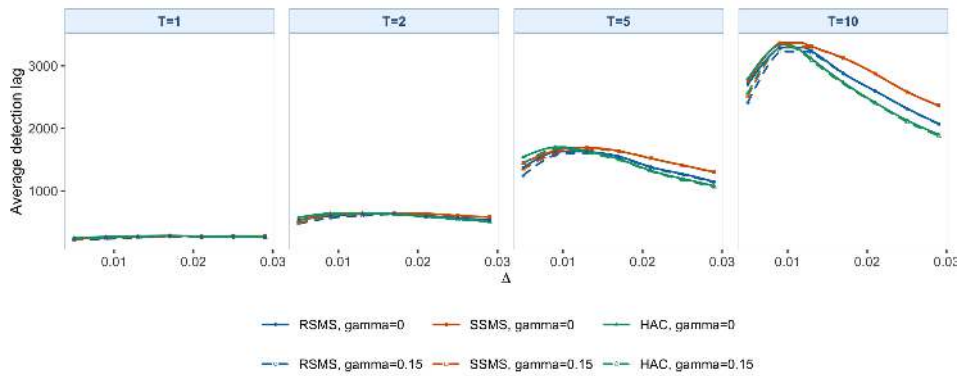
S3. SUPPLEMENTARY SIMULATION RESULTS



(a) BB DGP.

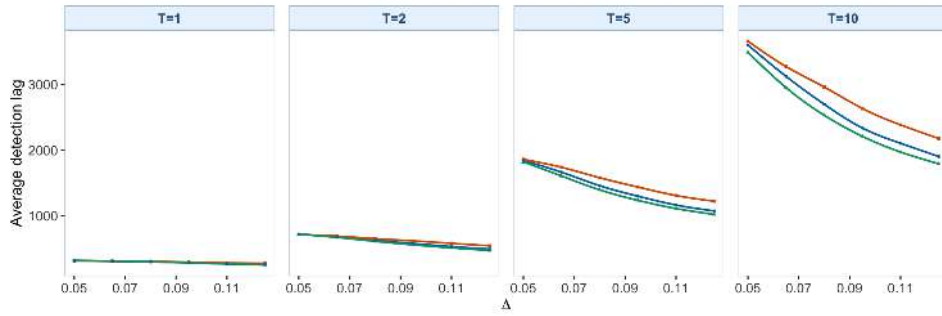


(b) IID DGP.

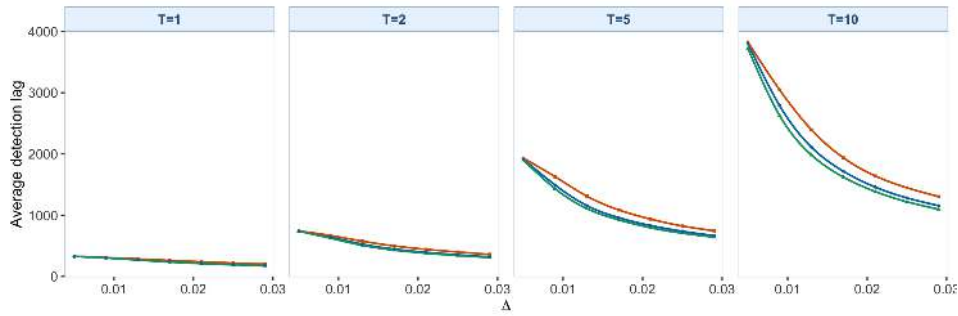


(c) fMA(1) DGP.

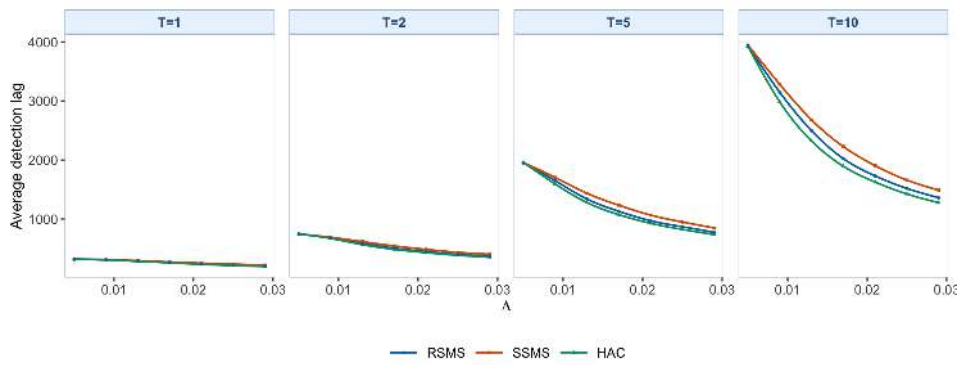
Figure S3.15: KS ADD curves for the smooth-change setting. Lower curves indicate earlier post-break stopping, and the four internal columns in each subfigure correspond to  $T = 1, 2, 5, 10$ . The legend below the final subfigure identifies the six method-boundary combinations.



(a) BB DGP.



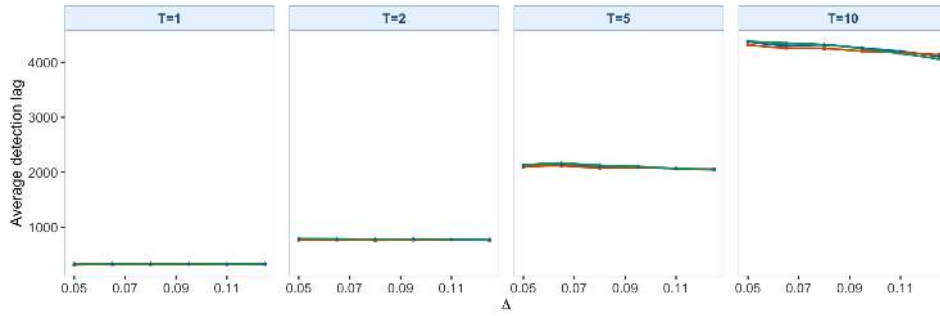
(b) IID DGP.



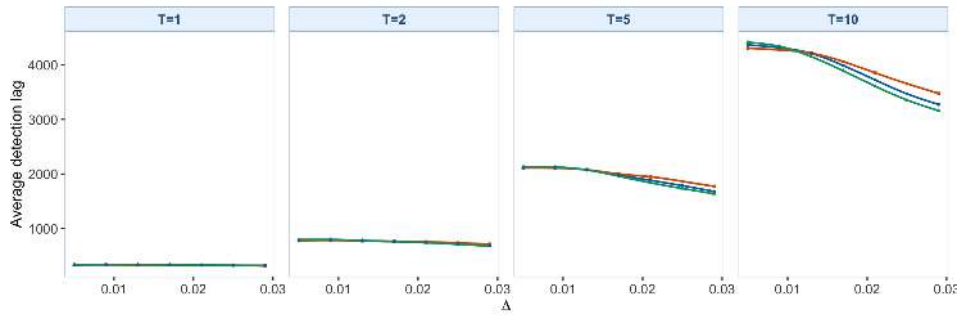
(c) fMA(1) DGP.

Figure S3.16: Late-weighted weighted-CvM ADD curves for the level-shift setting. The four internal columns in each subfigure correspond to  $T = 1, 2, 5, 10$ . The legend below the final subfigure identifies RSMS, SSMS, and HAC.

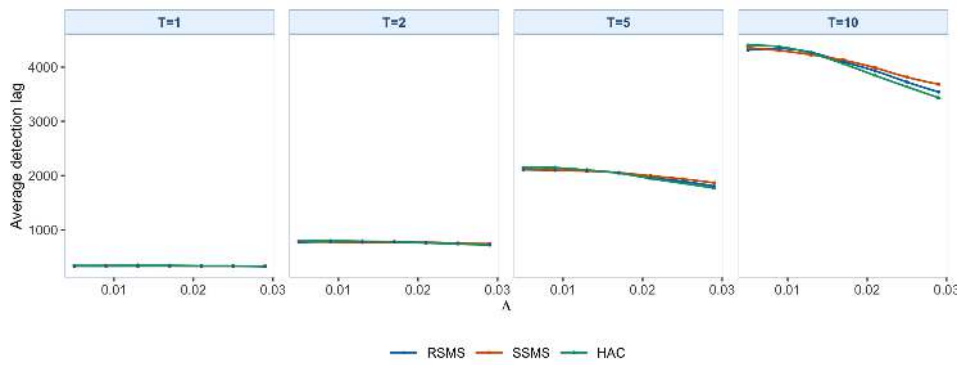
S3. SUPPLEMENTARY SIMULATION RESULTS



(a) BB DGP.

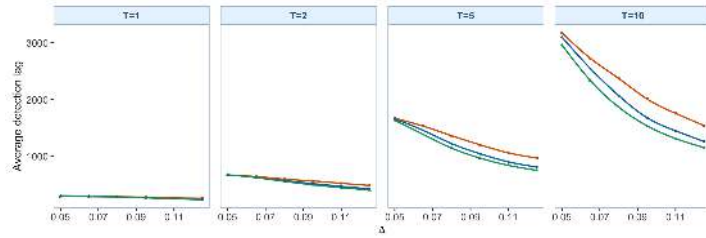


(b) IID DGP.

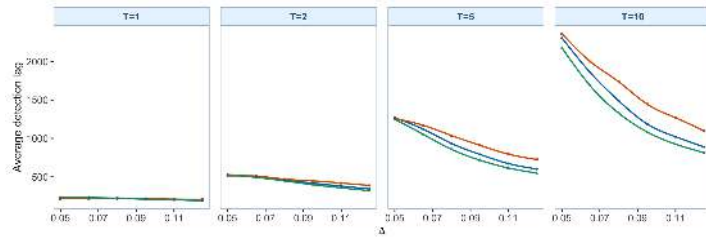


(c) fMA(1) DGP.

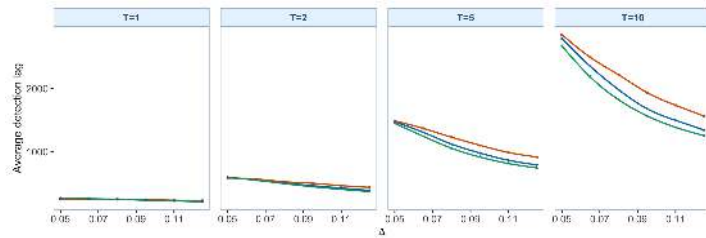
Figure S3.17: Late-weighted weighted-CvM ADD curves for the smooth-change setting. The four internal columns in each subfigure correspond to  $T = 1, 2, 5, 10$ . The legend below the final subfigure identifies RSMS, SSMS, and HAC.



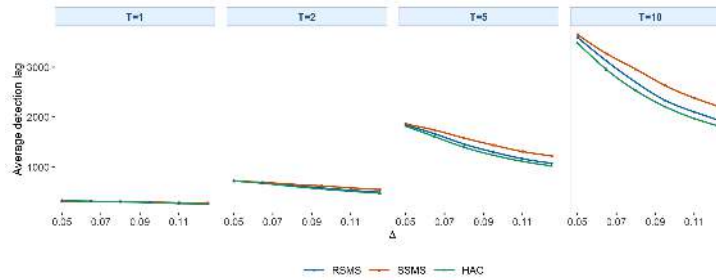
(a) Uniform weight  $w_U$ .



(b) Early-emphasis weight  $w_E$ .



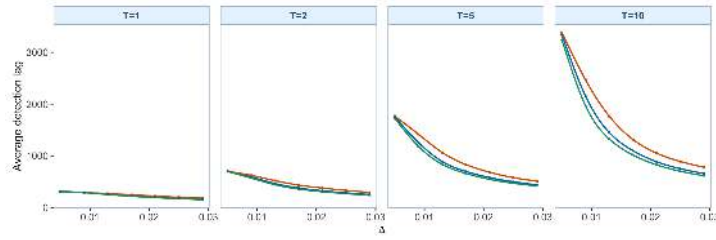
(c) Mid-emphasis weight  $w_M$ .



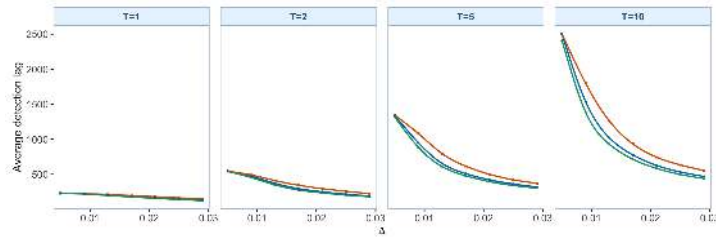
(d) Late-emphasis weight  $w_L$ .

Figure S3.18: Weighted-CvM ADD curves for the level-shift setting under the BB DGP. Each subfigure uses BB errors, and the four internal columns correspond to  $T = 1, 2, 5, 10$ . The legend below the final subfigure identifies RSMS, SSMS, and HAC.

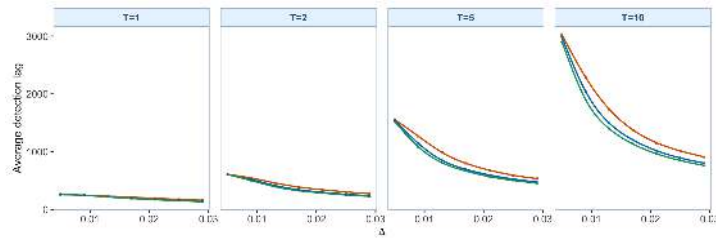
### S3. SUPPLEMENTARY SIMULATION RESULTS



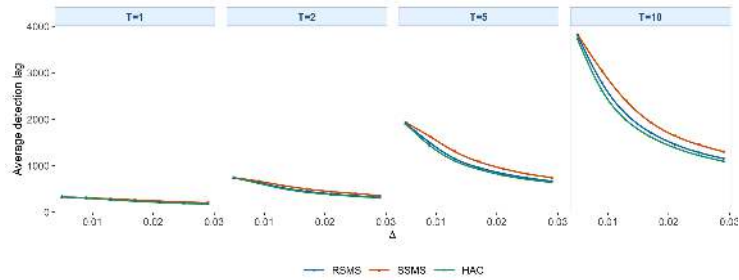
(a) Uniform weight  $w_U$ .



(b) Early-emphasis weight  $w_E$ .

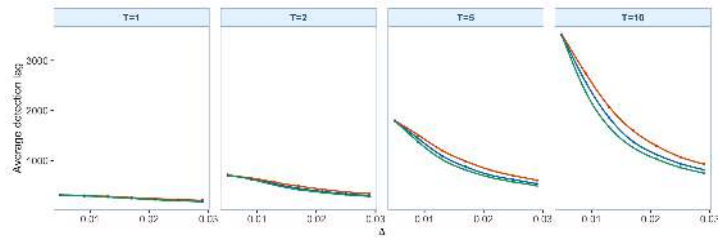


(c) Mid-emphasis weight  $w_M$ .

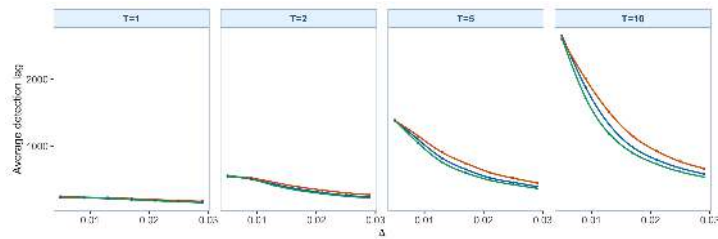


(d) Late-emphasis weight  $w_L$ .

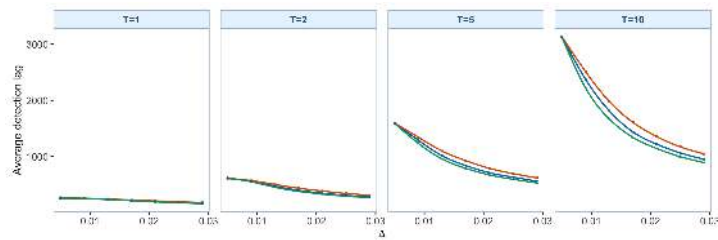
Figure S3.19: Weighted-CvM ADD curves for the level-shift setting under the IID DGP. Each subfigure uses IID errors, and the four internal columns correspond to  $T = 1, 2, 5, 10$ . The legend below the final subfigure identifies RSMS, SSMS, and HAC.



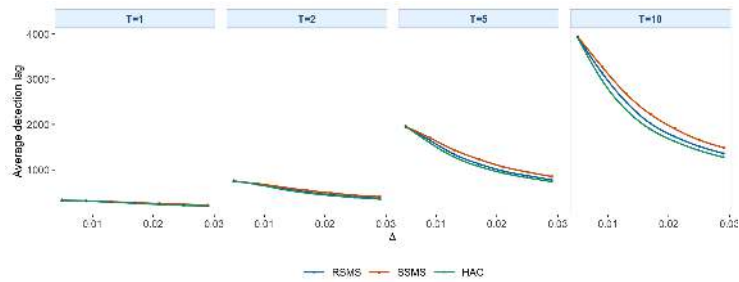
(a) Uniform weight  $w_U$ .



(b) Early-emphasis weight  $w_E$ .



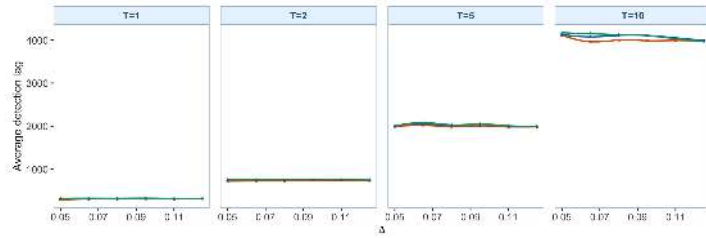
(c) Mid-emphasis weight  $w_M$ .



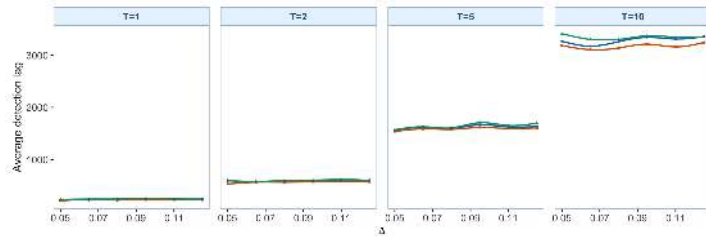
(d) Late-emphasis weight  $w_L$ .

Figure S3.20: Weighted-CvM ADD curves for the level-shift setting under the fMA(1) DGP. Each subfigure uses fMA(1) errors, and the four internal columns correspond to  $T = 1, 2, 5, 10$ . The legend below the final subfigure identifies RSMS, SSMS, and HAC.

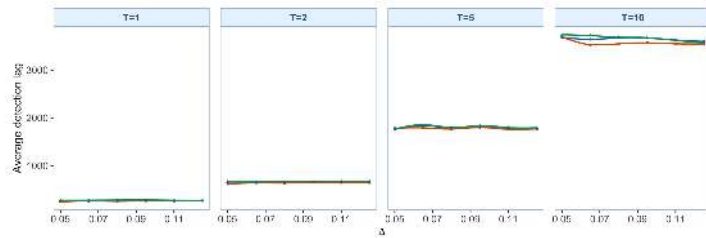
S3. SUPPLEMENTARY SIMULATION RESULTS



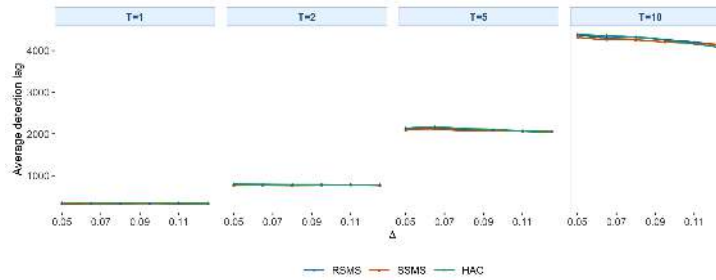
(a) Uniform weight  $w_U$ .



(b) Early-emphasis weight  $w_E$ .

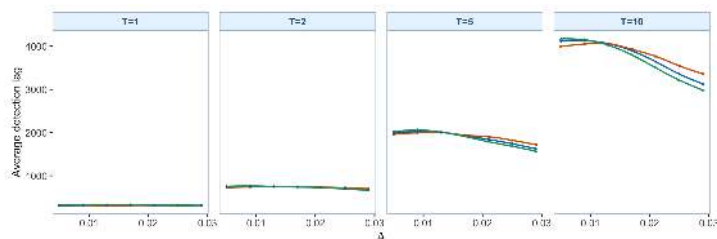


(c) Mid-emphasis weight  $w_M$ .

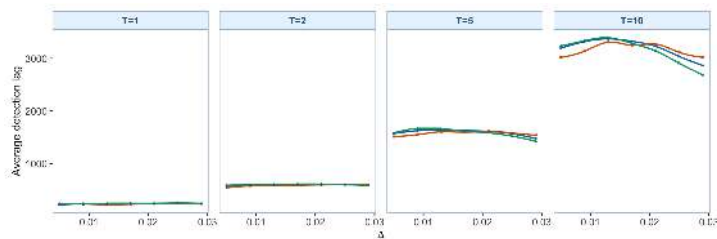


(d) Late-emphasis weight  $w_L$ .

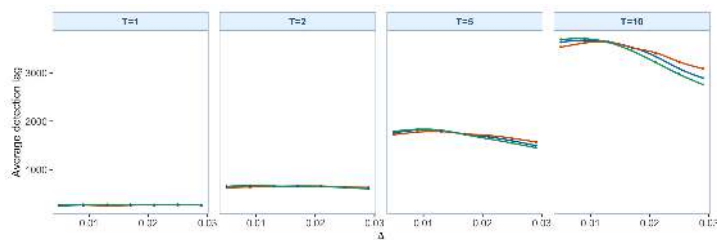
Figure S3.21: Weighted-CvM ADD curves for the smooth-change setting under the BB DGP. Each subfigure uses BB errors, and the four internal columns correspond to  $T = 1, 2, 5, 10$ . The legend below the final subfigure identifies RSMS, SSMS, and HAC.



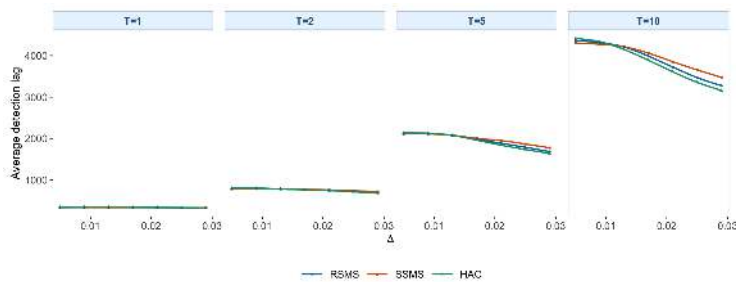
(a) Uniform weight  $w_U$ .



(b) Early-emphasis weight  $w_E$ .



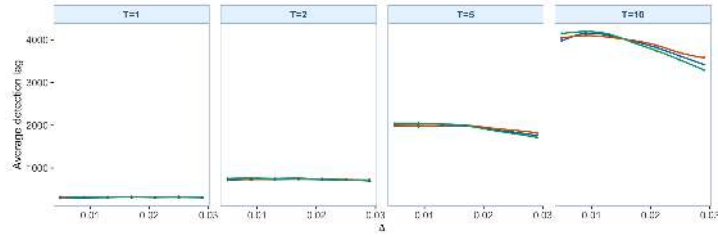
(c) Mid-emphasis weight  $w_M$ .



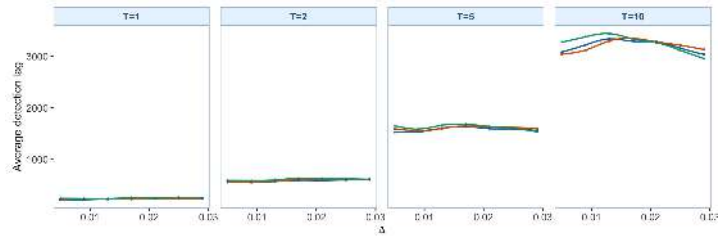
(d) Late-emphasis weight  $w_L$ .

Figure S3.22: Weighted-CvM ADD curves for the smooth-change setting under the IID DGP. Each subfigure uses IID errors, and the four internal columns correspond to  $T = 1, 2, 5, 10$ . The legend below the final subfigure identifies RSMS, SSMS, and HAC.

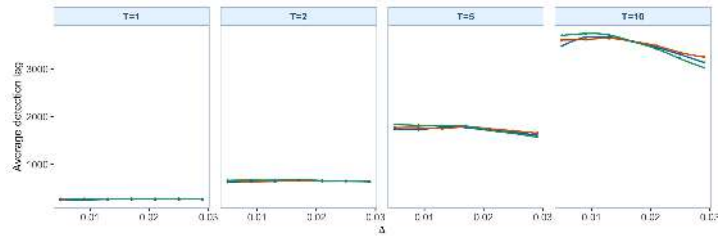
S3. SUPPLEMENTARY SIMULATION RESULTS



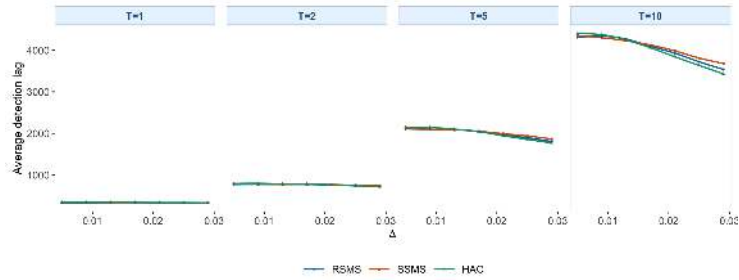
(a) Uniform weight  $w_U$ .



(b) Early-emphasis weight  $w_E$ .



(c) Mid-emphasis weight  $w_M$ .



(d) Late-emphasis weight  $w_L$ .

Figure S3.23: Weighted-CvM ADD curves for the smooth-change setting under the fMA(1) DGP. Each subfigure uses fMA(1) errors, and the four internal columns correspond to  $T = 1, 2, 5, 10$ . The legend below the final subfigure identifies RSMS, SSMS, and HAC.

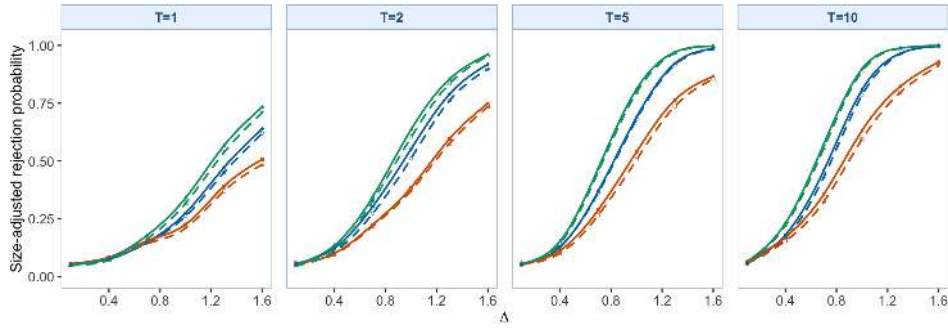
weighted-CvM, the late and uniform weights give the more stable delay patterns across these simulation settings, so the main paper treats weighted-CvM as a diagnostic companion to the KS statistic rather than as the main monitoring statistic.

### **S3.5 Localized-break simulation results for the main monitoring statistics**

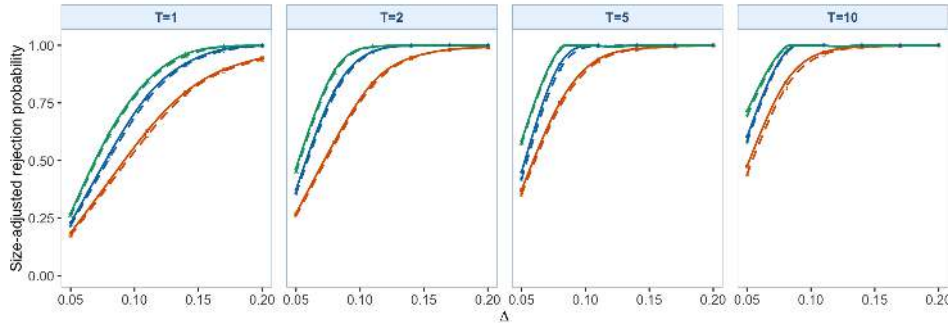
The localized-change setting changes only part of the function rather than the whole curve. The figures below report KS and late-weighted weighted-CvM results for BB, fIID, and fMA(1).

The localized-change setting shows that the ordering in Appendix S3.1 is not driven only by global level shifts. Across the three DGPs, RSMS remains above SSMS in most size-adjusted comparisons. HAC often has higher rejection rates and shorter ADD, but those differences should be interpreted together with its empirical size under the null.

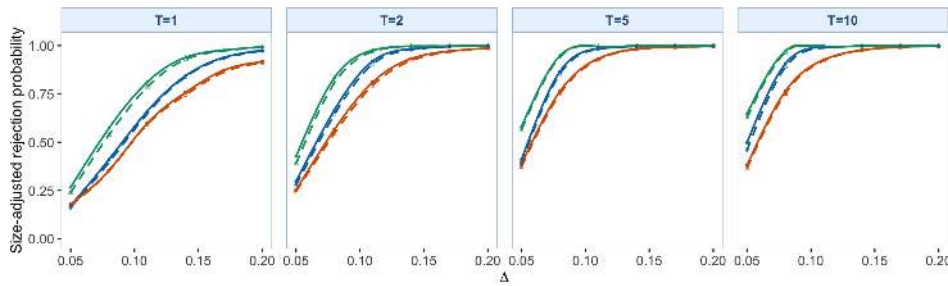
S3. SUPPLEMENTARY SIMULATION RESULTS



(a) BB DGP.



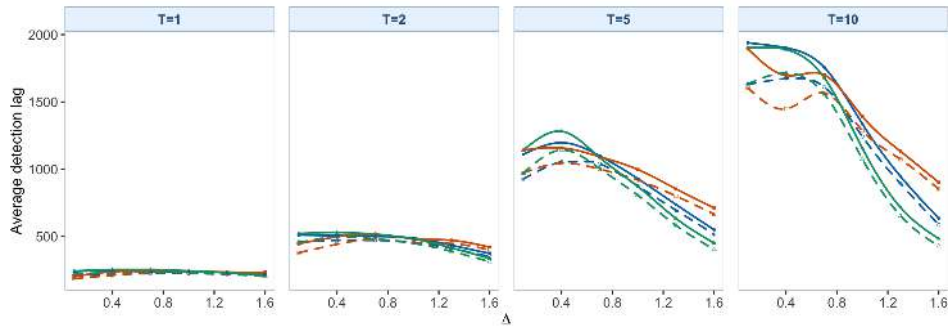
(b) IID DGP.



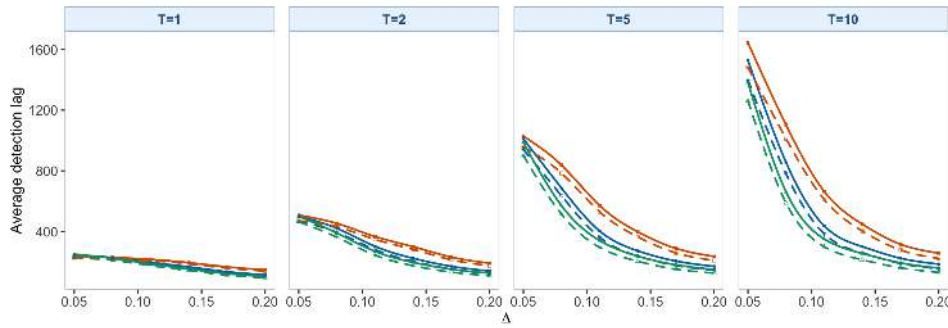
— RSMS,  $\gamma=0$       - - SSMS,  $\gamma=0$       - - HAC,  $\gamma=0$   
 - - RSMS,  $\gamma=0.15$       - - SSMS,  $\gamma=0.15$       - - HAC,  $\gamma=0.15$

(c) fMA(1) DGP.

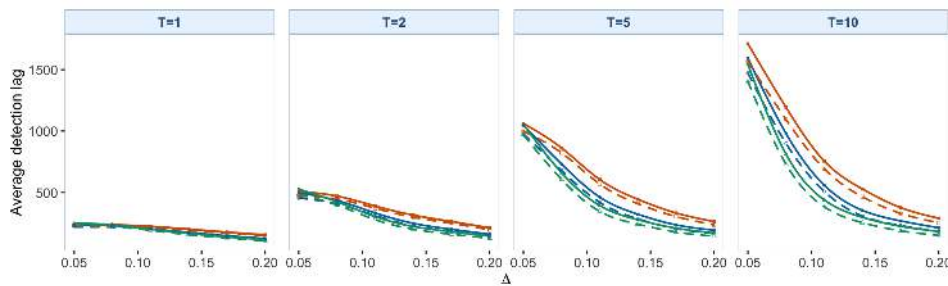
Figure S3.24: KS SAP curves for the localized-change setting. The four internal columns in each subfigure correspond to  $T = 1, 2, 5, 10$ . The legend below the final subfigure identifies the six method-boundary combinations.



(a) BB DGP.



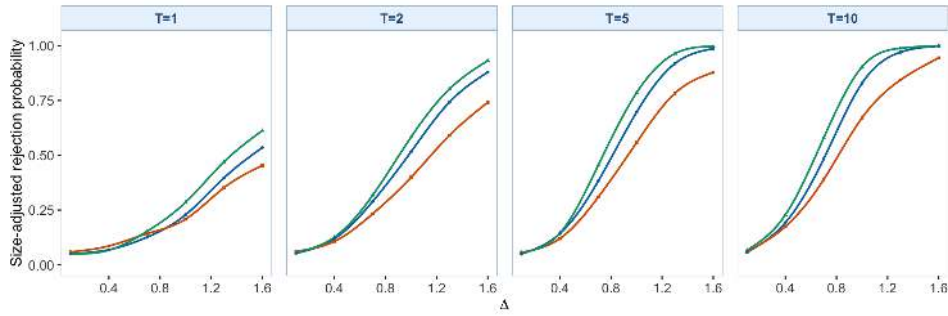
(b) fIID DGP.



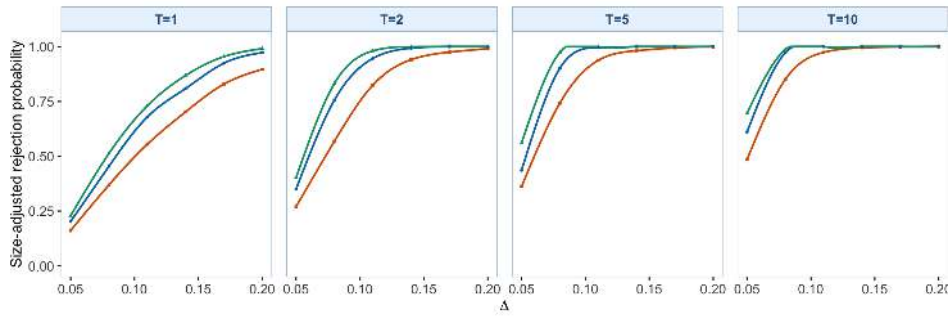
(c) fMA(1) DGP.

Figure S3.25: KS ADD curves for the localized-change setting. The four internal columns in each subfigure correspond to  $T = 1, 2, 5, 10$ . The legend below the final subfigure identifies the six method-boundary combinations.

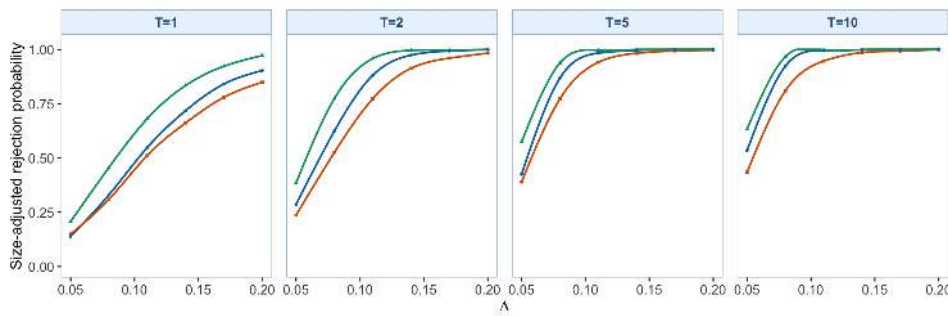
S3. SUPPLEMENTARY SIMULATION RESULTS



(a) BB DGP.



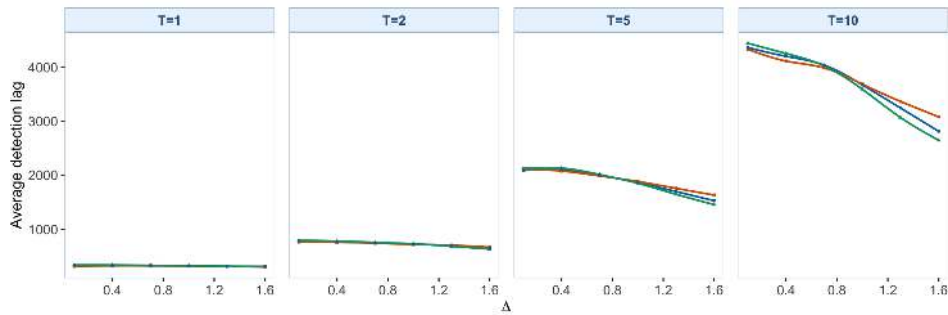
(b) IID DGP.



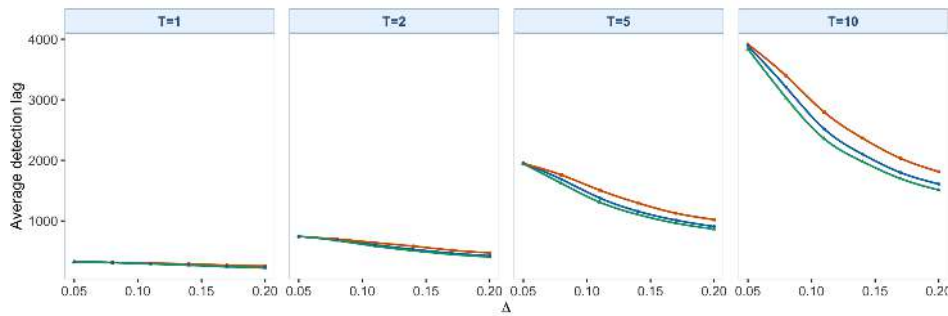
— RSMS — SSMS — HAC

(c) fMA(1) DGP.

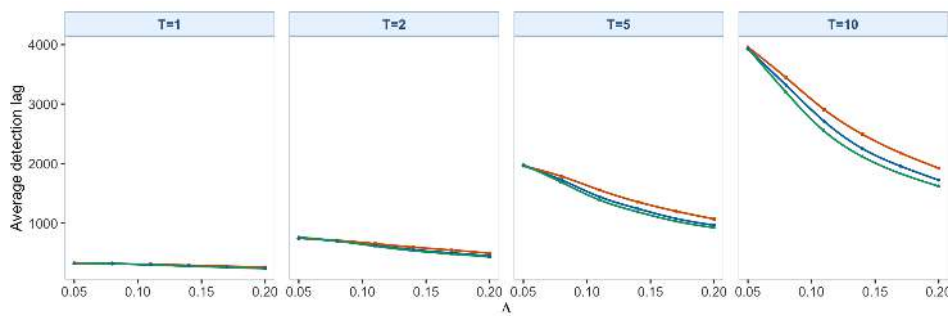
Figure S3.26: Late-weighted weighted-CvM SAP curves for the localized-change setting. The four internal columns in each subfigure correspond to  $T = 1, 2, 5, 10$ . The legend below the final subfigure identifies RSMS, SSMS, and HAC.



(a) BB DGP.



(b) IID DGP.



— RSMS — SSMS — HAC

(c) fMA(1) DGP.

Figure S3.27: Late-weighted weighted-CvM ADD curves for the localized-change setting. The four internal columns in each subfigure correspond to  $T = 1, 2, 5, 10$ . The legend below the final subfigure identifies RSMS, SSMS, and HAC.

### S3.6 Contaminated-training results for the main KS statistics

The main paper reports the fMA(1) contaminated-training figure and summarizes the three-DGP average over the mild range  $b_{\text{train}} \leq 0.005$ . This subsection gives the full three-DGP version. The setting has  $m = 1000$ ,  $T = 2$ , and a monitoring break at  $s^*/(mT) = 0.8$ .

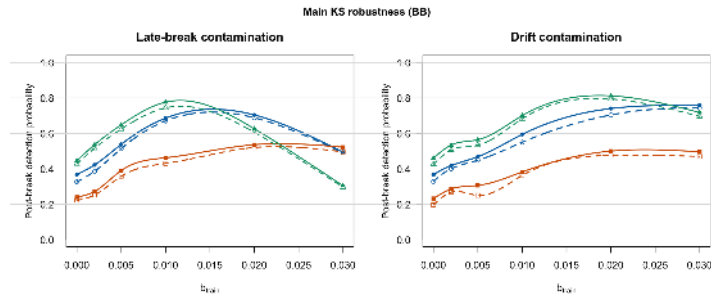
Table S3.4: Main KS contamination summary over the mild range  $b_{\text{train}} \leq 0.005$ .

DGP	Standardization	Post-break detection	Pre-break stopping
BB	RSMS	41.5	4.5
BB	SSMS	27.3	3.7
BB	HAC	51.9	5.5
fIID	RSMS	67.0	29.5
fIID	SSMS	66.5	15.7
fIID	HAC	61.2	37.2
fMA(1)	RSMS	53.9	15.5
fMA(1)	SSMS	38.5	9.7
fMA(1)	HAC	57.4	22.9
Overall	RSMS	54.2	16.5
Overall	SSMS	44.1	9.7
Overall	HAC	56.8	21.9

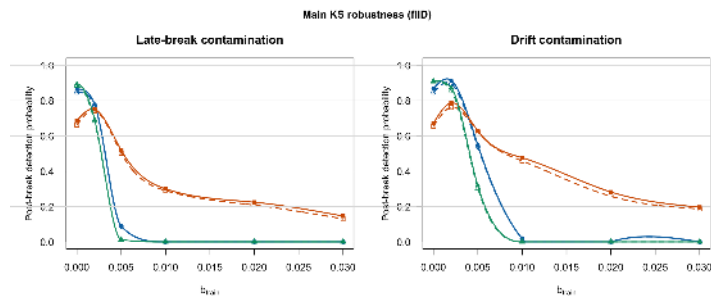
Note: Entries are percentages, averaged over late-break and drift contamination, both boundary exponents, and  $b_{\text{train}} \in \{0, 0.002, 0.005\}$ . The post-break column reports  $100 \times P(s^* < \tau_m \leq \lfloor mT \rfloor)$ , where  $\tau_m$  is the method-specific stopping time, and the pre-break column reports  $100 \times P(\tau_m \leq s^*)$ .

The full three-DGP results support the same conclusion as the main-paper summary. RSMS is usually close to HAC in post-break detection, but HAC has a higher pre-break stopping rate in fIID and fMA(1). SSMS stops less often before the monitoring break, but it also has weaker post-break detection in BB and fMA(1). This is why the paper treats RSMS KS as the main self-normalized statistic in the contaminated-training study.

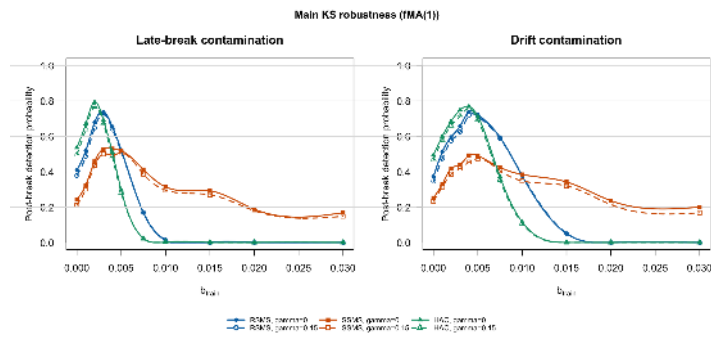
Contamination checks for selected CUSUM and MOSUM statistics follow. They are sensitivity checks using the same FPCA compression rather



(a) BB DGP.



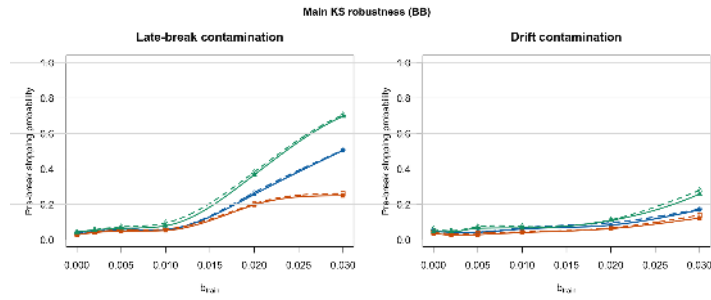
(b) fIID DGP.



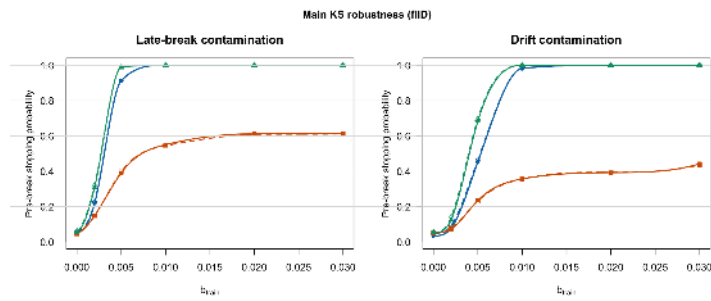
(c) fMA(1) DGP.

Figure S3.28: Post-break detection probabilities for the main KS statistics under contaminated training samples. Within each subfigure, the left internal panel is late-break contamination and the right internal panel is drift contamination. The legend below the final subfigure identifies the six method-boundary combinations.

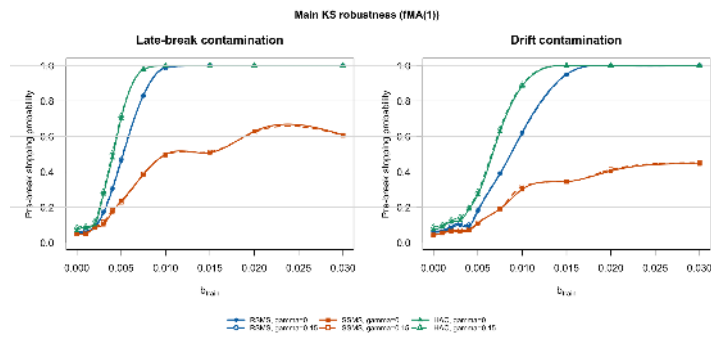
### S3. SUPPLEMENTARY SIMULATION RESULTS



(a) BB DGP.



(b) IID DGP.



(c) fMA(1) DGP.

Figure S3.29: Pre-break stopping probabilities for the main KS statistics under contaminated training samples. Within each subfigure, the left internal panel is late-break contamination and the right internal panel is drift contamination. The legend below the final subfigure identifies the six method-boundary combinations.

than the paper's default monitoring statistics.

### S3.7 Selected supplementary CUSUM and MOSUM monitoring statistics

Table S3.5: Effect of mild training contamination on the reported CUSUM-style monitoring statistics under the fMA(1) setting. Entries are post-break detection probabilities (in %) for each contamination setting and  $b_{\text{train}}$ , averaged over 1000 Monte Carlo replications. Configuration: level-shift setting, fMA(1) errors,  $m = 1000$ ,  $T = 2$ ,  $s^*/(mT) = 0.8$ , and  $\alpha = 0.05$ .

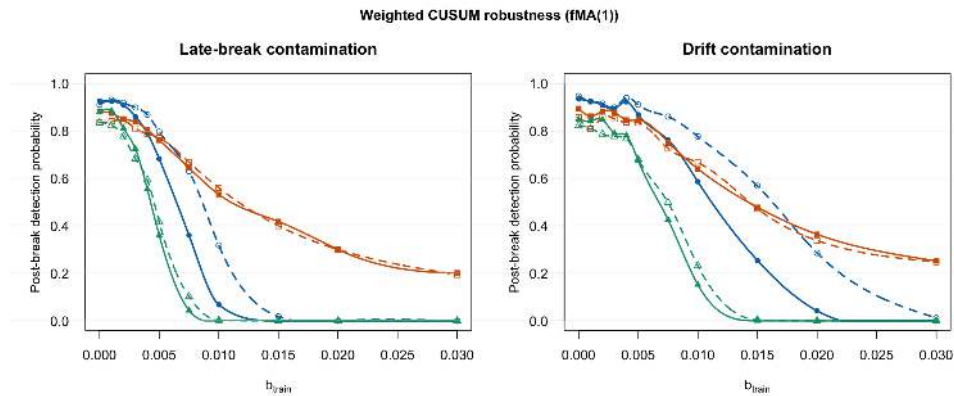
Panel A: Late-break contamination						
Method	$b_{\text{train}}$					
	0.000	0.002	0.005	0.010	0.020	0.030
RSMS Weighted CUSUM, $\gamma = 0$	92.6	90.8	68.2	6.8	0.0	0.0
RSMS Weighted CUSUM, $\gamma = 0.15$	91.0	91.8	79.6	31.8	0.0	0.0
SSMS Weighted CUSUM, $\gamma = 0$	88.0	85.0	76.0	53.2	30.0	20.2
SSMS Weighted CUSUM, $\gamma = 0.15$	83.6	84.4	77.0	56.0	30.0	19.4
HAC Weighted CUSUM, $\gamma = 0$	88.0	81.0	36.0	0.0	0.0	0.0
HAC Weighted CUSUM, $\gamma = 0.15$	83.4	77.6	41.6	0.2	0.0	0.0
RSMS Page-CUSUM, $\gamma = 0$	94.0	92.0	58.4	2.4	0.0	0.0
RSMS Page-CUSUM, $\gamma = 0.15$	94.4	91.2	60.0	2.8	0.0	0.0
SSMS Page-CUSUM, $\gamma = 0$	78.2	81.4	67.6	41.6	24.0	20.8
SSMS Page-CUSUM, $\gamma = 0.15$	85.4	84.2	69.2	44.8	25.2	21.4
HAC Page-CUSUM, $\gamma = 0$	92.8	89.4	31.4	0.0	0.0	0.0
HAC Page-CUSUM, $\gamma = 0.15$	91.8	87.8	31.2	0.0	0.0	0.0

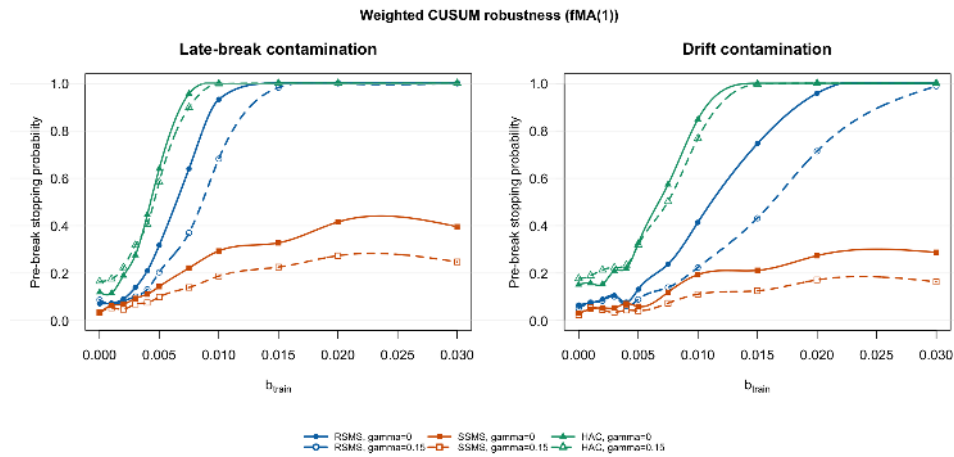
Panel B: Drift contamination						
Method	$b_{\text{train}}$					
	0.000	0.002	0.005	0.010	0.020	0.030
RSMS Weighted CUSUM, $\gamma = 0$	93.4	90.8	86.8	58.6	4.2	0.0
RSMS Weighted CUSUM, $\gamma = 0.15$	94.6	91.4	91.0	77.6	28.6	1.2
SSMS Weighted CUSUM, $\gamma = 0$	89.4	88.2	84.6	64.0	36.4	25.2
SSMS Weighted CUSUM, $\gamma = 0.15$	85.6	85.8	83.4	66.6	33.8	24.8
HAC Weighted CUSUM, $\gamma = 0$	84.8	84.6	67.4	15.2	0.0	0.0
HAC Weighted CUSUM, $\gamma = 0.15$	82.2	78.6	68.0	23.2	0.0	0.0
RSMS Page-CUSUM, $\gamma = 0$	93.4	90.6	84.8	46.0	0.4	0.0
RSMS Page-CUSUM, $\gamma = 0.15$	93.8	90.6	84.6	48.6	1.4	0.0
SSMS Page-CUSUM, $\gamma = 0$	80.4	81.8	77.4	55.0	31.4	27.0
SSMS Page-CUSUM, $\gamma = 0.15$	86.2	85.6	80.2	58.8	31.6	26.8
HAC Page-CUSUM, $\gamma = 0$	91.4	89.4	73.4	13.6	0.0	0.0
HAC Page-CUSUM, $\gamma = 0.15$	90.2	87.8	71.2	14.0	0.0	0.0

Note: The weighted-CUSUM rows use the fixed segment-length weight  $\omega(\ell) = \ell^{-1/2}$ . The Page-CUSUM rows are reported as restart comparators and should be read together with weighted CUSUM and the premature-stopping panels.

The reported CUSUM-style statistics provide a robustness check for the contaminated-training experiment by comparing post-break detection



(a) Post-break detection probabilities for the reported CUSUM-style supplementary statistics. The left internal panel is late-break contamination and the right internal panel is drift contamination.



(b) Pre-break stopping probabilities for the reported CUSUM-style supplementary statistics. The left internal panel is late-break contamination and the right internal panel is drift contamination.

Figure S3.30: Effect of mild training contamination on weighted-CUSUM monitoring under the  $fMA(1)$  setting,  $m = 1000$ ,  $T = 2$ , and  $s^*/(mT) = 0.8$ . The legend below the final subfigure identifies the six method-boundary combinations. The corresponding Page-CUSUM results are reported in Table S3.5.

S3. SUPPLEMENTARY SIMULATION RESULTS

---

with pre-break stopping under the same contaminated training samples. In the mild range  $b_{\text{train}} \leq 0.005$ , RSMS weighted CUSUM has an average post-break detection probability of 88.5% in the fMA(1) setting. RSMS Page-CUSUM is close, at 85.7%, but the weighted-CUSUM rows are more favorable when post-break detection and pre-break stopping are read together. The SSMS rows are more conservative: premature-stopping rates are lower, but so is post-break detection. HAC weighted CUSUM and HAC Page-CUSUM remain competitive in raw post-break detection at the mildest contamination levels, but Figure S3.30 reports higher pre-break stopping probabilities.

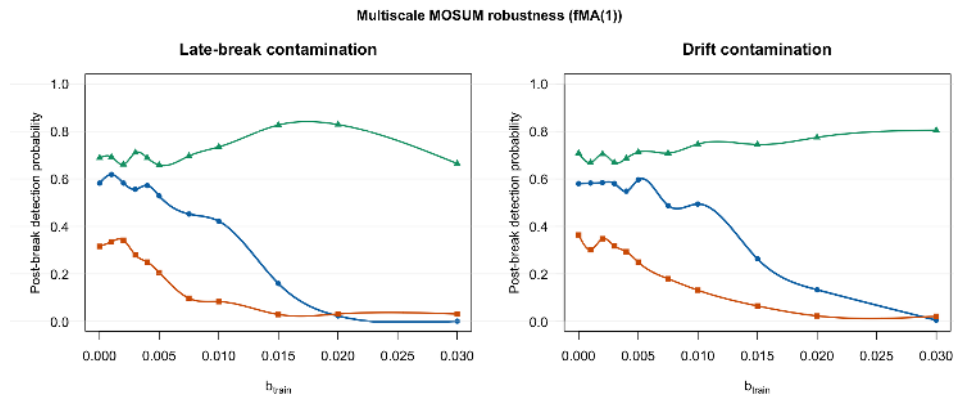
Table S3.6: Effect of mild training contamination on post-break detection for the multiscale MOSUM statistic under the fMA(1) setting. Entries are post-break detection probabilities (in %) for each contamination setting and  $b_{\text{train}}$ , averaged over 1000 Monte Carlo replications. Configuration: level-shift setting, fMA(1) errors,  $m = 1000$ ,  $T = 2$ ,  $s^*/(mT) = 0.8$ , and  $\alpha = 0.05$ . The multiscale scan uses the bandwidth set  $\mathcal{H} = \{0.05, 0.10, 0.20\}$  with equal scale weights.

<b>Panel A: Late-break contamination</b>						
Method	$b_{\text{train}}$					
	0.000	0.002	0.005	0.010	0.020	0.030
RSMS Multiscale MOSUM	58.2	58.2	52.8	42.2	2.4	0.2
SSMS Multiscale MOSUM	31.6	34.2	20.6	8.4	3.2	3.2
HAC Multiscale MOSUM	68.8	66.0	65.8	73.4	82.8	66.4

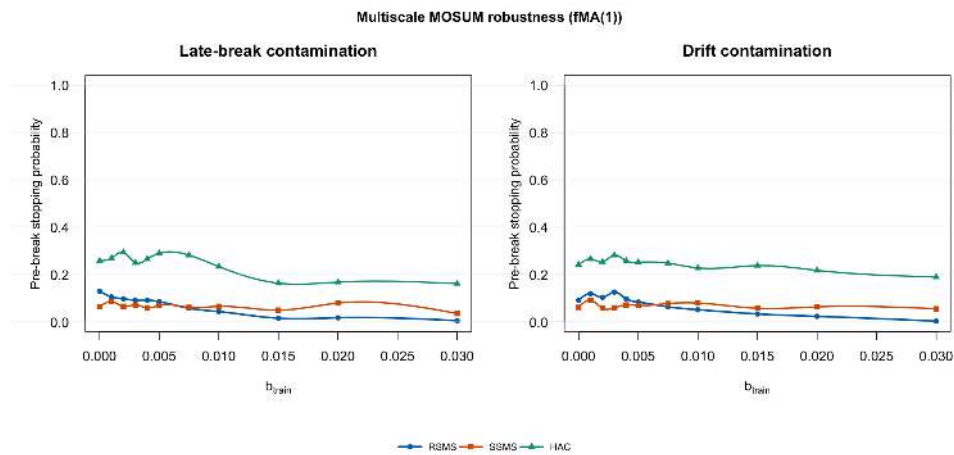
  

<b>Panel B: Drift contamination</b>						
Method	$b_{\text{train}}$					
	0.000	0.002	0.005	0.010	0.020	0.030
RSMS Multiscale MOSUM	58.0	58.4	59.6	49.4	13.4	0.6
SSMS Multiscale MOSUM	36.4	34.8	25.0	13.2	2.4	2.2
HAC Multiscale MOSUM	70.8	70.4	71.2	74.6	77.4	80.4

Note: The multiscale scan uses the bandwidth set  $\mathcal{H} = \{0.05, 0.10, 0.20\}$  with equal scale weights.



(a) Post-break detection probabilities for the multiscale MOSUM statistic. The left internal panel is late-break contamination and the right internal panel is drift contamination.



(b) Pre-break stopping probabilities for the same multiscale MOSUM statistic. The left internal panel is late-break contamination and the right internal panel is drift contamination.

Figure S3.31: Effect of mild training contamination on multiscale MOSUM monitoring under the fMA(1) setting,  $m = 1000$ ,  $T = 2$ , and  $s^*/(mT) = 0.8$ . The legend below the final subfigure identifies RSMS, SSMS, and HAC.

The multiscale MOSUM rows separate the statistic form from the standardization. HAC multiscale MOSUM has the highest post-break detection rates in this table, including beyond the mild contamination range, but Figure S3.31 also reports much higher premature-stopping rates. RSMS multiscale MOSUM increases post-break detection relative to SSMS while keeping premature stopping below HAC. In this fMA(1) experiment, RSMS weighted CUSUM gives a clearer tradeoff between post-break detection and premature stopping, so the discussion emphasizes that statistic.

## S4 Supplementary Monitoring Statistics

This section defines supplementary CUSUM and MOSUM monitoring statistics that use the same FPCA-compressed score stream as the main paper. The comparison separates the statistic form from the standardization. The statistic form determines whether the monitoring statistic uses the full post-training sum, restarts over recent segments, compares adjacent windows, or scans over several window widths. The standardization determines whether nuisance scale and dependence are handled by a HAC LRV estimator, Shao's self-normalizer, or the adjusted-range self-normalizer. This separation follows the sequential-monitoring taxonomy reviewed by Aue and Kirch (2024): the statistic form determines how score information

is accumulated over time, while standardization controls nuisance scale under dependence.

To match the critical-value tables, we write  $q$  for the retained score dimension in this appendix; it plays the same role here as the retained dimension  $K$  in the paper. Define the raw scores based on the training-sample eigenfunctions and their training mean by

$$a_t = (\langle X_t, \hat{\phi}_1 \rangle, \dots, \langle X_t, \hat{\phi}_q \rangle)^\top \in \mathbb{R}^q, \quad t \geq 1, \quad \bar{a}_m = m^{-1} \sum_{t=1}^m a_t.$$

The centered score vector is  $z_t = a_t - \bar{a}_m$ , equivalently

$$z_t = (\langle X_t - \hat{\mu}_m, \hat{\phi}_1 \rangle, \dots, \langle X_t - \hat{\mu}_m, \hat{\phi}_q \rangle)^\top.$$

Thus  $\sum_{t=1}^m z_t = 0$  on the training sample, and the monitoring-statistic contrasts below use the same training-centered score stream as the main paper.

The generic long-run covariance of the retained score stream is written as  $\Sigma_q$ , and the corresponding training-sample standardization objects are denoted by  $\hat{\Gamma}_m$  (HAC),  $D_m$  (Shao self-normalizer), and  $\tilde{R}_m$  (adjusted-range self-normalizer). For integers  $0 \leq j < k$ , define

$$C_m(k) = \sum_{t=m+1}^{m+k} z_t, \quad C_m(j, k) = \sum_{t=m+j+1}^{m+k} z_t,$$

so that  $C_m(k)$  is the full post-training score sum up to time  $k$ , whereas  $C_m(j, k)$  is the score contrast on the shorter segment  $(m + j, m + k]$ . For MOSUM-type statistics with bandwidth  $G_m = \lfloor mh \rfloor$ ,  $h > 0$ , define also the adjacent-window contrast

$$\Delta_m(k; G_m) = \sum_{t=m+k-G_m+1}^{m+k} z_t - \sum_{t=m+k-2G_m+1}^{m+k-G_m} z_t, \quad 2G_m \leq k.$$

#### S4.1 Interpretation of the numerator and denominator

Each monitoring statistic below has the same basic structure. The numerator is a quadratic form in one of the score contrasts above. It converts a  $q$ -dimensional deviation from the no-change restriction into a scalar measure of instability. The denominator has two roles. First, the standardizer or self-normalizer ( $\widehat{\Gamma}_m$ ,  $D_m$ , or  $\widetilde{R}_m$ ) removes nuisance scale and serial dependence. Second, the time-length factor puts contrasts computed over different segment lengths on a common scale. For full-history and restart-type statistics this uses the standard boundary

$$g_\gamma(s) = (1 + s) \left( \frac{s}{1 + s} \right)^\gamma, \quad \gamma \in [0, 1/2),$$

which is the same boundary family used in the main paper. For MOSUM-type statistics, the relevant variance scale is proportional to the window

length, so the denominator is of order  $G_m$  rather than of order  $m$ . The parameter  $\gamma$  controls how sharply the boundary penalizes very early monitoring times; larger  $\gamma$  reduces early boundary crossings near the start of the monitoring period. Boundary-weighted sequential monitoring of this kind follows the econometric monitoring logic of Chu et al. (1996) and the CUSUM-monitoring review of Aue and Kirch (2024).

Under the same strong-approximation assumptions used in the paper,

$$\frac{1}{\sqrt{m}}C_m(\lfloor ms \rfloor) \Rightarrow U_q(s), \quad \frac{1}{\sqrt{m}}C_m(\lfloor mu \rfloor, \lfloor mv \rfloor) \Rightarrow \mathbb{U}_q(u, v),$$

where

$$U_q(s) = B_q(1+s) - (1+s)B_q(1), \quad \mathbb{U}_q(u, v) = U_q(v) - U_q(u), \quad 0 \leq u < v,$$

and  $B_q$  is a standard  $q$ -dimensional Brownian motion. For MOSUM-type limits it is convenient to write

$$\Delta_h U_q(s) = U_q(s) - 2U_q(s-h) + U_q(s-2h), \quad s \geq 2h.$$

Thus the null laws below are Gaussian functionals of either the one-parameter bridge  $U_q$ , the two-parameter increment field  $\mathbb{U}_q$ , or the local-window field  $\Delta_h U_q$ .

## S4.2 How the literature compares these monitoring statistics

This subsection places the supplementary statistics in the existing monitoring literature. CUSUM and Page-CUSUM monitoring are discussed in Aue and Kirch (2024), and weighted-CUSUM statistics for short detection delay are developed by Kutta and Dörnemann (2025). MOSUM and multiscale MOSUM methods are treated by Eichinger and Kirch (2018) and Cho and Kirch (2022); Kutta et al. (2026) provide a functional full-window CUSUM statistic after dimension reduction. For the broader functional-data and object-valued context, Chu et al. (1996) explain why repeated retrospective tests are invalid for monitoring, Berkes et al. (2009) give an FPCA-based mean-change test, Aue et al. (2018) avoid dimension reduction, Aston and Kirch (2012) study dependent and epidemic functional changes, Horváth et al. (2010) test a functional autoregressive operator, Aue et al. (2014) study monitoring in dependent functional regression, Kutta and Kokoszka (2025) treat Banach-space monitoring, Bastian et al. (2024) study multiple functional changes, Boniece et al. (2025) use empirical energy distance for dependent functional observations, Zhang et al. (2026) study object-valued time series, Sharipov et al. (2016) develop a Hilbert-space block bootstrap, and Hörmann et al. (2015) develop dynamic FPCA. Full-history statistics are simple and often effective for early breaks, but they can dilute late

changes because many pre-change monitoring observations remain in the cumulative sum. Restart-type statistics such as Page-CUSUM address this issue by maximizing over recent starting points. MOSUM statistics localize the contrast by comparing adjacent windows, which can improve sensitivity to late or localized changes but introduces a bandwidth choice.

### S4.3 Kernel-based LRV monitoring statistics

Assume throughout this subsection that the same weak-dependence, score-process, and HAC LRV conditions used in the main paper hold for a fixed finite horizon  $T < \infty$ . The stopping time is always the first boundary crossing of the corresponding statistic path, with the convention that the stopping time equals  $\infty$  if no crossing occurs.

**Full-Window CUSUM** The full-window monitoring statistic with kernel-based LRV scaling is

$$\mathcal{F}_m^H(k) = \frac{C_m(k)^\top \widehat{\Gamma}_m^{-1} C_m(k)}{m g_\gamma(k/m)^2}, \quad 1 \leq k \leq \lfloor mT \rfloor.$$

The numerator uses the entire post-training score history up to time  $k$ , so it is large when the cumulative score imbalance from the start of monitoring is large. The denominator rescales that cumulative contrast by the natural  $m$ -

order variance and the monitoring boundary  $g_\gamma$ . The finite-horizon stopping time is

$$\tau_{m,\alpha}^{\text{FC,H}}(T) = \inf \left\{ 1 \leq k \leq \lfloor mT \rfloor : \mathcal{F}_m^{\text{H}}(k) > c_\alpha^{\text{FC,H}}(T, q, \gamma) \right\},$$

Under  $H_0$ ,

$$\sup_{1 \leq k \leq \lfloor mT \rfloor} \mathcal{F}_m^{\text{H}}(k) \Rightarrow \sup_{0 < s \leq T} \frac{U_q(s)^\top \Sigma_q^{-1} U_q(s)}{g_\gamma(s)^2},$$

**Page-CUSUM** A restart-type statistic is obtained by scanning all lower endpoints:

$$\mathcal{P}_m^{\text{H}}(k) = \max_{0 \leq j < k} \frac{C_m(j, k)^\top \widehat{\Gamma}_m^{-1} C_m(j, k)}{m g_\gamma \{(k - j)/m\}^2}, \quad 1 \leq k \leq \lfloor mT \rfloor.$$

Here the numerator is the standardized score imbalance over the recent segment ending at time  $k$  that gives the largest value. This avoids forcing all monitoring observations since time  $m + 1$  into the same contrast and is therefore less prone than full-window CUSUM to dilution from old pre-change observations. The stopping time is

$$\tau_{m,\alpha}^{\text{Page,H}}(T) = \inf \left\{ 1 \leq k \leq \lfloor mT \rfloor : \mathcal{P}_m^{\text{H}}(k) > c_\alpha^{\text{Page,H}}(T, q, \gamma) \right\},$$

Under  $H_0$ ,

$$\sup_{1 \leq k \leq \lfloor mT \rfloor} \mathcal{P}_m^H(k) \Rightarrow \sup_{0 < v \leq T} \sup_{0 \leq u < v} \frac{\mathbb{U}_q(u, v)^\top \Sigma_q^{-1} \mathbb{U}_q(u, v)}{g_\gamma(v - u)^2},$$

**MOSUM** Fix a bandwidth sequence  $G_m = \lfloor mh \rfloor$  with  $h \in (0, T/2)$ . The adjacent-window HAC monitoring statistic is

$$\mathcal{O}_m^H(k; G_m) = \frac{\Delta_m(k; G_m)^\top \widehat{\Gamma}_m^{-1} \Delta_m(k; G_m)}{G_m}, \quad 2G_m \leq k \leq \lfloor mT \rfloor.$$

The numerator compares the most recent block of length  $G_m$  with the immediately preceding block of the same length, so MOSUM reacts to local rather than full-history discrepancies. The denominator is  $G_m$  because the variance of a local window contrast is proportional to the window length.

The stopping time is

$$\tau_{m, \alpha}^{\text{MOS, H}}(T; h) = \inf \left\{ 2G_m \leq k \leq \lfloor mT \rfloor : \mathcal{O}_m^H(k; G_m) > c_\alpha^{\text{MOS, H}}(T, q, h) \right\},$$

Under  $H_0$ ,

$$\sup_{2G_m \leq k \leq \lfloor mT \rfloor} \mathcal{O}_m^H(k; G_m) \Rightarrow \sup_{2h \leq s \leq T} \frac{\Delta_h U_q(s)^\top \Sigma_q^{-1} \Delta_h U_q(s)}{h},$$

**Weighted-CUSUM and multiscale MOSUM** Let  $\omega : [0, \infty) \rightarrow (0, \infty)$  be a deterministic segment-length weight chosen so that the limiting supremum is finite under the null. A weighted-CUSUM monitoring statistic can be written as

$$\mathcal{W}_m^H(k) = \max_{0 \leq j < k} \omega\{(k-j)/m\} \frac{C_m(j, k)^\top \widehat{\Gamma}_m^{-1} C_m(j, k)}{m g_\gamma\{(k-j)/m\}^2}, \quad 1 \leq k \leq \lfloor mT \rfloor.$$

Relative to Page-CUSUM, the additional segment-length weight  $\omega$  allows the monitoring statistic to emphasize shorter or longer recent segments.

The stopping time is

$$\tau_{m, \alpha}^{\text{wC,H}}(T) = \inf \left\{ 1 \leq k \leq \lfloor mT \rfloor : \mathcal{W}_m^H(k) > c_\alpha^{\text{wC,H}}(T, q, \gamma, \omega) \right\}.$$

Under  $H_0$ ,

$$\sup_{1 \leq k \leq \lfloor mT \rfloor} \mathcal{W}_m^H(k) \Rightarrow \sup_{0 < v \leq T} \sup_{0 \leq u < v} \omega(v-u) \frac{\mathbb{U}_q(u, v)^\top \Sigma_q^{-1} \mathbb{U}_q(u, v)}{g_\gamma(v-u)^2},$$

A multiscale MOSUM monitoring statistic is obtained by scanning a set of bandwidths  $\mathcal{H} \subset (0, \infty)$ :

$$\mathcal{MS}_m^H(k) = \max_{h \in \mathcal{H}_m(k)} a(h) \mathcal{O}_m^H(k; \lfloor mh \rfloor), \quad \mathcal{H}_m(k) = \{h \in \mathcal{H} : 2\lfloor mh \rfloor \leq k\},$$

where  $a(h)$  is a deterministic scale weight. The numerator remains the local MOSUM contrast, while  $a(h)$  governs how heavily each window width enters the scan. The associated stopping time is the first crossing of a critical value  $c_\alpha^{\text{MS,H}}(T, q, \mathcal{H}, a)$ . Under  $H_0$ ,

$$\sup_{1 \leq k \leq \lfloor mT \rfloor} \mathcal{MS}_m^{\text{H}}(k) \Rightarrow \sup_{0 < s \leq T} \sup_{h \in \mathcal{H}(s)} a(h) \frac{\Delta_h U_q(s)^\top \Sigma_q^{-1} \Delta_h U_q(s)}{h},$$

where  $\mathcal{H}(s) = \{h \in \mathcal{H} : 2h \leq s\}$ . This statistic reduces sensitivity to any single bandwidth choice by scanning the chosen bandwidth set.

#### S4.4 Replacing HAC by Shao's or adjusted-range SN

The same statistic forms can be paired with the self-normalizers from the main paper. For Shao's version one replaces  $\widehat{\Gamma}_m^{-1}$  everywhere above by  $D_m^{-1}$ . For the adjusted-range version, the monitoring contrasts are first transformed by the same training-sample whitening matrix used to construct  $\widetilde{R}_m$ :

$$\begin{aligned} \widetilde{C}_m(k) &= \widehat{W}_m C_m(k), \\ \widetilde{C}_m(j, k) &= \widehat{W}_m C_m(j, k), \\ \widetilde{\Delta}_m(k; G_m) &= \widehat{W}_m \Delta_m(k; G_m). \end{aligned}$$

The adjusted-range versions then use these whitened contrasts with  $\tilde{R}_m^{-2}$ .

Thus, for example,

$$\mathcal{F}_m^S(k) = \frac{C_m(k)^\top D_m^{-1} C_m(k)}{m g_\gamma(k/m)^2}, \quad \mathcal{F}_m^R(k) = \frac{\tilde{C}_m(k)^\top \tilde{R}_m^{-2} \tilde{C}_m(k)}{m g_\gamma(k/m)^2}.$$

Analogous substitutions define the Page-CUSUM, MOSUM, weighted-CUSUM, and multiscale MOSUM paths under Shao's and adjusted-range SN; for MOSUM-type RSMS statistics,  $\Delta_m(k; G_m)$  is replaced by  $\tilde{\Delta}_m(k; G_m)$ . The stopping times are unchanged, except that the critical values must be taken from the corresponding self-normalized null laws.

At the limit level, the same Gaussian fields appear as in the HAC formulas, but the inverse covariance matrix is replaced by the relevant self-normalizer limit. Writing  $V_q$  and  $R_q$  for the  $q$ -dimensional analogs of the Shao and adjusted-range self-normalizer limits from the paper, the substitutions are  $\Sigma_q^{-1} \mapsto V_q^{-1}$  for Shao's SN and, after the corresponding whitening transformation,  $\Sigma_q^{-1} \mapsto R_q^{-2}$  for adjusted-range SN. For example,

$$\sup_{1 \leq k \leq \lfloor mT \rfloor} \mathcal{P}_m^S(k) \Rightarrow \sup_{0 < v \leq T} \sup_{0 \leq u < v} \frac{\mathbb{U}_q(u, v)^\top V_q^{-1} \mathbb{U}_q(u, v)}{g_\gamma(v - u)^2},$$

whereas, with  $\widetilde{\Delta}_h U_q(s)$  denoting the corresponding whitened MOSUM limit,

$$\sup_{2G_m \leq k \leq \lfloor mT \rfloor} \mathcal{O}_m^R(k; G_m) \Rightarrow \sup_{2h \leq s \leq T} \frac{\widetilde{\Delta}_h U_q(s)^\top R_q^{-2} \widetilde{\Delta}_h U_q(s)}{h}.$$

Thus the comparison separates the statistic form (full-history, restart, moving-window, or multiscale) from the standardization device (HAC, Shao, or adjusted range). The simulations can then distinguish changes due to the statistic form from changes due to SN standardization.

#### S4.5 Critical values for the supplementary CUSUM and MOSUM statistics

This subsection collects simulated critical values for the supplementary CUSUM and MOSUM statistics introduced in Appendix S4. The tables use the same score-dimension grid  $q = 1, \dots, 30$ . The finite horizons are  $T = 1, 2, 5, 10$ , and the nominal levels are  $\alpha = 0.01, 0.05, 0.10$ , as in the main paper. For Page-CUSUM and weighted-CUSUM, which use boundary exponent  $\gamma$ , separate panels report  $\gamma = 0$  and  $\gamma = 0.15$ . For multiscale MOSUM, the reported specification uses the bandwidth set  $\mathcal{H} = \{0.05, 0.10, 0.20\}$  and equal scale weights. To keep the notation readable, every later table row labeled ‘‘Multiscale MOSUM’’ refers to this same bandwidth set.

The Monte Carlo setup for these supplementary critical values uses

10,000 Brownian replications and a finite-horizon monitoring grid of 10,000 points. The weighted-CUSUM entries are reported for the inverse-square-root segment-length weight  $\omega(\ell) = \ell^{-1/2}$ . The Page-CUSUM and weighted-CUSUM critical values use the same geometric lag-scan approximation as the simulation implementation, rather than an exact all-endpoint/all-lag scan. The full-window CUSUM and fixed-bandwidth MOSUM critical-value blocks below use the same simulated-critical-value scheme. These larger 10,000/5,000 Monte Carlo counts are used only for the critical-value tables. The appendix raw-power, SAP, and ADD summaries for the supplementary statistics use 1000 Monte Carlo replications per simulation setting, matching the main paper.

**Page-CUSUM** Table S4.1 reports the full-window CUSUM critical-value block. Tables S4.2, S4.3, and S4.4 report the critical values for the HAC LRV-scaled, Shao's self-normalized, and adjusted-range self-normalized Page-CUSUM statistics.

**Multiscale MOSUM** The fixed-bandwidth MOSUM critical-value blocks report  $h \in \{0.10, 0.20\}$  for the HAC and adjusted-range standardizations. Tables S4.7, S4.8, and S4.9 report the multiscale MOSUM critical values for  $\mathcal{H} = \{0.05, 0.10, 0.20\}$  with equal scale weights.

Table S4.1: Finite-horizon simulated critical values (entries are critical values, not percentages) for the HAC LRV-scaled full-window CUSUM statistic for two boundary exponents  $\gamma \in \{0, 0.15\}$

Panel A: $\gamma = 0$												
$q$	$T = 1$			$T = 2$			$T = 5$			$T = 10$		
	1%	5%	10%	1%	5%	10%	1%	5%	10%	1%	5%	10%
1	3.8897	2.4187	1.8582	5.1645	3.2753	2.4947	6.4415	4.1746	3.1654	6.7604	4.4033	3.3627
2	5.0580	3.5456	2.8446	6.9083	4.7451	3.8035	8.6843	5.9458	4.7844	9.5251	6.4444	5.1802
3	6.2030	4.4415	3.6436	8.0986	6.0667	5.0416	10.5399	7.6145	6.2598	11.4749	8.1617	6.7160
4	7.1129	5.3328	4.4734	9.5782	7.1224	6.0417	12.0484	9.0370	7.5287	13.1479	9.7085	8.0966
5	8.2088	6.0862	5.2045	10.7983	8.1998	7.0581	13.4024	10.3315	8.7457	14.9022	11.2227	9.5054
6	8.9260	6.8736	5.9349	12.0803	9.1225	7.9247	14.7953	11.6228	9.9762	16.4669	12.7126	10.8719
7	9.6203	7.5919	6.6033	13.1270	10.1861	8.8704	16.1828	12.9008	11.1618	17.9612	14.0819	12.1472
8	10.5306	8.3211	7.2410	14.2087	11.0596	9.7473	17.4547	14.0318	12.2787	19.5614	15.4511	13.2900
9	11.3316	9.0586	7.9112	15.2147	12.1319	10.5902	19.0501	15.1412	13.4113	20.9872	16.6421	14.6830
10	12.0971	9.7010	8.5982	16.0701	13.0072	11.5090	20.3971	16.3724	14.4919	22.5730	17.8894	15.7671
11	12.8133	10.4291	9.2061	17.3378	13.9453	12.3636	21.8522	17.5536	15.5037	23.8203	19.2151	16.9738
12	13.6319	11.1044	9.8826	18.1794	14.9429	13.1431	23.1260	18.6596	16.6183	25.3023	20.5183	18.0758
13	14.3010	11.7574	10.5572	19.2029	15.8063	14.0716	24.2775	19.8725	17.7539	26.6256	21.6257	19.2051
14	15.0578	12.4051	11.2157	19.9127	16.8252	14.8907	25.1624	21.0261	18.8709	27.6209	22.7512	20.3761
15	15.7558	13.0701	11.8554	20.8028	17.6241	15.6848	26.6127	22.1054	19.8178	28.8364	23.9980	21.5093
16	16.5553	13.7807	12.4460	21.7818	18.4869	16.5833	27.9238	23.0268	20.9347	30.0258	25.2295	22.5808
17	17.3972	14.3661	13.0892	22.7941	19.3132	17.3745	28.9303	24.0896	21.9422	31.6356	26.3850	23.7552
18	17.8391	15.0214	13.6520	23.7174	20.1295	18.2166	29.8804	25.2993	22.9153	32.5755	27.4880	24.8544
19	18.6830	15.6849	14.2382	24.9433	20.9246	19.0152	31.1807	26.4503	23.9157	33.8633	28.6688	25.9366
20	19.3963	16.2663	14.8186	25.7027	21.7310	19.7791	32.4650	27.4213	25.0195	35.3278	29.6477	27.0269
21	20.0191	16.9228	15.4039	26.5708	22.6241	20.6229	33.6156	28.5236	26.1288	36.7910	30.9006	28.1480
22	20.6630	17.5881	16.0274	27.6435	23.5145	21.4992	34.6427	29.5883	27.0711	38.2301	32.0817	29.2401
23	21.2702	18.2137	16.6216	28.5797	24.3085	22.2810	35.9496	30.7033	28.0976	39.1644	33.3541	30.4586
24	22.0553	18.8652	17.1867	29.5889	25.1037	23.0618	37.1361	31.7053	29.0084	40.3717	34.3721	31.5594
25	22.6443	19.5015	17.7808	30.1917	25.9290	23.8844	38.1624	32.7101	30.0824	41.1616	35.4493	32.6838
26	23.4009	20.1459	18.3432	31.2947	26.6799	24.6815	39.0888	33.6894	31.0220	42.4942	36.5753	33.6519
27	24.1508	20.7435	18.9843	32.1918	27.5112	25.4675	40.5345	34.8608	31.9131	43.7514	37.6584	34.6640
28	24.6515	21.2785	19.5324	33.2928	28.3471	26.2641	41.4247	35.9745	32.9364	45.0433	38.7346	35.7423
29	25.3075	21.9769	20.1603	34.1754	29.1869	26.9623	42.5850	36.8023	33.9777	46.6471	39.8725	36.8915
30	26.0585	22.5600	20.7684	35.2730	29.9116	27.7636	43.7568	37.8502	34.9522	47.6279	40.8907	37.8980

Panel B: $\gamma = 0.15$												
$q$	$T = 1$			$T = 2$			$T = 5$			$T = 10$		
	1%	5%	10%	1%	5%	10%	1%	5%	10%	1%	5%	10%
1	4.9440	3.1446	2.4724	6.0931	3.8939	3.0191	7.1172	4.6545	3.5949	7.3702	4.7775	3.6764
2	6.4458	4.5791	3.6977	8.0462	5.6190	4.5286	9.4677	6.5574	5.3511	10.1207	6.8848	5.5986
3	7.7948	5.7215	4.7384	9.4696	7.1185	5.9522	11.3906	8.3857	6.8819	12.0788	8.6545	7.1875
4	8.9097	6.8094	5.7361	11.0860	8.3138	7.1142	13.0518	9.8310	8.2836	14.0804	10.3009	8.6318
5	10.3262	7.7052	6.6155	12.5723	9.5246	8.2303	14.5043	11.2698	9.5821	15.6292	11.9080	10.0900
6	11.3173	8.7046	7.5493	13.8496	10.6407	9.2142	15.9577	12.6014	10.8700	17.3030	13.4238	11.5277
7	12.1376	9.6058	8.3855	15.2356	11.8046	10.3358	17.4616	13.9154	12.1560	18.9099	14.8289	12.9051
8	13.3484	10.5474	9.1906	16.4834	12.8003	11.2951	18.8224	15.1657	13.3581	20.3900	16.2984	14.0630
9	14.1557	11.4163	10.0490	17.5362	14.0136	12.2890	20.5383	16.3821	14.5601	21.9834	17.5114	15.5154
10	15.1331	12.2240	10.8489	18.4083	15.0357	13.2593	21.9557	17.6143	15.7147	23.5759	18.7585	16.6281
11	15.9783	13.0946	11.6490	19.8666	16.1051	14.3016	23.4267	18.9377	16.7859	24.8375	20.1784	17.8512
12	17.0249	13.9487	12.4682	20.8687	17.1825	15.1966	24.7599	20.0802	17.9521	26.4403	21.4751	19.0326
13	17.8366	14.7546	13.2532	21.8859	18.2351	16.2161	25.9616	21.4052	19.1908	27.9539	22.5776	20.2460
14	18.9464	15.5661	14.0931	22.7893	19.3323	17.1095	26.9276	22.5859	20.3308	28.8485	23.7948	21.4116
15	19.7465	16.4393	14.8731	23.8828	20.1736	18.1434	28.4551	23.7180	21.3573	30.0520	24.9857	22.5924
16	20.7049	17.3222	15.6027	24.8680	21.2013	19.0800	29.7569	24.7160	22.4680	31.2787	26.3135	23.6629
17	21.6099	18.0208	16.4267	26.0857	22.1542	20.0241	30.8119	25.8399	23.5834	32.9633	27.5633	24.8208
18	22.3654	18.7688	17.1100	27.0404	23.0870	20.9184	31.9776	27.0869	24.5883	34.0590	28.6808	26.0239
19	23.3184	19.6526	17.8683	28.3675	23.9693	21.8388	33.2366	28.2605	25.6137	35.2354	29.8555	27.1578
20	24.2271	20.3243	18.6051	29.3426	24.9043	22.7695	34.8311	29.2643	26.8300	36.7011	30.9887	28.2752
21	25.0487	21.1365	19.3163	30.2821	25.9503	23.6719	36.1331	30.5031	27.9960	38.1849	32.2498	29.3564
22	25.8097	21.9799	20.0491	31.4750	26.8987	24.6669	37.1750	31.6338	28.9963	39.7179	33.5067	30.5425
23	26.5189	22.7243	20.7791	32.5829	27.9115	25.5134	38.2247	32.8357	30.0606	40.6842	34.7546	31.7387
24	27.0609	23.4921	21.5058	33.7258	28.6519	26.3765	39.5966	33.8627	31.0539	41.7474	35.7922	32.8740
25	28.1879	24.2556	22.1874	34.5635	29.7101	27.3515	40.7580	34.9886	32.1796	42.8775	36.9003	34.0411
26	29.2038	25.1714	22.8803	35.5583	30.5632	28.3045	42.0434	35.9760	33.1639	44.1013	38.0039	35.0765
27	30.1038	25.8795	23.6460	36.8480	31.4724	29.0666	43.1605	37.2504	34.1740	45.3552	39.1876	36.0543
28	30.8275	26.5231	24.3306	37.9700	32.3698	30.0316	44.1953	38.2928	35.2697	46.8225	40.3167	37.1338
29	31.5360	27.4323	25.0885	38.7772	33.3652	30.8632	45.5001	39.3507	36.3769	48.5372	41.5475	38.4245
30	32.3666	28.1299	25.7883	39.9907	34.1938	31.7728	46.5979	40.3951	37.3299	49.5635	42.5772	39.3924

S4. SUPPLEMENTARY MONITORING STATISTICS

Table S4.2: Finite-horizon simulated critical values (entries are critical values, not percentages) for the HAC LRV-scaled Page-CUSUM statistic for two boundary exponents  $\gamma \in \{0, 0.15\}$

Panel A: $\gamma = 0$												
$q$	$T = 1$			$T = 2$			$T = 5$			$T = 10$		
	1%	5%	10%	1%	5%	10%	1%	5%	10%	1%	5%	10%
1	4.1341	2.7639	2.2317	5.7324	3.8686	3.1262	7.4754	5.1726	4.2327	8.1085	5.9034	4.8755
2	5.3489	3.8433	3.2103	7.4712	5.3776	4.4411	9.6027	7.0752	5.8865	10.9245	7.9136	6.7534
3	6.3952	4.7259	3.9800	8.6902	6.5074	5.6326	11.5840	8.6230	7.3710	12.9965	9.6320	8.2971
4	7.2552	5.5197	4.7698	10.0511	7.6508	6.5846	12.9273	9.8838	8.5842	14.5658	11.2241	9.6791
5	8.2518	6.2390	5.4588	11.2425	8.6276	7.5267	14.3701	11.1823	9.8095	16.1958	12.6659	11.1213
6	8.9915	7.0429	6.1322	12.3447	9.6173	8.3984	15.6414	12.4865	10.9616	17.6882	14.2556	12.4595
7	9.8195	7.7548	6.7507	13.4028	10.6328	9.2776	17.0919	13.7651	12.1442	19.2469	15.4808	13.6975
8	10.5464	8.4316	7.4528	14.3456	11.5027	10.1425	18.1903	14.9450	13.2639	20.8253	16.7495	14.9536
9	11.2519	9.1688	8.1043	15.2643	12.4934	11.0968	20.0034	16.0617	14.3401	22.3303	18.1781	16.1671
10	11.9236	9.7387	8.7443	16.3842	13.4056	11.9211	21.3256	17.1816	15.4467	23.5979	19.3865	17.2671
11	12.5721	10.4526	9.3429	17.4206	14.2666	12.7605	22.5583	18.3168	16.3463	24.9622	20.6738	18.5060
12	13.5204	11.0990	9.9858	18.3264	15.1924	13.6223	23.6469	19.4154	17.4887	26.5113	21.7646	19.5093
13	14.1392	11.7559	10.5986	19.3789	16.0146	14.3924	24.9217	20.6029	18.5987	27.8225	22.9442	20.7348
14	14.8598	12.3980	11.2328	20.2359	16.9870	15.1910	25.8398	21.6965	19.6208	29.0138	24.0222	21.9100
15	15.4807	13.0294	11.8486	21.0512	17.7973	16.0288	27.0122	22.7330	20.6262	30.0064	25.2287	23.0059
16	16.3795	13.6935	12.4640	21.9656	18.6125	16.8383	28.2646	23.7383	21.6593	31.3112	26.4687	23.9877
17	17.0400	14.3824	13.1260	22.9593	19.4768	17.6792	29.1025	24.8122	22.5886	32.5862	27.5202	25.1764
18	17.6911	14.9322	13.6962	23.7680	20.2828	18.4845	30.2951	25.8558	23.6006	33.5539	28.7062	26.3174
19	18.3998	15.6290	14.3036	24.8876	21.0784	19.2375	31.5609	27.0327	24.6583	34.8100	29.8267	27.3544
20	19.0283	16.2009	14.8103	25.9467	21.9096	20.0279	32.9834	27.9258	25.7060	36.1819	30.9115	28.3431
21	19.6643	16.8985	15.4178	26.6328	22.7181	20.8676	33.9649	29.1358	26.7404	37.4754	32.0682	29.4934
22	20.4106	17.4865	16.0180	27.7070	23.6528	21.6561	34.9090	30.1967	27.6371	38.7259	33.1727	30.6694
23	21.0304	18.0854	16.6160	28.7998	24.4655	22.4528	36.1276	31.2249	28.6778	39.7776	34.3415	31.7035
24	21.7368	18.7521	17.1594	29.7764	25.1785	23.1938	37.4824	32.1313	29.6800	40.7875	35.5308	32.7512
25	22.3716	19.3661	17.7648	30.2693	26.1250	23.9390	38.5727	33.1678	30.6959	41.8184	36.5658	33.7939
26	23.0701	19.9177	18.2667	31.2619	26.8408	24.7527	39.4919	34.1402	31.7143	43.2665	37.6642	34.8599
27	23.7926	20.5156	18.9097	32.1772	27.5737	25.4567	40.8630	35.1542	32.6365	44.4885	38.7127	35.9937
28	24.4424	21.1626	19.4288	33.3496	28.2945	26.2751	41.8898	36.2829	33.6170	45.8112	39.7740	37.0758
29	25.1714	21.7490	20.0411	34.1831	29.0879	27.0479	43.1399	37.2431	34.5574	46.8300	40.8110	38.0872
30	25.6613	22.3780	20.6006	34.9073	29.9717	27.8033	43.9732	38.3338	35.4749	47.9173	41.9681	39.0443

Panel B: $\gamma = 0.15$												
$q$	$T = 1$			$T = 2$			$T = 5$			$T = 10$		
	1%	5%	10%	1%	5%	10%	1%	5%	10%	1%	5%	10%
1	5.5729	3.8487	3.1595	7.1057	4.9610	4.0996	8.6635	6.2489	5.2108	9.2758	6.9545	5.8593
2	7.1262	5.2617	4.4159	8.9358	6.7438	5.6362	10.9752	8.3005	7.0797	12.1430	9.1779	7.9429
3	8.2775	6.3467	5.4221	10.3778	8.1149	7.0420	12.9754	10.0287	8.6874	14.2201	11.0072	9.5895
4	9.4952	7.3236	6.4076	11.9364	9.2583	8.1422	14.4391	11.3420	9.9944	16.1777	12.6547	11.0910
5	10.6354	8.2489	7.2821	13.4146	10.4488	9.2096	16.0217	12.7630	11.2882	17.7535	14.2487	12.5152
6	11.6854	9.2142	8.1308	14.5733	11.5634	10.2268	17.4178	14.1381	12.5370	19.2577	15.7489	13.9772
7	12.6733	10.0194	8.9511	15.9491	12.7190	11.2556	18.8801	15.5032	13.8326	20.8890	17.1300	15.3169
8	13.5773	11.0414	9.7666	17.0171	13.7972	12.2348	20.3538	16.7528	15.0124	22.4010	18.4649	16.6250
9	14.4970	11.8775	10.5741	18.0448	14.8383	13.2886	21.9527	17.9919	16.1942	23.9315	19.8959	17.8726
10	15.3290	12.7171	11.3923	19.1385	15.9389	14.2800	23.4618	19.1650	17.3548	25.6382	21.2210	19.0655
11	16.1923	13.4662	12.1409	20.3348	16.9309	15.2046	24.7335	20.3338	18.3910	26.8427	22.4784	20.2620
12	17.2727	14.2958	12.8947	21.3265	17.9005	16.2400	25.9062	21.5213	19.4985	28.3047	23.5738	21.4030
13	18.0775	15.1006	13.7303	22.5861	18.9547	17.1665	27.3249	22.7115	20.7597	29.8338	24.9426	22.6333
14	18.9328	15.9339	14.5070	23.6325	19.9815	18.0801	28.4276	23.8849	21.8701	31.0928	26.0336	23.9023
15	19.7048	16.7090	15.2545	24.6215	20.8203	19.0283	29.6579	25.0053	22.9241	32.1149	27.1851	25.0481
16	20.6864	17.5757	16.0359	25.5748	21.7503	19.9083	30.7517	26.1494	23.9410	33.3158	28.4288	26.1295
17	21.5525	18.4115	16.8073	26.5991	22.8270	20.8369	31.5479	27.2134	24.9475	34.4597	29.6100	27.3026
18	22.3169	19.1005	17.5345	27.6489	23.6670	21.7498	32.9768	28.5243	26.0700	35.6735	30.8649	28.3788
19	23.1104	19.9065	18.2689	28.8365	24.6892	22.6737	34.1923	29.7051	27.1145	37.0556	32.0242	29.4617
20	24.0742	20.6291	19.0031	30.0801	25.6380	23.5349	35.9146	30.6544	28.2262	38.4857	33.2012	30.6519
21	24.7325	21.4520	19.7160	30.9706	26.5654	24.4741	36.8741	31.8145	29.3697	39.7484	34.2589	31.7638
22	25.6617	22.1602	20.4638	32.0990	27.4834	25.4164	37.9204	32.8808	30.2714	40.9914	35.3493	32.8897
23	26.3438	22.9417	21.2042	33.1667	28.5366	26.2741	39.2842	34.0313	31.4699	42.1051	36.5755	33.9922
24	27.2863	23.7836	21.8713	34.2920	29.4540	27.0587	40.3889	35.0148	32.4640	43.1020	37.8608	35.1131
25	28.1278	24.5771	22.5219	35.0664	30.3409	28.0306	41.7411	36.1812	33.5419	44.3209	38.9846	36.1485
26	28.9758	25.2842	23.2023	36.1151	31.2284	28.8702	42.6907	37.1247	34.5637	45.7960	39.9819	37.3689
27	30.0301	26.0079	23.9460	37.0201	32.0980	29.7453	44.3080	38.2241	35.5683	46.7817	41.2650	38.3971
28	30.7172	26.6956	24.6452	38.1713	32.9651	30.5942	45.2837	39.3527	36.6077	48.2095	42.3688	39.6408
29	31.4760	27.5270	25.3719	39.0473	33.7789	31.4942	46.4123	40.4990	37.6384	49.4165	43.3990	40.5970
30	32.2685	28.2270	26.1086	40.0436	34.8160	32.3231	47.3567	41.4737	38.6036	50.5068	44.5633	41.6852

Table S4.3: Finite-horizon simulated critical values (entries are critical values, not percentages) for Shao's self-normalized Page-CUSUM statistic for two boundary exponents  $\gamma \in \{0, 0.15\}$

Panel A: $\gamma = 0$												
$q$	$T = 1$			$T = 2$			$T = 5$			$T = 10$		
	1%	5%	10%	1%	5%	10%	1%	5%	10%	1%	5%	10%
1	75.4484	39.5813	28.3125	99.1654	55.9085	41.3008	135.6335	79.8760	57.5734	159.6649	91.7064	68.6130
2	127.8024	80.7400	60.1817	180.8797	112.5572	87.0635	243.0116	148.4945	116.5196	284.4811	181.0735	139.6732
3	189.3501	124.1967	97.0866	262.5255	172.2332	138.0639	364.7775	235.4196	186.3063	401.1712	268.7959	220.8696
4	265.1460	175.9364	140.8475	362.5448	236.9659	192.2780	484.0590	326.7266	261.3939	534.8674	370.6637	304.7768
5	329.5695	230.8853	188.9953	483.8135	324.0647	261.4064	602.7441	431.0530	351.7114	698.8763	495.0926	409.9273
6	409.7629	290.1166	242.0344	568.1662	403.7235	336.2255	753.4986	543.1960	451.8169	865.5483	609.9607	519.4460
7	492.9881	356.8666	299.0539	688.4976	496.5144	419.8368	892.3904	663.8031	555.2648	1066.8201	750.1636	639.9137
8	592.4970	429.1527	363.5852	809.2123	597.4018	505.4562	1083.9556	794.3535	669.4904	1215.5710	897.2794	773.1334
9	687.2940	514.7317	438.8460	946.1866	711.3724	599.6714	1245.6783	926.9775	792.9478	1404.1586	1056.3992	910.0917
10	800.3817	600.1844	509.9848	1102.3349	827.4071	703.5739	1442.3273	1072.7074	927.7257	1615.3214	1227.2374	1059.4916
11	915.3471	691.8682	589.4400	1273.9275	953.4678	811.8482	1651.4672	1235.7146	1066.9379	1824.8188	1393.2652	1208.9638
12	1055.8272	778.8748	674.2493	1417.6089	1081.0998	931.5732	1810.3943	1405.6489	1210.5600	2048.0994	1586.7243	1382.7739
13	1154.4728	885.6533	761.7489	1563.8333	1213.4715	1049.9383	2049.5088	1582.7774	1375.4248	2300.6431	1779.8041	1505.1600
14	1281.6835	985.6161	853.7116	1723.2345	1347.5320	1176.6692	2269.1702	1757.3469	1539.3280	2536.7809	1972.3982	1741.6175
15	1409.9544	1087.8635	955.8084	1899.4627	1506.6101	1309.6824	2530.5884	1947.9850	1711.1758	2802.4730	2205.7046	1925.5255
16	1551.2900	1214.8422	1060.4454	2114.6631	1662.3082	1456.9487	2743.5847	2135.7361	1884.4361	3129.8197	2425.6870	2126.3512
17	1712.4645	1334.2876	1168.1429	2310.9484	1829.6096	1602.2912	2976.5533	2343.1195	2067.6387	3435.1379	2679.0653	2354.0022
18	1869.2499	1471.5881	1283.5053	2547.3115	2018.7318	1756.1396	3246.2895	2553.6317	2266.9516	3723.8529	2949.1350	2578.3630
19	2002.6594	1589.9705	1403.2741	2810.3076	2204.0370	1923.1521	3528.1985	2789.1451	2478.8237	3989.7086	3195.0047	2797.7302
20	2192.3803	1728.7533	1525.7999	3023.3967	2376.5281	2087.6438	3805.7460	3011.2007	2682.7319	4305.7887	3457.3040	3058.6169
21	2334.8715	1853.7140	1653.8041	3221.7801	2562.8849	2250.0864	4096.8351	3266.4829	2906.0791	4588.4528	3719.4513	3310.2068
22	2522.7270	2008.0836	1779.5920	3484.4018	2759.0722	2434.1515	4422.4231	3518.3074	3125.3422	4957.5477	3990.9795	3549.7534
23	2687.3104	2149.2536	1917.0053	3714.1598	2973.2092	2610.5215	4670.3336	3762.8091	3366.4612	5300.8981	4257.6072	3822.8735
24	2878.1451	2316.3749	2053.6491	3951.0104	3173.7009	2808.7001	4978.9486	4038.6996	3599.8916	5598.4807	4583.0813	4088.7261
25	3071.4246	2489.9341	2203.1243	4172.3604	3351.0653	2990.7133	5332.8313	4329.5987	3873.9238	6021.1047	4899.2938	4371.5865
26	3309.4517	2651.8410	2357.4470	4406.4640	3587.5677	3198.2912	5636.4846	4650.6985	4139.6459	6373.9694	5203.0531	4651.3767
27	3524.2641	2816.9045	2515.9048	4615.8460	3812.6232	3405.9257	6033.5540	4934.1044	4393.2674	6725.9631	5500.6226	4925.7981
28	3684.6050	2987.3730	2678.0562	4888.0705	4058.6327	3637.1771	6384.5027	5250.5172	4678.7887	7107.7006	5819.3406	5233.3937
29	3823.6312	3190.3548	2848.9309	5199.2525	4311.8533	3869.2157	6770.1519	5545.5249	4972.3938	7466.1098	6162.6224	5550.0390
30	4064.6586	3365.9632	3029.4591	5497.6684	4548.4548	4102.7838	7123.8993	5856.8012	5282.1223	7775.2360	6459.9520	5873.1821

Panel B: $\gamma = 0.15$												
$q$	$T = 1$			$T = 2$			$T = 5$			$T = 10$		
	1%	5%	10%	1%	5%	10%	1%	5%	10%	1%	5%	10%
1	104.1054	57.9103	42.5467	130.6884	76.3412	56.9144	165.2977	101.8997	74.1421	193.0998	114.4309	86.5959
2	176.9953	115.1943	88.2612	227.5814	147.2841	116.3083	294.4857	182.8254	147.5624	328.2133	219.2877	173.1883
3	258.9072	174.3490	130.1042	331.0898	222.0739	181.7133	433.5325	285.4499	229.4180	461.5014	324.4718	268.1823
4	357.6219	242.9769	199.6807	440.8556	304.2013	251.0536	570.5174	396.6798	321.7318	622.6426	439.9521	365.1151
5	442.4328	317.7575	264.5934	579.9375	408.0399	336.8261	699.2417	512.2806	427.1778	791.3859	578.4290	486.9237
6	550.9996	399.7937	335.8804	696.4594	509.3743	429.3155	862.0332	642.0984	542.9786	985.6507	710.3035	610.8587
7	656.6197	482.5362	413.0866	838.8430	622.7451	529.4857	1038.5027	777.7390	663.1731	1176.6194	864.9387	742.8449
8	789.6835	578.9588	494.9558	984.2827	740.3919	637.6204	1240.3215	925.0742	791.9493	1374.4068	1035.5992	895.6810
9	906.8679	688.3391	589.6261	1148.9654	877.3829	753.1616	1420.6481	1072.9671	934.2732	1559.8800	1201.9113	1048.7910
10	1065.2060	800.6795	687.4739	1345.4486	1008.2885	871.9973	1625.5343	1254.1037	1083.6665	1796.4561	1394.0889	1213.8182
11	1204.7572	924.8247	790.0442	1543.6103	1168.1537	999.3468	1863.2938	1430.0693	1251.7027	2009.2053	1570.7590	1379.7581
12	1363.4374	1031.6506	902.8862	1714.4707	1315.7512	1145.0605	2065.5962	1610.6987	1408.4249	2253.1731	1792.2598	1577.5632
13	1494.4646	1166.6761	1012.1627	1872.0257	1478.6475	1290.6695	2313.8594	1811.1893	1598.3815	2529.9561	2007.4417	1772.9597
14	1675.3059	1297.8701	1136.7181	2084.8103	1636.9997	1437.5898	2540.3294	2007.6233	1773.0854	2788.9480	2207.2415	1953.6660
15	1837.7599	1443.2349	1263.6214	2272.4896	1821.1624	1597.0856	2830.3004	2231.7789	1964.0005	3088.8184	2447.8027	2173.2286
16	2010.7191	1592.4911	1403.2826	2508.5373	2005.8729	1757.1634	3074.1459	2436.1734	2156.4763	3403.3949	2698.0447	2393.2522
17	2205.6661	1748.9937	1537.4026	2738.2929	2209.1720	1938.7467	3344.3299	2647.5335	2364.6622	3769.5634	2975.0356	2630.9695
18	2402.0496	1913.5872	1694.9395	3011.9816	2416.9811	2118.6725	3636.7254	2878.7105	2588.6284	4035.8323	3239.9756	2882.8814
19	2586.9067	2079.5749	1844.9402	3297.1616	2635.5924	2318.4263	3975.9019	3148.4639	2818.1691	4313.7166	3525.6345	3137.7833
20	2800.3397	2250.2205	2002.0676	3573.2207	2824.3387	2507.1874	4242.9848	3390.4934	3044.8844	4671.1082	3809.8982	3411.9382
21	3005.7925	2414.1565	2162.4693	3765.0282	3061.6100	2707.7098	4557.8171	3665.5294	3290.3994	4943.0478	4110.2858	3678.0735
22	3242.3672	2612.5714	2330.5834	4084.5595	3296.1926	2918.2602	4912.5651	3938.2605	3533.9423	5337.7594	4389.2640	3939.1080
23	3470.5533	2797.6464	2497.3081	4354.6127	3539.4045	3136.0188	5212.2384	4203.2897	3791.3973	5759.9936	4678.9930	4229.7892
24	3685.5117	3007.3720	2688.2319	4640.0731	3768.7441	3375.4382	5540.3382	4499.5548	4064.4543	6093.9422	5002.4640	4517.6552
25	3931.3740	3231.9349	2873.6189	4864.5089	3989.9911	3594.5911	5921.4239	4852.8575	4355.7217	6520.8480	5348.7754	4825.7167
26	4221.1073	3422.2287	3077.0083	5187.0162	4252.9554	3833.2636	6222.8325	5196.3150	4665.7079	6891.9313	5683.9897	5125.7712
27	4478.7528	3619.8439	3268.9014	5442.1321	4541.1283	4069.9876	6584.0765	5492.3672	4943.8717	7209.2994	6002.9144	5418.3000
28	4709.5810	3851.7546	3485.8123	5781.5338	4737.4354	4327.7552	6975.1239	5843.0019	5239.4203	7617.1826	6333.3000	5765.8480
29	4888.6162	4097.8841	3706.1200	6049.6299	5082.2989	4607.8370	7388.8592	6163.2717	5599.4709	8019.0920	6690.3634	6076.6568
30	5186.7503	4344.3073	3909.1254	6416.8595	5361.4913	4869.9496	7827.6545	6525.7029	5884.1951	8411.7919	7056.9542	6423.9019

S4. SUPPLEMENTARY MONITORING STATISTICS

Table S4.4: Finite-horizon simulated critical values (entries are critical values, not percentages) for the adjusted-range self-normalized Page-CUSUM statistic for two boundary exponents  $\gamma \in \{0, 0.15\}$

Panel A: $\gamma = 0$												
$q$	$T = 1$			$T = 2$			$T = 5$			$T = 10$		
	1%	5%	10%	1%	5%	10%	1%	5%	10%	1%	5%	10%
1	4.1166	2.3154	1.7858	5.3261	3.3713	2.5946	7.5161	4.7030	3.6798	8.6392	5.4964	4.3538
2	5.0628	3.2960	2.6109	7.0888	4.6374	3.7785	9.3385	6.3682	5.1459	11.1165	7.4286	6.0743
3	5.9724	3.9973	3.2566	8.3829	5.7087	4.6787	10.9794	7.7804	6.3955	13.1830	9.0226	7.4384
4	6.7211	4.7359	3.9060	9.5232	6.5444	5.4444	12.4140	9.0445	7.4373	14.6457	10.4181	8.6680
5	7.3383	5.3556	4.4541	10.3491	7.4531	6.2439	13.7837	9.9460	8.4404	16.0058	11.5916	9.7957
6	7.9639	5.9689	5.0204	11.1426	8.2727	6.9838	14.9786	10.9216	9.4081	17.1947	12.7509	10.9627
7	8.6712	6.4759	5.5268	12.0238	9.0245	7.7226	16.0068	11.9682	10.3358	18.5966	14.0095	12.0344
8	9.3708	7.0412	6.0509	12.8571	9.7763	8.3689	17.3111	13.0936	11.1264	19.9835	14.9592	12.9159
9	10.0288	7.5461	6.5650	13.7472	10.5434	9.0722	18.6757	13.9758	12.1157	21.3934	16.0285	14.0122
10	10.4809	8.0226	7.0479	14.4609	11.3031	9.7415	19.7833	14.8907	13.0105	22.1614	17.1054	14.9824
11	11.0534	8.5750	7.5709	15.3799	12.0498	10.4352	20.7531	15.7614	13.8834	23.3332	18.1644	15.9749
12	11.6100	9.0387	7.9850	16.1097	12.7078	11.0705	21.4877	16.6665	14.6539	24.4151	19.0626	16.8885
13	12.1812	9.6092	8.4841	16.7811	13.4057	11.7366	22.3752	17.6250	15.4737	25.5810	19.9786	17.7610
14	12.8003	10.1031	8.9788	17.5860	14.0868	12.4476	23.4593	18.5151	16.2681	26.5769	20.8698	18.5779
15	13.3731	10.6531	9.4579	18.2017	14.7307	12.9978	24.3630	19.3237	17.0626	27.2981	21.8985	19.4022
16	13.9416	11.1540	9.9061	19.1649	15.4031	13.6114	25.3425	20.1300	17.9019	28.1482	22.6783	20.3292
17	14.4397	11.6395	10.3523	19.7815	15.9111	14.2217	26.2381	20.9760	18.6541	29.4873	23.6507	21.2206
18	14.8575	12.1087	10.8433	20.4718	16.5522	14.7729	27.2089	21.7844	19.5033	30.3303	24.8005	22.0305
19	15.2546	12.5916	11.3495	21.0919	17.2649	15.4341	28.2439	22.6623	20.2947	31.5001	25.5701	22.9139
20	15.7997	13.0628	11.8611	21.9463	17.9006	16.0749	29.1042	23.4417	21.0735	32.2920	26.4946	23.7889
21	16.3390	13.4825	12.2243	22.7361	18.6315	16.7702	30.0419	24.3094	21.9048	33.3290	27.4192	24.6745
22	16.9538	14.0102	12.6904	23.3295	19.3007	17.3539	30.8017	25.1763	22.6343	34.5086	28.4060	25.6435
23	17.4198	14.4766	13.1213	24.0055	19.8520	17.8887	31.8194	25.9269	23.3940	35.1525	29.2532	26.4164
24	17.8677	14.9865	13.5552	24.6332	20.4943	18.4972	32.7343	26.6843	24.1911	35.9345	30.1106	27.3109
25	18.4843	15.4100	14.0057	25.4684	21.0333	19.0639	33.4105	27.4824	24.9648	36.9041	30.9486	28.2141
26	19.0257	15.8450	14.4319	26.1074	21.7206	19.6213	34.2732	28.2761	25.6452	37.6895	31.8559	29.0172
27	19.4797	16.3054	14.8344	26.9672	22.3527	20.1538	35.2711	29.1223	26.4111	38.5071	32.6549	29.8362
28	19.9000	16.7944	15.3053	27.4866	22.9866	20.8105	35.7573	29.8994	27.1395	39.5478	33.5760	30.6706
29	20.5208	17.2505	15.7514	28.1603	23.5851	21.3641	36.6406	30.5872	28.0405	40.4405	34.5021	31.4227
30	20.9741	17.7179	16.1937	28.7786	24.1842	21.9801	37.5437	31.3576	28.6703	41.2096	35.3289	32.3624

Panel B: $\gamma = 0.15$												
$q$	$T = 1$			$T = 2$			$T = 5$			$T = 10$		
	1%	5%	10%	1%	5%	10%	1%	5%	10%	1%	5%	10%
1	5.4805	3.3190	2.6227	6.8003	4.4216	3.5000	8.8350	5.7944	4.6424	10.2991	6.7545	5.3943
2	6.6773	4.5979	3.7015	8.9306	5.9546	4.9001	10.9713	7.7254	6.3249	12.9208	8.7869	7.3420
3	7.9847	5.5456	4.5359	10.1921	7.2117	5.9734	12.6542	9.2084	7.7035	14.9918	10.5606	8.8726
4	8.8954	6.3909	5.3762	11.6793	8.1617	6.8955	14.1668	10.5235	8.8613	16.5449	11.9269	10.1304
5	9.5958	7.1708	6.0753	12.5139	9.2658	7.8101	15.6846	11.5894	9.9423	17.8877	13.3026	11.3927
6	10.5304	7.9488	6.7352	13.5498	10.1403	8.6641	17.0404	12.6290	10.9585	19.1969	14.6080	12.5967
7	11.2391	8.5817	7.4209	14.5333	11.0019	9.5283	18.3379	13.7291	11.8953	20.3384	15.8038	13.7190
8	12.0828	9.2875	8.0692	15.4745	11.9309	10.2672	19.4018	14.8077	12.9039	22.0930	16.8363	14.6332
9	12.8727	9.8972	8.6755	16.3610	12.8259	11.1180	20.8586	15.8825	13.8766	23.4761	18.0548	15.8205
10	13.4983	10.5370	9.3010	17.3553	13.6422	11.8578	22.0261	16.8980	14.9392	24.5084	19.0899	16.8725
11	14.2960	11.1592	9.8769	18.3479	14.3584	12.6585	23.1403	17.8692	15.7488	25.3828	20.1228	17.7739
12	14.8963	11.8170	10.4739	19.1569	15.1778	13.4163	23.8376	18.7773	16.5513	26.6054	21.0572	18.7600
13	15.6747	12.4471	11.1054	19.8049	15.9613	14.1451	24.8117	19.8053	17.4789	27.6686	21.9161	19.6585
14	16.5268	13.0903	11.7203	20.7174	16.7079	14.8906	26.0235	20.5556	18.4257	28.6773	22.8909	20.5745
15	17.1879	13.7155	12.2964	21.3000	17.4203	15.5356	26.8018	21.5407	19.2835	29.6400	23.9661	21.5578
16	17.9764	14.3440	12.8942	22.4271	18.1866	16.2927	27.9469	22.4468	20.1650	30.6413	24.8409	22.4596
17	18.5493	14.9833	13.4535	23.1499	18.9111	16.9233	29.0979	23.3076	20.9374	31.6340	25.9205	23.3269
18	19.0587	15.5093	14.0059	24.0024	19.6461	17.6180	30.1225	24.2598	21.7623	32.9051	26.9852	24.1223
19	19.5465	16.1140	14.6078	24.7285	20.4980	18.3369	30.9873	25.1030	22.6158	33.7399	27.8385	25.0783
20	20.2157	16.7174	15.2144	25.7319	21.1853	19.0958	32.1236	25.7984	23.5179	34.6889	28.7951	25.9362
21	21.0386	17.3140	15.7056	26.5289	21.9636	19.8296	33.0035	26.8164	24.3405	35.8078	29.7102	26.8567
22	21.5982	17.9530	16.2968	27.3691	22.6372	20.5331	33.8600	27.7384	25.0500	36.9172	30.6750	27.8532
23	22.3432	18.5584	16.8687	27.9612	23.4280	21.1848	34.7948	28.6247	25.8338	37.7669	31.5909	28.7406
24	22.7163	19.1243	17.3748	28.7441	24.0496	21.8511	35.7594	29.3198	26.5795	38.3657	32.4762	29.6661
25	23.4875	19.6617	17.8978	29.5575	24.7375	22.4782	36.6006	30.0799	27.5229	39.3423	33.4759	30.6128
26	24.2160	20.2766	18.4462	30.2414	25.3594	23.1112	37.6037	31.0953	28.2184	40.1098	34.2843	31.3554
27	24.8249	20.8244	18.9434	31.4619	26.1339	23.7598	38.6503	31.9653	29.0185	40.9548	35.2855	32.2932
28	25.2940	21.3879	19.4902	32.1814	26.9164	24.4619	39.2631	32.6589	29.8297	42.1078	36.1904	33.1931
29	25.9981	21.9639	20.0347	32.8504	27.7041	25.1380	40.0750	33.4948	30.6827	43.0001	37.0646	33.9668
30	26.6373	22.5468	20.5849	33.4247	28.4015	25.8128	40.8594	34.3185	31.5158	43.9648	37.9663	34.9046

Table S4.5: Finite-horizon simulated critical values (entries are critical values, not percentages) for the HAC LRV-scaled MOSUM statistic for two bandwidth fractions  $h \in \{0.10, 0.20\}$

Panel A: $h = 0.10$												
$q$	$T = 1$			$T = 2$			$T = 5$			$T = 10$		
	1%	5%	10%	1%	5%	10%	1%	5%	10%	1%	5%	10%
1	30.0409	22.9562	19.9711	31.7866	25.3491	22.4792	34.3586	27.6727	24.7617	35.3192	28.1990	25.4765
2	36.7210	29.3603	26.2207	38.8917	31.6533	28.7837	40.4834	33.8465	31.1095	41.9681	34.8355	31.7553
3	42.2650	34.5321	31.2704	44.3757	37.0969	33.8807	47.3910	39.3866	36.2024	46.6086	40.2241	37.0563
4	47.1022	39.3747	35.7778	48.8697	41.7509	38.5099	51.2286	43.7639	40.7349	51.7518	44.7076	41.5481
5	51.3215	43.7166	39.8631	53.3383	45.9892	42.5951	55.5004	48.2623	44.9476	56.2566	49.0055	45.8212
6	55.6134	47.5536	43.8920	57.7337	50.1128	46.3818	60.3810	52.2496	48.8632	61.0737	53.1837	49.6871
7	59.8511	51.3443	47.5133	60.9946	54.0737	50.2539	65.0443	56.5712	52.9383	65.9609	57.4712	53.8309
8	63.8084	55.3034	51.2704	65.6766	57.8220	54.0097	69.1552	60.2835	56.6084	69.9658	61.2427	57.7513
9	67.5944	58.9085	54.7374	70.3362	61.4308	57.5264	73.1920	64.2620	60.3210	73.3093	65.0266	61.3673
10	71.5594	62.0963	58.0216	74.2969	64.6549	61.0781	76.7955	67.8817	63.8656	76.9277	68.4023	64.7049
11	75.8347	65.6242	61.5755	77.5679	68.3689	64.2817	80.5817	71.4736	67.3877	80.8015	71.9762	68.0254
12	79.0532	68.7140	64.4733	81.6738	71.8626	67.6201	83.8626	75.2347	70.8484	84.1270	75.4667	71.6712
13	81.7632	72.3023	67.5572	85.0261	75.3745	71.0598	87.5349	78.2391	74.0979	87.6474	78.8327	75.0152
14	85.3916	75.1603	70.7475	88.6501	78.9664	74.3693	91.1945	81.7317	77.4838	91.1545	82.3900	78.3622
15	88.8934	78.7970	73.9991	91.7459	82.3638	77.8151	94.0336	85.0890	80.8445	95.4247	85.7971	81.6807
16	92.4464	82.2060	77.2197	95.4163	85.3422	80.9944	97.1676	88.3127	83.9497	98.8291	89.3813	84.8842
17	95.9608	85.3983	80.5157	98.5199	88.6224	84.1053	101.0913	91.4716	87.1489	102.2373	92.7359	88.1079
18	98.4010	88.2280	83.2317	101.7115	91.7077	87.1671	104.6048	94.2493	90.2843	105.8765	95.9342	91.3172
19	101.5893	91.4220	86.6007	104.8879	94.9618	90.4355	107.6704	97.3811	93.2294	108.9075	98.6935	94.3188
20	104.9670	94.3184	89.2730	108.2042	98.1292	93.3774	111.1147	100.6389	96.1774	112.0788	101.9630	97.3526
21	108.3068	97.4815	92.3560	110.9588	101.3029	96.6366	113.7749	103.5349	99.1598	115.1871	105.3161	100.5440
22	111.0714	100.7941	95.2608	114.3197	104.0900	99.2676	116.8962	106.6377	102.2446	118.4037	108.6233	103.6138
23	115.1284	103.6576	98.3882	118.0493	107.2367	102.0516	120.0618	109.9099	105.3505	121.7080	111.6358	106.7487
24	118.6548	106.5796	101.4071	120.1492	110.2418	105.3337	123.6848	112.8698	108.3162	124.6663	114.5207	109.9388
25	121.9391	109.6368	104.5454	123.4985	113.0944	108.3103	126.7924	116.0103	111.3299	127.4906	117.6305	112.9293
26	124.3354	112.5890	107.1102	126.5474	116.1934	111.1245	129.3502	118.9019	114.3091	130.9579	120.5583	115.6918
27	127.0387	115.4133	110.2177	130.0951	119.1850	113.8956	132.9100	122.3937	117.0933	133.8994	123.6907	118.4157
28	130.8390	118.3140	113.0448	132.9558	122.1475	117.0400	135.6571	125.1032	120.0509	136.7740	126.4352	121.3135
29	133.3180	121.4724	115.9512	135.9188	125.3104	119.8427	138.8604	128.3528	123.0140	140.4218	129.2885	124.2110
30	135.6885	124.4442	118.5509	138.3758	127.9013	122.6776	142.1318	130.8817	125.9759	143.1477	132.0552	127.0720
Panel B: $h = 0.20$												
$q$	$T = 1$			$T = 2$			$T = 5$			$T = 10$		
	1%	5%	10%	1%	5%	10%	1%	5%	10%	1%	5%	10%
1	26.8516	19.7488	16.6418	29.7733	22.9293	19.8575	32.5406	26.3663	23.3875	34.0932	27.7009	24.8091
2	32.7974	25.8475	22.6058	36.6053	29.6306	26.5146	39.5219	32.4791	29.4557	40.9454	34.0611	30.9560
3	38.3479	30.8476	27.2312	42.8040	34.7569	31.2849	44.7624	37.8004	34.4425	46.5723	39.2908	36.3310
4	43.1999	35.3661	31.6687	47.5622	39.4480	35.6810	49.5576	42.6186	39.1681	51.7428	44.0471	40.6430
5	47.4824	39.4351	35.6542	52.0008	43.3484	40.0186	53.9685	47.0370	43.5097	56.5092	48.5014	44.9994
6	51.4484	43.5156	39.4628	55.8510	47.7056	43.5829	58.3508	51.1498	47.5648	60.5528	52.7820	49.0316
7	55.6794	46.8202	42.9439	60.0330	51.3923	47.5925	63.1834	54.7366	51.2119	64.2568	56.4876	53.0285
8	59.1703	50.8205	46.4188	64.2188	55.3243	51.2243	66.7625	58.6589	54.8160	68.9594	60.2800	56.7376
9	63.5625	54.5381	50.0272	67.8436	58.5758	54.6455	70.3839	62.2829	58.4423	72.5532	64.2169	60.3326
10	67.0588	57.6760	53.3777	70.6549	61.9115	57.9241	73.8554	65.6524	61.8189	75.9752	67.8054	63.8290
11	70.1631	61.0190	56.5840	74.4941	65.5850	61.4711	78.2226	69.3146	65.2932	80.1376	71.1244	67.5148
12	73.4926	64.2410	59.7944	78.3673	69.1425	64.6530	82.3249	72.7158	68.8004	83.6086	74.8335	70.8105
13	76.6706	67.3704	62.8445	82.1432	72.4320	67.9617	85.3574	75.8974	71.9492	87.0423	78.2173	74.1882
14	80.0418	70.5776	65.8590	85.2864	75.4975	71.3211	88.8386	79.5766	75.2114	90.3403	81.7286	77.5096
15	84.0802	73.7347	68.8633	88.4347	78.9028	74.3645	92.2103	83.3200	78.4583	94.0639	85.0087	80.7992
16	87.4322	76.9562	71.9205	92.3336	82.2312	77.4168	95.1558	86.2379	81.7586	97.7637	88.6536	84.0640
17	90.7474	79.7943	74.8178	95.7965	85.5749	80.5893	98.0015	89.1243	84.8006	101.0656	91.5276	87.1595
18	93.6207	83.1320	77.7933	99.6187	88.5643	83.5238	101.4448	92.2353	87.6681	104.4112	94.4892	90.3666
19	97.0491	86.1430	80.7262	103.1162	91.5781	86.6554	105.0556	95.2033	90.7787	107.8551	97.6908	93.3728
20	99.7415	89.2297	83.7679	106.1907	94.4498	89.6990	108.3711	98.6898	93.7538	111.3282	101.0138	96.1448
21	102.7708	92.4134	86.7880	109.0796	97.7427	92.4798	110.9299	101.6920	96.9791	113.8511	104.2964	99.3406
22	107.0216	94.9982	89.7889	111.9224	100.6927	95.5144	114.4548	104.5929	99.8999	117.3357	107.1821	102.1669
23	109.3955	98.0091	92.6702	114.6483	103.7361	98.6038	117.2681	107.6863	102.9734	119.7443	110.1936	105.1935
24	112.6213	100.8341	95.5399	117.7340	106.8201	101.5103	121.0695	110.9708	105.8419	123.3394	113.2957	108.4736
25	116.0632	103.9978	98.4317	121.1339	109.7475	104.3375	124.2170	114.0034	108.7367	126.4131	116.1696	111.4165
26	119.0756	106.9471	101.2572	124.1982	112.4969	107.1242	127.8945	116.9054	112.0091	129.4324	119.2565	114.3528
27	122.0908	109.7164	104.1169	127.0093	115.5822	110.1059	131.1018	120.0060	114.7644	133.2633	122.5152	117.2193
28	124.6389	112.6474	106.7532	129.9711	118.1516	112.9430	133.8766	123.1914	117.6789	136.3651	125.0015	120.2743
29	127.2651	115.5013	109.4675	132.3366	121.3769	115.6704	137.0042	126.0768	120.5752	139.1865	128.0725	123.0440
30	130.4464	118.1710	112.1605	136.4386	124.2826	118.4286	140.4643	129.2154	123.4041	142.2166	131.1393	125.8662

S4. SUPPLEMENTARY MONITORING STATISTICS

Table S4.6: Finite-horizon simulated critical values (entries are critical values, not percentages) for the adjusted-range self-normalized MOSUM statistic for two bandwidth fractions  $h \in \{0.10, 0.20\}$

Panel A: $h = 0.10$												
$q$	$T = 1$			$T = 2$			$T = 5$			$T = 10$		
	1%	5%	10%	1%	5%	10%	1%	5%	10%	1%	5%	10%
1	31.0543	21.4546	17.3059	35.6399	24.5829	20.2594	40.3685	28.6062	23.6858	42.5687	30.9127	25.5724
2	38.3165	27.7122	23.4387	42.7298	31.4275	26.6964	46.6925	35.4634	29.9992	50.8268	37.9316	32.6500
3	42.5584	32.4345	27.9954	47.7389	36.7527	31.6960	53.0207	40.9217	35.4716	56.9638	43.5280	38.0962
4	46.9735	36.4895	31.9339	52.1703	40.8281	35.8874	56.4268	44.8067	39.6720	61.2296	47.6879	42.4473
5	50.5587	40.3458	35.5897	55.1244	44.3791	39.3941	61.6938	48.6794	43.5848	65.7906	51.2952	45.7998
6	54.3870	43.8161	38.8256	58.8503	47.6616	42.8261	65.8629	52.1184	46.8412	70.4619	55.4766	49.6997
7	58.2227	46.9348	41.8582	63.2388	50.9419	45.8808	69.9763	55.6927	50.2069	73.7238	59.4513	53.2715
8	62.5904	50.1069	45.0973	66.5894	54.2427	49.0056	73.7464	58.8717	53.2371	77.4179	63.2434	56.8052
9	65.5321	52.9299	47.8388	69.7919	57.3810	51.9567	76.9132	61.9771	56.7759	80.4633	66.3060	59.9787
10	69.1894	55.7694	50.5044	73.1730	60.2772	54.7326	79.9700	65.1130	59.6876	83.4500	69.2194	62.9681
11	71.3605	58.5525	53.2092	75.6859	62.8198	57.5244	83.1652	68.2526	62.3808	86.0388	72.1523	66.0342
12	73.9892	61.3284	55.7886	78.7893	65.8103	60.2407	85.8690	71.3055	65.3524	88.8407	75.2678	68.9589
13	77.4691	64.2108	58.3225	81.5784	68.4372	62.8937	88.7415	74.2104	68.0439	91.6088	77.9737	71.6132
14	79.6284	66.8216	60.9816	84.7795	71.7253	65.5328	92.1165	76.7820	70.6799	94.4293	80.6059	74.4083
15	81.3365	69.3465	63.6462	87.2500	74.1261	67.9494	94.4236	79.3181	73.3277	97.6324	83.7589	77.2091
16	83.9109	72.0331	66.0375	89.9434	76.4564	70.6384	96.6525	81.9477	75.9642	99.7166	86.4179	79.9023
17	87.0552	74.3059	68.6490	92.4570	78.9391	73.0922	98.5784	84.4938	78.6784	102.7749	88.9903	82.3706
18	89.8542	76.7874	70.8806	94.9927	81.4712	75.5944	100.8306	86.8195	81.2222	105.0631	91.2521	84.7211
19	92.2295	79.0286	73.2782	97.2822	83.9976	78.0391	102.9741	89.7837	83.7234	107.4236	93.5531	87.3815
20	95.4742	81.2550	75.3776	99.7911	86.6994	80.6279	106.6501	92.2843	86.1231	110.0901	96.2215	89.7636
21	97.3036	83.4499	77.6380	102.9719	89.2988	83.0320	108.5206	94.8145	88.4821	112.5431	98.6046	92.3079
22	101.1764	86.1104	80.1405	105.4679	91.8061	85.3023	110.8844	97.1323	90.7979	115.0312	100.9943	94.7719
23	102.7101	88.2603	82.3944	107.2639	94.1482	87.7085	113.6135	99.7935	93.3623	118.3106	103.7075	97.1170
24	105.2965	90.6602	84.5605	109.6442	96.5620	90.3802	115.0688	102.2028	95.5713	120.5657	106.0444	99.5043
25	107.8800	92.7588	86.9090	112.5512	98.7168	92.5740	117.8927	104.8287	98.0323	123.1860	108.2611	101.8471
26	110.3892	95.5845	89.0688	115.9603	100.9074	94.7729	119.2353	107.1538	100.1277	125.2353	110.7765	104.3448
27	112.6515	97.8350	91.3728	116.8098	103.3083	97.1967	121.4889	109.1583	102.9004	127.8138	113.0884	106.6985
28	114.5770	100.2352	93.3719	119.4415	105.6940	99.5721	124.3324	111.4990	105.1671	130.8219	115.5049	108.9276
29	117.5742	102.2967	95.5410	121.3723	107.9041	101.4538	127.4841	113.7894	107.4346	132.6145	118.0104	111.3525
30	118.8322	104.5551	97.8899	123.7670	110.1940	103.6728	129.3094	116.0444	109.7760	134.5738	120.3368	113.8546

Panel B: $h = 0.20$												
$q$	$T = 1$			$T = 2$			$T = 5$			$T = 10$		
	1%	5%	10%	1%	5%	10%	1%	5%	10%	1%	5%	10%
1	26.7211	17.6046	13.9445	31.2632	21.8787	17.7316	37.7122	26.1786	21.6169	41.9925	29.5406	24.3568
2	33.7831	23.2895	19.4963	38.5666	28.4697	23.9235	44.4505	33.0745	28.0543	48.9407	36.3831	31.3049
3	38.2499	27.7394	23.6256	44.6730	33.3331	28.6214	49.0799	38.1529	33.1640	55.3534	42.3764	36.6309
4	42.6767	31.7745	27.3459	48.4922	37.6408	32.5304	53.8458	42.7656	37.6101	59.4184	47.0487	41.0471
5	45.4443	35.0784	30.6970	53.0848	41.2975	36.0643	57.4055	46.2698	41.2715	63.9612	50.6103	44.7205
6	49.7839	38.5017	33.8095	56.3091	44.5686	39.4030	62.2476	49.9591	44.7730	67.9643	54.4266	48.4459
7	52.7201	41.5905	36.5607	59.6877	48.1400	42.9378	65.0362	53.5733	47.8862	71.4788	57.8961	51.8314
8	55.7822	44.4939	39.4038	63.0907	51.5388	45.8790	67.7608	56.5522	50.8139	74.5551	61.1704	55.3853
9	58.7190	47.3736	42.3750	65.8132	54.0707	48.4931	71.3976	59.8029	54.2149	77.7497	64.4055	58.4455
10	60.9931	50.0964	45.1869	69.3055	56.6615	51.0486	74.4682	62.7835	57.0593	80.3795	67.5694	61.5189
11	63.7774	52.6473	47.7810	72.3766	59.6443	54.0561	77.3918	65.6517	60.1620	83.7294	70.3093	64.5398
12	67.9729	55.1142	50.2203	75.2969	62.2793	56.9521	81.9574	68.5242	62.6421	87.1843	73.1739	67.4679
13	70.9941	57.4650	52.6622	77.4362	65.1637	59.4270	85.2697	71.4863	65.2125	90.1971	75.7989	70.1048
14	73.0475	60.3705	55.0409	80.4621	67.8206	62.0220	88.6323	74.3011	68.0200	92.7058	78.7607	72.6265
15	74.8709	62.9382	57.3751	83.5313	70.2807	64.4683	90.8500	76.7151	70.7068	95.4532	80.9682	75.2499
16	77.7659	65.5340	59.8896	86.6297	72.9830	67.1044	92.9858	79.2483	73.6134	97.7765	83.8046	77.5920
17	80.1075	67.7378	62.1235	88.9483	75.4523	69.5264	95.5411	81.9638	75.8259	100.3182	86.5492	80.2798
18	82.8811	70.2983	64.5508	90.9049	78.2434	71.8934	98.0643	84.5480	78.6596	103.2605	89.4022	82.9149
19	85.5858	72.5047	66.8240	93.9954	80.8974	74.3040	100.2167	86.9012	81.0777	105.8906	91.9500	85.5184
20	87.7450	75.0411	69.2300	96.5540	82.9935	76.9034	102.2192	89.1803	83.3999	108.3090	94.4931	88.0406
21	89.3456	77.2281	71.5623	99.0116	85.1660	79.4211	104.9281	91.8117	85.8656	110.8261	96.8027	90.5866
22	92.1810	79.6455	73.7936	100.9512	87.7541	81.6283	108.0520	94.1263	88.1145	112.5795	99.3847	93.1145
23	94.2830	82.0301	76.0229	103.0892	89.8520	83.6978	110.5475	96.7271	90.6520	115.2597	101.9125	95.4976
24	97.1320	83.8593	78.1269	105.7120	92.3031	86.1257	113.6621	99.2727	92.9635	119.6887	104.7735	97.9783
25	99.3108	86.1522	80.2689	107.7001	94.7112	88.3019	116.2860	101.5637	95.3312	122.5977	106.9254	100.3366
26	100.8605	88.5306	82.5507	109.6368	96.7471	90.5666	117.8316	104.0702	97.9250	125.1533	109.1596	102.5354
27	103.3850	90.6138	84.5639	111.8508	99.2068	92.7111	120.0510	106.2922	100.2106	127.2948	111.5061	105.0595
28	105.6054	93.0323	86.8413	114.4174	101.3849	94.8459	123.3156	108.7302	102.2317	128.6505	113.8061	107.2344
29	108.2133	95.2081	88.8727	117.4403	103.6914	96.8192	125.7184	111.2826	104.7273	131.4777	116.1742	109.3873
30	110.6552	97.4386	91.0497	119.0834	105.5330	99.2014	127.4973	113.6704	107.1416	132.9900	118.4805	112.0585

Table S4.7: Finite-horizon simulated critical values (entries are critical values, not percentages) for the HAC LRV-scaled multiscale MOSUM statistic with bandwidth set  $\mathcal{H} = \{0.05, 0.10, 0.20\}$  and equal scale weights

q	T = 1			T = 2			T = 5			T = 10		
	1%	5%	10%	1%	5%	10%	1%	5%	10%	1%	5%	10%
1	31.2624	24.1507	21.0678	33.5441	26.8817	23.8347	35.9777	29.7860	26.7108	37.5633	30.5138	27.6863
2	38.2595	30.7794	27.5170	40.8844	33.4446	30.2963	42.9026	36.0571	32.9291	43.9171	37.1802	34.1408
3	43.8595	36.0210	32.5813	46.6343	38.8505	35.6650	48.6908	41.4877	38.3186	49.4333	42.6296	39.5260
4	48.5653	40.8490	37.1835	51.7224	43.7216	40.2595	53.3031	46.1654	42.8869	54.8480	47.3783	44.1113
5	53.4992	44.9946	41.5403	55.5173	48.0483	44.4430	57.4894	50.6140	47.2822	59.5071	51.8188	48.5509
6	57.3416	49.0967	45.4076	60.0290	51.9350	48.4991	62.7355	54.7861	51.4681	64.2323	56.2467	52.7103
7	61.8953	52.9867	48.9813	63.8585	56.0627	52.2381	67.7081	59.0711	55.3755	67.9673	60.1795	56.6841
8	65.9331	56.9860	52.8992	67.7398	59.8059	56.1789	72.0019	62.7266	59.1627	72.6257	64.4856	60.5783
9	69.8709	60.5854	56.4811	72.4767	63.5083	59.7312	75.5834	66.7734	63.0345	75.9546	68.0092	64.2873
10	73.4751	64.0480	59.8740	76.0899	67.1106	63.0841	79.3258	70.4578	66.4270	79.9652	71.5969	67.8056
11	77.3248	67.3322	63.3017	80.3604	70.7838	66.6049	83.3440	74.0643	70.0181	83.7215	75.3140	71.3227
12	80.6978	70.6845	66.2225	84.0696	74.3420	70.1895	86.4514	77.7668	73.6728	87.3428	78.8652	74.8651
13	83.9822	74.1867	69.5489	86.9920	77.9512	73.5079	90.4074	81.2353	77.0320	90.6761	82.5450	78.3128
14	87.5862	77.3035	72.8972	91.0859	81.4942	76.8122	93.4110	84.6940	80.5419	94.7649	85.9883	81.8693
15	90.7443	80.8971	75.9935	94.3035	84.8466	80.3287	96.7360	88.0207	83.9595	99.2291	89.4879	85.1404
16	94.1229	84.1230	79.3267	97.7682	87.9598	83.5402	100.9357	91.2273	86.9915	102.1420	92.7887	88.8149
17	97.0445	87.3776	82.6182	101.6377	91.1886	86.7489	104.1498	94.1910	90.0719	105.4997	96.1709	91.7845
18	100.4359	90.6436	85.6521	104.9787	94.2919	89.7632	107.6729	97.2532	93.0255	109.7626	99.3719	94.9466
19	103.6685	93.4249	88.7406	108.1354	97.6903	92.9129	110.4700	100.5287	96.1721	112.8908	102.6614	97.9756
20	106.9117	96.6623	91.6440	111.0143	101.1290	96.1237	113.6261	104.1254	99.1466	115.6785	105.8059	101.2453
21	110.2622	99.8182	94.7466	114.8893	104.4943	99.2820	116.7743	106.8867	102.2791	118.6630	109.2380	104.5528
22	114.1729	102.7441	97.5119	118.1240	106.8954	102.0633	120.0672	109.9888	105.4943	122.1109	112.2287	107.4614
23	117.5826	105.8301	100.7186	120.7925	109.9727	105.2956	123.1333	112.8162	108.5384	125.2230	115.0285	110.5563
24	120.5957	109.2360	103.7970	124.1287	112.9248	108.3486	126.2941	116.4100	111.6916	128.3032	118.1944	113.5250
25	123.8223	111.9398	106.8558	127.2943	116.1473	111.0728	129.5261	119.5921	114.8162	131.2164	121.2964	116.4674
26	126.3543	115.0338	109.7135	129.5086	118.8389	114.0812	132.3304	122.4347	117.4808	134.7591	124.2627	119.6815
27	129.3171	117.8086	112.7031	133.8979	122.1290	117.0835	136.0097	125.8396	120.8280	137.9587	127.3186	122.7259
28	132.1645	120.8501	115.4952	136.8811	125.2779	119.9417	139.6023	128.7828	123.7403	140.9411	130.5281	125.3963
29	135.5278	123.9359	118.3033	138.7646	128.2183	122.9671	142.4188	131.6496	126.9664	144.2637	133.5025	128.3947
30	138.1063	127.1204	121.2981	141.6536	131.2629	125.8754	145.7660	134.8611	129.8317	146.9545	136.3358	131.2947

Table S4.8: Finite-horizon simulated critical values (entries are critical values, not percentages) for Shao's self-normalized multiscale MOSUM statistic with bandwidth set  $\mathcal{H} = \{0.05, 0.10, 0.20\}$  and equal scale weights

q	T = 1		T = 2		T = 5		T = 10					
	1%	5%	1%	5%	1%	5%	1%	5%				
1	665.3880	413.7148	313.1398	771.2993	486.0873	366.4957	890.8790	550.8419	428.0911	927.4016	606.4142	467.7151
2	1113.5912	760.4857	616.0878	1257.7229	877.5951	723.7739	1383.0912	990.4244	818.2689	1494.6746	1062.4074	885.5598
3	1606.9296	1113.5465	945.3773	1761.1184	1298.2300	1095.3490	1970.6469	1447.3662	1226.0402	2002.6364	1524.9221	1310.9210
4	2105.6092	1526.4546	1299.2890	2328.7676	1735.3593	1503.0692	2506.8896	1921.6936	1667.2620	2591.3533	1999.2851	1760.9030
5	2613.4514	1983.8849	1690.9686	2914.7236	2205.3233	1921.9992	3190.8197	2417.3895	2133.2644	3225.9035	2530.0404	2245.1444
6	3121.8097	2453.0498	2146.7167	3480.3001	2713.1820	2386.7885	3783.0126	2981.3349	2636.8232	3896.4179	3122.7310	2761.3474
7	3713.6009	2976.6887	2595.1727	4073.3289	3240.2373	2877.2328	4380.9105	3538.1888	3151.3573	4476.8062	3660.5664	3296.7556
8	4375.7378	3491.1095	3080.2262	4781.8543	3825.1116	3433.7998	5127.1245	4144.3429	3719.2096	5227.3121	4283.7793	3864.3447
9	5052.6245	4061.0094	3605.3940	5489.1594	4431.7404	3987.2927	5864.8963	4781.6761	4302.0105	5998.1253	4949.6969	4549.0907
10	5783.3241	4645.7288	4164.9032	6166.6130	5059.1988	4570.2841	6552.8475	5389.6610	4911.1749	6770.8610	5624.8719	5106.3642
11	6561.2915	5203.7682	4686.5166	6925.8249	5703.4467	5162.2776	7248.4539	6056.6993	5546.8161	7479.9910	6268.5303	5751.5621
12	7254.8592	5824.6721	5286.2984	7612.2217	6385.0185	5803.4658	8078.8586	6776.4153	6221.7695	8303.5965	6954.1085	6394.7862
13	7910.9589	6525.9890	5896.0481	8362.9015	7089.5098	6424.9427	8840.5953	7603.1250	6902.9272	9225.5430	7749.4850	7135.1887
14	8744.2865	7226.7852	6541.7988	9319.9800	7763.7026	7098.9985	9645.0068	8285.1372	7658.6551	10115.7275	8505.7269	7870.1651
15	9515.5829	8006.6305	7287.8482	10169.0939	8525.6361	7806.9704	10452.8227	9039.7748	8385.0606	11090.4671	9295.0687	8611.5409
16	10568.7154	8713.9845	7973.9921	10933.8044	9365.9582	8571.9482	11325.6254	9793.2122	9119.9239	11850.2428	10080.6637	9352.8641
17	11331.3557	9455.3189	8683.8520	12036.5510	10136.4211	9316.8986	12333.5073	10618.8331	9884.5295	12850.2905	10991.2685	10193.8591
18	12190.6390	10234.7828	9374.5291	12916.3309	10934.2724	10107.4331	13350.0576	11508.7139	10688.7115	13850.7154	11831.0654	11021.7742
19	13079.2606	11071.2619	10173.4976	13786.8973	11735.4346	10877.5585	14420.4102	12474.5681	11572.2048	14830.3194	12749.9607	11913.0851
20	13857.5322	11913.2929	10967.5724	14893.1937	12645.2399	11706.2192	15419.7896	13368.7427	12470.1840	15727.4231	13683.1510	12798.3235
21	14946.3344	12771.4511	11793.9047	15962.4223	13611.0963	12577.4578	16282.0344	14215.9639	13326.5160	16808.5947	14638.7026	13688.4301
22	15948.8335	13692.1997	12648.0393	16971.7119	14552.0624	13508.2706	17361.5393	15204.5755	14227.2760	17817.0340	15635.5969	14666.9684
23	16996.8381	14583.2135	13499.7842	18060.9012	15550.0940	14390.4054	18620.1287	16223.3887	15223.7712	18802.6366	16642.8591	15636.7431
24	18000.1382	15565.7951	14419.6004	18936.8435	16522.8647	15345.8333	19881.8142	17264.2155	16179.4088	19847.7048	17633.3372	16647.7062
25	19201.2109	16581.8716	15317.9920	20041.2140	17487.8579	16337.1942	20873.0273	18259.5928	17155.3991	21105.2255	18759.2528	17651.8278
26	20320.6868	17498.7505	16210.7986	21178.3662	18447.5597	17283.8225	21916.7057	19394.5684	18193.7425	22242.4848	19749.0086	18670.7610
27	21468.7589	18542.8700	17197.1479	22240.1426	19551.0432	18295.8526	23199.3234	20502.6927	19282.7592	23436.2493	20912.8440	19735.9577
28	22679.8313	19524.1427	18184.6506	23541.1052	20694.2500	19339.9274	24615.2059	21692.0448	20384.4016	24914.3190	22015.2124	20807.4328
29	23818.9107	20516.6591	19159.9156	24727.7478	21746.5622	20329.9638	25765.1239	22724.7831	21478.3776	26015.1405	23278.0883	21922.1505
30	25005.3559	21683.7359	20147.3029	26000.3199	22920.7586	21388.8537	26874.6296	23832.0246	22548.9898	27247.3494	24483.0169	23086.1212

S4. SUPPLEMENTARY MONITORING STATISTICS

Table S4.9: Finite-horizon simulated critical values (entries are critical values, not percentages) for the adjusted-range self-normalized multiscale MOSUM statistic with bandwidth set  $\mathcal{H} = \{0.05, 0.10, 0.20\}$  and equal scale weights

q	T = 1			T = 2			T = 5			T = 10		
	1%	5%	10%	1%	5%	10%	1%	5%	10%	1%	5%	10%
1	33.2616	22.7608	18.4798	37.7248	26.3791	21.8734	43.5213	30.8835	25.4640	46.4982	33.5769	28.1113
2	40.2516	28.8900	24.7231	44.1517	33.7466	28.6106	49.3196	37.7647	32.4626	54.4264	41.3625	35.1804
3	44.5960	34.0881	29.3946	50.0912	38.8006	33.7647	55.3655	43.1890	37.8979	60.2794	47.0818	41.2164
4	48.9839	38.1681	33.3415	54.9719	43.0536	38.0170	59.7364	47.7057	42.4111	65.3400	51.5407	45.5313
5	51.9442	41.9695	37.0077	58.7853	46.8251	41.7432	64.0893	51.5458	46.1658	69.6275	55.2963	49.4002
6	55.8876	45.7864	40.4325	62.6258	50.1721	44.9403	68.5510	55.1338	49.7439	74.2153	59.4447	53.3623
7	59.9459	49.0912	43.6420	66.2814	54.0436	48.3400	72.9490	58.7186	53.2378	77.5700	63.5684	56.9419
8	64.0635	52.1943	46.8687	70.1303	57.1403	51.5569	76.6762	62.2874	56.5547	81.1293	67.4035	60.5919
9	67.8130	55.3873	49.7391	72.7199	60.0837	54.6321	79.6704	65.5590	59.7083	84.9103	70.6064	63.8836
10	71.0651	57.4408	52.3931	75.9379	63.1318	57.3636	83.0623	68.7116	62.8373	87.3746	73.3895	66.9669
11	73.9805	60.4983	55.1762	78.7884	66.1270	60.1868	87.3320	71.4748	65.6571	90.1851	76.1621	69.9132
12	76.2817	63.4695	57.4756	82.6874	68.8337	62.8952	89.8614	75.0064	68.7282	93.3529	79.1700	72.6955
13	80.2074	66.0352	60.2388	84.7991	71.6072	65.7136	93.2441	77.9153	71.5315	96.7788	81.8360	75.5536
14	82.0578	68.4689	62.9183	88.1220	74.7299	68.5639	96.3132	80.6445	74.1954	98.7302	84.7961	78.2247
15	84.7255	71.2103	65.3848	90.7704	77.5152	70.9594	98.1538	83.1646	76.8163	102.1397	87.6320	80.7792
16	86.9469	74.0343	67.9972	92.7683	80.2360	73.4805	100.5819	85.3943	79.4582	103.5128	90.1328	83.5886
17	89.3775	76.3798	70.7686	95.8724	82.5308	75.9638	103.4924	88.0068	82.1331	105.8569	92.6317	86.3029
18	92.3587	79.0109	73.1096	97.9632	84.8046	78.7131	105.4163	91.0078	84.6688	109.8114	95.3247	88.9210
19	94.6837	81.2209	75.3916	100.6783	87.3586	81.4005	108.2816	93.7444	87.0588	112.5632	97.3766	91.4123
20	97.1373	83.4039	77.6341	104.3244	90.0078	83.7409	110.2846	96.1570	89.4124	114.6926	100.1598	93.9315
21	99.0424	85.8146	79.8651	106.2351	92.3225	86.0454	112.4390	98.4655	92.2254	117.5545	102.7534	96.5210
22	103.1219	88.2975	82.4038	108.5434	94.8786	88.6283	114.7924	101.0489	94.5875	119.6685	105.2108	98.8842
23	105.5131	90.3708	84.5815	110.7419	97.4819	90.8853	116.9835	103.5540	96.9236	122.9475	107.9967	101.2856
24	108.0365	92.8504	86.7964	113.2498	99.8443	93.3813	118.7632	106.0403	99.3723	125.8650	110.4257	103.6620
25	110.1216	95.3807	89.2528	115.7946	102.1010	95.6290	121.5196	108.5165	101.7702	128.4802	112.2799	106.0171
26	112.6084	97.7986	91.3319	117.6207	104.1365	97.8278	123.6539	110.6293	104.1752	129.9519	114.8609	108.5827
27	113.8435	99.9918	93.5944	120.1194	106.6155	100.3825	126.3035	112.9453	106.4965	132.7889	117.3650	110.9377
28	117.2975	102.1801	95.7677	122.3891	109.1722	102.4977	129.0236	115.3662	109.0257	135.4354	119.6989	113.3531
29	120.6776	104.6036	98.1851	124.8218	111.2441	104.5459	131.8489	117.8264	111.5620	137.6509	122.6113	115.7693
30	121.6989	106.8013	100.5271	127.1137	113.5859	106.7110	133.3900	120.3004	113.8333	140.3597	124.8599	118.3007

**Weighted-CUSUM** Tables S4.10, S4.11, and S4.12 report the critical values for the weighted-CUSUM statistic with inverse-square-root segment-length weight  $\omega(\ell) = \ell^{-1/2}$ .

Table S4.10: Finite-horizon simulated critical values (entries are critical values, not percentages) for the HAC LRV-scaled weighted-CUSUM statistic with inverse-square-root weight  $\omega(\ell) = \ell^{-1/2}$  and two boundary exponents  $\gamma \in \{0, 0.15\}$

Panel A: $\gamma = 0$												
$q$	$T = 1$			$T = 2$			$T = 5$			$T = 10$		
	1%	5%	10%	1%	5%	10%	1%	5%	10%	1%	5%	10%
1	6.0203	4.3565	3.7286	6.6623	5.0681	4.3731	7.5580	5.8762	5.1185	7.8087	6.3020	5.5596
2	7.3180	5.7283	4.9787	8.3544	6.5319	5.7336	9.2413	7.4130	6.6412	9.7518	7.9475	7.1253
3	8.4717	6.7599	5.9473	9.6010	7.7296	6.8538	10.4682	8.7110	7.8179	11.2305	9.2145	8.3335
4	9.5232	7.6793	6.8449	10.6004	8.6382	7.8070	11.4924	9.7033	8.8091	12.3824	10.3647	9.4128
5	10.4892	8.5775	7.7068	11.7033	9.5517	8.6741	12.6566	10.6505	9.7767	13.6636	11.4165	10.4460
6	11.4698	9.3576	8.4977	12.7180	10.5046	9.5252	13.8495	11.5671	10.6637	14.7640	12.4560	11.3841
7	12.3139	10.1945	9.2617	13.4936	11.4416	10.4007	14.9059	12.5724	11.5881	15.4720	13.4206	12.3375
8	13.1960	11.0172	10.0255	14.5285	12.2836	11.1654	15.6772	13.5479	12.4467	16.5562	14.3082	13.2562
9	14.1161	11.7975	10.7482	15.3464	13.1278	11.9883	16.6128	14.4371	13.2987	17.5179	15.2554	14.0930
10	14.7500	12.5432	11.5031	16.2683	13.8404	12.7724	17.5102	15.3158	14.1552	18.3630	16.0774	14.9732
11	15.4792	13.2134	12.1848	17.2228	14.6585	13.5143	18.2865	16.0761	14.9095	19.2461	16.8652	15.7511
12	16.3620	13.9418	12.8971	17.8405	15.4673	14.2822	19.2650	16.8989	15.7048	20.3171	17.6185	16.4956
13	17.2247	14.7320	13.5877	18.7678	16.1860	14.9759	20.2202	17.7409	16.5459	21.1387	18.5577	17.2881
14	17.9459	15.4588	14.2918	19.4934	16.9713	15.7243	20.9593	18.5015	17.3191	21.8512	19.3638	18.0908
15	18.6660	16.2334	14.9831	20.2386	17.6585	16.3826	21.7888	19.2322	18.0427	22.4645	20.2272	18.8552
16	19.5633	16.8848	15.6836	20.9106	18.4110	17.0840	22.6733	19.9681	18.7831	23.4142	20.9956	19.6567
17	20.2601	17.6351	16.3401	21.6591	19.1579	17.8494	23.4879	20.6658	19.5274	24.2532	21.6558	20.3891
18	20.9652	18.2633	17.0060	22.3662	19.8769	18.6075	24.1196	21.4412	20.1805	25.2166	22.3744	21.1664
19	21.6697	18.9384	17.6426	23.1950	20.6310	19.2943	25.1132	22.1621	20.9533	25.9006	23.2063	21.9270
20	22.2798	19.7059	18.2919	23.9874	21.3655	20.0060	25.9369	22.9421	21.6804	26.6324	23.9773	22.6357
21	22.9440	20.3220	18.8929	24.7319	22.0559	20.6182	26.7207	23.6455	22.3938	27.3839	24.7692	23.3805
22	23.6816	20.9947	19.5602	25.5362	22.7176	21.2882	27.2881	24.5134	23.0879	28.1958	25.4485	24.1553
23	24.6270	21.6374	20.2117	26.3688	23.4059	21.9929	27.9822	25.2254	23.7663	29.0106	26.2294	24.8323
24	25.4426	22.3459	20.9086	27.2368	24.1125	22.6944	28.6865	25.9354	24.4013	29.6568	27.0032	25.5002
25	26.0451	22.9899	21.5080	27.7996	24.8258	23.3485	29.5354	26.6027	25.1461	30.4728	27.6073	26.2630
26	26.8514	23.6749	22.1650	28.4612	25.5378	24.0013	30.3980	27.3204	25.8271	31.2511	28.3653	26.9289
27	27.4989	24.2811	22.7333	29.4067	26.2524	24.6323	31.1681	28.1209	26.5233	32.1024	29.1357	27.6612
28	28.1136	24.9321	23.3097	30.0501	27.0047	25.3630	31.9926	28.7251	27.1938	32.8216	29.8430	28.3270
29	28.7278	25.6786	23.9520	30.7899	27.5590	25.9748	32.7542	29.5165	27.8977	33.6576	30.4840	29.0184
30	29.4098	26.3553	24.5804	31.4577	28.2641	26.6924	33.4287	30.1542	28.6354	34.2634	31.2034	29.6921

Panel B: $\gamma = 0.15$												
$q$	$T = 1$			$T = 2$			$T = 5$			$T = 10$		
	1%	5%	10%	1%	5%	10%	1%	5%	10%	1%	5%	10%
1	10.6011	8.3443	7.4422	10.8688	9.0340	8.0941	12.0431	9.8227	8.8351	12.3328	10.2856	9.2937
2	12.5155	10.3448	9.3566	13.3252	11.1357	10.1242	14.1889	12.0154	10.9209	14.6690	12.4561	11.4616
3	14.1219	11.8658	10.8718	15.0640	12.7808	11.6835	15.9566	13.7573	12.6821	16.7695	14.2903	13.2116
4	15.6854	13.3160	12.2353	16.4769	14.1359	13.1126	17.4439	15.1559	14.0722	18.3900	15.8082	14.6655
5	16.9600	14.5554	13.5198	17.9371	15.5395	14.3848	19.0045	16.5382	15.4314	19.8677	17.2809	16.1496
6	18.4490	15.8841	14.6886	19.4932	16.8214	15.6334	20.4381	17.9233	16.7358	21.2833	18.5910	17.5032
7	19.6117	17.0388	15.8520	20.7377	18.0943	16.8607	22.0452	19.2744	18.0693	22.5396	19.9299	18.7232
8	20.8733	18.2343	16.9950	22.0278	19.2558	18.0251	23.4044	20.4340	19.2265	24.0778	21.2070	19.9165
9	22.1049	19.3656	18.1700	23.1550	20.4245	19.0719	24.7867	21.8208	20.3802	25.3414	22.3903	21.1247
10	23.2566	20.3906	19.1961	24.3886	21.6073	20.2206	25.8020	22.9671	21.5747	26.7803	23.5343	22.3455
11	24.2647	21.5024	20.1997	25.6047	22.6971	21.3466	27.0134	24.0662	22.6801	27.7981	24.7436	23.3589
12	25.5500	22.6715	21.2271	26.8006	23.7903	22.4249	28.1264	25.1714	23.7897	29.0473	25.9026	24.5057
13	26.8333	23.7810	22.2957	27.8951	24.8508	23.3772	29.1722	26.3327	24.9019	29.9557	27.0387	25.6396
14	27.9247	24.7355	23.3474	28.8818	25.9159	24.4759	30.4697	27.4767	25.9838	31.2787	28.1196	26.6991
15	29.0150	25.8454	24.3393	30.0351	27.0452	25.4717	31.6764	28.5803	27.0697	32.2990	29.2147	27.8352
16	30.0595	26.8590	25.3548	31.0329	27.9906	26.5148	32.8210	29.6339	28.1310	33.4511	30.2571	28.8477
17	30.9629	27.8306	26.2638	32.1483	28.9354	27.5283	34.0587	30.6442	29.0456	34.8244	31.3285	29.8400
18	31.9531	28.7998	27.2180	33.2577	30.0228	28.5512	34.8854	31.7403	30.1319	35.8177	32.4215	30.8810
19	33.0556	29.7553	28.1510	34.3931	31.0722	29.5388	36.3547	32.8426	31.2264	36.8447	33.4115	31.8694
20	34.0224	30.6719	29.0620	35.2878	32.0971	30.5366	37.5530	33.8727	32.2329	37.9982	34.4473	32.9667
21	35.1636	31.6838	30.0633	36.5983	33.0930	31.4608	38.4179	34.8908	33.2161	39.0107	35.5370	33.9589
22	36.1547	32.6170	31.0259	37.9098	34.0827	32.4261	39.5802	35.8356	34.1061	39.9461	36.5250	34.9577
23	37.0306	33.5510	31.9140	38.8454	35.0638	33.3857	40.3859	36.8311	35.1469	41.0471	37.5972	35.9446
24	37.9552	34.5983	32.9455	40.0298	36.1028	34.3240	41.3655	37.8061	36.1656	41.9367	38.5331	36.9226
25	39.2084	35.6511	33.8020	40.9863	36.9958	35.2561	42.3354	38.8539	37.0761	43.0407	39.5378	37.8639
26	40.2276	36.5858	34.7481	41.9585	38.0483	36.2133	43.3360	39.8200	38.0288	43.9942	40.5328	38.9268
27	41.1669	37.3938	35.5845	42.7680	39.0274	37.1132	44.3722	40.7572	38.9955	45.0338	41.4895	39.8566
28	42.0240	38.2839	36.4581	43.7696	39.8406	38.0538	45.2998	41.7691	39.9626	46.0671	42.3984	40.8328
29	43.3092	39.1859	37.3004	44.5964	40.8333	38.9790	46.3623	42.7471	40.9239	46.8980	43.3760	41.7737
30	44.1194	40.1136	38.1981	45.5097	41.7784	39.8749	47.4156	43.6530	41.8237	47.9173	44.3167	42.6669

S4. SUPPLEMENTARY MONITORING STATISTICS

Table S4.11: Finite-horizon simulated critical values (entries are critical values, not percentages) for Shao's self-normalized weighted-CUSUM statistic with inverse-square-root weight  $\omega(\ell) = \ell^{-1/2}$  and two boundary exponents  $\gamma \in \{0, 0.15\}$

Panel A: $\gamma = 0$												
$q$	$T = 1$			$T = 2$			$T = 5$			$T = 10$		
	1%	5%	10%	1%	5%	10%	1%	5%	10%	1%	5%	10%
1	120.5657	71.8590	54.8569	137.1105	85.3163	65.3241	163.0324	104.3744	79.2262	179.8601	114.8201	88.9391
2	202.2018	136.0689	108.4716	233.0006	160.3969	130.9817	270.2819	185.1416	154.2588	297.0822	209.3370	170.4058
3	295.6652	202.3564	165.4670	329.4476	237.1517	195.5365	392.8886	275.9310	231.4956	416.5156	303.3396	257.0415
4	392.5379	275.2998	231.9532	435.8014	318.9168	269.1419	516.1250	374.4321	318.7365	545.9701	405.9167	346.1020
5	475.7402	356.8138	300.5671	551.5522	412.9426	354.6973	635.8703	474.6795	408.9924	685.2573	523.4068	452.5217
6	585.9357	441.9376	382.1112	668.1016	510.7795	440.8807	765.8368	583.9874	512.2447	812.8828	630.6148	560.9369
7	687.5097	532.6513	463.9762	795.4524	618.0496	539.0026	902.7968	704.1632	615.1492	975.3427	765.8365	676.7146
8	819.5008	633.4449	549.6980	929.2326	733.1336	639.8978	1046.4369	826.8202	731.7432	1132.8963	892.0712	800.4280
9	953.9975	741.3100	648.4529	1069.9179	848.6982	750.2649	1188.0849	963.0918	846.6628	1286.6539	1031.1486	921.6804
10	1086.1047	855.1525	752.3328	1226.2883	960.9432	857.4594	1353.3561	1094.8778	972.9298	1454.9618	1182.0994	1055.6887
11	1231.0391	970.3031	860.3611	1374.5320	1093.6491	972.1340	1536.4781	1244.8531	1116.1415	1617.1034	1316.1850	1191.3271
12	1377.1524	1093.8672	965.6126	1550.9545	1238.5722	1104.0900	1715.7556	1384.0513	1247.8043	1786.3400	1479.6739	1336.3380
13	1552.2583	1222.8065	1085.4754	1710.6669	1377.2561	1238.2132	1897.0947	1554.8869	1405.7553	1992.9848	1650.2740	1493.0512
14	1706.2546	1343.6472	1207.2104	1865.5107	1522.5098	1369.0678	2078.4238	1710.4970	1546.9491	2166.1913	1812.6489	1644.1424
15	1875.7389	1482.7300	1329.0035	2042.1379	1683.3690	1504.9008	2256.7525	1885.6700	1706.1081	2355.0107	1988.1438	1807.6377
16	2024.6104	1641.3292	1470.7624	2216.2041	1836.8134	1650.9412	2416.1922	2039.8329	1861.2874	2583.2925	2162.0041	1981.4272
17	2184.4512	1797.5952	1610.0073	2412.6057	2003.0358	1811.6656	2681.5677	2225.5529	2021.1144	2814.9500	2358.1306	2156.4895
18	2378.6194	1967.2694	1755.3395	2624.1581	2170.8142	1967.3724	2895.3296	2420.2886	2195.7021	3089.9968	2567.6762	2344.3855
19	2570.2604	2112.0757	1909.0299	2814.6034	2366.4930	2135.7111	3118.2986	2615.2885	2378.8062	3273.9265	2779.4009	2537.7079
20	2762.6709	2281.9130	2064.0594	3046.5908	2550.2161	2294.6010	3347.0688	2797.0918	2558.4284	3545.3557	2998.5709	2744.8179
21	2942.6264	2463.0993	2215.7993	3244.6402	2732.0979	2479.1424	3566.2691	3009.1143	2752.5622	3767.2093	3202.0744	2939.9103
22	3144.0638	2639.2711	2381.2988	3496.4742	2910.9765	2662.4652	3793.8527	3222.2859	2960.4023	3996.4312	3423.4353	3164.7956
23	3341.5534	2807.8164	2556.0938	3724.2461	3129.3474	2843.8683	4058.0291	3444.9532	3156.4864	4279.2527	3653.2792	3376.6866
24	3591.2640	2994.5894	2742.2144	3944.0992	3317.7756	3035.1613	4301.0122	3675.2750	3368.7193	4538.9871	3874.5356	3573.2470
25	3807.5355	3196.1720	2924.7390	4171.3178	3525.4518	3218.7226	4523.9005	3889.7284	3583.7003	4830.5688	4121.9075	3820.4114
26	4091.7839	3384.1011	3108.0571	4386.3181	3717.7650	3437.1946	4765.5621	4136.9695	3813.3686	5123.3657	4367.7424	4047.7424
27	4267.3251	3600.0747	3295.4164	4605.5708	3949.7543	3633.5953	5157.7576	4348.9616	4033.3964	5358.1680	4594.3298	4270.7626
28	4503.4606	3829.0251	3486.9603	4916.1226	4177.4063	3848.4644	5404.4947	4620.9545	4282.9943	5616.1667	4857.1911	4510.1687
29	4753.8951	4032.9141	3700.9909	5164.8547	4409.4273	4070.8452	5733.3144	4879.4960	4517.7348	5880.9984	5135.7511	4759.9598
30	5003.9566	4274.6578	3894.8399	5404.4524	4637.8751	4277.2816	6015.0013	5136.1238	4754.7093	6130.4609	5377.8067	4992.8882
Panel B: $\gamma = 0.15$												
$q$	$T = 1$			$T = 2$			$T = 5$			$T = 10$		
	1%	5%	10%	1%	5%	10%	1%	5%	10%	1%	5%	10%
1	241.0078	158.0220	120.9642	259.1545	173.7869	134.3030	289.4477	190.2088	147.1151	317.6430	200.8661	162.0289
2	398.2017	276.7549	228.3732	421.5675	309.8271	257.0519	466.2755	335.8235	279.9596	502.5077	359.3578	298.9897
3	542.8559	404.2843	341.8809	592.4441	442.6851	380.5335	682.4086	487.8520	414.9898	678.6176	515.0839	443.3961
4	720.2362	541.5787	466.9012	771.0920	589.2245	509.2817	850.0711	643.0337	556.8881	880.1896	671.0897	589.8848
5	893.1751	682.1445	597.6185	958.2322	743.5754	658.1004	1028.5820	808.7439	708.9300	1081.2213	858.6138	756.2053
6	1069.6636	843.8855	737.2168	1158.4774	905.5790	804.7836	1236.1892	982.9284	876.7245	1295.2172	1039.5276	903.8866
7	1239.4266	999.5448	889.9184	1354.0044	1098.6214	973.4543	1440.7340	1181.3515	1051.4529	1497.0954	1233.5675	1114.2626
8	1460.2665	1168.3018	1042.4261	1564.5170	1273.7414	1137.3236	1637.7316	1365.1104	1233.1714	1750.4683	1429.0170	1296.1650
9	1688.3131	1350.5233	1214.4940	1766.5134	1460.3066	1317.6195	1883.5479	1562.7770	1423.4137	1969.4597	1631.2741	1489.4545
10	1840.2198	1533.7470	1388.8504	1991.8638	1659.4180	1497.6179	2137.7220	1765.7070	1610.3849	2224.9947	1840.9413	1686.3162
11	2135.5229	1739.0011	1572.5954	2238.7058	1845.5994	1683.2055	2385.6957	1982.4910	1823.1557	2463.3302	2076.2464	1888.2500
12	2377.7645	1925.8193	1745.7962	2476.2550	2060.7006	1890.0947	2633.0068	2209.3566	2026.9829	2745.7768	2282.4746	2115.5571
13	2620.2023	2145.9720	1943.1646	2782.6262	2287.3317	2082.8126	2905.2722	2465.0937	2260.4357	3022.2756	2564.7048	2355.5690
14	2845.7683	2370.0371	2160.9479	2973.6209	2519.5111	2310.9050	3184.9520	2706.6398	2483.1113	3309.3571	2814.4629	2589.8378
15	3090.1317	2601.0265	2375.0307	3269.4734	2762.6632	2523.3483	3463.3146	2959.3123	2723.4296	3572.4468	3075.2641	2835.9318
16	3400.3670	2829.9336	2589.4410	3535.8382	2993.6632	2763.5217	3778.5683	3204.6743	2961.6929	3852.5231	3335.7356	3096.3683
17	3669.7752	3076.9812	2811.8347	3823.4741	3256.4864	3008.5212	4058.4064	3488.0386	3233.5691	4197.9003	3611.7239	3353.0370
18	3950.6080	3347.0548	3081.4715	4101.6726	3493.2370	3243.0597	4369.5747	3750.6951	3481.0961	4506.8395	3913.3289	3627.2815
19	4214.7982	3603.5410	3316.9836	4415.0757	3777.7183	3511.1478	4653.5905	4064.1775	3767.1039	4791.6023	4218.6364	3914.0390
20	4458.8237	3876.5963	3571.7412	4735.1140	4079.9348	3782.2298	4941.6719	4322.7601	4038.6905	5124.4162	4519.1782	4205.8428
21	4786.1404	4125.2768	3825.3372	5008.5555	4372.5822	4049.2784	5320.6423	4633.9836	4307.1271	5508.7160	4819.6223	4495.8879
22	5109.7869	4395.2631	4081.6062	5387.7090	4637.5456	4314.2291	5667.3115	4953.2942	4614.4567	5951.1224	5132.9374	4801.8914
23	5433.1160	4664.6860	4340.7649	5736.1010	4905.4494	4609.4979	6045.8818	5258.0963	4928.2423	6252.3357	5485.9622	5122.9524
24	5780.9929	4969.4351	4605.8895	6067.7511	5265.1396	4893.2251	6330.6493	5579.2514	5231.2167	6652.7772	5808.3413	5422.0830
25	6135.2564	5297.3026	4901.8819	6457.5421	5580.7934	5204.5051	6686.6582	5944.7295	5548.8767	7108.4943	6174.8205	5767.2674
26	6552.5806	5626.3459	5208.6971	6801.6401	5896.0664	5508.9667	7113.2159	6292.3559	5884.3967	7474.7613	6509.8806	6098.2555
27	6909.5851	5963.9141	5527.6467	7148.1171	6226.5898	5812.4560	7603.9844	6664.1794	6233.8624	7820.2287	6862.2138	6448.9812
28	7210.4441	6297.3607	5860.5215	7542.0196	6585.1578	6159.8418	7977.6443	7003.8613	6571.5230	8222.0529	7218.4427	6790.8642
29	7625.7763	6597.9338	6179.2813	7915.8504	6942.7115	6487.5440	8481.0736	7392.4681	6914.5081	8637.3985	7587.5331	7152.1528
30	7969.6973	6936.4906	6485.9033	8267.9831	7293.4593	6824.6126	8827.4585	7763.8553	7271.8854	8975.9945	8001.6704	7526.3252

Table S4.12: Finite-horizon simulated critical values (entries are critical values, not percentages) for the adjusted-simulated self-normalized weighted-CUSUM statistic with inverse-square-root weight  $\omega(\ell) = \ell^{-1/2}$  and two boundary exponents  $\gamma \in \{0, 0.15\}$

Panel A: $\gamma = 0$												
$q$	$T = 1$			$T = 2$			$T = 5$			$T = 10$		
	1%	5%	10%	1%	5%	10%	1%	5%	10%	1%	5%	10%
1	5.9112	3.9754	3.2335	6.9251	4.7637	3.9263	8.4226	5.7950	4.8052	9.2008	6.5235	5.3695
2	7.2942	5.2638	4.3686	8.4840	6.1770	5.1907	9.9565	7.2838	6.1758	11.2502	8.2004	6.9955
3	8.2863	6.1595	5.2225	9.6839	7.2716	6.1979	11.3033	8.4987	7.2975	12.9055	9.4537	8.2639
4	9.2639	6.9513	6.0075	10.6854	8.1315	7.0281	12.4093	9.5291	8.2204	13.9470	10.5558	9.1830
5	9.9704	7.6727	6.6979	11.7452	8.9355	7.8050	13.2110	10.3199	9.0568	14.9163	11.5065	10.1069
6	10.7228	8.3741	7.3249	12.7031	9.6369	8.5284	14.0316	11.0809	9.8368	15.9912	12.4234	10.9887
7	11.5665	9.0257	7.9686	13.4142	10.4154	9.2216	14.8315	11.8974	10.5358	16.6585	13.3134	11.8569
8	12.2486	9.6255	8.5860	14.1662	11.0742	9.8961	15.7347	12.7260	11.2540	17.3903	14.0716	12.5892
9	12.8861	10.2322	9.1387	14.9227	11.8684	10.5564	16.7671	13.4486	11.9955	18.2130	14.8543	13.3211
10	13.3701	10.8310	9.6853	15.5935	12.5113	11.1585	17.7115	14.2237	12.7174	18.7477	15.5014	14.0743
11	14.0046	11.4156	10.2756	16.2635	13.0059	11.7322	18.4102	14.8398	13.3609	19.3671	16.1653	14.7081
12	14.6991	12.0353	10.7896	16.8148	13.6257	12.3206	19.0930	15.4548	14.0024	20.0580	16.8166	15.3579
13	15.4221	12.5988	11.3573	17.5580	14.2565	12.9157	19.7874	16.1492	14.6723	20.7505	17.4751	15.9890
14	15.9969	13.1111	11.9041	18.0238	14.8360	13.5052	20.4260	16.7507	15.2784	21.4818	18.1605	16.6627
15	16.5300	13.7677	12.4278	18.7568	15.4348	14.0638	21.0634	17.4236	15.8692	22.2303	18.8422	17.2658
16	17.3090	14.3041	12.9682	19.3697	15.9636	14.5726	21.9557	17.9501	16.4658	22.8637	19.4834	17.8596
17	17.9009	14.7969	13.4818	20.0697	16.5459	15.0902	22.4259	18.6474	17.0262	23.5989	20.1312	18.4526
18	18.6961	15.3123	13.9441	20.4723	17.1551	15.6555	23.1234	19.1872	17.5656	24.0727	20.7019	19.1075
19	19.0298	15.7151	14.4444	21.1053	17.7069	16.2812	23.6240	19.7753	18.2426	24.6834	21.2850	19.6788
20	19.5387	16.2268	14.9317	21.6333	18.3857	16.8239	24.1167	20.3975	18.8586	25.4133	21.9919	20.2598
21	20.0658	16.7961	15.4400	22.1798	18.9070	17.3940	24.8046	21.0043	19.3766	25.8827	22.5380	20.8986
22	20.6758	17.3603	15.9174	22.7810	19.4660	17.9368	25.2891	21.5955	19.9256	26.7619	23.1276	21.5376
23	21.2399	17.9503	16.4752	23.2820	20.0441	18.4195	25.7241	22.1084	20.4421	27.2582	23.7999	22.1293
24	21.6999	18.4589	16.9769	23.9581	20.6479	18.9352	26.3484	22.6678	21.0123	27.7802	24.2789	22.6668
25	22.1572	18.9472	17.4296	24.3994	21.1523	19.4710	27.1243	23.2198	21.5975	28.4417	24.9370	23.2590
26	22.6903	19.4984	17.9259	25.1041	21.6573	19.9939	27.7109	23.8164	22.0890	29.2228	25.4950	23.8159
27	23.1484	19.8876	18.3550	25.6385	22.1779	20.5024	28.2236	24.4526	22.6414	29.8356	26.0850	24.3710
28	23.7005	20.4046	18.8517	26.2338	22.7423	21.0329	28.7451	25.0047	23.1211	30.5360	26.6417	25.0191
29	24.4816	20.9473	19.2962	26.5498	23.2208	21.5192	29.1080	25.5737	23.7483	31.0615	27.1321	25.4991
30	24.9695	21.5262	19.7954	26.9799	23.7646	22.0201	29.6803	26.0875	24.2970	31.4024	27.7039	26.0219

Panel B: $\gamma = 0.15$												
$q$	$T = 1$			$T = 2$			$T = 5$			$T = 10$		
	1%	5%	10%	1%	5%	10%	1%	5%	10%	1%	5%	10%
1	11.3901	8.4354	6.9600	12.4850	9.2430	7.7778	14.3774	10.3727	8.7969	15.5683	11.4413	9.5283
2	13.6392	10.3914	8.8898	14.8751	11.3843	9.8395	16.6482	12.6415	10.9089	18.2521	13.8644	11.9350
3	15.2706	11.7932	10.2809	16.8492	12.9788	11.3093	18.4078	14.2998	12.5694	20.7079	15.8368	13.7960
4	16.5228	13.0591	11.5220	18.2383	14.3706	12.6379	20.4873	15.7896	13.9342	21.9334	17.1890	15.2202
5	17.7444	14.0935	12.6085	19.3788	15.4717	13.8020	21.3972	17.1202	15.1861	23.2788	18.4659	16.4784
6	18.9769	15.2147	13.5125	20.6195	16.5945	14.7940	22.3862	18.1624	16.2694	24.8184	19.7313	17.6408
7	19.8245	16.1732	14.5938	21.9745	17.5811	15.8531	23.6232	19.3113	17.3797	25.9275	21.0151	18.8830
8	21.0200	17.0106	15.4338	23.0784	18.6662	16.8018	24.6714	20.4272	18.4455	26.7434	22.1198	19.9388
9	22.1012	17.9908	16.2982	24.0385	19.5832	17.7243	25.9591	21.4698	19.4526	28.1143	23.2457	20.9654
10	23.0155	18.8778	17.1246	24.9404	20.4821	18.5504	26.9248	22.5182	20.4236	29.0909	24.1376	21.9064
11	23.8544	19.7060	17.9766	26.0123	21.3405	19.4353	27.9591	23.4328	21.2960	29.8835	25.0330	22.9002
12	24.4258	20.5034	18.8333	26.8257	22.2253	20.3325	28.9623	24.3364	22.2028	30.9154	26.0544	23.7611
13	25.3766	21.3914	19.6314	27.5869	23.0606	21.1704	29.9306	25.1812	23.1090	31.8893	26.8583	24.7422
14	26.1081	22.1548	20.4384	28.4042	23.9577	21.9644	30.6707	26.0710	24.0345	33.2367	27.8376	25.7032
15	26.9349	22.9640	21.1812	29.2931	24.8749	22.7995	31.5786	26.9644	24.8379	33.8133	28.7647	26.5399
16	27.6789	23.7340	21.9205	29.9096	25.6722	23.5425	32.2762	27.8532	25.7470	34.8584	29.5943	27.3548
17	28.7789	24.4466	22.5956	30.5222	26.3688	24.3280	33.4371	28.7279	26.5480	35.5916	30.4487	28.2749
18	29.4895	25.2734	23.3702	31.4581	27.1638	25.1949	34.0921	29.5187	27.2725	36.2328	31.2843	29.1124
19	30.1934	25.9440	24.0751	32.1855	27.9458	26.0424	34.8565	30.2907	28.2147	37.1624	32.0437	29.9469
20	31.1433	26.5645	24.7303	33.0274	28.7832	26.7419	35.7063	31.0783	29.0417	37.7964	32.9745	30.6772
21	31.9542	27.3187	25.5012	33.9873	29.4422	27.3959	36.6459	31.8606	29.8308	38.5420	33.8020	31.4491
22	32.7693	28.1751	26.1788	34.6948	30.2891	28.1606	37.4659	32.6613	30.5399	39.5350	34.5957	32.3435
23	33.3914	29.0151	26.9544	35.3871	30.9548	28.8331	38.0960	33.4251	31.1753	40.2841	35.3908	33.2007
24	34.3053	29.7696	27.7145	36.3673	31.8852	29.6013	38.8213	34.2322	31.9367	41.0344	36.0657	33.9030
25	34.9707	30.4755	28.2861	37.0556	32.5307	30.2811	39.8457	35.0179	32.6776	41.8319	36.9215	34.7044
26	35.7432	31.1457	29.0311	37.7491	33.3412	31.0733	40.5773	35.7643	33.4124	42.5564	37.6674	35.5439
27	36.3088	31.6901	29.7969	38.8121	34.0737	31.7868	41.3479	36.5405	34.1057	43.2997	38.4152	36.2778
28	36.9178	32.4278	30.4532	39.2535	34.6876	32.4959	41.9547	37.2020	34.8781	44.3073	39.1526	37.0547
29	37.6486	33.2456	31.1236	39.8434	35.3950	33.2384	43.0414	37.9201	35.6704	45.1919	39.8714	37.7663
30	38.5717	34.0359	31.8444	40.5605	36.0921	33.9069	43.6587	38.6185	36.4008	45.8213	40.7115	38.4681

**S4.6 Alternative FPCA-compressed monitoring statistics**

Table S4.13 reports empirical size for the supplementary CUSUM and MOSUM statistics. The scenario-specific tables and subfigures that follow keep the DGP-specific break grids visible, so the weighted-CUSUM, Page-CUSUM, and multiscale MOSUM comparisons are not compressed to weak and strong endpoints.

Table S4.13: Null rejection rates (in %) at the 5% level for the FPCA-compressed Page-CUSUM, weighted-CUSUM, and multiscale MOSUM monitoring statistics with  $m = 500$ . Columns keep the DGP and monitoring horizon  $T \in \{1, 2, 5, 10\}$  explicit.

Method	BB				fIID				fMA(1)			
	$T=1$	$T=2$	$T=5$	$T=10$	$T=1$	$T=2$	$T=5$	$T=10$	$T=1$	$T=2$	$T=5$	$T=10$
RSMS weighted CUSUM, $\gamma = 0$	9.3	8.5	8.4	4.9	8.3	11.2	9.0	7.1	14.8	14.6	11.6	10.1
SSMS weighted CUSUM, $\gamma = 0$	5.3	5.5	5.2	3.5	6.4	6.7	7.7	5.9	5.2	4.8	5.0	4.0
HAC weighted CUSUM, $\gamma = 0$	8.8	9.6	9.4	8.6	13.4	14.5	16.3	16.6	10.1	11.3	10.4	11.0
RSMS weighted CUSUM, $\gamma = 0.15$	8.8	8.4	8.4	5.0	10.2	12.6	8.9	7.7	18.7	17.8	14.5	12.9
SSMS weighted CUSUM, $\gamma = 0.15$	4.0	4.7	5.1	3.5	5.9	6.9	6.7	5.7	22.9	19.2	13.4	12.1
HAC weighted CUSUM, $\gamma = 0.15$	11.3	11.3	12.8	10.0	19.9	20.9	21.1	23.8	20.3	20.1	17.5	17.6
RSMS Page-CUSUM, $\gamma = 0$	9.0	7.0	6.6	5.1	8.0	10.0	10.4	7.1	19.7	9.7	8.5	7.8
SSMS Page-CUSUM, $\gamma = 0$	3.9	5.3	5.2	5.2	6.0	6.5	6.8	5.9	5.3	5.2	3.9	3.6
HAC Page-CUSUM, $\gamma = 0$	7.8	6.4	8.8	6.1	10.4	10.3	10.8	9.2	7.8	7.7	6.8	8.3
RSMS Page-CUSUM, $\gamma = 0.15$	9.4	7.7	7.3	5.5	8.2	9.4	10.0	7.1	11.4	10.6	9.1	9.0
SSMS Page-CUSUM, $\gamma = 0.15$	4.6	6.0	5.4	4.7	6.6	6.6	7.1	5.5	5.2	4.9	3.9	4.4
HAC Page-CUSUM, $\gamma = 0.15$	7.8	7.0	9.5	5.9	10.9	10.8	11.7	10.2	8.3	7.8	7.3	8.7
RSMS Multiscale MOSUM	14.8	13.2	10.9	6.8	17.2	19.3	14.1	10.3	24.3	22.8	19.4	16.7
SSMS Multiscale MOSUM	10.0	7.6	7.4	6.0	10.4	11.5	11.2	7.2	11.8	9.5	7.5	6.3
HAC Multiscale MOSUM	20.2	18.9	17.9	15.6	29.3	33.4	34.5	31.2	25.9	26.3	26.0	26.0

Table S4.13 reports empirical sizes that vary more across statistics than in the main KS/CvM section. Among the supplementary statistics, SSMS Page-CUSUM ranges from 3.6% to 7.1%, HAC weighted CUSUM ranges from 8.6% to 23.8%, and HAC multiscale MOSUM ranges from 15.6% to 34.5%. SSMS is again the most conservative standardizer, while HAC and some RSMS combinations are substantially oversized. This pattern matters for the multiscale MOSUM rows in the raw-power tables:

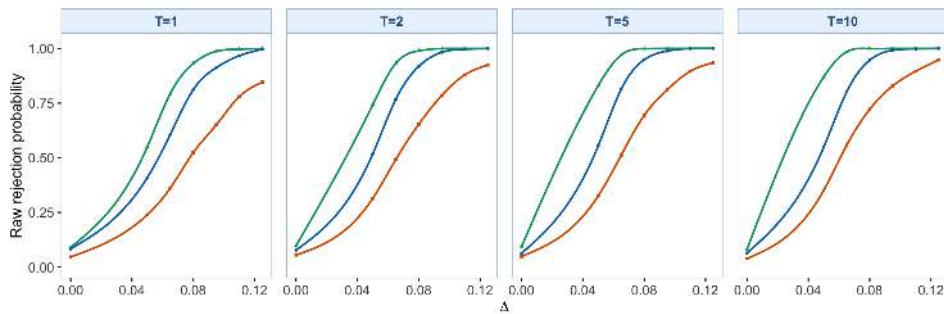
the statistic is built from a local adjacent-block contrast rather than a long accumulation statistic, and it is reported only for the bandwidth set  $\mathcal{H} = \{0.05, 0.10, 0.20\}$  with equal scale weights. The raw-power and ADD comparisons should therefore be read together with the empirical-size table rather than as comparisons among statistics with the same finite-sample size. All supplementary-statistic raw-power, SAP, and ADD summaries are based on 1000 Monte Carlo replications per simulation setting. In the raw-rejection subfigures below, the leftmost plotted point at  $\Delta = 0$  corresponds to empirical size, so the curves show size first and rejection under alternatives second.

**Level shift** For the level-shift setting, the tables keep the DGP, the horizon  $T$ , and the positive break grid explicit for the FPCA-compressed weighted-CUSUM, Page-CUSUM, and multiscale MOSUM statistics. The color figures are reported DGP by DGP, with the four internal columns corresponding to  $T = 1, 2, 5, 10$ .

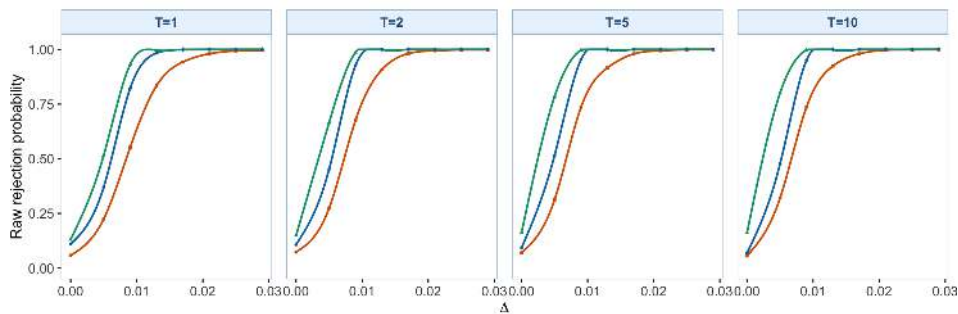
### **Raw power.**

For the level-shift setting, the raw-power tables and raw-rejection subfigures show Page-CUSUM with the highest reported rejection rates at each horizon  $T = 1, 2, 5, 10$ . Its mean raw power rises from 83.0% at  $T = 1$  to

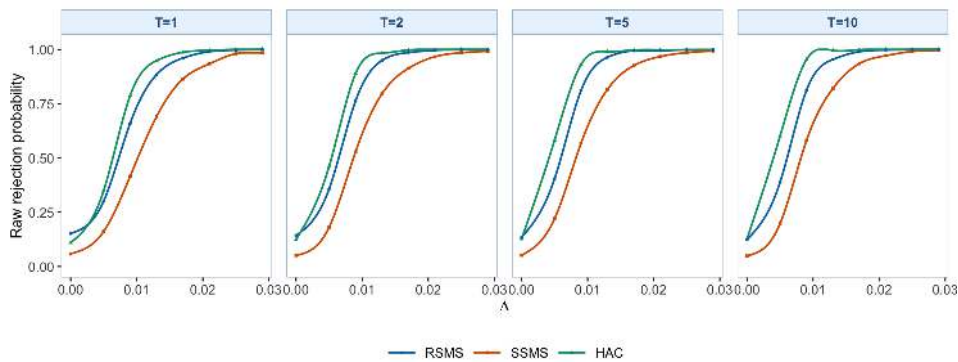




(a) BB errors; the four internal columns, from left to right, correspond to  $T = 1, 2, 5, 10$ .



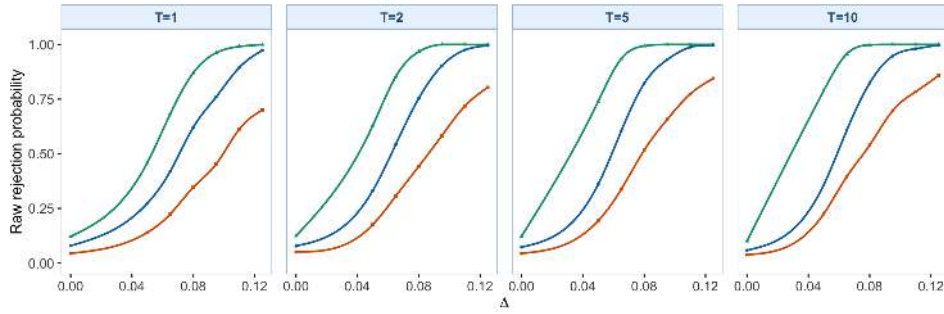
(b) IID errors; the four internal columns, from left to right, correspond to  $T = 1, 2, 5, 10$ .



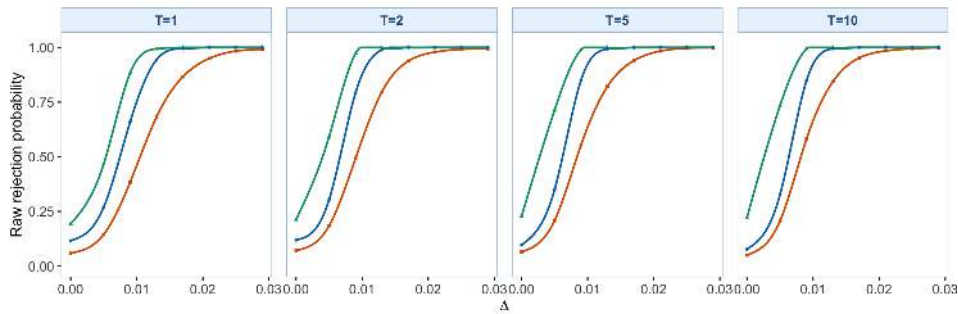
(c) fMA(1) errors; the four internal columns, from left to right, correspond to  $T = 1, 2, 5, 10$ .

Figure S4.1: Raw rejection curves for weighted CUSUM,  $\gamma = 0$  under the level-shift setting. Each subfigure fixes one DGP, and the four internal columns correspond to  $T = 1, 2, 5, 10$ . The legend below the final subfigure identifies RSMS, SSMS, and HAC.

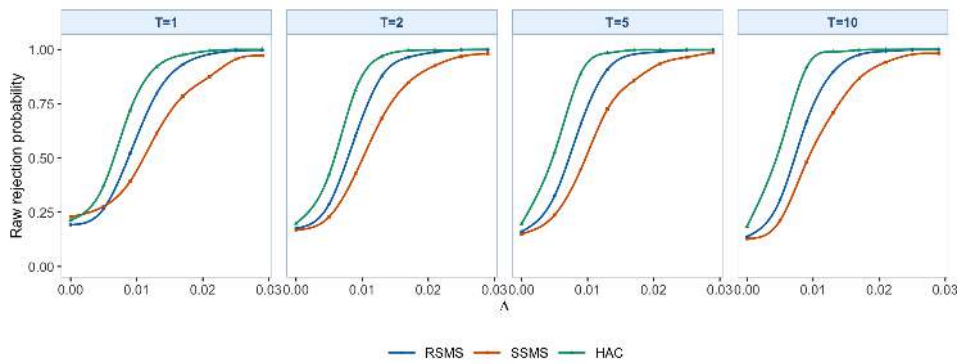
S4. SUPPLEMENTARY MONITORING STATISTICS



(a) BB errors; the four internal columns, from left to right, correspond to  $T = 1, 2, 5, 10$ .

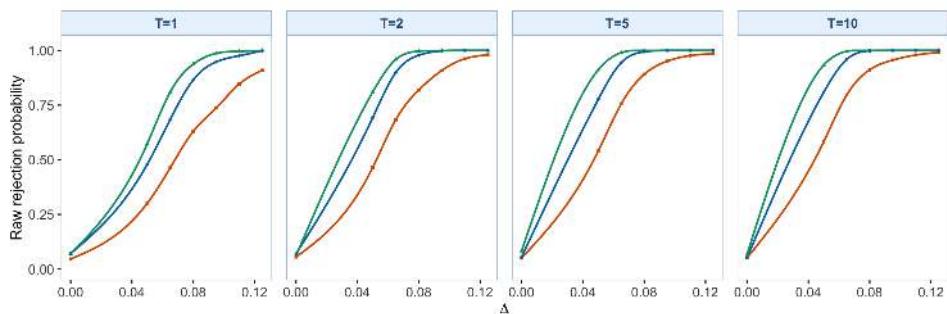


(b) IID errors; the four internal columns, from left to right, correspond to  $T = 1, 2, 5, 10$ .

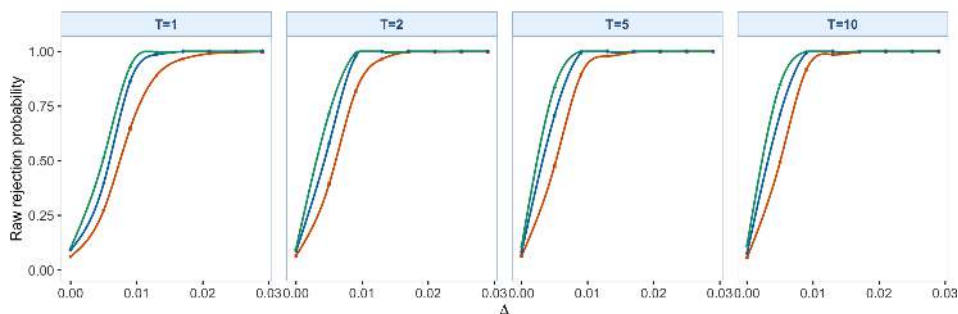


(c) fMA(1) errors; the four internal columns, from left to right, correspond to  $T = 1, 2, 5, 10$ .

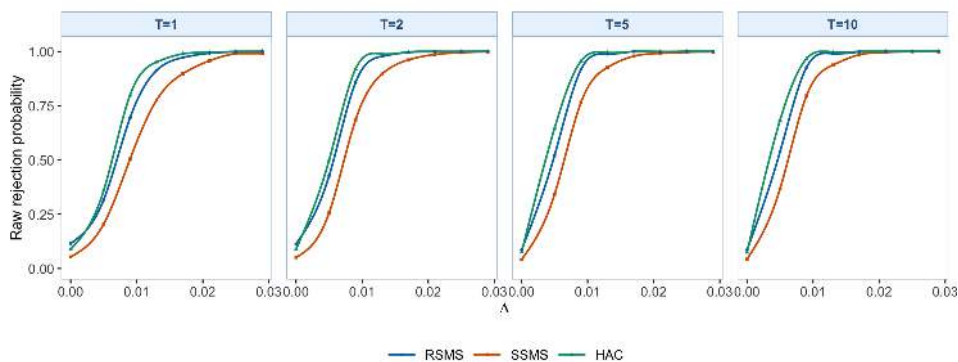
Figure S4.2: Raw rejection curves for weighted CUSUM,  $\gamma = 0.15$  under the level-shift setting. Each subfigure fixes one DGP, and the four internal columns correspond to  $T = 1, 2, 5, 10$ . The legend below the final subfigure identifies RSMS, SSMS, and HAC.



(a) BB errors; the four internal columns, from left to right, correspond to  $T = 1, 2, 5, 10$ .



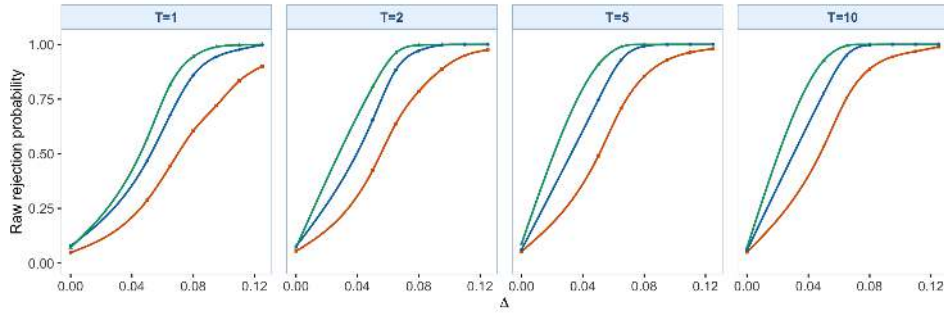
(b) IID errors; the four internal columns, from left to right, correspond to  $T = 1, 2, 5, 10$ .



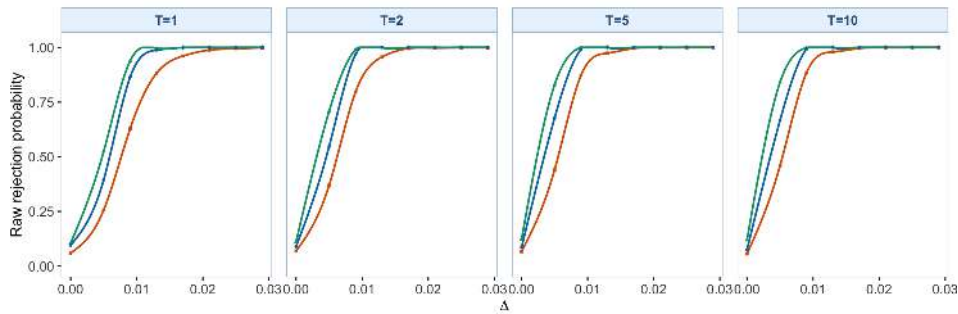
(c) fMA(1) errors; the four internal columns, from left to right, correspond to  $T = 1, 2, 5, 10$ .

Figure S4.3: Raw rejection curves for Page-CUSUM,  $\gamma = 0$  under the level-shift setting. Each subfigure fixes one DGP, and the four internal columns correspond to  $T = 1, 2, 5, 10$ . The legend below the final subfigure identifies RSMS, SSMS, and HAC.

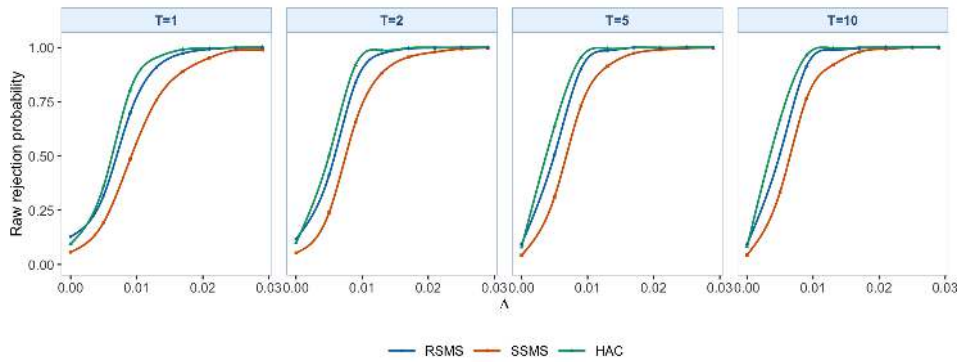
S4. SUPPLEMENTARY MONITORING STATISTICS



(a) BB errors; the four internal columns, from left to right, correspond to  $T = 1, 2, 5, 10$ .



(b) IID errors; the four internal columns, from left to right, correspond to  $T = 1, 2, 5, 10$ .



(c) fMA(1) errors; the four internal columns, from left to right, correspond to  $T = 1, 2, 5, 10$ .

Figure S4.4: Raw rejection curves for Page-CUSUM,  $\gamma = 0.15$  under the level-shift setting. Each subfigure fixes one DGP, and the four internal columns correspond to  $T = 1, 2, 5, 10$ . The legend below the final subfigure identifies RSMS, SSMS, and HAC.

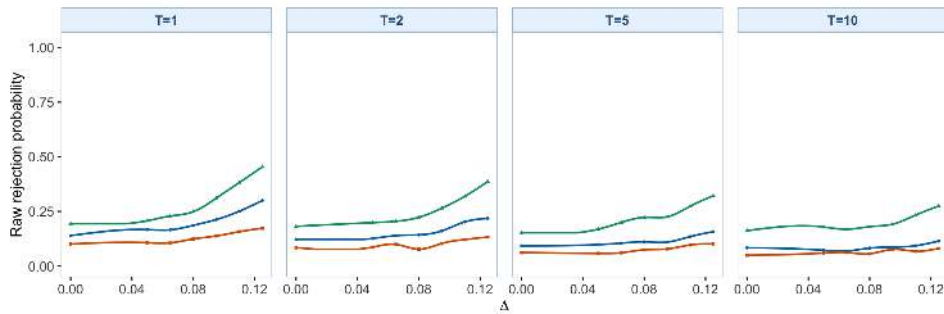
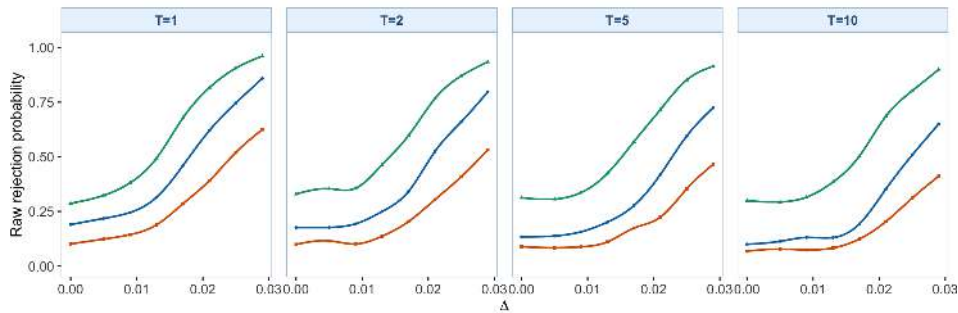
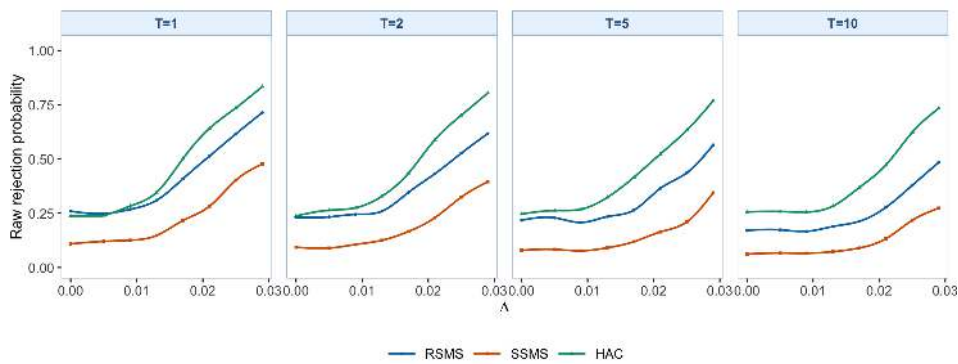
(a) BB errors; the four internal columns, from left to right, correspond to  $T = 1, 2, 5, 10$ .(b) IID errors; the four internal columns, from left to right, correspond to  $T = 1, 2, 5, 10$ .(c) fMA(1) errors; the four internal columns, from left to right, correspond to  $T = 1, 2, 5, 10$ .

Figure S4.5: Raw rejection curves for Multiscale MOSUM with bandwidth set  $\mathcal{H} = \{0.05, 0.10, 0.20\}$  under the level-shift setting. Each subfigure fixes one DGP, and the four internal columns correspond to  $T = 1, 2, 5, 10$ . The legend below the final subfigure identifies RSMS, SSMS, and HAC.

93.0% at  $T = 10$ , with most of the increase between  $T = 1$  and  $T = 2$ . Weighted CUSUM is the next closest supplementary statistic by raw power. Multiscale MOSUM uses local adjacent-window contrasts and has lower raw power in these global level-shift settings. The SSMS rows are more conservative than the corresponding RSMS rows.

**SAP.**

After empirical size adjustment, Page-CUSUM again has the highest reported rejection rates for the level-shift setting at each horizon  $T = 1, 2, 5, 10$ . Its mean SAP rises from 80.2% at  $T = 1$  to 92.2% at  $T = 10$ , with most of the increase between  $T = 1$  and  $T = 2$ . Weighted CUSUM is the next closest supplementary statistic by SAP. Multiscale MOSUM reports lower SAP in these global level-shift settings. The SSMS rows remain more conservative than the corresponding RSMS rows.

**ADD.**

The ADD tables and subfigures for the level-shift setting report shorter delays for several RSMS rows. Weighted CUSUM has lower ADD on most horizons, specifically  $T \in \{2, 5\}$ . Its mean ADD increases from 123.4 at  $T = 1$  to 572.8 at  $T = 10$  because stopping times are recorded on a longer scale as the monitoring horizon lengthens. Multiscale MOSUM has the largest average ADD among the supplementary statistics. The SSMS rows

Table S4.15: SAP (in %) for the FPCA-compressed alternative monitoring statistics under the level-shift setting. Panels separate the three DGPs, columns are grouped by monitoring horizon  $T \in \{1, 2, 5, 10\}$  and then by the positive break sizes  $\Delta$ , and the empirical size adjustment is computed separately for each simulation setting before averaging over  $s^* \in \{50, 200\}$ .

Method	Panel A: BB errors																							
	$T = 1$					$T = 2$					$T = 5$					$T = 10$								
	0.05	0.065	0.08	0.095	0.11	0.125	0.05	0.065	0.08	0.095	0.11	0.125	0.05	0.065	0.08	0.095	0.11	0.125	0.05	0.065	0.08	0.095	0.11	0.125
RSSM weighted CUSUM, $\gamma = 0$	32.0	50.8	77.5	86.6	94.8	39.0	42.2	69.5	87.7	96.8	99.5	100.0	46.9	74.2	92.3	98.1	99.8	100.0	55.6	80.5	94.8	99.2	99.8	100.0
RSSM weighted CUSUM, $\gamma = 0.15$	33.6	70.0	88.7	96.5	99.4	48.7	69.4	88.7	92.8	100.0	100.0	100.0	74.1	95.0	99.6	100.0	100.0	100.0	79.2	97.0	100.0	100.0	100.0	100.0
RSSM weighted CUSUM, $\gamma = 0.15$	20.8	33.8	53.5	70.2	85.5	95.8	95.8	64.4	43.4	67.5	55.8	96.0	99.1	23.0	47.3	71.6	87.9	96.8	99.0	36.2	61.5	82.7	95.0	99.8
RSSM weighted CUSUM, $\gamma = 0.15$	15.7	24.2	37.0	47.8	63.3	71.8	18.6	31.7	45.0	59.1	72.4	80.8	19.3	33.5	51.6	65.6	77.2	84.4	26.2	43.5	58.0	73.2	80.8	88.3
RSSM Page-CUSUM, $\gamma = 0$	32.7	59.6	79.7	90.7	96.5	99.4	92.7	99.4	92.7	99.4	99.4	92.7	99.4	92.7	99.4	92.7	99.4	92.7	99.4	92.7	99.4	92.7	99.4	92.7
RSSM Page-CUSUM, $\gamma = 0.15$	33.6	50.2	66.4	75.8	86.4	92.0	46.4	66.4	80.8	90.8	96.2	98.0	53.3	74.7	88.8	94.6	97.4	98.4	58.0	79.2	91.1	95.5	97.8	99.0
HAC Page-CUSUM, $\gamma = 0$	48.9	74.6	91.0	97.8	99.4	100.0	100.0	100.0	100.0	100.0	100.0	100.0	88.1	98.5	100.0	100.0	100.0	100.0	92.6	99.5	100.0	100.0	100.0	100.0
HAC Page-CUSUM, $\gamma = 0.15$	47.5	74.2	90.8	97.7	99.8	100.0	73.4	93.7	99.1	100.0	100.0	73.4	93.7	99.1	100.0	100.0	100.0	100.0	85.7	99.2	100.0	100.0	100.0	100.0
HAC Multiscale MOSUM	6.4	5.9	6.9	9.8	10.5	14.3	3.6	4.3	4.2	5.6	7.3	10.3	3.5	3.6	4.6	4.6	4.3	6.0	5.9	4.9	5.9	5.8	6.9	8.5
HAC Multiscale MOSUM	6.2	7.1	8.8	13.0	17.9	24.5	4.5	5.2	5.5	7.3	12.0	17.8	5.4	6.9	8.6	9.0	13.7	15.8	7.1	6.5	6.9	8.0	10.7	14.1

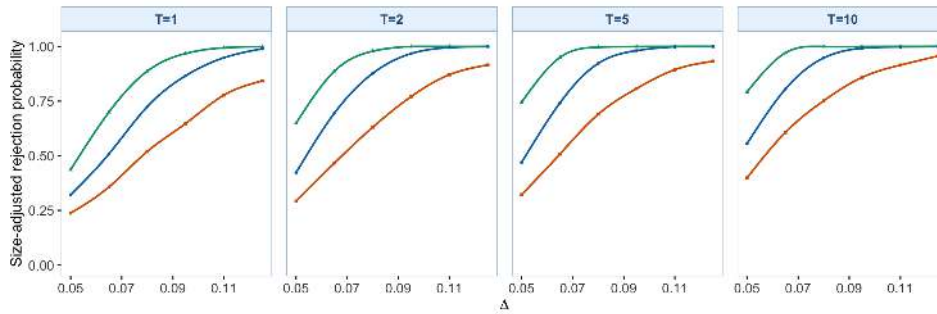
  

Method	Panel B: IID errors																											
	$T = 1$					$T = 2$					$T = 5$					$T = 10$												
	0.005	0.009	0.013	0.017	0.021	0.025	0.029	0.005	0.009	0.013	0.017	0.021	0.025	0.029	0.005	0.009	0.013	0.017	0.021	0.025	0.029	0.005	0.009	0.013	0.017	0.021	0.025	0.029
RSSM weighted CUSUM, $\gamma = 0$	29.8	72.8	98.0	99.8	100.0	100.0	100.0	31.8	85.8	99.6	100.0	100.0	100.0	40.8	91.4	99.8	100.0	100.0	100.0	100.0	41.6	91.9	100.0	100.0	100.0	100.0	100.0	
RSSM weighted CUSUM, $\gamma = 0.15$	19.5	49.3	78.8	91.5	97.0	99.2	99.5	23.5	61.3	87.2	100.0	100.0	100.0	24.1	64.3	186.5	100.0	100.0	100.0	100.0	30.2	70.5	100.0	100.0	100.0	100.0	100.0	
RSSM weighted CUSUM, $\gamma = 0.15$	17.3	54.7	89.8	100.0	100.0	100.0	15.7	62.5	95.8	99.8	100.0	100.0	100.0	26.7	76.3	98.2	100.0	100.0	100.0	100.0	27.6	75.5	98.8	100.0	100.0	100.0	100.0	
RSSM weighted CUSUM, $\gamma = 0.15$	12.8	24.7	60.2	83.4	100.0	100.0	24.2	82.5	73.8	100.3	100.0	100.0	100.0	17.1	48.9	77.2	100.0	100.0	100.0	100.0	19.6	53.8	80.4	100.0	100.0	100.0	100.0	
RSSM Page-CUSUM, $\gamma = 0$	31.9	80.4	97.6	99.8	100.0	100.0	48.1	94.8	100.0	100.0	100.0	100.0	100.0	63.9	98.0	100.0	100.0	100.0	100.0	100.0	63.9	98.0	100.0	100.0	100.0	100.0	100.0	
RSSM Page-CUSUM, $\gamma = 0.15$	36.0	85.6	99.1	100.0	100.0	100.0	56.4	96.2	100.0	100.0	100.0	100.0	100.0	75.4	98.7	100.0	100.0	100.0	100.0	100.0	75.4	98.7	100.0	100.0	100.0	100.0	100.0	
HAC Page-CUSUM, $\gamma = 0$	32.6	80.9	99.6	99.9	100.0	100.0	45.6	94.2	100.0	100.0	100.0	100.0	100.0	56.4	98.1	100.0	100.0	100.0	100.0	100.0	56.4	98.1	100.0	100.0	100.0	100.0	100.0	
HAC Page-CUSUM, $\gamma = 0.15$	36.6	86.9	99.1	100.0	100.0	100.0	57.1	98.2	100.0	100.0	100.0	100.0	100.0	72.6	99.7	100.0	100.0	100.0	100.0	100.0	72.6	99.7	100.0	100.0	100.0	100.0	100.0	
HAC Multiscale MOSUM	7.7	9.7	14.3	28.2	30.8	34.4	4.8	5.7	8.9	16.4	16.4	6.1	6.1	7.2	10.2	17.0	29.7	34.0	5.0	4.8	7.9	12.8	25.5	34.2	37.2	42.6	52.8	72.8
HAC Multiscale MOSUM	5.5	7.8	15.3	32.6	53.6	69.8	83.7	6.4	6.7	13.1	26.4	48.4	65.3	79.5	5.5	7.1	11.8	23.5	43.8	63.3	78.2	4.8	5.1	7.8	20.0	37.5	58.6	72.8

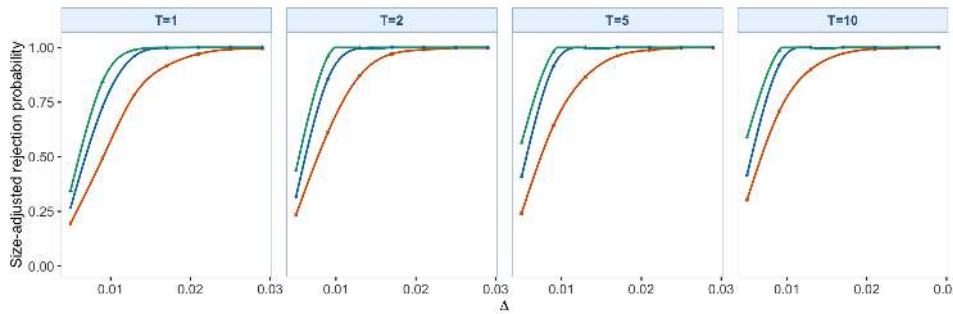
  

Method	Panel C: FMA(1) errors																											
	$T = 1$					$T = 2$					$T = 5$					$T = 10$												
	0.005	0.009	0.013	0.017	0.021	0.025	0.029	0.005	0.009	0.013	0.017	0.021	0.025	0.029	0.005	0.009	0.013	0.017	0.021	0.025	0.029	0.005	0.009	0.013	0.017	0.021	0.025	0.029
RSSM weighted CUSUM, $\gamma = 0$	13.4	43.6	75.5	91.5	97.5	99.3	99.6	22.1	62.5	90.7	97.4	99.0	99.8	25.8	70.2	92.7	98.5	99.0	99.8	99.8	26.2	71.0	91.7	98.3	99.2	99.9	99.8	
RSSM weighted CUSUM, $\gamma = 0.15$	6.9	26.6	56.1	80.4	93.1	97.1	98.7	11.0	37.0	74.6	91.3	96.4	98.7	15.0	44.4	79.8	93.0	97.2	98.9	99.5	16.1	50.5	81.8	95.0	98.2	99.6	99.8	
RSSM weighted CUSUM, $\gamma = 0.15$	14.0	51.5	82.4	93.3	98.2	99.2	99.2	15.3	47.7	60.7	90.8	99.2	99.8	25.0	75.0	95.0	98.8	99.4	99.8	99.8	28.0	90.0	96.0	99.3	99.6	100.0	100.0	
RSSM Page-CUSUM, $\gamma = 0$	18.2	54.2	81.1	94.0	98.4	99.9	99.9	32.1	78.6	99.9	99.9	99.9	99.9	45.0	88.8	98.1	99.8	99.6	100.0	99.9	45.5	89.3	98.4	99.6	99.8	100.0	100.0	
RSSM Page-CUSUM, $\gamma = 0.15$	18.2	54.2	81.1	94.0	98.4	99.9	99.9	32.1	78.6	99.9	99.9	99.9	99.9	45.0	88.8	98.1	99.8	99.6	100.0	99.9	45.5	89.3	98.4	99.6	99.8	100.0	100.0	
HAC Page-CUSUM, $\gamma = 0$	17.3	52.8	92.4	98.0	99.4	100.0	100.0	44.4	89.5	98.2	99.7	100.0	100.0	60.2	95.6	99.2	100.0	100.0	100.0	100.0	60.2	95.6	99.2	100.0	100.0	100.0	100.0	
HAC Page-CUSUM, $\gamma = 0.15$	17.3	52.8	92.4	98.0	99.4	100.0	100.0	44.4	89.5	98.2	99.7	100.0	100.0	60.2	95.6	99.2	100.0	100.0	100.0	100.0	60.2	95.6	99.2	100.0	100.0	100.0	100.0	
HAC Multiscale MOSUM	5.9	7.5	13.0	24.4	27.5	36.8	4.9	5.9	8.1	16.0	16.0	6.4	6.8	9.2	14.2	24.2	40.0	50.0	5.0	5.0	7.6	10.9	19.0	30.0	42.0	58.0	76.0	99.0
HAC Multiscale MOSUM	6.3	7.8	11.5	21.4	38.6	52.0	67.8	4.0	5.8	8.4	16.8	31.1	48.5	58.5	6.0	6.5	8.4	14.5	27.5	41.1	50.2	4.7	5.5	7.1	12.2	23.3	39.1	52.3

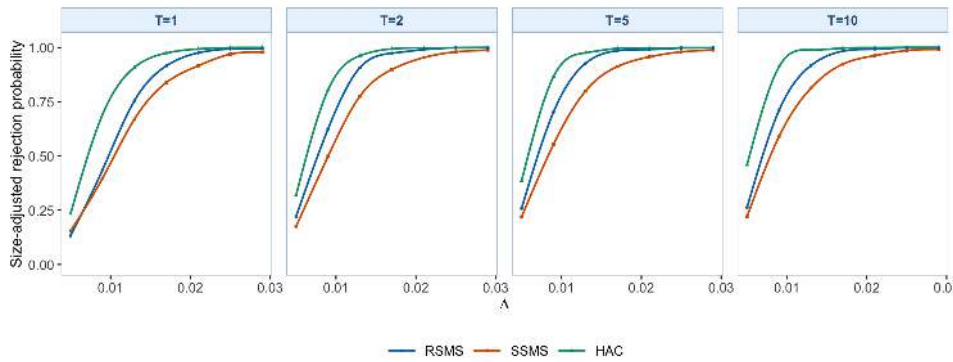
S4. SUPPLEMENTARY MONITORING STATISTICS



(a) BB errors; the four internal columns, from left to right, correspond to  $T = 1, 2, 5, 10$ .

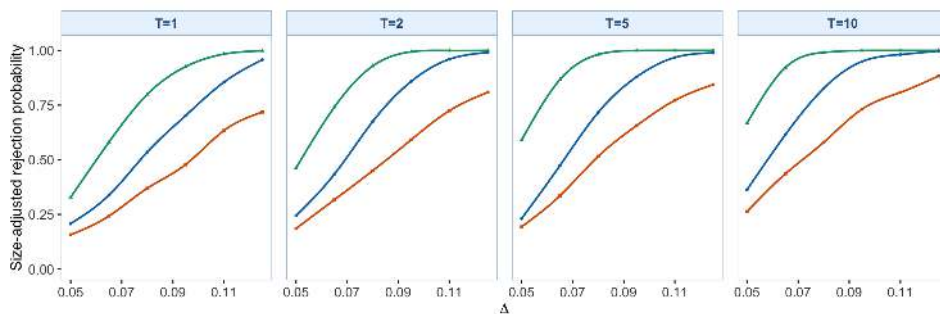


(b) IID errors; the four internal columns, from left to right, correspond to  $T = 1, 2, 5, 10$ .

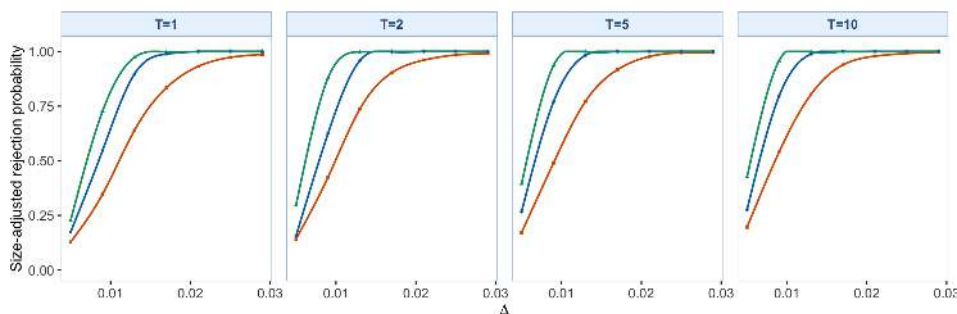


(c) fMA(1) errors; the four internal columns, from left to right, correspond to  $T = 1, 2, 5, 10$ .

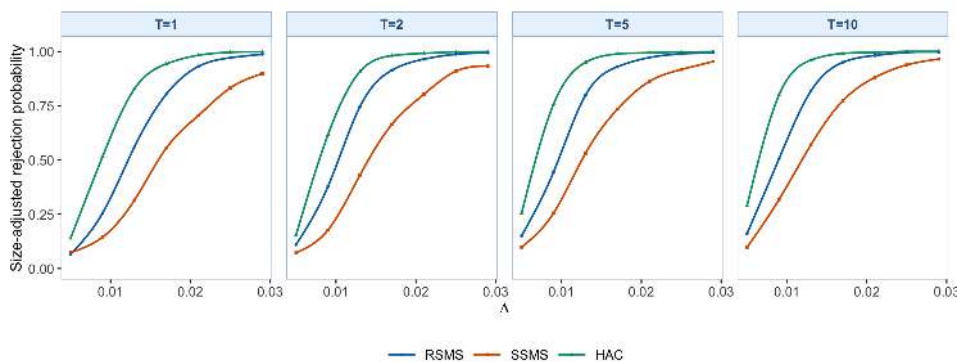
Figure S4.6: SAP curves for weighted CUSUM,  $\gamma = 0$  under the level-shift setting. Each subfigure fixes one DGP, and the four internal columns correspond to  $T = 1, 2, 5, 10$ . The legend below the final subfigure identifies RSMS, SSMS, and HAC.



(a) BB errors; the four internal columns, from left to right, correspond to  $T = 1, 2, 5, 10$ .



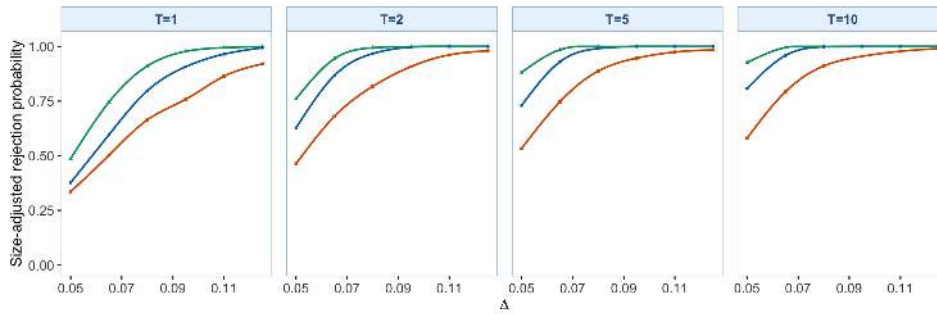
(b) IID errors; the four internal columns, from left to right, correspond to  $T = 1, 2, 5, 10$ .



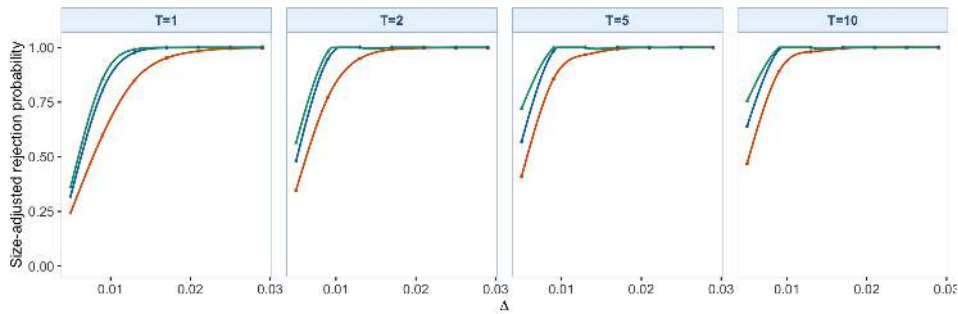
(c) fMA(1) errors; the four internal columns, from left to right, correspond to  $T = 1, 2, 5, 10$ .

Figure S4.7: SAP curves for weighted CUSUM,  $\gamma = 0.15$  under the level-shift setting. Each subfigure fixes one DGP, and the four internal columns correspond to  $T = 1, 2, 5, 10$ . The legend below the final subfigure identifies RSMS, SSMS, and HAC.

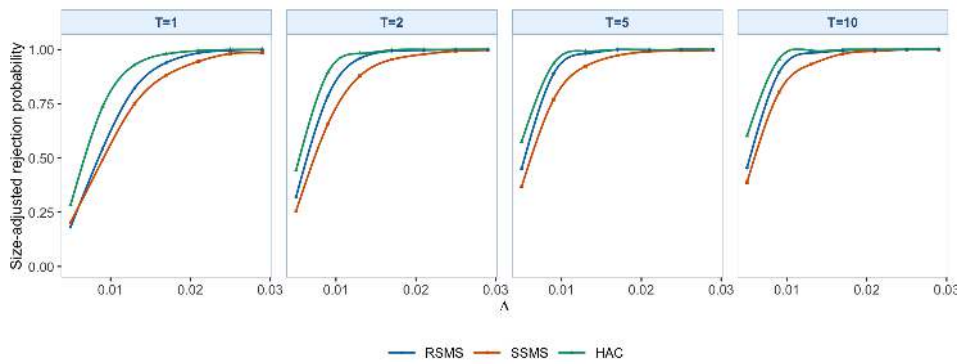
S4. SUPPLEMENTARY MONITORING STATISTICS



(a) BB errors; the four internal columns, from left to right, correspond to  $T = 1, 2, 5, 10$ .

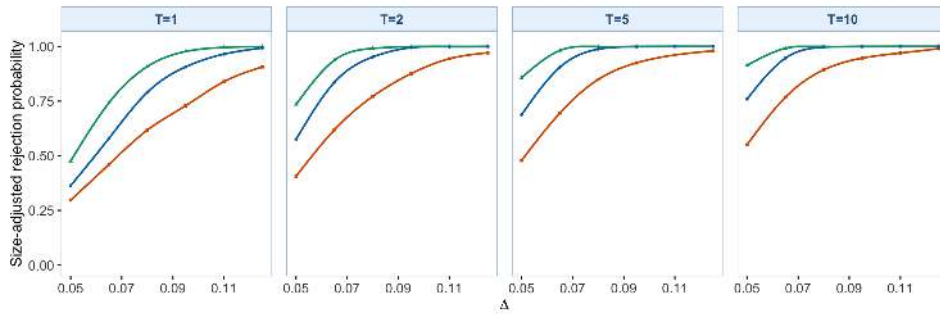


(b) IID errors; the four internal columns, from left to right, correspond to  $T = 1, 2, 5, 10$ .

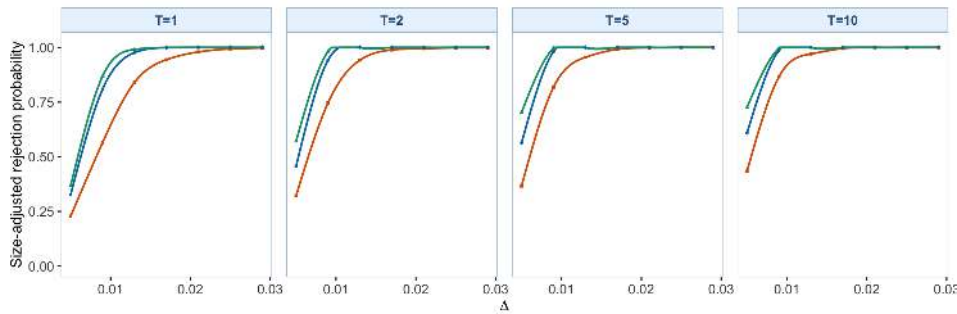


(c) fMA(1) errors; the four internal columns, from left to right, correspond to  $T = 1, 2, 5, 10$ .

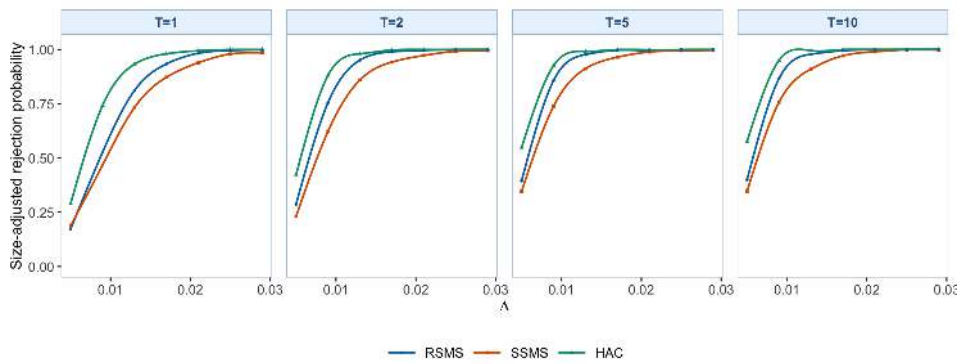
Figure S4.8: SAP curves for Page-CUSUM,  $\gamma = 0$  under the level-shift setting. Each subfigure fixes one DGP, and the four internal columns correspond to  $T = 1, 2, 5, 10$ . The legend below the final subfigure identifies RSMS, SSMS, and HAC.



(a) BB errors; the four internal columns, from left to right, correspond to  $T = 1, 2, 5, 10$ .



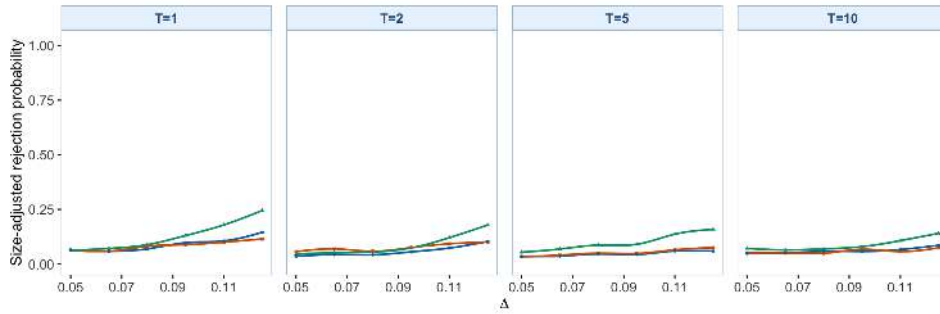
(b) IID errors; the four internal columns, from left to right, correspond to  $T = 1, 2, 5, 10$ .



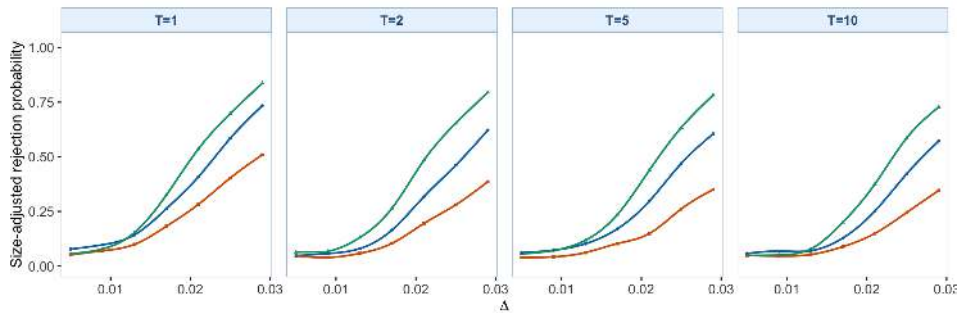
(c) fMA(1) errors; the four internal columns, from left to right, correspond to  $T = 1, 2, 5, 10$ .

Figure S4.9: SAP curves for Page-CUSUM,  $\gamma = 0.15$  under the level-shift setting. Each subfigure fixes one DGP, and the four internal columns correspond to  $T = 1, 2, 5, 10$ . The legend below the final subfigure identifies RSMS, SSMS, and HAC.

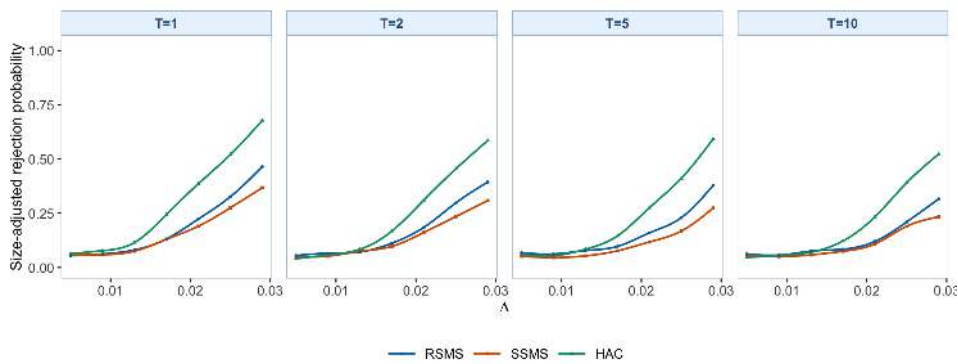
S4. SUPPLEMENTARY MONITORING STATISTICS



(a) BB errors; the four internal columns, from left to right, correspond to  $T = 1, 2, 5, 10$ .



(b) IID errors; the four internal columns, from left to right, correspond to  $T = 1, 2, 5, 10$ .



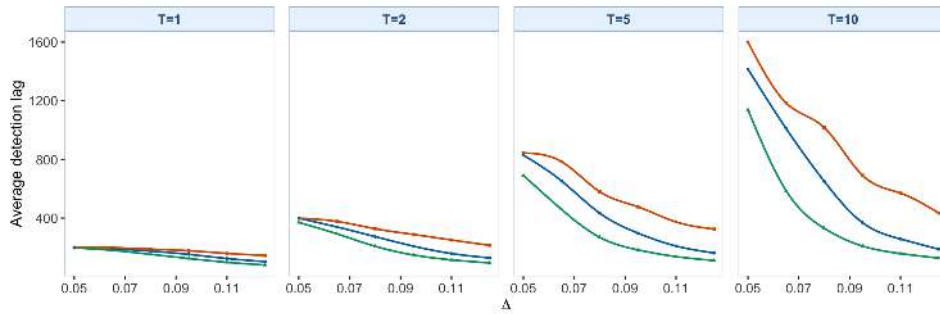
(c) fMA(1) errors; the four internal columns, from left to right, correspond to  $T = 1, 2, 5, 10$ .

Figure S4.10: SAP curves for Multiscale MOSUM with bandwidth set  $\mathcal{H} = \{0.05, 0.10, 0.20\}$  under the level-shift setting. Each subfigure fixes one DGP, and the four internal columns correspond to  $T = 1, 2, 5, 10$ . The legend below the final subfigure identifies RSMS, SSMS, and HAC.

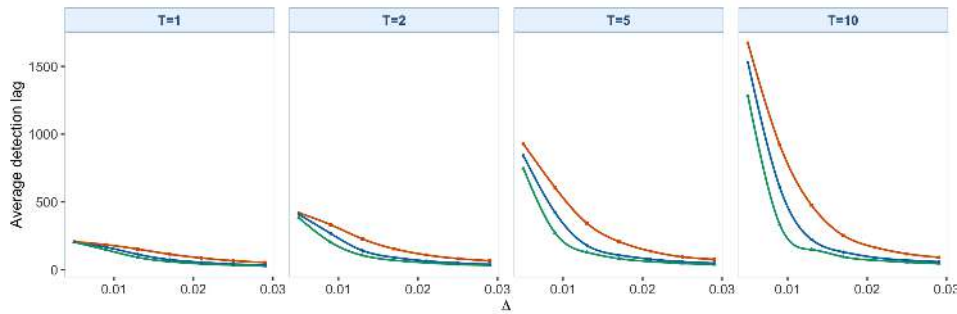
Table S4.16: ADD for the FPCA-compressed alternative monitoring statistics under the level-shift setting. Panels separate the three DGPs, columns are grouped by monitoring horizon  $T \in \{1, 2, 5, 10\}$  and then by the positive break sizes  $\Delta$ , entries are detection delays in monitoring observations, not percentages, and smaller entries indicate faster post-break detection after averaging over  $s^* \in \{50, 200\}$ .

Method	Panel A: BB errors									
	$T=1$		$T=2$		$T=5$		$T=10$		$T=10$	
	0.05	0.065	0.08	0.095	0.11	0.125	0.05	0.065	0.08	0.095
Method	Panel B: IID errors									
	$T=1$		$T=2$		$T=5$		$T=10$		$T=10$	
	0.05	0.065	0.08	0.095	0.11	0.125	0.05	0.065	0.08	0.095
Method	Panel C: FMA(1) errors									
	$T=1$		$T=2$		$T=5$		$T=10$		$T=10$	
	0.05	0.065	0.08	0.095	0.11	0.125	0.05	0.065	0.08	0.095
Method	Panel D: MDSUM									
	$T=1$		$T=2$		$T=5$		$T=10$		$T=10$	
	0.05	0.065	0.08	0.095	0.11	0.125	0.05	0.065	0.08	0.095
Method	Panel E: MDSUM									
	$T=1$		$T=2$		$T=5$		$T=10$		$T=10$	
	0.05	0.065	0.08	0.095	0.11	0.125	0.05	0.065	0.08	0.095
Method	Panel F: MDSUM									
	$T=1$		$T=2$		$T=5$		$T=10$		$T=10$	
	0.05	0.065	0.08	0.095	0.11	0.125	0.05	0.065	0.08	0.095
Method	Panel G: MDSUM									
	$T=1$		$T=2$		$T=5$		$T=10$		$T=10$	
	0.05	0.065	0.08	0.095	0.11	0.125	0.05	0.065	0.08	0.095
Method	Panel H: MDSUM									
	$T=1$		$T=2$		$T=5$		$T=10$		$T=10$	
	0.05	0.065	0.08	0.095	0.11	0.125	0.05	0.065	0.08	0.095
Method	Panel I: MDSUM									
	$T=1$		$T=2$		$T=5$		$T=10$		$T=10$	
	0.05	0.065	0.08	0.095	0.11	0.125	0.05	0.065	0.08	0.095
Method	Panel J: MDSUM									
	$T=1$		$T=2$		$T=5$		$T=10$		$T=10$	
	0.05	0.065	0.08	0.095	0.11	0.125	0.05	0.065	0.08	0.095
Method	Panel K: MDSUM									
	$T=1$		$T=2$		$T=5$		$T=10$		$T=10$	
	0.05	0.065	0.08	0.095	0.11	0.125	0.05	0.065	0.08	0.095
Method	Panel L: MDSUM									
	$T=1$		$T=2$		$T=5$		$T=10$		$T=10$	
	0.05	0.065	0.08	0.095	0.11	0.125	0.05	0.065	0.08	0.095
Method	Panel M: MDSUM									
	$T=1$		$T=2$		$T=5$		$T=10$		$T=10$	
	0.05	0.065	0.08	0.095	0.11	0.125	0.05	0.065	0.08	0.095
Method	Panel N: MDSUM									
	$T=1$		$T=2$		$T=5$		$T=10$		$T=10$	
	0.05	0.065	0.08	0.095	0.11	0.125	0.05	0.065	0.08	0.095
Method	Panel O: MDSUM									
	$T=1$		$T=2$		$T=5$		$T=10$		$T=10$	
	0.05	0.065	0.08	0.095	0.11	0.125	0.05	0.065	0.08	0.095
Method	Panel P: MDSUM									
	$T=1$		$T=2$		$T=5$		$T=10$		$T=10$	
	0.05	0.065	0.08	0.095	0.11	0.125	0.05	0.065	0.08	0.095
Method	Panel Q: MDSUM									
	$T=1$		$T=2$		$T=5$		$T=10$		$T=10$	
	0.05	0.065	0.08	0.095	0.11	0.125	0.05	0.065	0.08	0.095
Method	Panel R: MDSUM									
	$T=1$		$T=2$		$T=5$		$T=10$		$T=10$	
	0.05	0.065	0.08	0.095	0.11	0.125	0.05	0.065	0.08	0.095
Method	Panel S: MDSUM									
	$T=1$		$T=2$		$T=5$		$T=10$		$T=10$	
	0.05	0.065	0.08	0.095	0.11	0.125	0.05	0.065	0.08	0.095
Method	Panel T: MDSUM									
	$T=1$		$T=2$		$T=5$		$T=10$		$T=10$	
	0.05	0.065	0.08	0.095	0.11	0.125	0.05	0.065	0.08	0.095
Method	Panel U: MDSUM									
	$T=1$		$T=2$		$T=5$		$T=10$		$T=10$	
	0.05	0.065	0.08	0.095	0.11	0.125	0.05	0.065	0.08	0.095
Method	Panel V: MDSUM									
	$T=1$		$T=2$		$T=5$		$T=10$		$T=10$	
	0.05	0.065	0.08	0.095	0.11	0.125	0.05	0.065	0.08	0.095
Method	Panel W: MDSUM									
	$T=1$		$T=2$		$T=5$		$T=10$		$T=10$	
	0.05	0.065	0.08	0.095	0.11	0.125	0.05	0.065	0.08	0.095
Method	Panel X: MDSUM									
	$T=1$		$T=2$		$T=5$		$T=10$		$T=10$	
	0.05	0.065	0.08	0.095	0.11	0.125	0.05	0.065	0.08	0.095
Method	Panel Y: MDSUM									
	$T=1$		$T=2$		$T=5$		$T=10$		$T=10$	
	0.05	0.065	0.08	0.095	0.11	0.125	0.05	0.065	0.08	0.095
Method	Panel Z: MDSUM									
	$T=1$		$T=2$		$T=5$		$T=10$		$T=10$	
	0.05	0.065	0.08	0.095	0.11	0.125	0.05	0.065	0.08	0.095

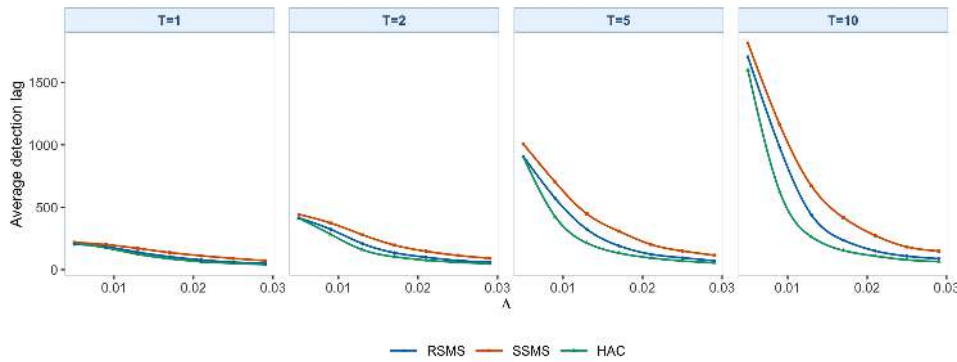
S4. SUPPLEMENTARY MONITORING STATISTICS



(a) BB errors; the four internal columns, from left to right, correspond to  $T = 1, 2, 5, 10$ .

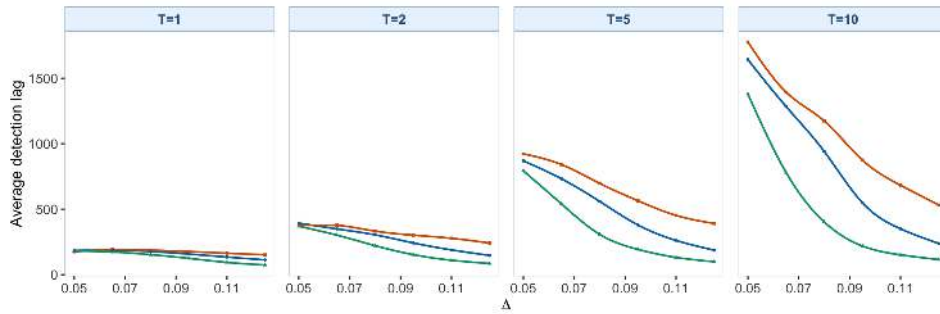


(b) IID errors; the four internal columns, from left to right, correspond to  $T = 1, 2, 5, 10$ .

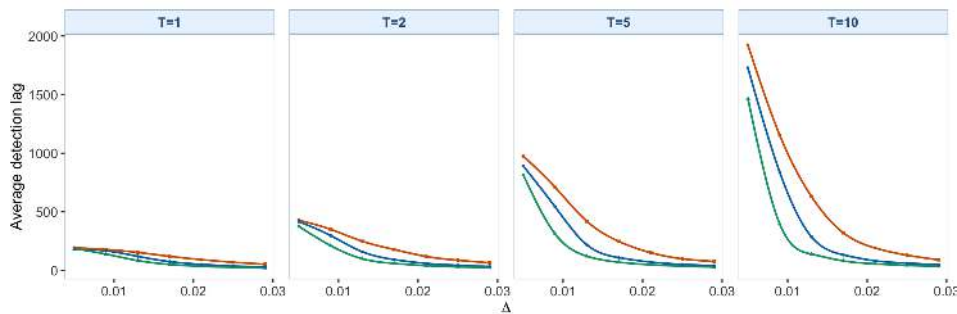


(c) fMA(1) errors; the four internal columns, from left to right, correspond to  $T = 1, 2, 5, 10$ .

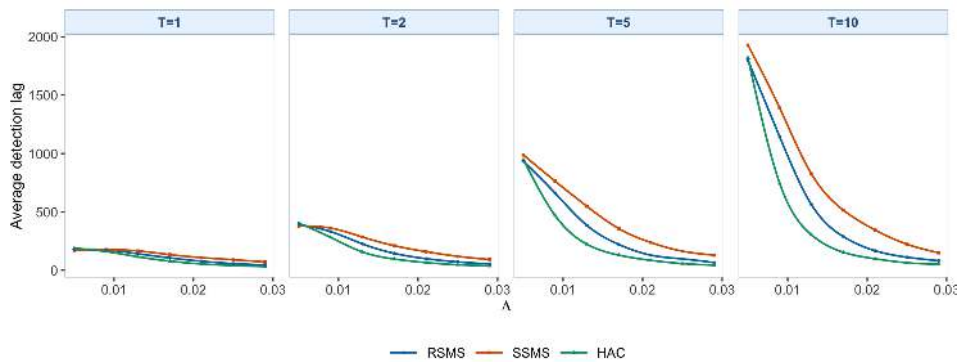
Figure S4.11: ADD curves for weighted CUSUM,  $\gamma = 0$  under the level-shift setting. Each subfigure fixes one DGP, and the four internal columns correspond to  $T = 1, 2, 5, 10$ . The legend below the final subfigure identifies RSMS, SSMS, and HAC.



(a) BB errors; the four internal columns, from left to right, correspond to  $T = 1, 2, 5, 10$ .



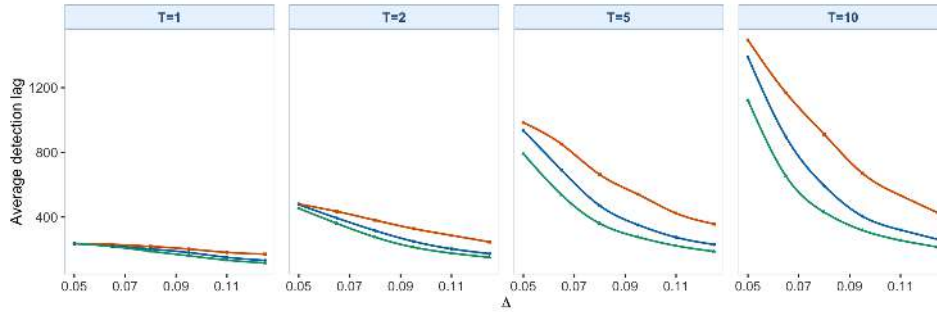
(b) fIID errors; the four internal columns, from left to right, correspond to  $T = 1, 2, 5, 10$ .



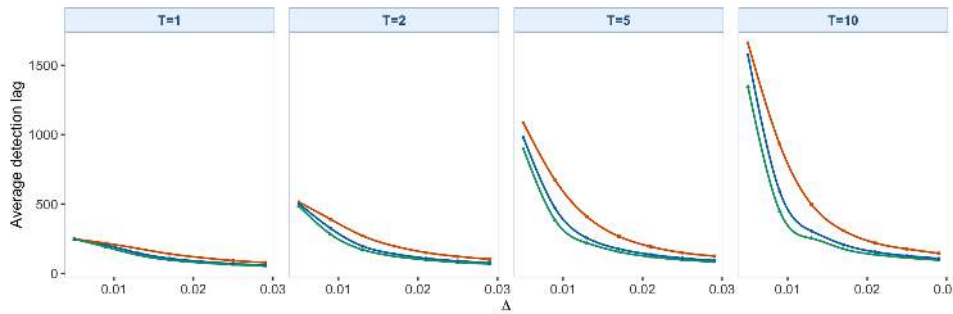
(c) fMA(1) errors; the four internal columns, from left to right, correspond to  $T = 1, 2, 5, 10$ .

Figure S4.12: ADD curves for weighted CUSUM,  $\gamma = 0.15$  under the level-shift setting. Each subfigure fixes one DGP, and the four internal columns correspond to  $T = 1, 2, 5, 10$ . The legend below the final subfigure identifies RSMS, SSMS, and HAC.

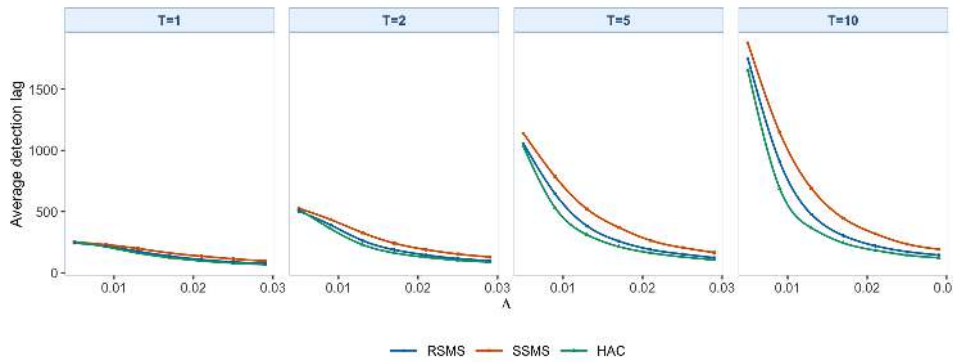
S4. SUPPLEMENTARY MONITORING STATISTICS



(a) BB errors; the four internal columns, from left to right, correspond to  $T = 1, 2, 5, 10$ .

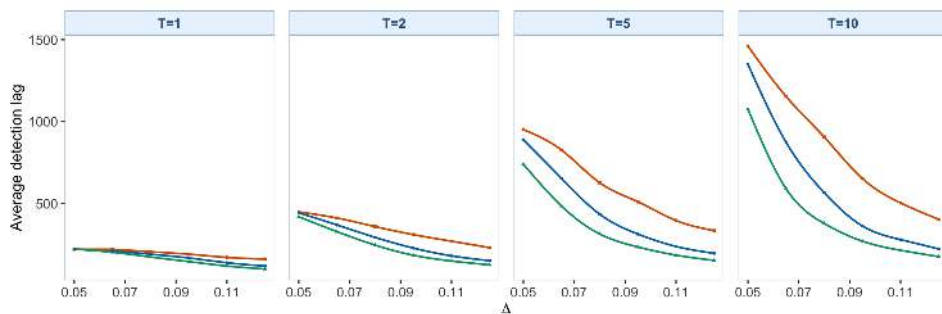


(b) IID errors; the four internal columns, from left to right, correspond to  $T = 1, 2, 5, 10$ .

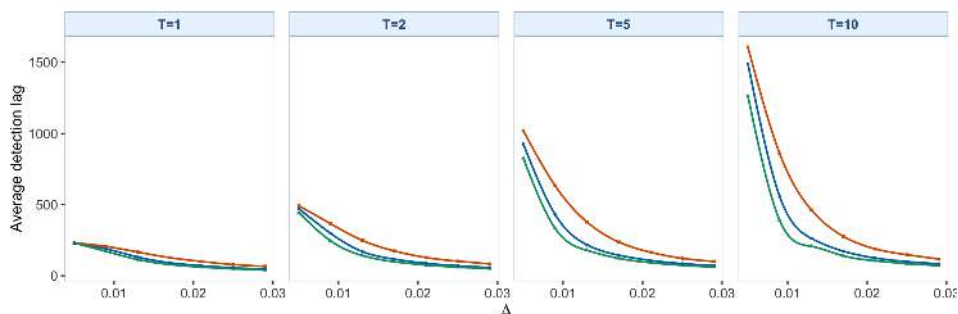


(c) fMA(1) errors; the four internal columns, from left to right, correspond to  $T = 1, 2, 5, 10$ .

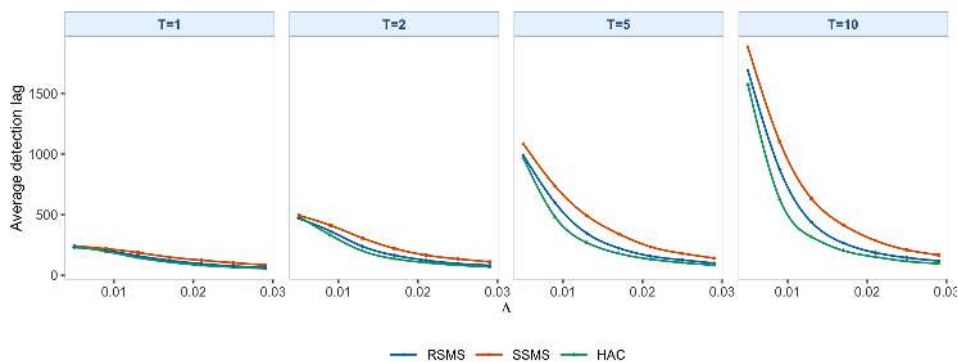
Figure S4.13: ADD curves for Page-CUSUM,  $\gamma = 0$  under the level-shift setting. Each subfigure fixes one DGP, and the four internal columns correspond to  $T = 1, 2, 5, 10$ . The legend below the final subfigure identifies RSMS, SSMS, and HAC.



(a) BB errors; the four internal columns, from left to right, correspond to  $T = 1, 2, 5, 10$ .



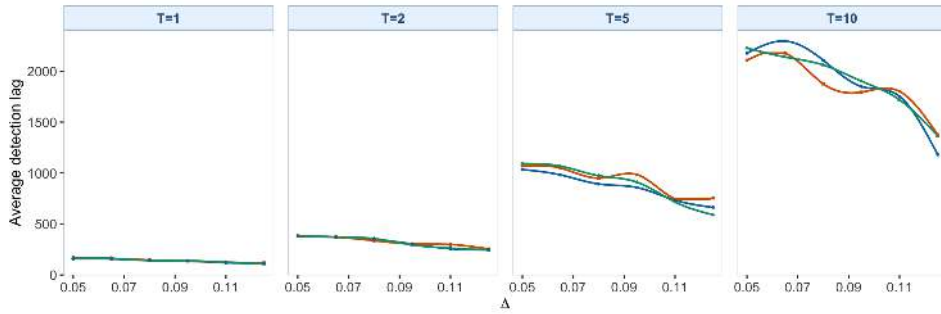
(b) IID errors; the four internal columns, from left to right, correspond to  $T = 1, 2, 5, 10$ .



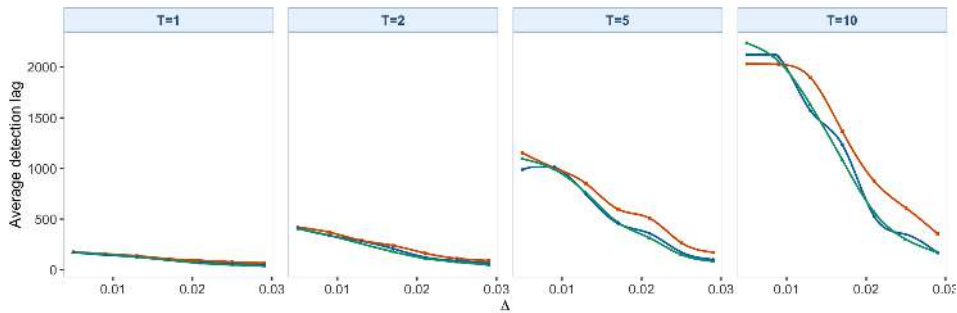
(c) fMA(1) errors; the four internal columns, from left to right, correspond to  $T = 1, 2, 5, 10$ .

Figure S4.14: ADD curves for Page-CUSUM,  $\gamma = 0.15$  under the level-shift setting. Each subfigure fixes one DGP, and the four internal columns correspond to  $T = 1, 2, 5, 10$ . The legend below the final subfigure identifies RSMS, SSMS, and HAC.

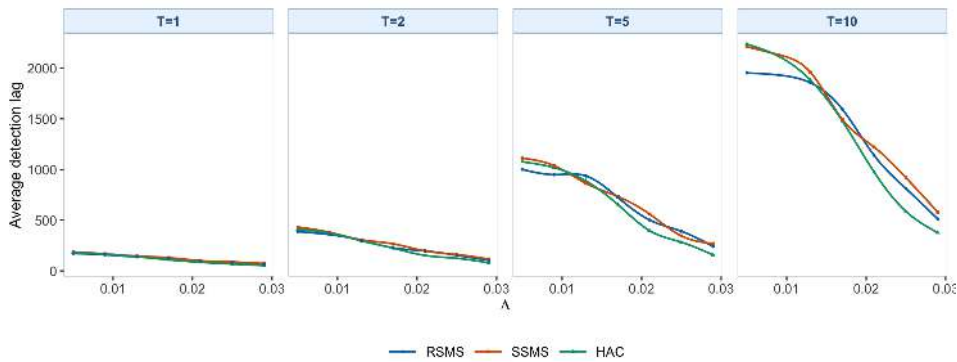
S4. SUPPLEMENTARY MONITORING STATISTICS



(a) BB errors; the four internal columns, from left to right, correspond to  $T = 1, 2, 5, 10$ .



(b) IID errors; the four internal columns, from left to right, correspond to  $T = 1, 2, 5, 10$ .



(c) fMA(1) errors; the four internal columns, from left to right, correspond to  $T = 1, 2, 5, 10$ .

Figure S4.15: ADD curves for Multiscale MOSUM with bandwidth set  $\mathcal{H} = \{0.05, 0.10, 0.20\}$  under the level-shift setting. Each subfigure fixes one DGP, and the four internal columns correspond to  $T = 1, 2, 5, 10$ . The legend below the final subfigure identifies RSMS, SSMS, and HAC.

remain conservative relative to the corresponding RSMS rows.

**Smooth change** For the smooth-change setting, the tables keep the DGP, the horizon  $T$ , and the positive break grid explicit for the FPCA-compressed weighted-CUSUM, Page-CUSUM, and multiscale MOSUM statistics. The color figures are reported DGP by DGP, with the four internal columns corresponding to  $T = 1, 2, 5, 10$ .

**Raw power.**

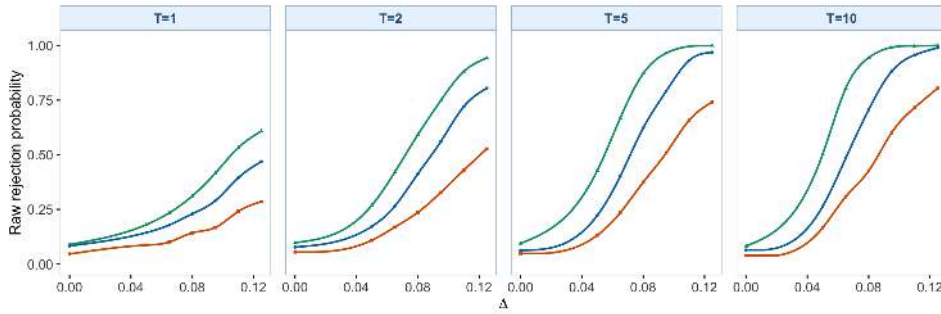
For the smooth-change setting, the raw-power tables and raw-rejection subfigures show Page-CUSUM with the highest reported rejection rates at each horizon  $T = 1, 2, 5, 10$ . Its mean raw power rises from 43.4% at  $T = 1$  to 83.3% at  $T = 10$ . Most of the gain occurs between  $T = 1$  and  $T = 2$ , with smaller increments thereafter, because the smooth-change drift needs time to accumulate. Weighted CUSUM is the next closest supplementary statistic by raw power, while multiscale MOSUM has lower raw power in these global settings. The SSMS rows are more conservative than the corresponding RSMS rows.

**SAP.**

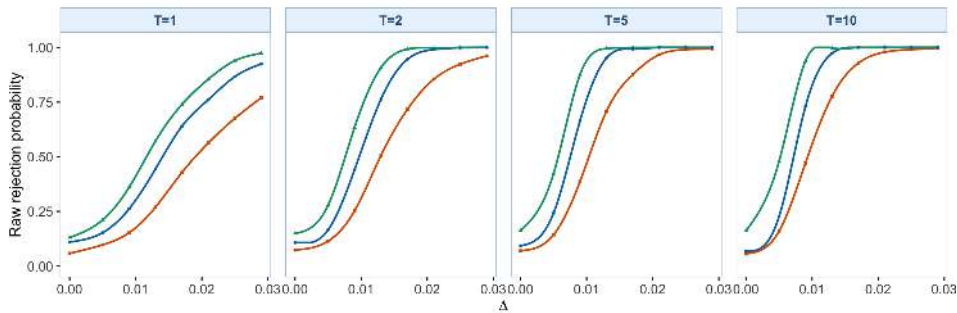
After empirical size adjustment, Page-CUSUM has the highest reported rejection rates for the smooth-change setting at each horizon  $T = 1, 2, 5, 10$ . Its mean SAP rises from 37.9% at  $T = 1$  to 81.9% at  $T = 10$ , with most of the increase between  $T = 1$  and  $T = 2$ . This horizon effect is pro-



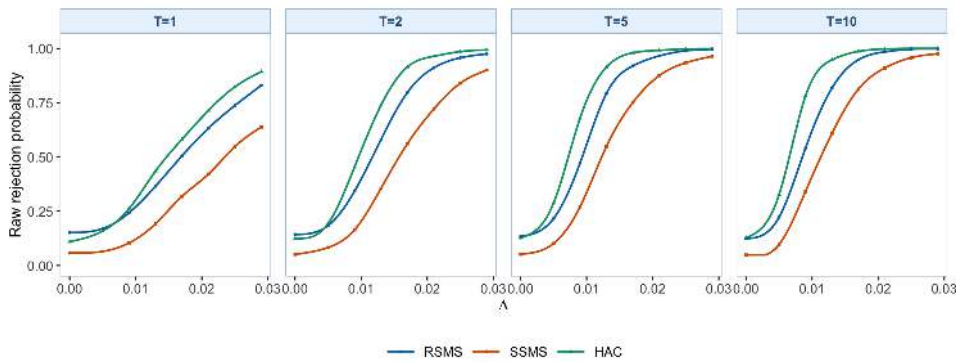
S4. SUPPLEMENTARY MONITORING STATISTICS



(a) BB errors; the four internal columns, from left to right, correspond to  $T = 1, 2, 5, 10$ .

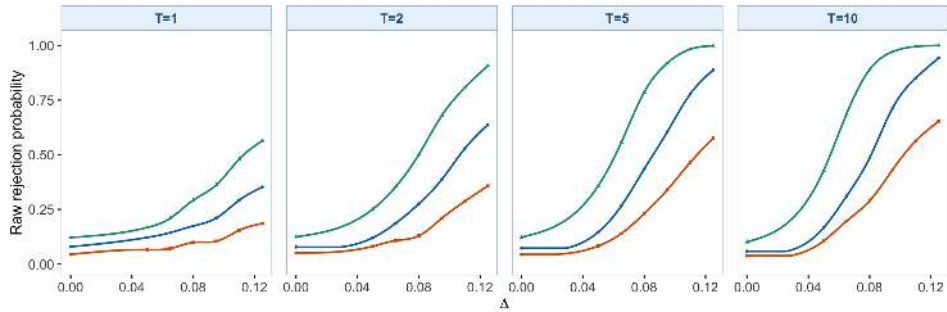


(b) fIID errors; the four internal columns, from left to right, correspond to  $T = 1, 2, 5, 10$ .

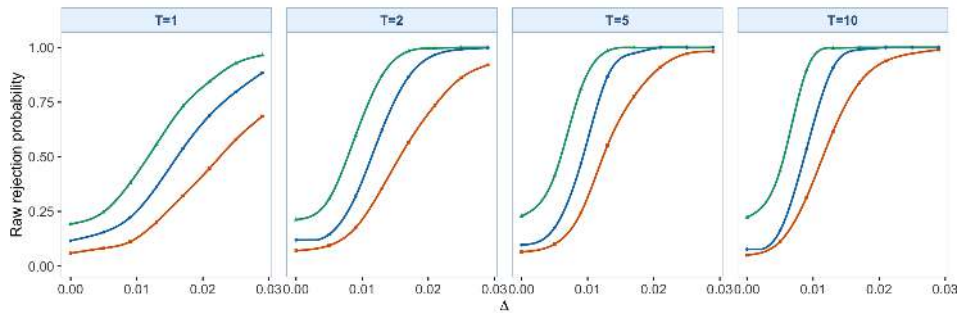


(c) fMA(1) errors; the four internal columns, from left to right, correspond to  $T = 1, 2, 5, 10$ .

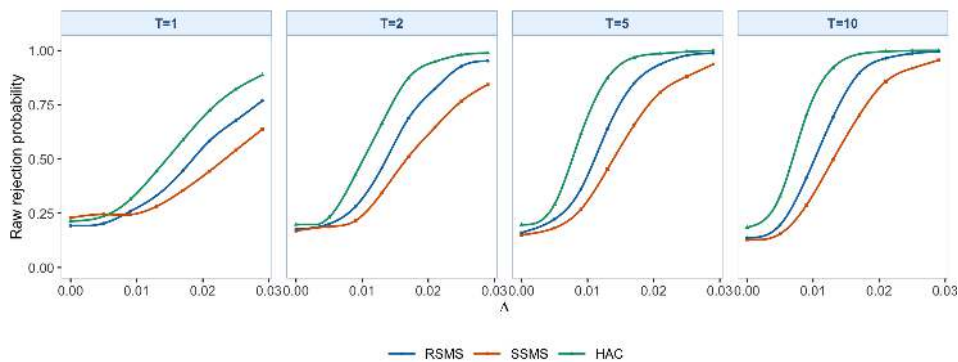
Figure S4.16: Raw rejection curves for weighted CUSUM,  $\gamma = 0$  under the smooth-change setting. Each subfigure fixes one DGP, and the four internal columns correspond to  $T = 1, 2, 5, 10$ . The legend below the final subfigure identifies RSMS, SSMS, and HAC.



(a) BB errors; the four internal columns, from left to right, correspond to  $T = 1, 2, 5, 10$ .



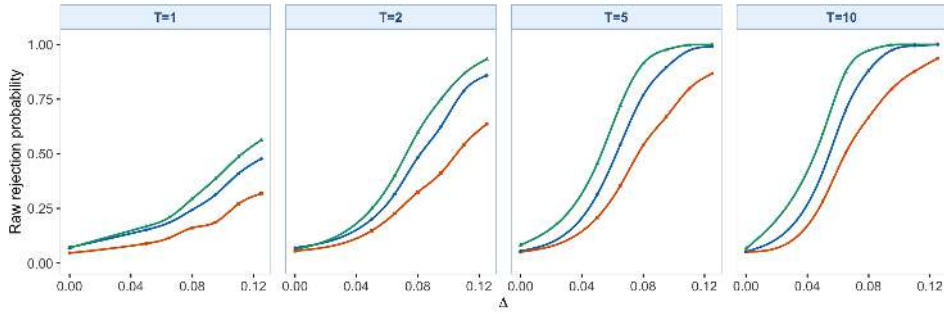
(b) IID errors; the four internal columns, from left to right, correspond to  $T = 1, 2, 5, 10$ .



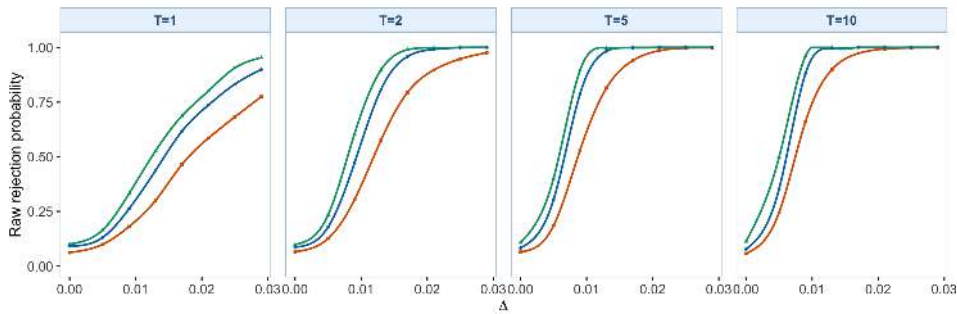
(c) fMA(1) errors; the four internal columns, from left to right, correspond to  $T = 1, 2, 5, 10$ .

Figure S4.17: Raw rejection curves for weighted CUSUM,  $\gamma = 0.15$  under the smooth-change setting. Each subfigure fixes one DGP, and the four internal columns correspond to  $T = 1, 2, 5, 10$ . The legend below the final subfigure identifies RSMS, SSMS, and HAC.

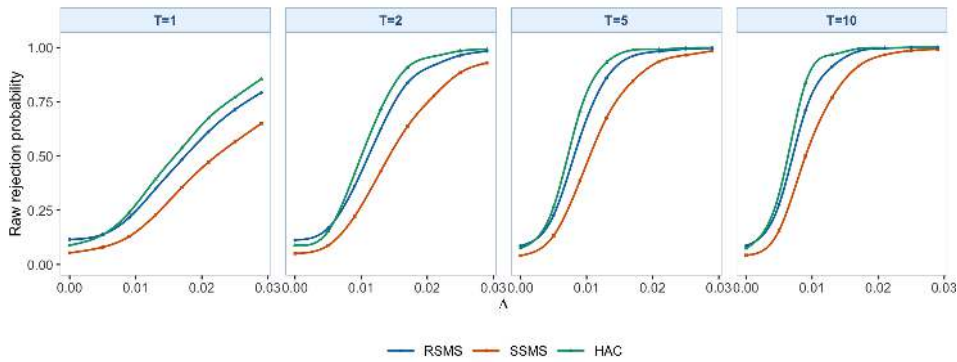
S4. SUPPLEMENTARY MONITORING STATISTICS



(a) BB errors; the four internal columns, from left to right, correspond to  $T = 1, 2, 5, 10$ .

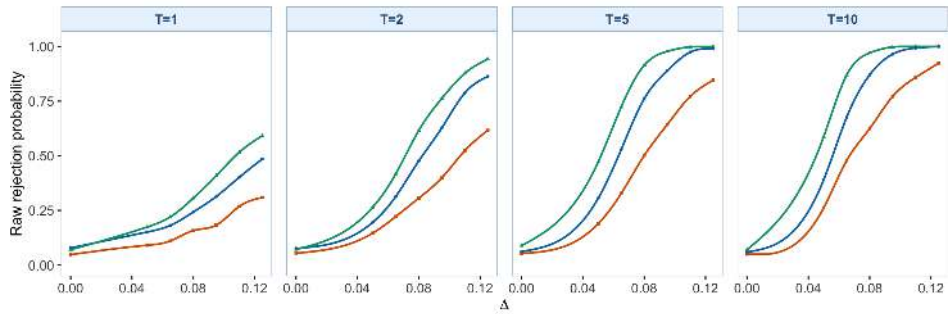


(b) IID errors; the four internal columns, from left to right, correspond to  $T = 1, 2, 5, 10$ .

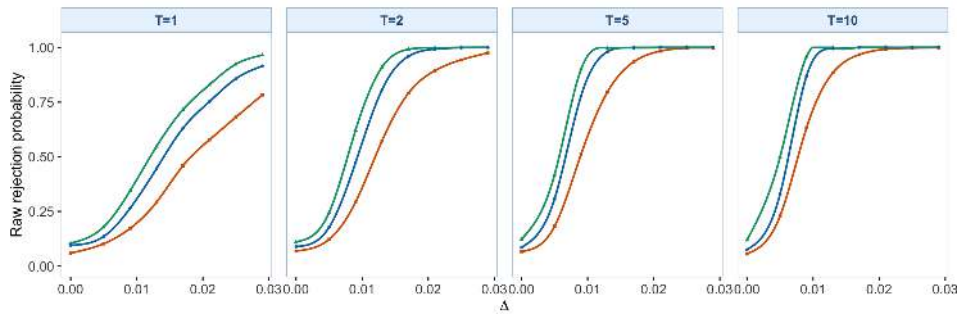


(c) fMA(1) errors; the four internal columns, from left to right, correspond to  $T = 1, 2, 5, 10$ .

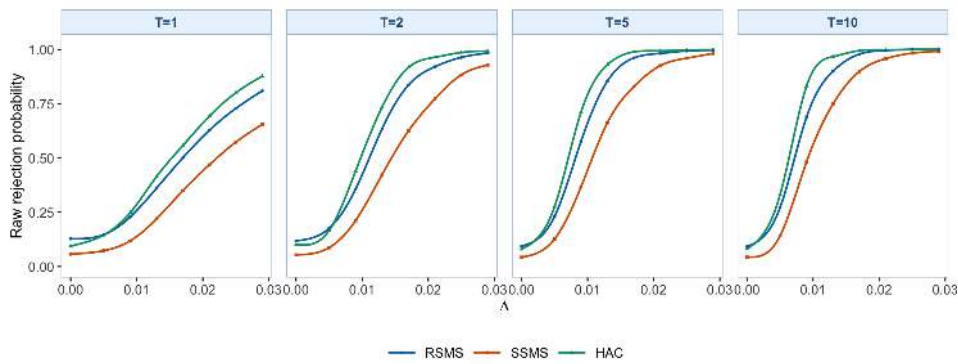
Figure S4.18: Raw rejection curves for Page-CUSUM,  $\gamma = 0$  under the smooth-change setting. Each subfigure fixes one DGP, and the four internal columns correspond to  $T = 1, 2, 5, 10$ . The legend below the final subfigure identifies RSMS, SSMS, and HAC.



(a) BB errors; the four internal columns, from left to right, correspond to  $T = 1, 2, 5, 10$ .



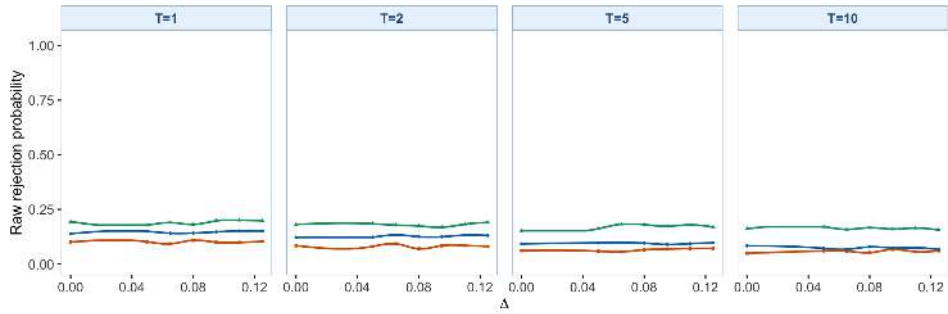
(b) IID errors; the four internal columns, from left to right, correspond to  $T = 1, 2, 5, 10$ .



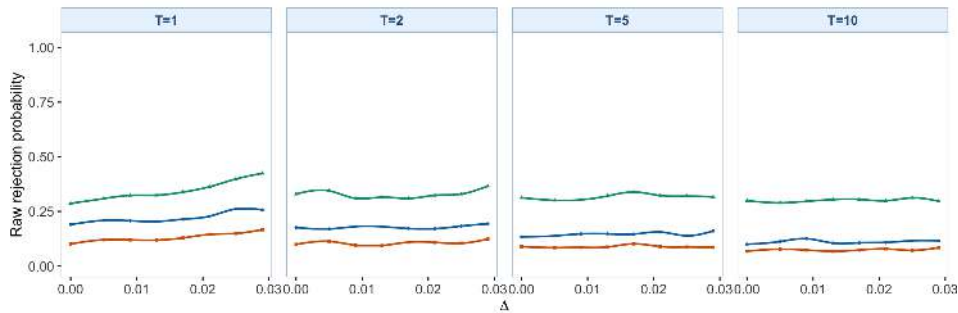
(c) fMA(1) errors; the four internal columns, from left to right, correspond to  $T = 1, 2, 5, 10$ .

Figure S4.19: Raw rejection curves for Page-CUSUM,  $\gamma = 0.15$  under the smooth-change setting. Each subfigure fixes one DGP, and the four internal columns correspond to  $T = 1, 2, 5, 10$ . The legend below the final subfigure identifies RSMS, SSMS, and HAC.

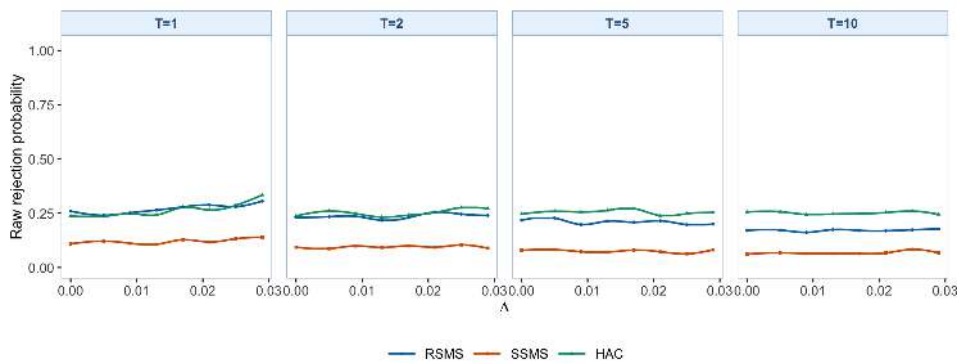
S4. SUPPLEMENTARY MONITORING STATISTICS



(a) BB errors; the four internal columns, from left to right, correspond to  $T = 1, 2, 5, 10$ .



(b) IID errors; the four internal columns, from left to right, correspond to  $T = 1, 2, 5, 10$ .



(c) fMA(1) errors; the four internal columns, from left to right, correspond to  $T = 1, 2, 5, 10$ .

Figure S4.20: Raw rejection curves for Multiscale MOSUM with bandwidth set  $\mathcal{H} = \{0.05, 0.10, 0.20\}$  under the smooth-change setting. Each subfigure fixes one DGP, and the four internal columns correspond to  $T = 1, 2, 5, 10$ . The legend below the final subfigure identifies RSMS, SSMS, and HAC.

Table S4.18: SAP (in %) for the FPCCA-compressed alternative monitoring statistics under the smooth-change setting. Panels separate the three DGPs, columns are grouped by monitoring horizon  $T \in \{1, 2, 5, 10\}$  and then by the positive break sizes  $\Delta$ , and the empirical size adjustment is computed separately for each simulation setting before averaging over  $s^* \in \{50, 200\}$ .

Method	Panel A: BB errors											
	$T = 1$		$T = 2$		$T = 5$		$T = 10$		$T = 10$			
Method	0.05	0.065	0.08	0.095	0.11	0.125	0.05	0.065	0.08	0.095	0.11	0.125
RSMS weighted CUSUM, $\gamma = 0$	9.6	12.1	16.8	21.2	30.3	39.0	11.7	20.5	32.3	47.9	64.1	75.0
RSMS weighted CUSUM, $\gamma = 0.15$	10.6	14.8	22.7	31.1	42.8	51.5	18.4	30.9	50.2	67.4	82.7	91.8
HAC weighted CUSUM, $\gamma = 0$	7.6	9.9	12.3	15.8	22.9	28.8	7.5	12.2	21.1	29.8	43.0	54.9
RSMS weighted CUSUM, $\gamma = 0.15$	7.4	8.2	12.0	11.8	17.2	20.8	8.7	11.3	13.5	21.7	29.6	37.0
RSMS Page-CUSUM, $\gamma = 0$	6.8	12.3	17.3	23.1	32.9	40.2	15.7	25.8	42.2	57.5	73.6	82.5
RSMS Page-CUSUM, $\gamma = 0.15$	6.8	12.3	17.3	23.1	32.9	40.2	15.7	25.8	42.2	57.5	73.6	82.5
HAC Page-CUSUM, $\gamma = 0$	11.1	13.4	18.2	21.1	29.5	35.2	14.5	22.6	32.2	41.0	53.6	63.5
RSMS Page-CUSUM, $\gamma = 0.15$	12.2	14.4	22.4	31.9	42.6	50.1	19.1	32.6	52.4	68.7	82.7	91.1
HAC Page-CUSUM, $\gamma = 0.15$	9.8	12.2	16.2	19.4	27.7	32.2	12.8	20.2	28.8	37.5	50.2	58.2
RSMS Multiscale MOSUM	11.6	14.9	22.6	32.3	43.0	51.0	18.6	32.2	51.9	69.0	83.7	91.8
HAC Multiscale MOSUM	5.7	5.0	5.0	5.5	4.7	5.4	3.2	4.0	3.4	3.2	4.7	4.6
FAC Multiscale MOSUM	6.3	4.9	5.0	5.7	4.9	5.4	3.2	4.5	3.8	3.2	4.1	3.8
FAC Multiscale MOSUM	5.3	4.9	5.0	5.7	4.9	5.4	3.2	4.1	3.8	3.2	4.1	3.8

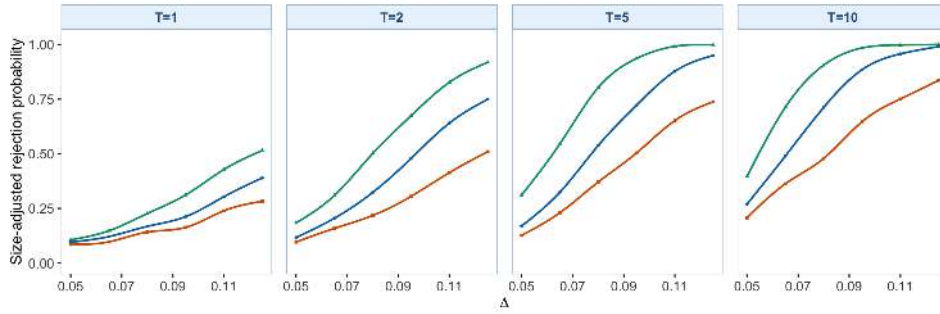
  

Method	Panel B: MID errors											
	$T = 1$		$T = 2$		$T = 5$		$T = 10$		$T = 10$			
Method	0.005	0.009	0.013	0.017	0.021	0.025	0.029	0.005	0.009	0.013	0.017	0.021
RSMS weighted CUSUM, $\gamma = 0$	10.0	18.3	33.2	54.7	69.3	81.0	88.0	9.0	21.7	44.6	69.8	97.6
RSMS weighted CUSUM, $\gamma = 0.15$	7.4	12.3	23.6	38.3	51.1	62.9	72.8	1.4	14.9	27.8	41.4	54.6
HAC weighted CUSUM, $\gamma = 0$	10.8	13.8	20.2	28.1	36.7	45.0	53.0	10.1	18.9	29.8	41.8	54.6
RSMS weighted CUSUM, $\gamma = 0.15$	6.7	19.2	18.2	39.3	41.6	63.3	64.0	6.8	14.0	29.5	50.3	61.4
HAC weighted CUSUM, $\gamma = 0.15$	8.9	19.3	37.0	67.8	78.2	86.7	86.7	11.3	37.2	72.2	92.5	98.6
RSMS Page-CUSUM, $\gamma = 0$	8.2	20.2	26.2	42.4	53.8	64.4	73.6	10.4	26.3	51.1	72.1	86.5
RSMS Page-CUSUM, $\gamma = 0.15$	8.2	20.2	26.2	42.4	53.8	64.4	73.6	10.4	26.3	51.1	72.1	86.5
HAC Page-CUSUM, $\gamma = 0$	10.0	20.4	38.5	57.3	70.8	81.5	88.2	11.5	37.5	72.4	93.0	98.6
RSMS Page-CUSUM, $\gamma = 0.15$	9.5	21.2	42.3	61.3	73.6	84.5	92.2	13.5	46.2	82.0	97.3	99.2
HAC Page-CUSUM, $\gamma = 0.15$	7.4	8.3	7.4	7.8	9.2	9.6	9.7	4.7	5.0	4.9	4.7	4.0
RSMS Multiscale MOSUM	5.2	5.5	5.3	5.8	6.3	7.0	8.2	6.1	5.5	5.2	5.3	5.2
FAC Multiscale MOSUM	5.2	5.5	5.3	5.8	6.3	7.0	8.2	6.1	5.5	5.2	5.3	5.2
FAC Multiscale MOSUM	5.2	5.5	5.3	5.8	6.3	7.0	8.2	6.1	5.5	5.2	5.3	5.2

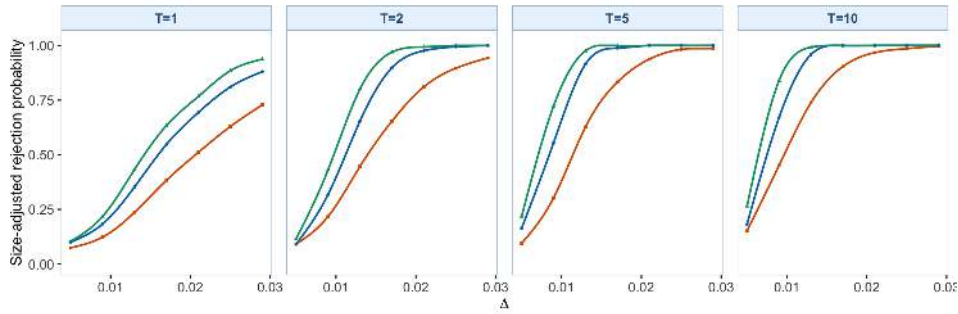
  

Method	Panel C: FMA(1) errors											
	$T = 1$		$T = 2$		$T = 5$		$T = 10$		$T = 10$			
Method	0.005	0.009	0.013	0.017	0.021	0.025	0.029	0.005	0.009	0.013	0.017	0.021
RSMS weighted CUSUM, $\gamma = 0$	5.3	9.7	18.4	30.5	45.9	58.0	68.0	9.0	20.2	44.6	68.7	83.9
RSMS weighted CUSUM, $\gamma = 0.15$	7.0	10.5	19.1	31.1	42.7	53.0	62.8	7.8	17.3	33.0	53.3	63.8
HAC weighted CUSUM, $\gamma = 0$	4.1	6.6	10.2	20.0	33.0	46.0	56.5	5.8	11.3	26.1	43.4	60.1
RSMS weighted CUSUM, $\gamma = 0.15$	6.2	7.1	2.0	10.0	10.7	29.7	37.7	3.2	6.0	14.4	22.9	38.0
HAC weighted CUSUM, $\gamma = 0.15$	6.2	12.3	20.0	31.4	48.5	58.9	68.0	10.6	26.4	52.5	73.5	85.0
RSMS Page-CUSUM, $\gamma = 0$	8.1	12.3	22.4	34.2	48.3	61.4	74.8	9.1	23.8	46.3	64.3	81.4
RSMS Page-CUSUM, $\gamma = 0.15$	8.1	12.3	22.4	34.2	48.3	61.4	74.8	9.1	23.8	46.3	64.3	81.4
HAC Page-CUSUM, $\gamma = 0$	9.7	11.7	21.4	31.2	48.3	61.4	74.8	10.1	25.1	51.1	73.9	87.8
RSMS Page-CUSUM, $\gamma = 0.15$	9.9	19.2	34.8	50.1	63.7	75.2	85.1	11.8	34.7	67.0	97.5	97.5
HAC Page-CUSUM, $\gamma = 0.15$	5.2	5.6	5.4	6.2	6.8	7.5	8.2	4.9	5.6	5.6	5.7	5.7
RSMS Multiscale MOSUM	5.2	5.6	5.4	6.2	6.8	7.5	8.2	4.9	5.6	5.6	5.7	5.7
HAC Multiscale MOSUM	5.4	5.7	6.2	7.1	7.6	7.9	8.2	4.0	4.5	4.5	4.8	4.8
FAC Multiscale MOSUM	5.4	5.7	6.2	7.1	7.6	7.9	8.2	4.0	4.5	4.5	4.8	4.8

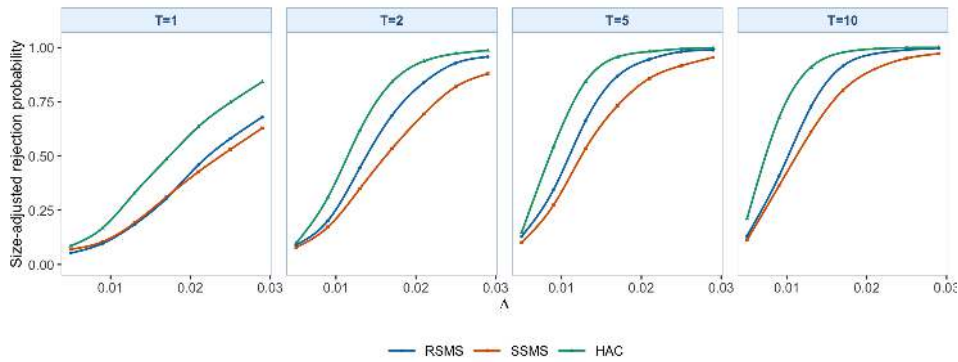
S4. SUPPLEMENTARY MONITORING STATISTICS



(a) BB errors; the four internal columns, from left to right, correspond to  $T = 1, 2, 5, 10$ .

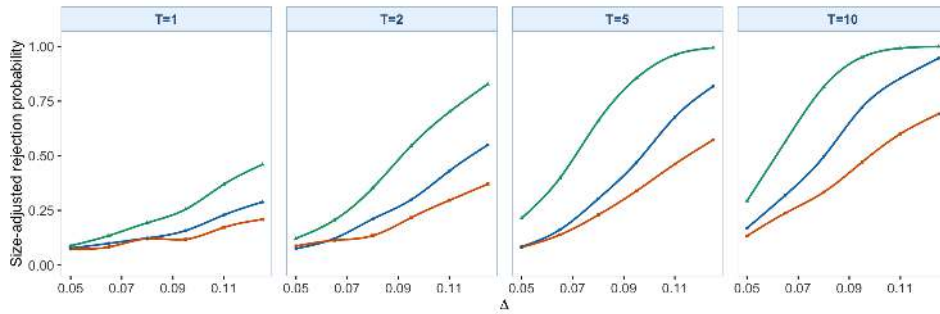


(b) IID errors; the four internal columns, from left to right, correspond to  $T = 1, 2, 5, 10$ .

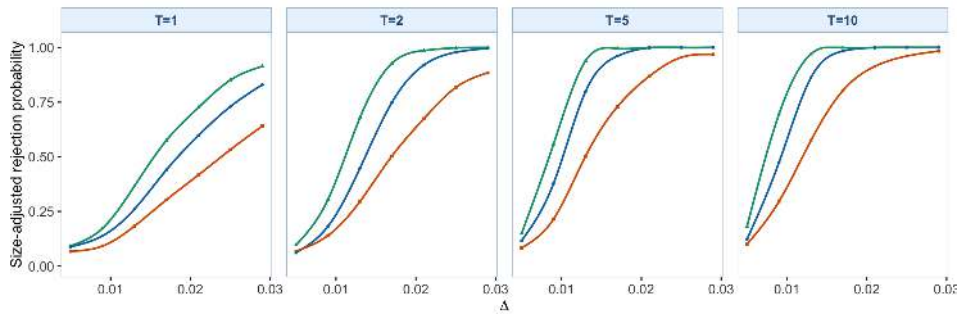


(c) fMA(1) errors; the four internal columns, from left to right, correspond to  $T = 1, 2, 5, 10$ .

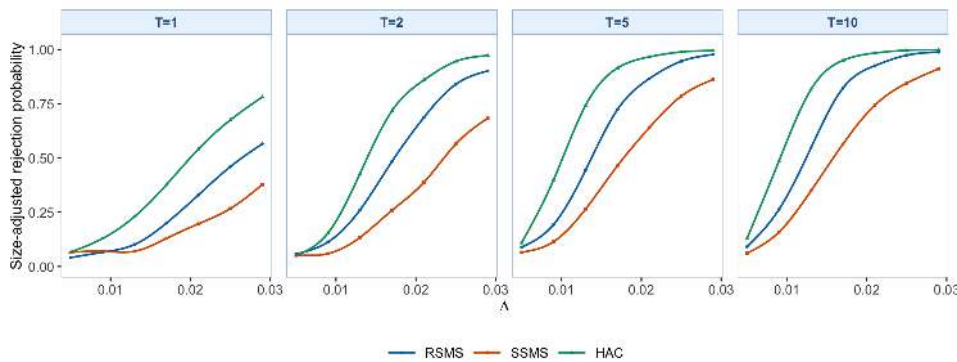
Figure S4.21: SAP curves for weighted CUSUM,  $\gamma = 0$  under the smooth-change setting. Each subfigure fixes one DGP, and the four internal columns correspond to  $T = 1, 2, 5, 10$ . The legend below the final subfigure identifies RSMS, SSMS, and HAC.



(a) BB errors; the four internal columns, from left to right, correspond to  $T = 1, 2, 5, 10$ .



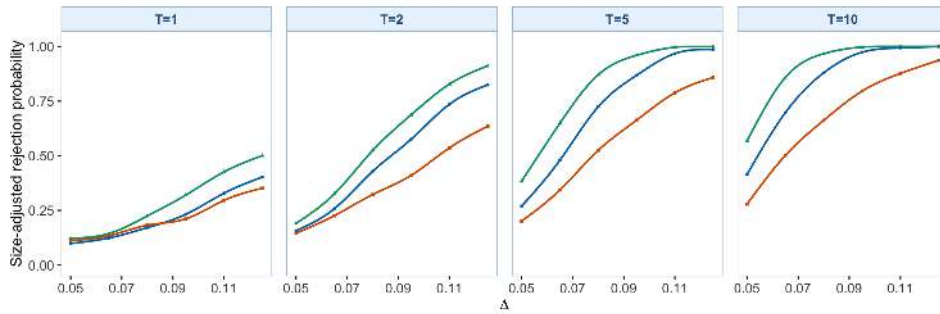
(b) IID errors; the four internal columns, from left to right, correspond to  $T = 1, 2, 5, 10$ .



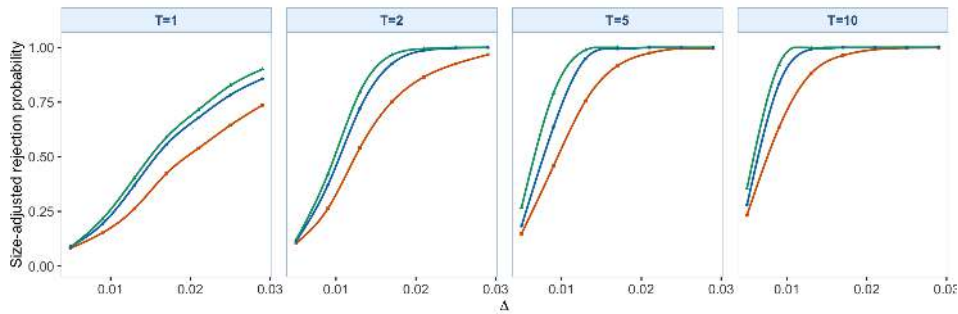
(c) fMA(1) errors; the four internal columns, from left to right, correspond to  $T = 1, 2, 5, 10$ .

Figure S4.22: SAP curves for weighted CUSUM,  $\gamma = 0.15$  under the smooth-change setting. Each subfigure fixes one DGP, and the four internal columns correspond to  $T = 1, 2, 5, 10$ . The legend below the final subfigure identifies RSMS, SSMS, and HAC.

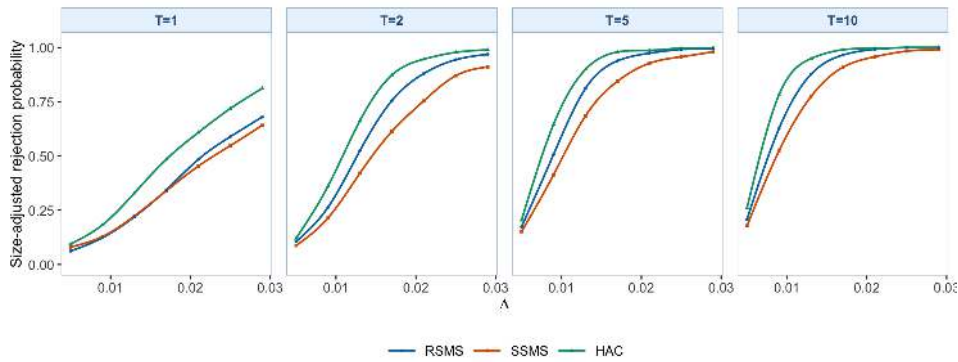
S4. SUPPLEMENTARY MONITORING STATISTICS



(a) BB errors; the four internal columns, from left to right, correspond to  $T = 1, 2, 5, 10$ .

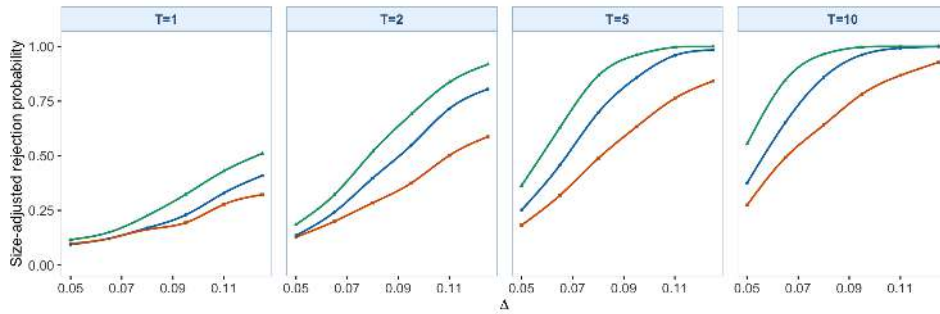


(b) IID errors; the four internal columns, from left to right, correspond to  $T = 1, 2, 5, 10$ .

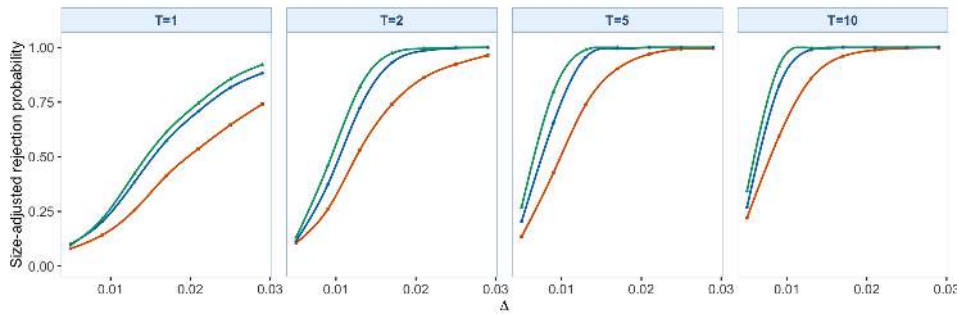


(c) fMA(1) errors; the four internal columns, from left to right, correspond to  $T = 1, 2, 5, 10$ .

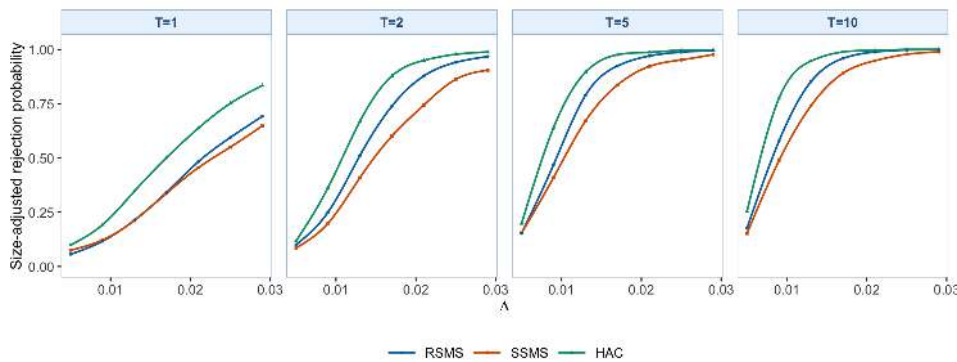
Figure S4.23: SAP curves for Page-CUSUM,  $\gamma = 0$  under the smooth-change setting. Each subfigure fixes one DGP, and the four internal columns correspond to  $T = 1, 2, 5, 10$ . The legend below the final subfigure identifies RSMS, SSMS, and HAC.



(a) BB errors; the four internal columns, from left to right, correspond to  $T = 1, 2, 5, 10$ .



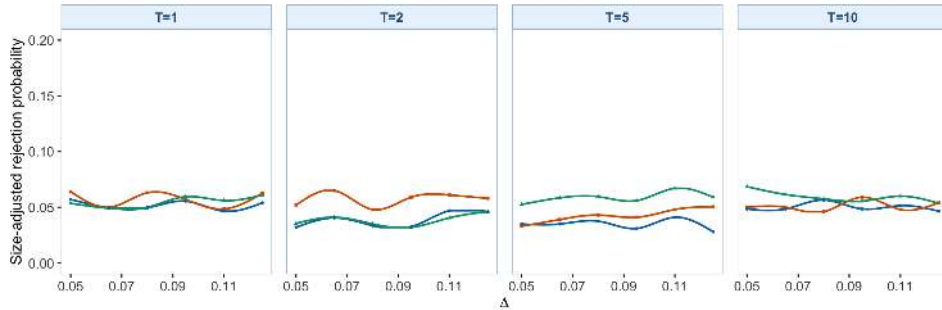
(b) IID errors; the four internal columns, from left to right, correspond to  $T = 1, 2, 5, 10$ .



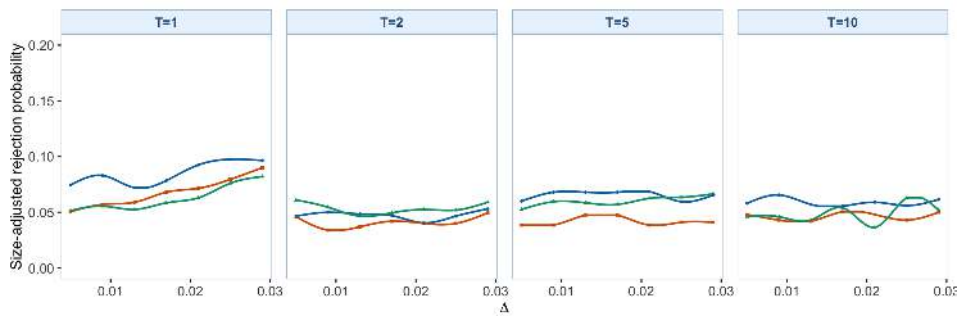
(c) fMA(1) errors; the four internal columns, from left to right, correspond to  $T = 1, 2, 5, 10$ .

Figure S4.24: SAP curves for Page-CUSUM,  $\gamma = 0.15$  under the smooth-change setting. Each subfigure fixes one DGP, and the four internal columns correspond to  $T = 1, 2, 5, 10$ . The legend below the final subfigure identifies RSMS, SSMS, and HAC.

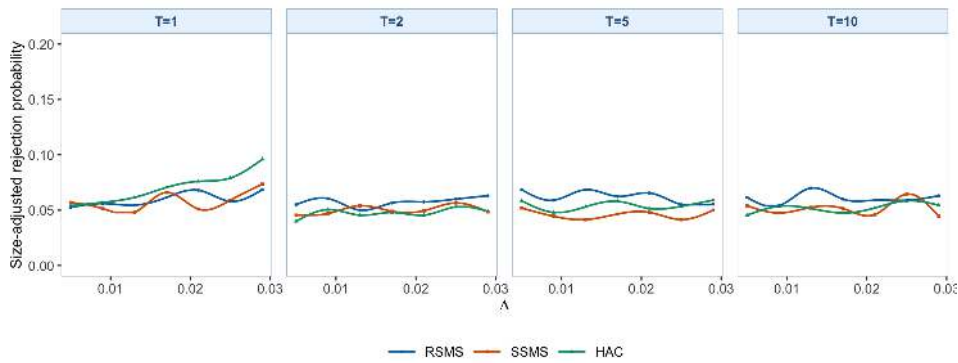
S4. SUPPLEMENTARY MONITORING STATISTICS



(a) BB errors; the four internal columns, from left to right, correspond to  $T = 1, 2, 5, 10$ .



(b) fIID errors; the four internal columns, from left to right, correspond to  $T = 1, 2, 5, 10$ .



(c) fMA(1) errors; the four internal columns, from left to right, correspond to  $T = 1, 2, 5, 10$ .

Figure S4.25: SAP curves for Multiscale MOSUM with bandwidth set  $\mathcal{H} = \{0.05, 0.10, 0.20\}$  under the smooth-change setting. Each subfigure fixes one DGP, and the four internal columns correspond to  $T = 1, 2, 5, 10$ . The legend below the final subfigure identifies RSMS, SSMS, and HAC. Because the curves after empirical size adjustment remain concentrated near zero, the vertical axis is restricted to  $[0, 0.20]$  to make the cross-method differences visible.

nounced for smooth change, where the drift needs time to accumulate. Weighted CUSUM is the next closest supplementary statistic by SAP. Multiscale MOSUM reports lower SAP in these global smooth-change settings, partly because empirical size is substantially distorted for HAC and for several RSMS multiscale MOSUM entries. The SSMS rows remain more conservative than the corresponding RSMS rows.

**ADD.**

The ADD tables and subfigures for the smooth-change setting report shorter delays for several RSMS rows. Multiscale MOSUM has lower ADD at every horizon  $T = 1, 2, 5, 10$ . Its mean ADD increases from 184.2 at  $T = 1$  to 2209.3 at  $T = 10$  because stopping times are recorded on a longer scale as the monitoring horizon lengthens. Page-CUSUM has the largest average ADD among the supplementary statistics. The SSMS rows remain conservative relative to the corresponding RSMS rows.

S4. SUPPLEMENTARY MONITORING STATISTICS

Table S4.19: ADD for the FPCA-compressed alternative monitoring statistics under the smooth-change setting. Panels separate the three DGPs, columns are grouped by monitoring horizon  $T \in \{1, 2, 5, 10\}$  and then by the positive break sizes  $\Delta$ , entries are detection delays in monitoring observations, not percentages, and smaller entries indicate faster post-break detection after averaging over  $s^* \in \{50, 200\}$ .

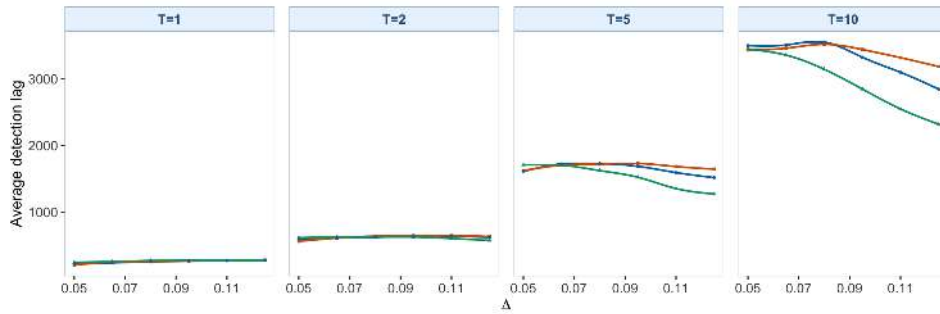
Method	Panel A: BB errors												
	T = 1		T = 2		T = 5		T = 10		T = 10				
	0.05	0.065	0.08	0.095	0.11	0.125	0.05	0.065	0.08	0.095	0.11	0.125	
RSMS weighted CUSUM, $\gamma = 0$	206.4	219.9	261.4	274.1	271.3	276.6	613.9	622.7	648.5	638.3	623.2	1611.7	1703.3
HAC weighted CUSUM, $\gamma = 0$	246.9	256.8	264.5	274.7	271.5	276.6	625.6	627.2	637.5	637.5	637.5	1708.6	1705.1
RSMS weighted CUSUM, $\gamma = 0.15$	198.3	241.4	233.4	250.0	260.0	272.2	513.3	584.3	626.2	653.1	654.6	1664.3	1601.6
HAC weighted CUSUM, $\gamma = 0.15$	215.6	238.8	254.5	262.9	268.9	271.5	546.2	596.8	611.6	625.0	617.7	1590.8	1646.6
RSMS Page-CUSUM, $\gamma = 0$	249.7	262.8	281.5	279.4	281.0	289.7	620.8	633.4	672.0	660.7	644.0	1722.2	1770.5
HAC Page-CUSUM, $\gamma = 0$	275.9	285.8	286.7	290.0	287.4	288.6	673.6	673.5	675.0	668.4	640.6	1610.9	1779.7
RSMS Page-CUSUM, $\gamma = 0.15$	242.3	247.7	277.2	272.3	276.7	283.8	596.2	637.6	664.0	652.0	658.0	1756.0	1757.4
HAC Page-CUSUM, $\gamma = 0.15$	251.6	274.2	283.5	283.4	285.4	283.6	649.6	654.0	658.5	620.6	591.2	1765.9	1747.5
RSMS Multiscale MOSUM	175.2	184.1	172.4	192.5	184.4	189.2	418.6	397.1	421.3	406.8	429.7	1101.9	1102.7
HAC Multiscale MOSUM	188.4	188.1	180.2	189.1	193.9	182.7	417.5	431.3	453.5	429.9	441.8	1155.6	1175.4

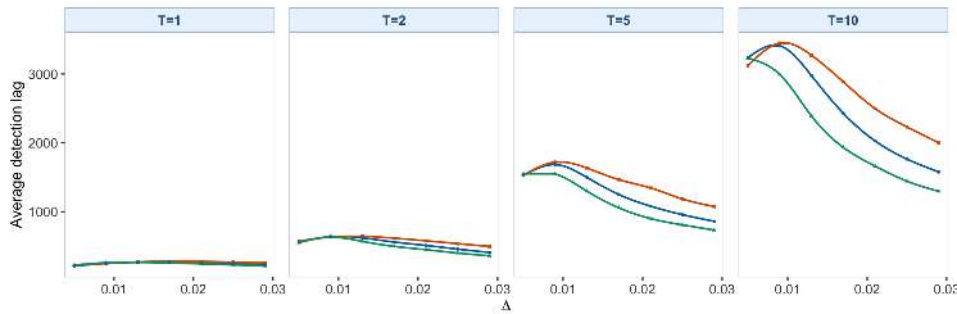
Method	Panel B: fIID errors												
	T = 1		T = 2		T = 5		T = 10		T = 10				
	0.005	0.009	0.013	0.017	0.021	0.025	0.005	0.009	0.013	0.017	0.021	0.025	
RSMS weighted CUSUM, $\gamma = 0$	210.0	245.9	268.5	276.9	274.4	265.6	558.3	637.1	617.1	573.8	576.8	1534.4	1605.3
HAC weighted CUSUM, $\gamma = 0$	178.6	225.1	253.0	256.4	261.6	255.6	509.3	584.2	623.4	604.8	546.8	1492.6	1535.3
RSMS weighted CUSUM, $\gamma = 0.15$	186.3	232.5	261.3	274.6	270.2	274.2	517.3	601.3	633.4	633.4	536.1	1374.9	1673.7
HAC weighted CUSUM, $\gamma = 0.15$	243.5	281.9	282.9	286.5	273.8	266.4	638.8	678.6	648.6	582.3	532.9	1485.4	1705.7
RSMS Page-CUSUM, $\gamma = 0$	268.8	280.1	285.3	276.7	263.7	255.6	623.4	650.6	623.4	549.6	498.8	1432.7	1657.5
HAC Page-CUSUM, $\gamma = 0$	237.3	271.4	275.6	272.1	266.0	253.5	607.0	665.5	638.8	577.5	517.5	1693.1	1793.4
RSMS Page-CUSUM, $\gamma = 0.15$	251.4	272.0	267.2	254.9	241.2	222.9	608.7	661.8	603.8	572.2	477.5	1430.1	1628.8
HAC Page-CUSUM, $\gamma = 0.15$	180.5	181.7	179.9	186.5	190.2	200.2	423.6	433.4	436.5	429.9	416.7	1116.7	1116.7
RSMS Multiscale MOSUM	182.3	187.1	186.5	187.0	188.1	190.3	404.2	409.9	407.5	404.7	416.2	1033.9	1033.9
HAC Multiscale MOSUM	182.3	187.1	186.5	187.0	188.1	190.3	404.2	409.9	407.5	404.7	416.2	1033.9	1033.9

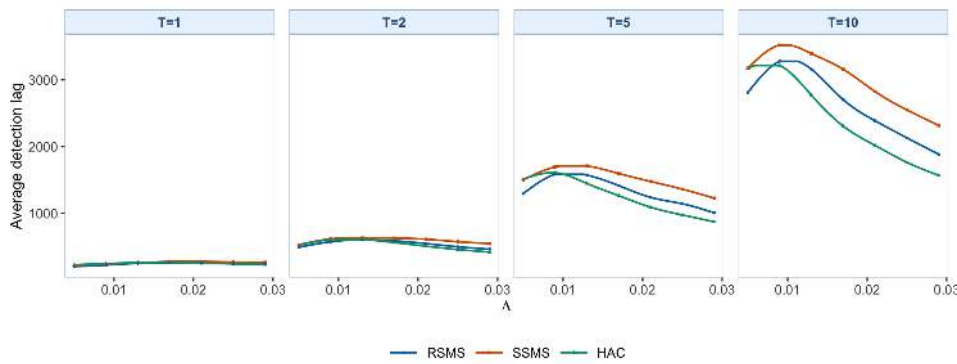
Method	Panel C: fMA(1) errors												
	T = 1		T = 2		T = 5		T = 10		T = 10				
	0.005	0.009	0.013	0.017	0.021	0.025	0.005	0.009	0.013	0.017	0.021	0.025	
RSMS weighted CUSUM, $\gamma = 0$	222.3	245.8	260.3	286.5	280.2	274.3	247.0	336.3	318.5	333.7	331.0	618.3	570.5
HAC weighted CUSUM, $\gamma = 0$	230.8	250.0	263.2	297.9	257.2	246.1	233.3	326.5	309.2	311.3	304.6	510.3	460.0
RSMS weighted CUSUM, $\gamma = 0.15$	171.1	182.3	203.0	228.3	236.4	243.9	249.8	407.3	448.7	428.9	376.4	597.9	675.5
HAC weighted CUSUM, $\gamma = 0.15$	246.4	246.9	274.0	275.6	271.6	267.8	259.0	482.2	511.3	542.3	514.1	529.7	497.9
RSMS Page-CUSUM, $\gamma = 0$	285.5	278.1	284.7	289.7	259.3	256.8	254.4	628.2	678.4	659.3	631.1	554.1	507.9
HAC Page-CUSUM, $\gamma = 0$	236.5	252.3	267.5	272.6	267.9	260.0	255.0	558.0	621.7	633.2	608.9	560.8	480.6
RSMS Page-CUSUM, $\gamma = 0.15$	249.0	262.8	272.6	279.4	269.1	257.9	245.9	609.0	657.4	637.4	590.2	535.5	437.4
HAC Page-CUSUM, $\gamma = 0.15$	191.3	184.6	183.0	170.0	184.4	191.4	185.3	436.3	423.7	399.1	420.3	428.8	445.7
RSMS Multiscale MOSUM	186.9	187.2	191.9	176.3	184.4	191.4	197.7	425.3	420.0	415.0	418.6	417.2	423.2
HAC Multiscale MOSUM	186.9	187.2	191.9	176.3	184.4	191.4	197.7	425.3	420.0	415.0	418.6	417.2	423.2



(a) BB errors; the four internal columns, from left to right, correspond to  $T = 1, 2, 5, 10$ .



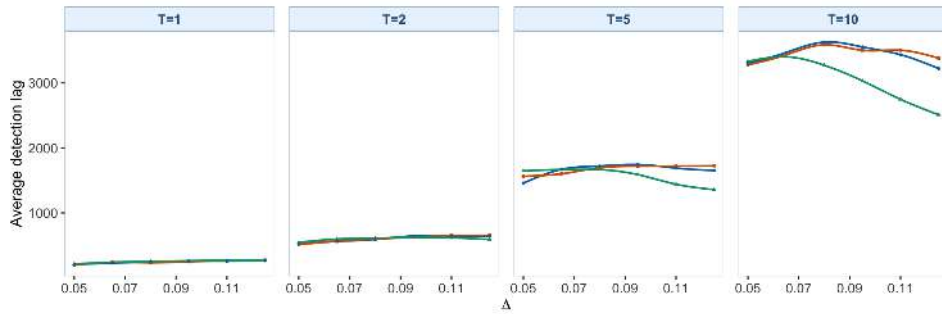
(b) IID errors; the four internal columns, from left to right, correspond to  $T = 1, 2, 5, 10$ .



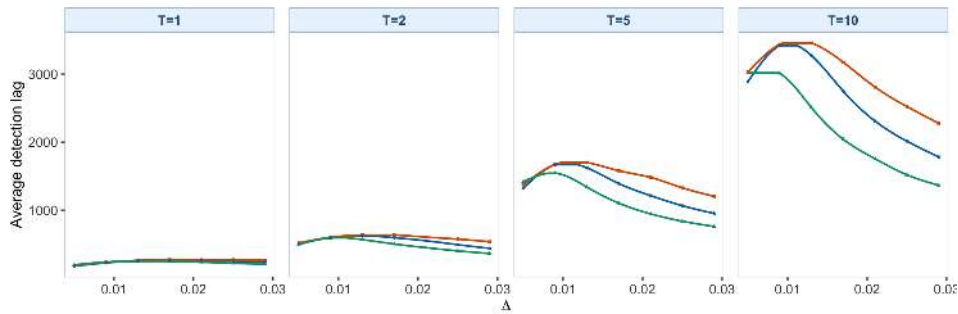
(c) fMA(1) errors; the four internal columns, from left to right, correspond to  $T = 1, 2, 5, 10$ .

Figure S4.26: ADD curves for weighted CUSUM,  $\gamma = 0$  under the smooth-change setting. Each subfigure fixes one DGP, and the four internal columns correspond to  $T = 1, 2, 5, 10$ . The legend below the final subfigure identifies RSMS, SSMS, and HAC.

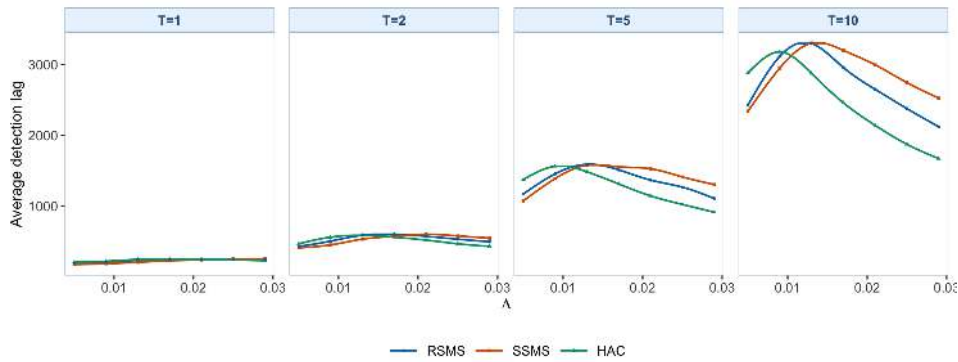
S4. SUPPLEMENTARY MONITORING STATISTICS



(a) BB errors; the four internal columns, from left to right, correspond to  $T = 1, 2, 5, 10$ .

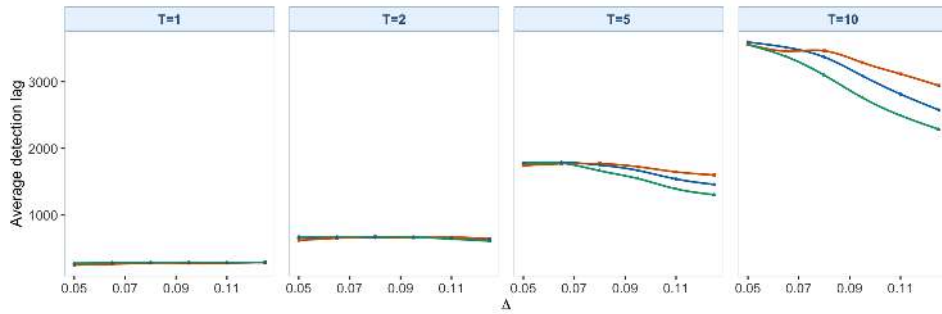


(b) IID errors; the four internal columns, from left to right, correspond to  $T = 1, 2, 5, 10$ .

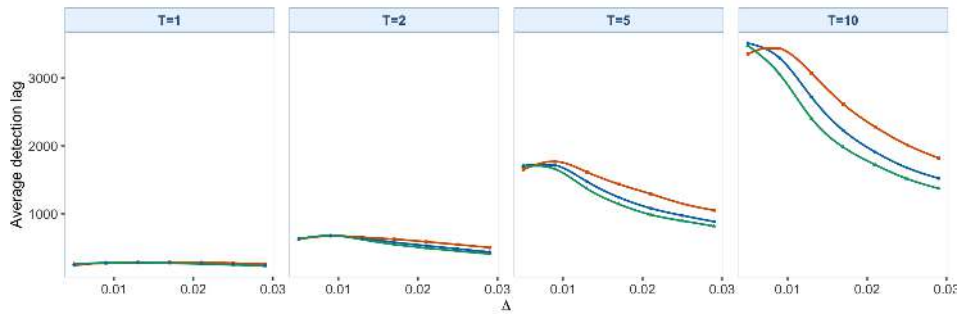


(c) fMA(1) errors; the four internal columns, from left to right, correspond to  $T = 1, 2, 5, 10$ .

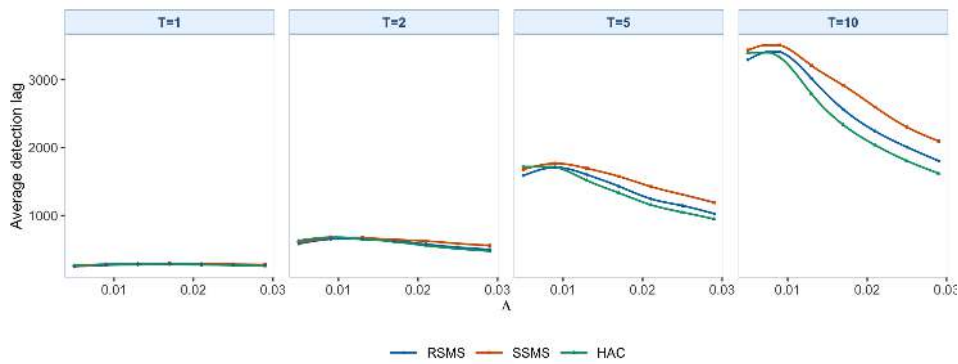
Figure S4.27: ADD curves for weighted CUSUM,  $\gamma = 0.15$  under the smooth-change setting. Each subfigure fixes one DGP, and the four internal columns correspond to  $T = 1, 2, 5, 10$ . The legend below the final subfigure identifies RSMS, SSMS, and HAC.



(a) BB errors; the four internal columns, from left to right, correspond to  $T = 1, 2, 5, 10$ .



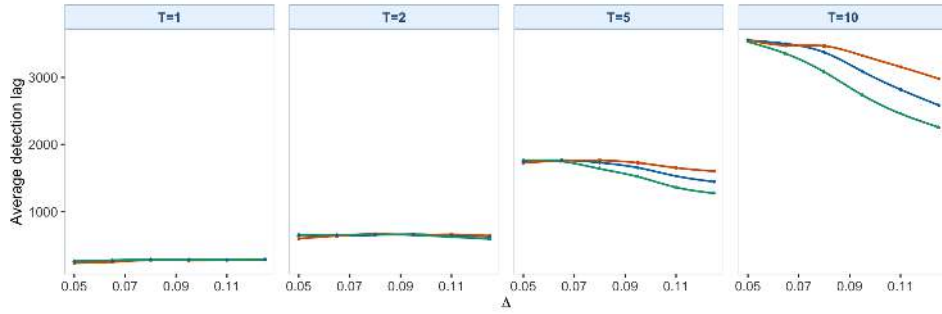
(b) IID errors; the four internal columns, from left to right, correspond to  $T = 1, 2, 5, 10$ .



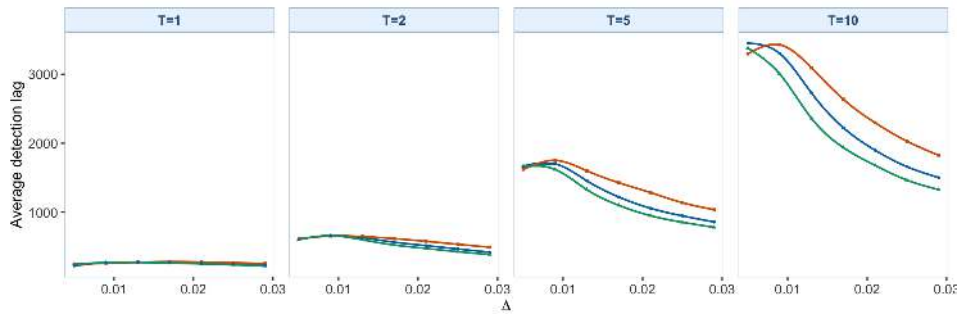
(c) fMA(1) errors; the four internal columns, from left to right, correspond to  $T = 1, 2, 5, 10$ .

Figure S4.28: ADD curves for Page-CUSUM,  $\gamma = 0$  under the smooth-change setting. Each subfigure fixes one DGP, and the four internal columns correspond to  $T = 1, 2, 5, 10$ . The legend below the final subfigure identifies RSMS, SSMS, and HAC.

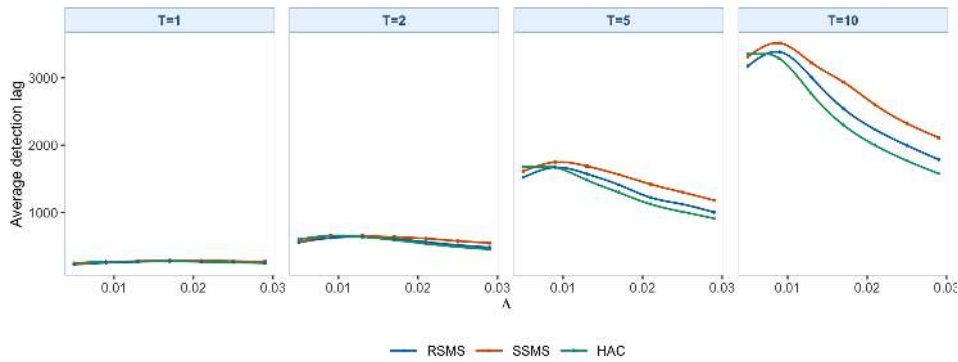
S4. SUPPLEMENTARY MONITORING STATISTICS



(a) BB errors; the four internal columns, from left to right, correspond to  $T = 1, 2, 5, 10$ .

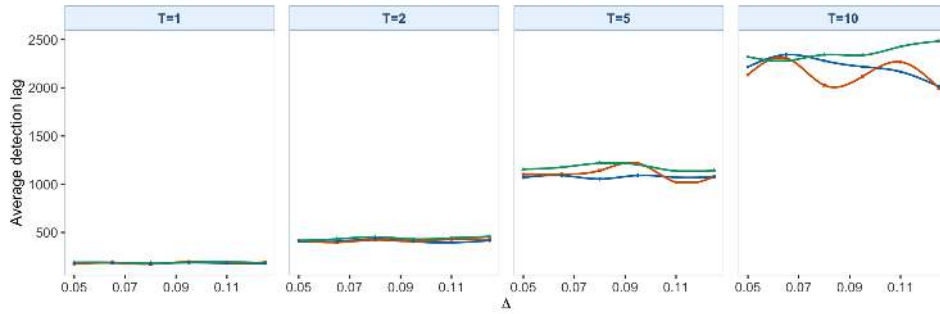


(b) IID errors; the four internal columns, from left to right, correspond to  $T = 1, 2, 5, 10$ .

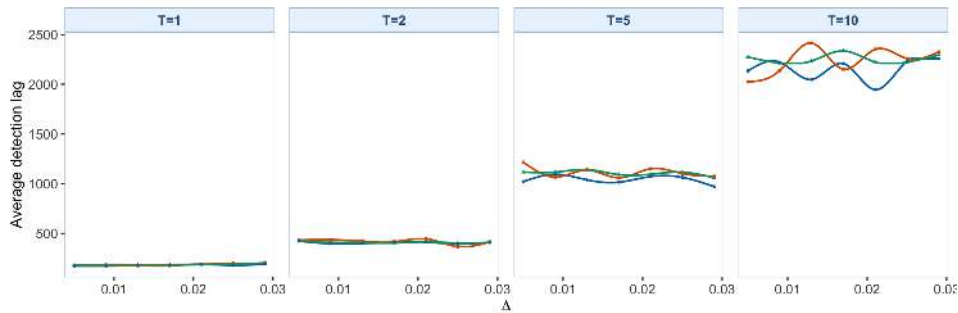


(c) fMA(1) errors; the four internal columns, from left to right, correspond to  $T = 1, 2, 5, 10$ .

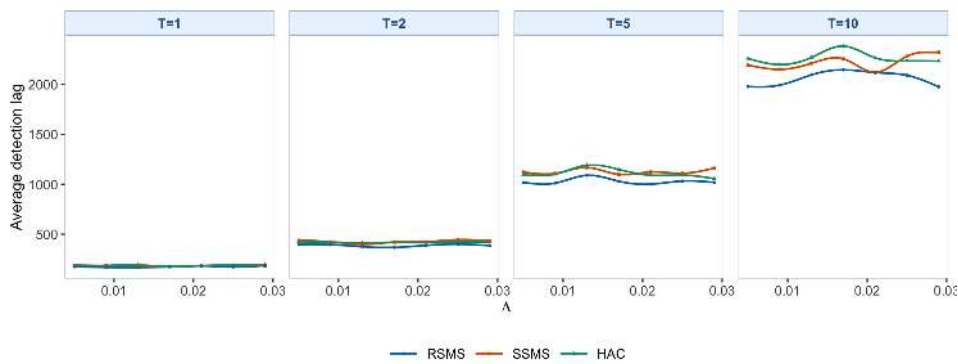
Figure S4.29: ADD curves for Page-CUSUM,  $\gamma = 0.15$  under the smooth-change setting. Each subfigure fixes one DGP, and the four internal columns correspond to  $T = 1, 2, 5, 10$ . The legend below the final subfigure identifies RSMS, SSMS, and HAC.



(a) BB errors; the four internal columns, from left to right, correspond to  $T = 1, 2, 5, 10$ .



(b) IID errors; the four internal columns, from left to right, correspond to  $T = 1, 2, 5, 10$ .



(c) fMA(1) errors; the four internal columns, from left to right, correspond to  $T = 1, 2, 5, 10$ .

Figure S4.30: ADD curves for Multiscale MOSUM with bandwidth set  $\mathcal{H} = \{0.05, 0.10, 0.20\}$  under the smooth-change setting. Each subfigure fixes one DGP, and the four internal columns correspond to  $T = 1, 2, 5, 10$ . The legend below the final subfigure identifies RSMS, SSMS, and HAC.

**Localized change** For the localized-change setting, the tables keep the DGP, the horizon  $T$ , and the positive break grid explicit for the FPCA-compressed weighted-CUSUM, Page-CUSUM, and multiscale MOSUM statistics. The color figures are reported DGP by DGP, with the four internal columns corresponding to  $T = 1, 2, 5, 10$ .

**Raw power.**

For the localized-change setting, the raw-power tables and raw-rejection subfigures show Page-CUSUM with the highest reported rejection rates at each horizon  $T = 1, 2, 5, 10$ . Its mean raw power rises from 64.5% at  $T = 1$  to 78.4% at  $T = 10$ . Most of the gain occurs between  $T = 1$  and  $T = 2$ , with smaller increments thereafter. Weighted CUSUM is the next closest supplementary statistic by raw power. Multiscale MOSUM is more local and has lower raw power in these reported simulation settings. The SSMS rows are more conservative than the corresponding RSMS rows.

**SAP.**

After empirical size adjustment, Page-CUSUM has the highest reported rejection rates for the localized-change setting at each horizon  $T = 1, 2, 5, 10$ . Its mean SAP rises from 60.6% at  $T = 1$  to 77.2% at  $T = 10$ . Most of the gain occurs between  $T = 1$  and  $T = 2$ , with smaller increments thereafter. Weighted CUSUM is the next closest supplementary

Table S4.20: Raw power (in %) for the FPCA-compressed alternative monitoring statistics under the localized-change setting. Panels separate the three DGPs, columns are grouped by monitoring horizon  $T \in \{1, 2, 5, 10\}$  and then by the positive break sizes  $\Delta$ , and entries average over the two break locations  $s^* \in \{50, 200\}$ .

Method	Panel A: BB errors																						
	$T = 1$					$T = 2$					$T = 5$					$T = 10$							
	0.1	0.4	0.7	1	1.3	1.6	1.6	1.6	1.6	1.6	1.6	1.6	1.6	1.6	1.6	1.6	1.6	1.6	1.6	1.6			
SSMS weighted CUSUM, $\gamma = 0$	9.7	12.5	20.7	33.5	54.4	76.0	6.9	12.4	26.0	46.2	72.0	87.6	7.4	11.4	27.3	49.9	76.4	90.2	5.7	12.0	24.9	51.8	75.6
HAC weighted CUSUM, $\gamma = 0$	10.1	14.6	27.7	48.1	74.1	89.4	9.2	17.1	32.5	66.9	88.9	98.2	8.1	19.6	48.4	78.2	96.5	99.6	10.2	23.1	51.0	81.8	97.2
SSMS weighted CUSUM, $\gamma = 0.15$	9.4	10.7	15.0	22.1	38.0	55.1	8.1	10.8	17.2	28.7	49.4	69.0	7.4	9.3	18.8	33.2	55.6	74.4	5.3	9.6	15.8	31.1	54.4
HAC weighted CUSUM, $\gamma = 0.15$	11.1	14.5	24.5	39.1	61.9	81.8	12.6	17.1	32.8	56.0	80.9	94.9	11.7	18.9	39.1	68.8	91.3	98.0	12.7	21.4	43.5	73.7	93.5
SSMS Page-CUSUM, $\gamma = 0$	8.7	12.2	18.1	28.3	40.6	42.2	5.2	9.3	14.5	23.0	40.5	63.0	6.2	11.3	20.2	51.0	73.5	82.3	5.7	13.8	23.2	54.4	75.5
HAC Page-CUSUM, $\gamma = 0$	8.9	13.7	29.5	51.0	76.2	90.5	7.3	17.8	44.0	73.9	93.2	99.2	7.3	21.8	56.7	87.2	98.6	100.0	7.2	28.2	61.4	93.0	99.0
SSMS Page-CUSUM, $\gamma = 0.15$	5.9	8.4	15.3	23.6	41.3	54.8	6.1	14.5	34.1	59.7	84.0	95.6	6.7	14.7	38.5	68.2	92.2	98.5	6.2	16.4	39.5	73.0	93.2
HAC Page-CUSUM, $\gamma = 0.15$	9.1	13.0	23.4	39.4	61.4	81.8	6.4	10.7	21.9	37.8	59.5	78.5	4.5	9.8	24.2	44.8	67.8	83.6	4.8	12.6	26.0	48.4	70.8
SSMS Multiscale MOSUM	17.9	19.1	17.6	20.2	23.1	23.8	18.5	18.0	17.7	17.8	19.8	21.7	16.0	18.1	18.6	17.3	19.2	18.2	17.1	16.1	16.5	16.0	17.4

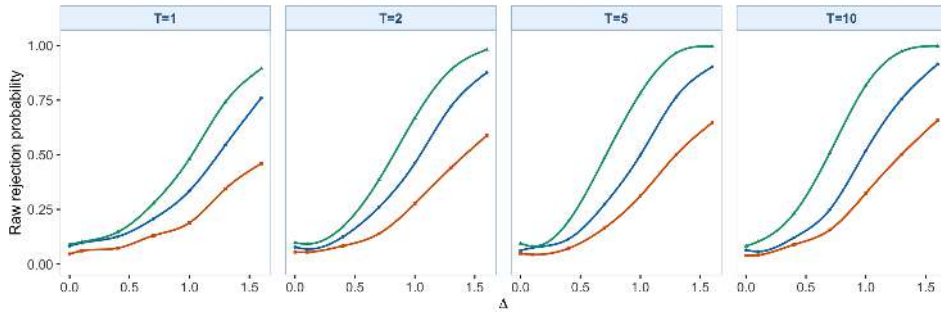
  

Method	Panel B: IID errors																						
	$T = 1$					$T = 2$					$T = 5$					$T = 10$							
	0.05	0.08	0.11	0.14	0.17	0.2	0.05	0.08	0.11	0.14	0.17	0.2	0.05	0.08	0.11	0.14	0.17	0.2	0.05	0.08	0.11	0.14	0.17
SSMS weighted CUSUM, $\gamma = 0$	32.2	65.6	91.3	98.8	100.0	100.0	39.3	79.4	97.4	100.0	100.0	100.0	43.0	84.7	99.0	100.0	100.0	42.3	84.0	99.1	100.0	100.0	100.0
HAC weighted CUSUM, $\gamma = 0$	45.4	82.5	97.8	100.0	100.0	100.0	62.1	96.3	99.9	100.0	100.0	100.0	70.8	98.8	100.0	100.0	100.0	74.6	98.6	100.0	100.0	100.0	100.0
SSMS weighted CUSUM, $\gamma = 0.15$	23.2	47.9	78.3	94.8	99.4	100.0	26.9	60.9	89.8	98.8	100.0	100.0	27.8	68.8	93.7	99.6	100.0	28.9	66.0	94.2	99.8	100.0	100.0
HAC weighted CUSUM, $\gamma = 0.15$	11.9	29.0	47.1	68.5	83.8	91.5	16.8	34.0	61.2	80.4	91.9	95.5	18.7	40.6	67.5	84.7	94.3	97.1	18.6	42.9	69.7	86.1	93.0
SSMS Page-CUSUM, $\gamma = 0$	35.0	70.5	93.7	99.3	100.0	100.0	57.8	90.5	99.7	100.0	100.0	100.0	61.9	96.8	100.0	100.0	100.0	64.5	97.5	100.0	100.0	100.0	100.0
HAC Page-CUSUM, $\gamma = 0$	44.8	89.0	98.2	100.0	100.0	100.0	65.6	97.5	100.0	100.0	100.0	100.0	77.4	99.6	100.0	100.0	100.0	81.0	99.9	100.0	100.0	100.0	100.0
SSMS Page-CUSUM, $\gamma = 0.15$	21.5	49.2	71.9	88.6	95.2	98.2	35.5	65.3	88.0	96.6	99.6	38.4	75.6	94.0	98.4	99.6	100.0	41.0	77.5	95.0	98.4	99.8	100.0
HAC Page-CUSUM, $\gamma = 0.15$	20.9	22.1	26.7	31.4	40.5	51.4	17.2	19.4	29.3	23.9	31.2	41.2	13.9	15.2	16.2	19.1	22.9	32.7	11.9	10.4	11.1	13.0	17.9
SSMS Multiscale MOSUM	20.9	22.1	26.7	31.4	40.5	51.4	17.2	19.4	29.3	23.9	31.2	41.2	13.9	15.2	16.2	19.1	22.9	32.7	11.9	10.4	11.1	13.0	17.9
HAC Multiscale MOSUM	30.4	33.7	42.5	49.5	61.1	72.9	32.2	34.6	46.8	46.1	56.9	68.8	30.6	32.9	35.8	41.4	50.8	60.6	31.9	31.8	32.3	37.5	47.5

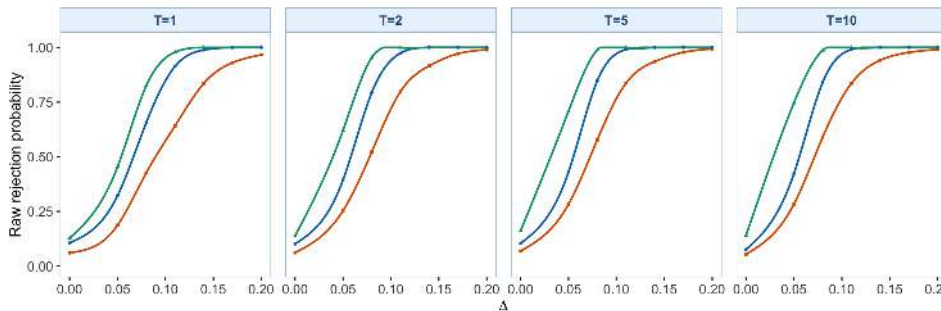
  

Method	Panel C: FMA(1) errors																							
	$T = 1$					$T = 2$					$T = 5$					$T = 10$								
	0.05	0.08	0.11	0.14	0.17	0.2	0.05	0.08	0.11	0.14	0.17	0.2	0.05	0.08	0.11	0.14	0.17	0.2	0.05	0.08	0.11	0.14	0.17	
SSMS weighted CUSUM, $\gamma = 0$	29.9	58.5	83.0	97.8	99.5	99.2	36.5	70.6	92.3	98.5	99.6	100.0	39.0	78.9	95.3	99.9	100.0	39.2	76.8	94.8	99.4	99.6	100.0	
HAC weighted CUSUM, $\gamma = 0$	15.1	34.3	53.0	75.8	89.3	93.7	16.8	42.0	70.3	87.5	94.6	99.0	20.8	49.9	76.7	89.9	95.6	20.5	51.8	75.8	89.5	96.0	98.2	
SSMS weighted CUSUM, $\gamma = 0.15$	25.7	46.2	69.2	89.2	97.8	99.0	28.9	58.2	81.2	92.5	98.7	99.9	30.0	69.1	88.7	96.2	99.8	29.6	61.3	83.2	97.0	98.8	99.8	
HAC weighted CUSUM, $\gamma = 0.15$	35.7	62.3	88.9	98.4	99.6	99.8	45.0	75.3	97.0	99.8	99.8	100.0	51.8	93.0	99.0	99.7	100.0	50.0	92.1	96.2	99.8	99.9	100.0	
SSMS Page-CUSUM, $\gamma = 0$	30.9	62.9	86.7	97.1	99.2	99.9	45.2	82.5	97.9	99.8	99.8	100.0	51.8	91.0	99.2	99.9	100.0	50.0	92.1	96.2	99.8	99.9	100.0	
HAC Page-CUSUM, $\gamma = 0$	18.8	42.4	68.9	84.0	93.4	95.6	26.8	59.6	84.7	95.0	97.8	99.2	33.9	72.0	91.7	97.6	99.9	25.5	75.0	92.0	97.8	99.2	99.9	
SSMS Page-CUSUM, $\gamma = 0.15$	30.7	62.5	87.1	97.0	99.5	99.7	43.2	80.7	96.4	99.0	99.8	100.0	46.2	89.5	98.6	99.6	100.0	52.4	90.5	99.0	99.9	100.0	100.0	
HAC Page-CUSUM, $\gamma = 0.15$	18.0	40.0	67.2	82.8	92.8	95.5	24.1	56.9	82.5	94.0	97.4	99.0	30.7	68.2	89.9	97.0	99.0	29.4	32.2	70.2	90.1	96.9	99.8	
SSMS Multiscale MOSUM	25.4	44.4	71.2	93.8	41.6	20.9	24.4	41.0	99.2	100.0	99.9	100.0	65.5	98.4	99.7	100.0	100.0	69.8	97.8	99.9	100.0	100.0		
HAC Multiscale MOSUM	24.3	26.9	32.8	40.8	50.4	61.9	24.3	28.2	28.6	28.5	32.1	21.8	20.9	22.4	23.3	23.5	26.8	15.3	16.8	18.4	16.9	18.4	20.8	27.2

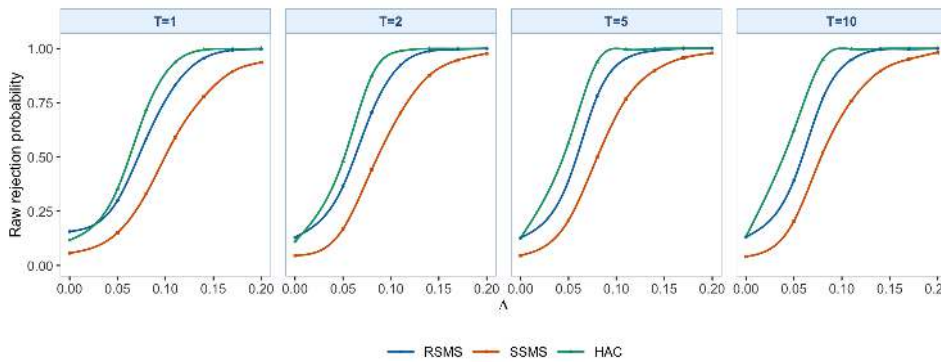
S4. SUPPLEMENTARY MONITORING STATISTICS



(a) BB errors; the four internal columns, from left to right, correspond to  $T = 1, 2, 5, 10$ .

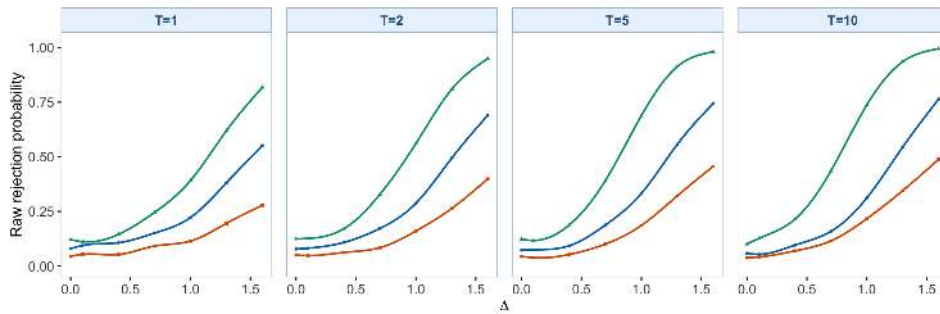


(b) IID errors; the four internal columns, from left to right, correspond to  $T = 1, 2, 5, 10$ .

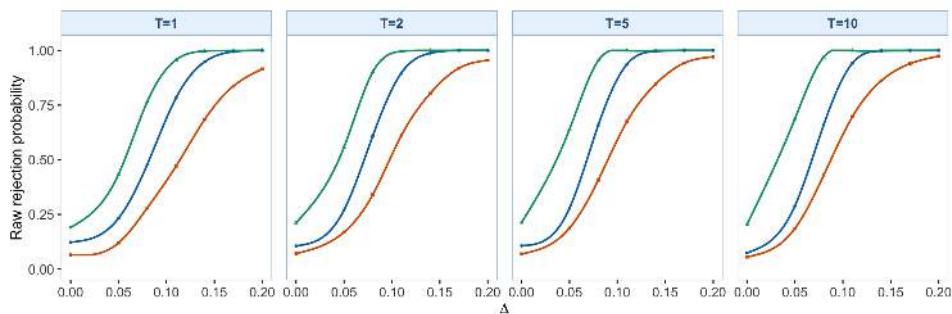


(c) fMA(1) errors; the four internal columns, from left to right, correspond to  $T = 1, 2, 5, 10$ .

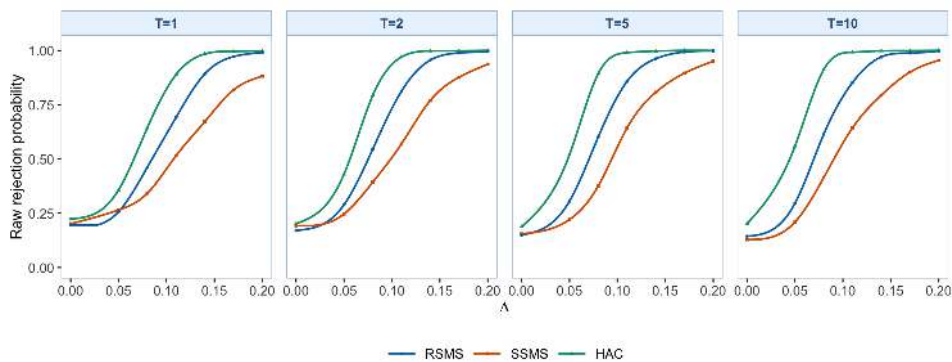
Figure S4.31: Raw rejection curves for weighted CUSUM,  $\gamma = 0$  under the localized-change setting. Each subfigure fixes one DGP, and the four internal columns correspond to  $T = 1, 2, 5, 10$ . The legend below the final subfigure identifies RSMS, SSMS, and HAC.



(a) BB errors; the four internal columns, from left to right, correspond to  $T = 1, 2, 5, 10$ .



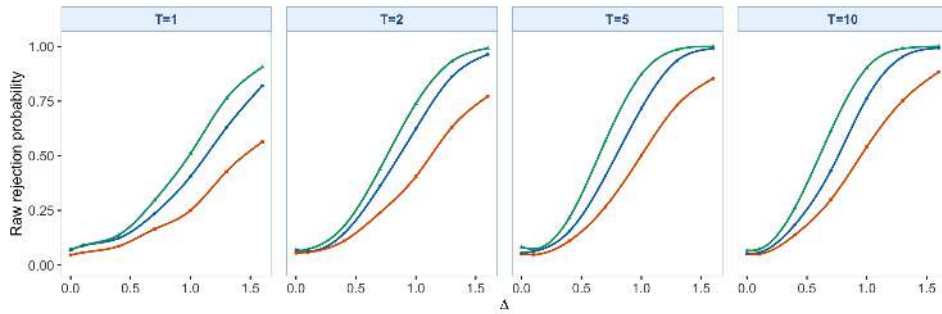
(b) IID errors; the four internal columns, from left to right, correspond to  $T = 1, 2, 5, 10$ .



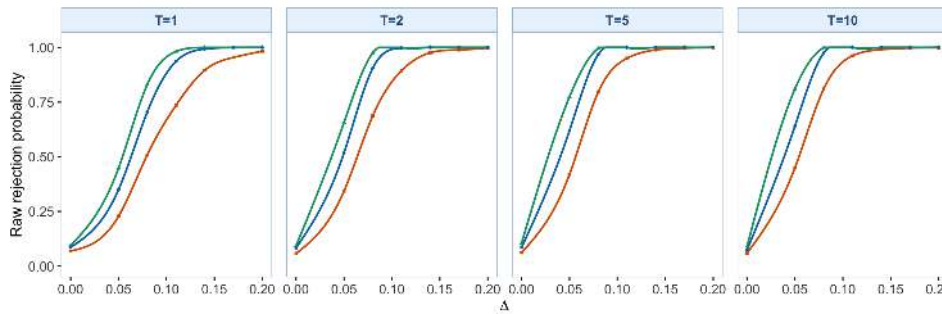
(c) fMA(1) errors; the four internal columns, from left to right, correspond to  $T = 1, 2, 5, 10$ .

Figure S4.32: Raw rejection curves for weighted CUSUM,  $\gamma = 0.15$  under the localized-change setting. Each subfigure fixes one DGP, and the four internal columns correspond to  $T = 1, 2, 5, 10$ . The legend below the final subfigure identifies RSMS, SSMS, and HAC.

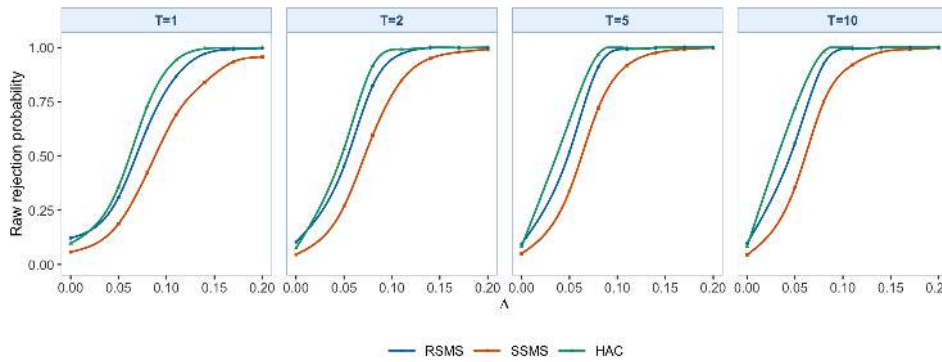
S4. SUPPLEMENTARY MONITORING STATISTICS



(a) BB errors; the four internal columns, from left to right, correspond to  $T = 1, 2, 5, 10$ .

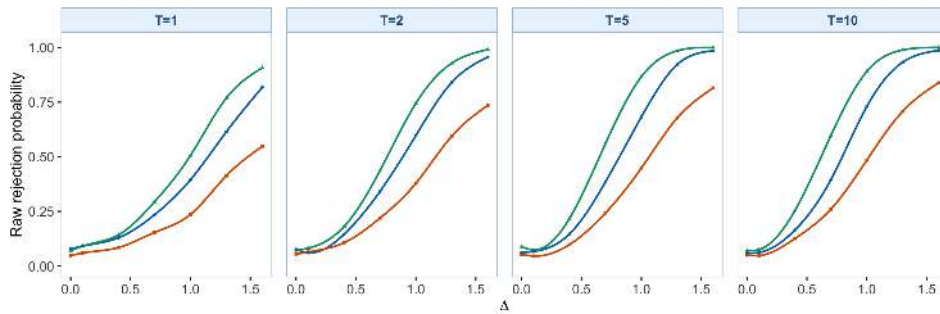


(b) IID errors; the four internal columns, from left to right, correspond to  $T = 1, 2, 5, 10$ .

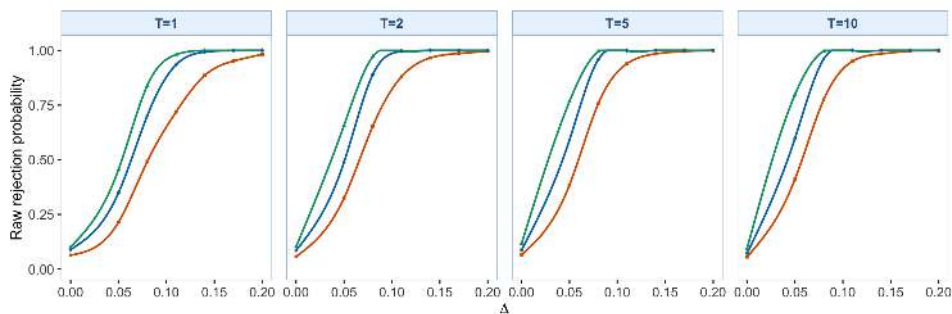


(c) fMA(1) errors; the four internal columns, from left to right, correspond to  $T = 1, 2, 5, 10$ .

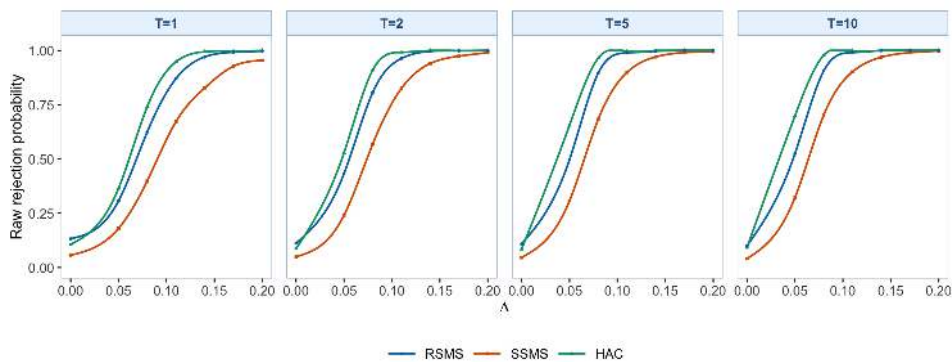
Figure S4.33: Raw rejection curves for Page-CUSUM,  $\gamma = 0$  under the localized-change setting. Each subfigure fixes one DGP, and the four internal columns correspond to  $T = 1, 2, 5, 10$ . The legend below the final subfigure identifies RSMS, SSMS, and HAC.



(a) BB errors; the four internal columns, from left to right, correspond to  $T = 1, 2, 5, 10$ .



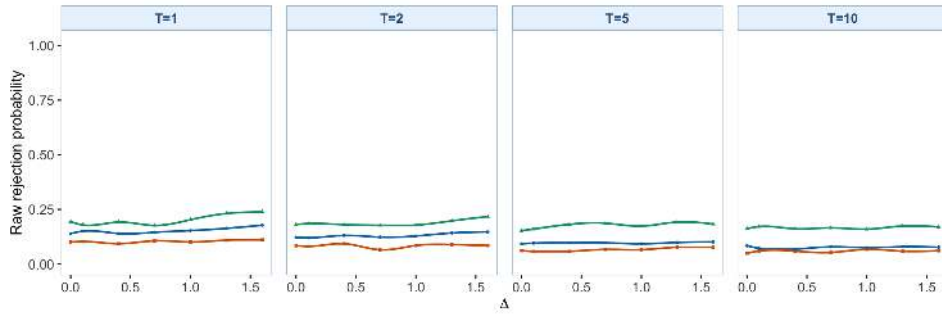
(b) IID errors; the four internal columns, from left to right, correspond to  $T = 1, 2, 5, 10$ .



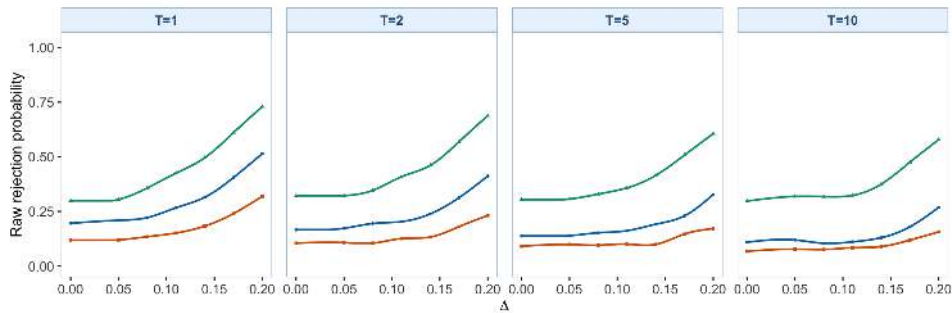
(c) fMA(1) errors; the four internal columns, from left to right, correspond to  $T = 1, 2, 5, 10$ .

Figure S4.34: Raw rejection curves for Page-CUSUM,  $\gamma = 0.15$  under the localized-change setting. Each subfigure fixes one DGP, and the four internal columns correspond to  $T = 1, 2, 5, 10$ . The legend below the final subfigure identifies RSMS, SSMS, and HAC.

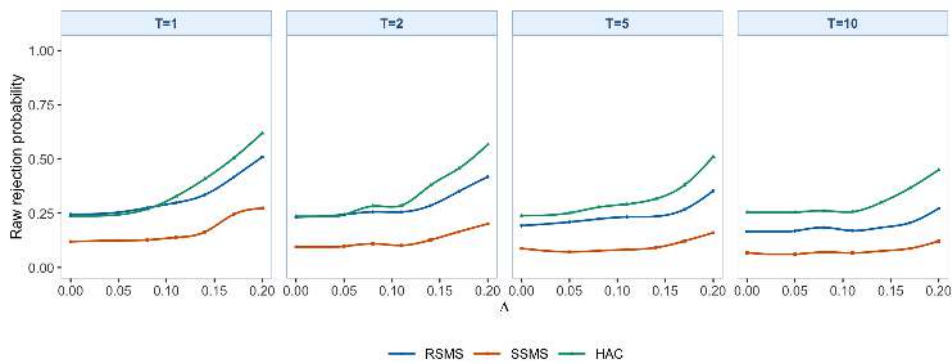
S4. SUPPLEMENTARY MONITORING STATISTICS



(a) BB errors; the four internal columns, from left to right, correspond to  $T = 1, 2, 5, 10$ .



(b) IID errors; the four internal columns, from left to right, correspond to  $T = 1, 2, 5, 10$ .



(c) fMA(1) errors; the four internal columns, from left to right, correspond to  $T = 1, 2, 5, 10$ .

Figure S4.35: Raw rejection curves for Multiscale MOSUM with bandwidth set  $\mathcal{H} = \{0.05, 0.10, 0.20\}$  under the localized-change setting. Each subfigure fixes one DGP, and the four internal columns correspond to  $T = 1, 2, 5, 10$ . The legend below the final subfigure identifies RSMS, SSMS, and HAC.

Table S4.21: SAP (in %) for the FPCA-compressed alternative monitoring statistics under the localized-change setting. Panels separate the three DGPs, columns are grouped by monitoring horizon  $T \in \{1, 2, 5, 10\}$  and then by the positive break sizes  $\Delta$ , and the empirical size adjustment is computed separately for each simulation setting before averaging over  $s^* \in \{50, 200\}$ .

Method	Panel A: BB errors																								
	$T = 1$		$T = 2$		$T = 5$		$T = 10$		$T = 10$																
	0.1	0.4	0.7	1	1.3	1.6	0.1	0.4	0.7	1	1.3														
RSMS weighted CUSUM, $\gamma = 0$	5.5	7.9	15.4	24.3	45.1	67.8	4.3	8.7	19.8	37.2	63.3	81.9	4.8	6.9	20.7	41.2	70.0	85.9	5.9	12.6	25.7	52.8	76.2	91.7	
SSMS weighted CUSUM, $\gamma = 0$	6.0	7.1	12.9	18.4	34.0	45.6	4.9	7.1	12.2	25.6	41.9	56.9	4.1	6.9	16.1	30.6	49.5	64.2	5.7	11.5	19.9	36.9	55.5	70.3	
HAC weighted CUSUM, $\gamma = 0$	5.3	8.7	18.9	37.1	63.8	83.8	4.9	10.9	28.5	57.6	84.5	96.6	4.7	11.6	34.7	68.7	92.9	98.9	5.6	14.3	39.0	74.4	94.8	99.6	
RSMS weighted CUSUM, $\gamma = 0.15$	6.1	7.2	10.5	16.4	30.6	47.1	4.5	5.9	11.5	20.3	38.5	59.5	5.8	4.7	10.1	21.6	43.2	62.5	5.5	9.8	16.4	31.9	55.0	77.0	
SSMS weighted CUSUM, $\gamma = 0.15$	6.3	6.5	10.3	15.1	29.9	47.1	4.3	6.2	9.0	16.9	27.4	40.8	3.8	5.2	10.1	18.4	31.9	45.4	5.8	9.3	14.1	25.9	39.2	53.3	
HAC weighted CUSUM, $\gamma = 0.15$	5.0	7.7	15.7	37.5	61.4	73.9	4.3	11.9	35.2	60.1	97.4	89.8	4.9	18.8	35.4	62.4	93.9	96.0	5.7	11.3	29.2	70.1	88.2	95.9	
RSMS Page-CUSUM, $\gamma = 0$	6.9	9.7	18.5	27.8	46.2	59.9	5.8	10.8	23.7	40.3	62.9	77.0	4.5	10.3	25.8	49.2	72.4	84.8	5.0	13.6	29.6	53.6	74.8	88.1	
SSMS Page-CUSUM, $\gamma = 0$	5.8	9.3	21.9	42.0	69.3	86.5	4.5	13.1	37.0	67.8	91.2	98.6	5.1	15.9	48.9	83.0	97.7	99.8	6.3	23.9	58.9	89.4	99.0	100.0	
HAC Page-CUSUM, $\gamma = 0$	5.2	7.0	16.0	30.0	52.3	73.8	5.8	9.8	27.3	50.9	78.4	92.6	4.5	11.2	32.7	62.5	89.1	97.8	5.5	15.0	37.3	70.8	49.9	71.8	
RSMS Page-CUSUM, $\gamma = 0.15$	6.6	9.0	16.2	24.8	42.2	55.5	5.5	9.3	18.9	35.7	56.6	70.8	4.4	9.3	23.3	43.8	66.9	81.0	5.3	13.2	27.8	49.9	71.8	84.7	
SSMS Page-CUSUM, $\gamma = 0.15$	5.6	8.9	21.3	41.7	68.7	86.8	4.7	14.0	34.9	64.9	89.2	98.4	4.6	13.9	48.2	89.0	97.2	99.8	6.2	22.6	55.2	87.2	98.6	100.0	
HAC Page-CUSUM, $\gamma = 0.15$	5.2	6.9	15.9	31.3	51.7	68.7	4.7	11.0	34.2	64.9	89.2	98.4	4.6	13.9	48.2	89.0	97.2	99.8	6.2	22.6	55.2	87.2	98.6	100.0	
RSMS Multiscale MOSUM	6.2	5.0	6.3	5.8	6.1	6.1	7.1	5.2	6.5	6.2	6.5	6.5	6.5	3.8	4.4	4.1	5.1	5.5	5.1	5.5	5.1	5.0	4.7	6.0	4.8
SSMS Multiscale MOSUM	5.1	5.0	5.5	6.4	7.1	8.5	3.8	4.1	3.6	3.4	5.0	5.9	5.1	5.9	6.3	5.7	7.8	6.7	6.8	6.2	6.2	5.9	5.8	6.4	6.2
HAC Multiscale MOSUM	5.1	5.0	5.5	6.4	7.1	8.5	3.8	4.1	3.6	3.4	5.0	5.9	5.1	5.9	6.3	5.7	7.8	6.7	6.8	6.2	6.2	5.9	5.8	6.4	6.2

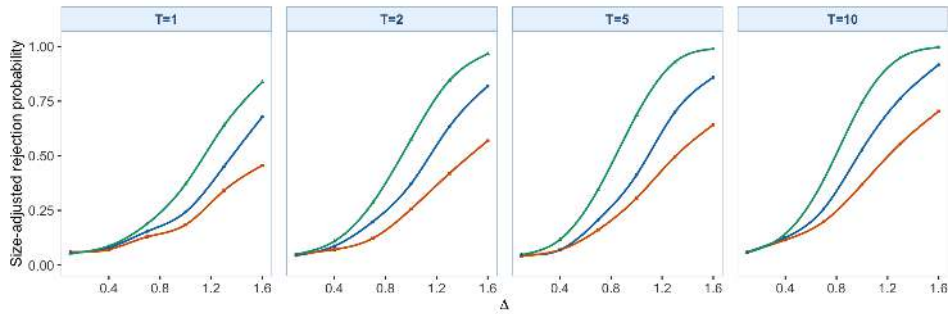
  

Method	Panel B: IID errors																								
	$T = 1$		$T = 2$		$T = 5$		$T = 10$		$T = 10$																
	0.05	0.08	0.11	0.14	0.17	0.2	0.05	0.08	0.11	0.14	0.17	0.2	0.05	0.08	0.11	0.14	0.17	0.2							
RSMS weighted CUSUM, $\gamma = 0$	23.2	54.5	85.2	97.3	99.8	100.0	26.5	68.0	95.0	99.7	100.0	100.0	31.1	76.2	97.8	99.9	100.0	100.0	35.9	78.6	98.0	100.0	100.0	100.0	
SSMS weighted CUSUM, $\gamma = 0$	25.8	37.2	58.7	78.6	90.9	95.3	29.9	43.6	74.4	88.9	96.0	98.0	24.2	48.4	77.8	89.8	96.4	98.4	52.8	55.6	80.8	92.3	97.1	98.6	
HAC weighted CUSUM, $\gamma = 0$	25.2	35.9	67.8	91.0	98.8	100.0	13.4	41.1	78.6	95.8	99.7	100.0	20.2	55.5	87.9	98.7	100.0	23.8	58.3	80.9	92.9	100.0	100.0	100.0	
RSMS weighted CUSUM, $\gamma = 0.15$	11.6	24.6	43.1	64.1	80.9	89.1	12.7	28.0	50.7	74.8	88.9	94.0	14.8	35.4	63.3	80.6	91.4	95.8	16.9	38.1	64.8	82.9	92.1	95.8	
SSMS weighted CUSUM, $\gamma = 0.15$	28.8	54.6	86.5	98.6	99.9	100.0	29.1	68.7	96.7	100.0	100.0	32.0	81.6	99.4	100.0	100.0	96.0	85.7	99.7	100.0	100.0	100.0	100.0	100.0	
HAC weighted CUSUM, $\gamma = 0.15$	20.2	46.8	69.8	87.3	94.7	97.4	30.0	63.9	86.8	96.2	98.7	99.5	35.4	73.1	92.5	98.1	99.6	100.0	41.9	78.1	95.5	98.6	99.7	99.9	
RSMS Page-CUSUM, $\gamma = 0$	28.4	62.0	92.0	98.7	99.9	100.0	38.3	82.8	98.4	100.0	100.0	46.2	90.7	99.7	100.0	100.0	100.0	69.6	99.0	100.0	100.0	100.0	100.0	100.0	
SSMS Page-CUSUM, $\gamma = 0$	28.4	71.1	94.2	99.6	100.0	100.0	48.5	93.3	99.9	100.0	100.0	63.7	98.6	100.0	100.0	100.0	100.0	69.6	99.0	100.0	100.0	100.0	100.0	100.0	
HAC Page-CUSUM, $\gamma = 0$	30.6	72.0	95.0	99.6	100.0	100.0	49.0	93.5	99.5	100.0	100.0	61.1	98.5	100.0	100.0	100.0	100.0	66.9	98.9	100.0	100.0	100.0	100.0	100.0	
RSMS Page-CUSUM, $\gamma = 0.15$	6.8	8.8	11.5	12.2	20.4	31.4	4.9	5.0	6.2	8.2	12.7	20.7	6.0	6.6	7.2	9.2	12.8	20.8	6.2	6.2	6.5	6.2	7.2	10.3	17.8
SSMS Page-CUSUM, $\gamma = 0.15$	5.3	5.9	7.8	8.6	13.9	23.9	4.0	4.6	5.6	8.6	12.6	21.5	35.8	5.2	4.9	4.4	5.0	7.4	5.0	5.0	5.0	5.0	5.0	5.0	5.0
HAC Page-CUSUM, $\gamma = 0.15$	4.9	6.4	9.7	13.8	23.9	40.1	4.6	6.2	8.6	12.6	21.5	35.8	5.2	4.9	4.4	5.0	7.4	11.1	18.8	50.6	4.8	4.8	5.5	8.2	15.9
RSMS Multiscale MOSUM	5.3	6.4	9.7	13.8	23.9	40.1	4.6	6.2	8.6	12.6	21.5	35.8	5.2	4.9	4.4	5.0	7.4	11.1	18.8	50.6	4.8	4.8	5.5	8.2	15.9
SSMS Multiscale MOSUM	5.3	6.4	9.7	13.8	23.9	40.1	4.6	6.2	8.6	12.6	21.5	35.8	5.2	4.9	4.4	5.0	7.4	11.1	18.8	50.6	4.8	4.8	5.5	8.2	15.9
HAC Multiscale MOSUM	5.3	6.4	9.7	13.8	23.9	40.1	4.6	6.2	8.6	12.6	21.5	35.8	5.2	4.9	4.4	5.0	7.4	11.1	18.8	50.6	4.8	4.8	5.5	8.2	15.9

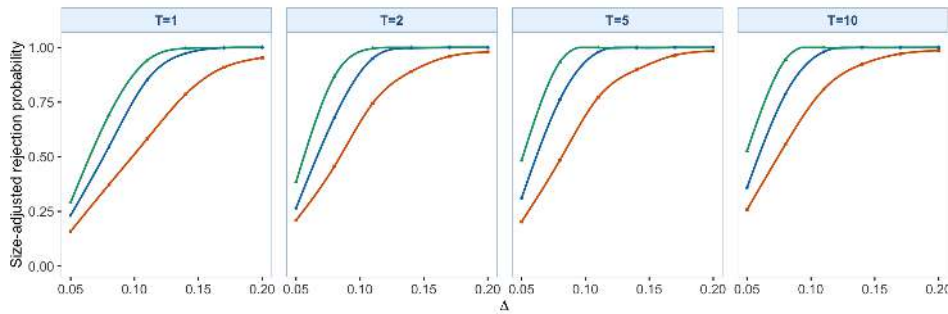
  

Method	Panel C: FMA(1) errors																							
	$T = 1$		$T = 2$		$T = 5$		$T = 10$		$T = 10$															
	0.05	0.08	0.11	0.14	0.17	0.2	0.05	0.08	0.11	0.14	0.17	0.2	0.05	0.08	0.11	0.14	0.17	0.2						
RSMS weighted CUSUM, $\gamma = 0$	11.8	33.0	63.8	88.0	95.9	99.0	22.4	56.7	85.3	96.6	99.2	99.8	24.8	63.5	89.3	97.6	99.6	100.0	26.7	64.3	90.2	98.0	99.2	99.8
SSMS weighted CUSUM, $\gamma = 0$	12.4	33.4	64.2	88.4	96.8	99.9	22.4	57.0	85.3	96.6	99.2	99.8	24.8	63.5	89.3	97.6	99.6	100.0	26.7	64.3	90.2	98.0	99.2	99.8
HAC weighted CUSUM, $\gamma = 0$	22.9	55.8	89.5	98.2	99.5	99.8	31.9	77.0	96.8	99.6	99.8	100.0	39.2	85.9	98.6	99.7	100.0	48.2	89.5	99.2	99.8	99.9	100.0	100.0
RSMS weighted CUSUM, $\gamma = 0.15$	6.0	17.0	41.5	69.7	89.0	96.0	12.4	29.7	62.9	89.6	98.0	98.0	14.6	38.9	67.4	88.9	97.8	99.2	17.2	44.3	72.8	92.1	97.6	99.4
SSMS weighted CUSUM, $\gamma = 0.15$	6.5	9.9	20.0	37.5	55.9	71.5	7.0	15.2	30.2	52.4	68.7	83.4	8.6	18.8	41.7	62.8	78.1	87.9	9.8	24.6	46.6	66.7	80.8	89.9
HAC weighted CUSUM, $\gamma = 0.15$	14.1	38.3	75.0	94.5	98.3	99.3	34.0	70.2	97.3	98.3	99.4	100.0	42.1	88.1	99.0	99.9	100.0	49.9	78.4	98.4	98.4	99.4	99.9	100.0
RSMS Page-CUSUM, $\gamma = 0$	17.6	40.8	67.0	82.2	91.8	95.2	25.7	62.6	82.6	94.0	97.6	98.8	36.9	75.8	91.7	97.6	99.2	99.6	38.1	75.8	92.0	97.7	99.0	99.8
SSMS Page-CUSUM, $\gamma = 0$	29.1	65.9	91.2	98.7	99.6	99.9	47.6	88.5	99.0	100.0	99.8	100.0	58.2	99.6	99.9	100.0	100.0	63.0	96.6	99.8	100.0	100.0	100.0	100.0
HAC Page-CUSUM, $\gamma = 0$	16.2	46.8	73.4	92.4	98.3	99.3	31.1	70.4	93.2	98.8	99.7	100.0	38.8	84.5	97.8	99.5	100.0	41.2	84.0	98.1	99.8	100.0	100.0	100.0
RSMS Page-CUSUM, $\gamma = 0.15$	28.6	62.0	91.7	99.2	99.6	99.9	45.2	86.9	98.4	100.0	99.8	100.0	57.1	94.5	99.6	99.9	100.0	60.7	96.7	98.7	99.8	100.0	100.0	100.0
SSMS Page-CUSUM, $\gamma = 0.15$	5.1	7.1	6.4	10.2	15.2	21.7	5.9	6.4	5.9	8.6	11.9	16.3	3.2	4.8	8.1	8.0	10.1	14.3	5.3	6.2	6.2	6.6	8.2	10.9
HAC Page-CUSUM, $\gamma = 0.15$	5.4	6.7	6.9	7.4	10.5	15.7	5.0	6.4	5.9	8.6	11.9	16.3	3.2	4.8	8.0	8.0	10.6	14.8	5.3	6.2	6.2	6.7	8.0	10.9
RSMS Multiscale MOSUM	5.8	7.3	8.4	16.2	24.3	37.7	4.0	5.5																

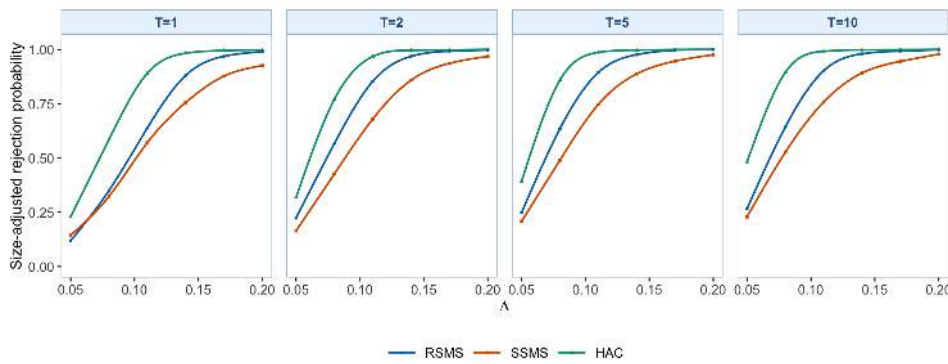
S4. SUPPLEMENTARY MONITORING STATISTICS



(a) BB errors; the four internal columns, from left to right, correspond to  $T = 1, 2, 5, 10$ .

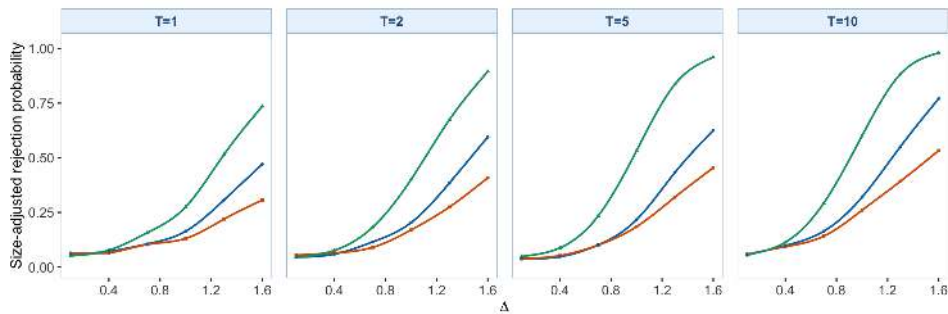


(b) IID errors; the four internal columns, from left to right, correspond to  $T = 1, 2, 5, 10$ .

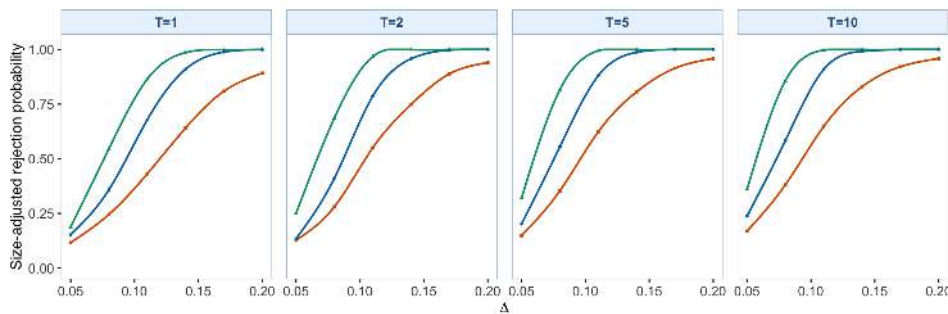


(c) fMA(1) errors; the four internal columns, from left to right, correspond to  $T = 1, 2, 5, 10$ .

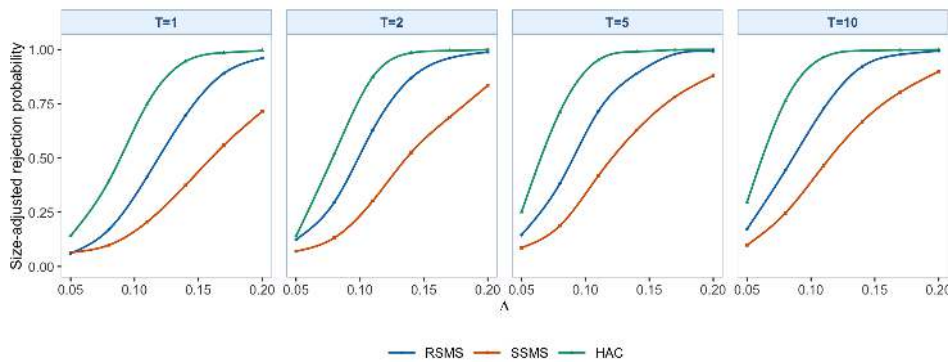
Figure S4.36: SAP curves for weighted CUSUM,  $\gamma = 0$  under the localized-change setting. Each subfigure fixes one DGP, and the four internal columns correspond to  $T = 1, 2, 5, 10$ . The legend below the final subfigure identifies RSMS, SSMS, and HAC.



(a) BB errors; the four internal columns, from left to right, correspond to  $T = 1, 2, 5, 10$ .



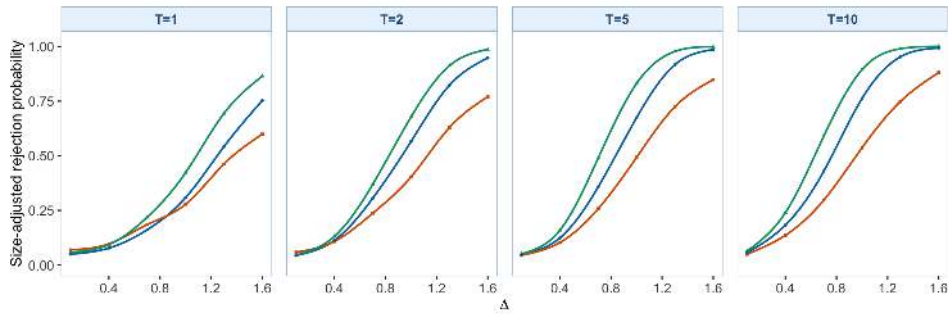
(b) IID errors; the four internal columns, from left to right, correspond to  $T = 1, 2, 5, 10$ .



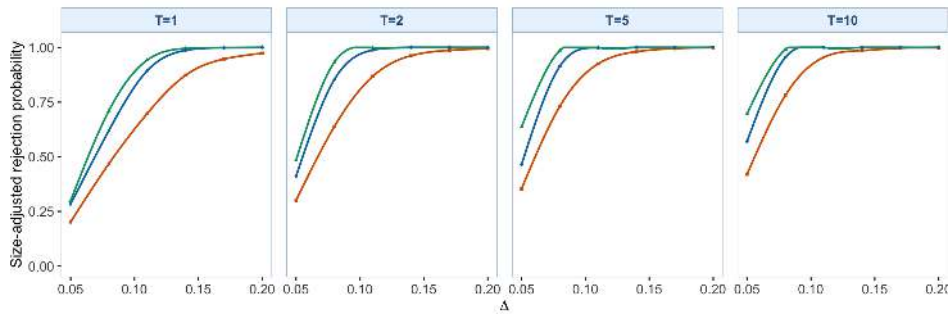
(c) fMA(1) errors; the four internal columns, from left to right, correspond to  $T = 1, 2, 5, 10$ .

Figure S4.37: SAP curves for weighted CUSUM,  $\gamma = 0.15$  under the localized-change setting. Each subfigure fixes one DGP, and the four internal columns correspond to  $T = 1, 2, 5, 10$ . The legend below the final subfigure identifies RSMS, SSMS, and HAC.

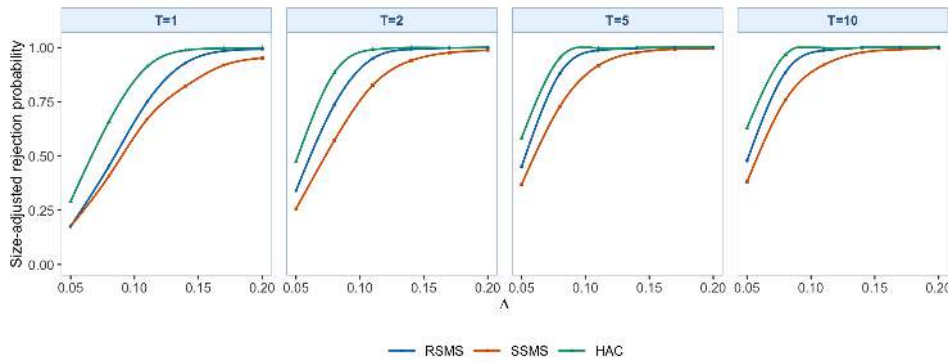
S4. SUPPLEMENTARY MONITORING STATISTICS



(a) BB errors; the four internal columns, from left to right, correspond to  $T = 1, 2, 5, 10$ .

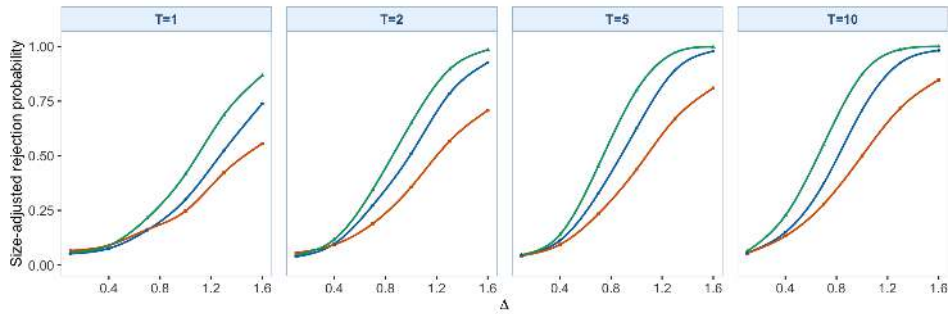


(b) IID errors; the four internal columns, from left to right, correspond to  $T = 1, 2, 5, 10$ .

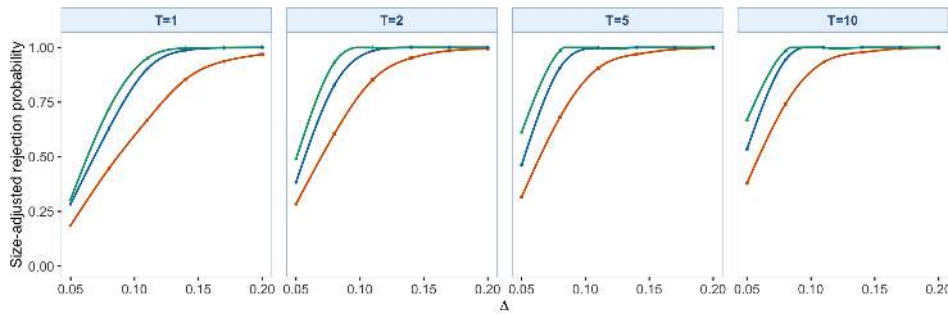


(c) fMA(1) errors; the four internal columns, from left to right, correspond to  $T = 1, 2, 5, 10$ .

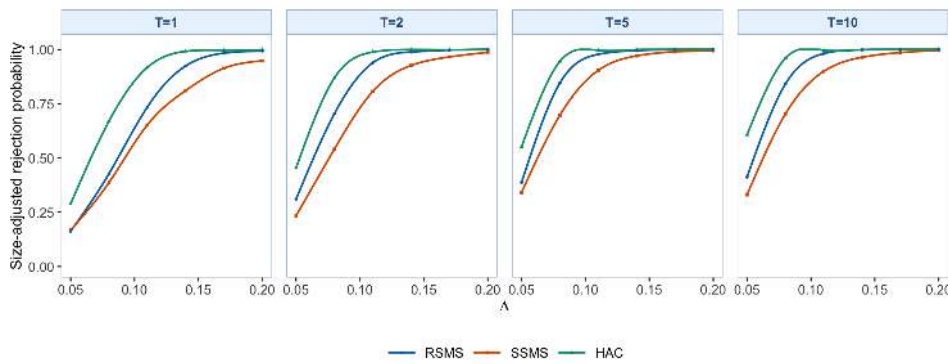
Figure S4.38: SAP curves for Page-CUSUM,  $\gamma = 0$  under the localized-change setting. Each subfigure fixes one DGP, and the four internal columns correspond to  $T = 1, 2, 5, 10$ . The legend below the final subfigure identifies RSMS, SSMS, and HAC.



(a) BB errors; the four internal columns, from left to right, correspond to  $T = 1, 2, 5, 10$ .



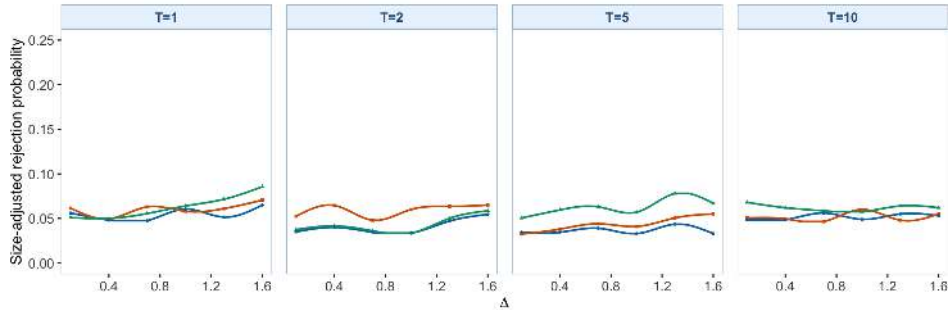
(b) IID errors; the four internal columns, from left to right, correspond to  $T = 1, 2, 5, 10$ .



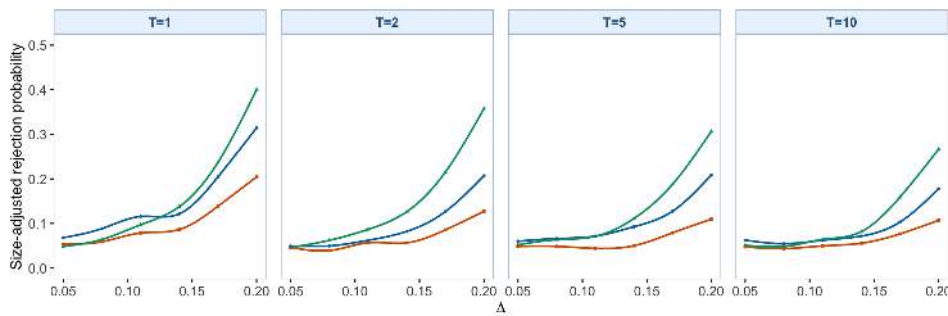
(c) fMA(1) errors; the four internal columns, from left to right, correspond to  $T = 1, 2, 5, 10$ .

Figure S4.39: SAP curves for Page-CUSUM,  $\gamma = 0.15$  under the localized-change setting. Each subfigure fixes one DGP, and the four internal columns correspond to  $T = 1, 2, 5, 10$ . The legend below the final subfigure identifies RSMS, SSMS, and HAC.

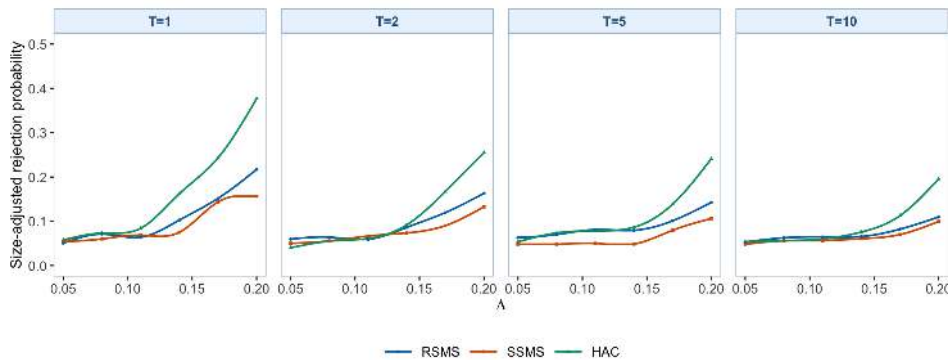
S4. SUPPLEMENTARY MONITORING STATISTICS



(a) BB errors; the four internal columns, from left to right, correspond to  $T = 1, 2, 5, 10$ .



(b) fIID errors; the four internal columns, from left to right, correspond to  $T = 1, 2, 5, 10$ .



(c) fMA(1) errors; the four internal columns, from left to right, correspond to  $T = 1, 2, 5, 10$ .

Figure S4.40: SAP curves for Multiscale MOSUM with bandwidth set  $\mathcal{H} = \{0.05, 0.10, 0.20\}$  under the localized-change setting. Each subfigure fixes one DGP, and the four internal columns correspond to  $T = 1, 2, 5, 10$ . The legend below the final subfigure identifies RSMS, SSMS, and HAC. To keep the three DGP panels visually distinguishable, the BB subfigure uses a 0–0.25 vertical range, while the fIID and fMA(1) subfigures use 0–0.50.

statistic by SAP. Multiscale MOSUM is more local and has lower SAP in these reported simulation settings. The SSMS rows remain more conservative than the corresponding RSMS rows.

**ADD.**

The ADD tables and subfigures for the localized-change setting report shorter delays for several RSMS rows. Weighted CUSUM has lower ADD on most horizons, specifically  $T \in \{2, 5\}$ . Its mean ADD increases from 156.6 at  $T = 1$  to 1006.5 at  $T = 10$  because stopping times are recorded on a longer scale as the monitoring horizon lengthens. Multiscale MOSUM has the largest average ADD among the supplementary statistics. The SSMS rows remain conservative relative to the corresponding RSMS rows.

S4. SUPPLEMENTARY MONITORING STATISTICS

Table S4.22: ADD for the FPCA-compressed alternative monitoring statistics under the localized-change setting. Panels separate the three DGPs, columns are grouped by monitoring horizon  $T \in \{1, 2, 5, 10\}$  and then by the positive break sizes  $\Delta$ , entries are detection delays in monitoring observations, not percentages, and smaller entries indicate faster post-break detection after averaging over  $s^* \in \{50, 200\}$ .

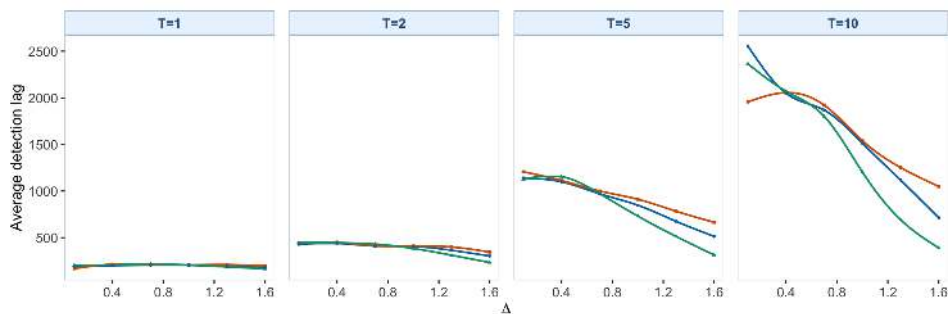
Method		Panel A: BB errors																	
		T = 1		T = 5		T = 10		T = 10		T = 10									
		0.1	0.4	0.7	1	1.3	1.6	0.1	0.4	0.7	1	1.3	1.6	0.1	0.4	0.7	1	1.3	1.6
RMS weighted CUSUM, $\gamma = 0$		189.1	200.8	205.6	207.4	191.3	180.5	438.9	438.5	410.5	405.9	364.4	302.7	1140.9	1008.9	970.7	817.9	674.9	513.3
RMS weighted CUSUM, $\gamma = 0.15$		204.2	213.8	209.8	206.8	197.1	183.5	443.4	448.9	411.6	401.2	389.6	345.3	1206.5	1122.6	1070.2	911.4	783.4	614.3
HAC weighted CUSUM, $\gamma = 0$		174.8	191.2	196.0	192.2	186.8	189.0	398.3	383.8	406.9	377.7	408.3	358.6	1240.7	1063.5	973.9	827.4	708.8	513.0
HAC weighted CUSUM, $\gamma = 0.15$		179.1	194.0	195.0	191.5	178.3	159.4	422.9	407.4	414.2	375.0	329.2	250.1	1241.6	1106.3	992.1	811.5	568.9	367.6
RMS Page-CUSUM, $\gamma = 0$		217.9	246.0	251.1	244.2	235.0	236.7	522.2	533.8	528.1	477.1	462.8	403.3	1381.0	1267.6	1149.9	1005.8	846.4	723.7
RMS Page-CUSUM, $\gamma = 0.15$		255.9	260.2	260.0	244.9	224.6	197.5	565.0	556.3	533.2	468.9	388.0	306.3	1332.3	1343.2	1149.4	855.4	578.6	404.0
HAC Page-CUSUM, $\gamma = 0$		206.8	226.4	236.9	230.2	224.7	215.8	492.9	496.3	505.0	452.5	442.0	384.6	1350.8	1246.4	1214.4	961.4	781.7	532.6
HAC Page-CUSUM, $\gamma = 0.15$		232.3	241.1	243.9	228.6	209.5	181.8	511.3	512.1	492.3	438.5	351.5	297.6	1273.8	1259.4	1041.4	781.7	532.6	358.8
RMS Multiscale MOSUM		176.2	181.7	165.8	178.8	160.4	162.2	414.9	398.3	401.4	379.0	383.2	368.7	1064.9	1063.6	1104.9	1177.0	941.6	1009.2
HAC Multiscale MOSUM		186.7	185.5	173.6	178.8	163.5	147.9	415.6	426.1	434.3	407.9	382.0	379.5	1163.4	1170.2	1184.3	1170.8	1018.7	992.3

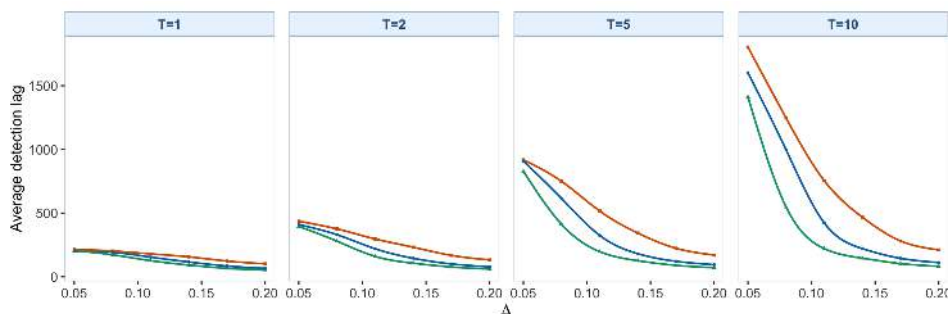
Method		Panel B: fIID errors																	
		T = 1		T = 5		T = 10		T = 10		T = 10									
		0.1	0.4	0.7	1	1.3	1.6	0.1	0.4	0.7	1	1.3	1.6	0.1	0.4	0.7	1	1.3	1.6
RMS weighted CUSUM, $\gamma = 0$		201.2	192.8	154.3	116.4	84.3	66.2	409.6	330.3	219.9	145.1	100.7	78.1	908.5	615.0	325.0	181.0	121.5	94.9
RMS weighted CUSUM, $\gamma = 0.15$		214.5	202.4	179.8	156.3	123.6	102.2	435.9	375.8	296.9	231.9	167.6	132.6	981.1	745.6	510.1	343.0	233.7	170.4
HAC weighted CUSUM, $\gamma = 0$		183.6	177.0	159.4	124.1	86.8	64.2	381.8	346.2	257.0	164.5	103.7	73.8	919.6	735.6	433.0	223.5	126.2	50.1
HAC weighted CUSUM, $\gamma = 0.15$		187.8	190.3	178.9	158.3	129.6	109.1	428.1	377.8	316.5	260.2	188.0	143.2	922.7	827.7	593.4	411.7	288.0	199.9
RMS Page-CUSUM, $\gamma = 0$		246.4	224.7	185.1	138.1	115.9	97.1	511.4	498.0	375.9	198.2	151.4	128.7	1036.8	667.3	383.0	256.0	191.8	157.2
RMS Page-CUSUM, $\gamma = 0.15$		245.5	230.0	207.4	181.5	148.4	128.3	512.6	449.3	343.8	276.6	209.0	174.9	1102.5	846.3	564.4	393.1	281.3	237.1
HAC Page-CUSUM, $\gamma = 0$		230.8	211.2	169.8	132.1	100.3	81.9	473.5	372.3	249.3	172.1	123.7	100.0	980.5	626.7	341.7	218.7	158.4	127.3
HAC Page-CUSUM, $\gamma = 0.15$		234.2	218.7	196.5	170.1	136.2	115.8	487.2	420.7	322.3	254.3	186.3	159.9	1030.9	799.9	536.0	361.2	258.4	197.4
RMS Multiscale MOSUM		173.5	170.9	147.9	136.9	119.0	112.3	380.2	402.1	375.0	315.9	261.2	202.9	1044.1	1022.7	948.2	798.9	510.6	420.4
HAC Multiscale MOSUM		177.2	166.0	147.7	125.0	101.3	84.2	401.9	367.6	329.7	278.5	213.7	148.4	1069.5	1035.8	931.8	720.9	541.4	424.6

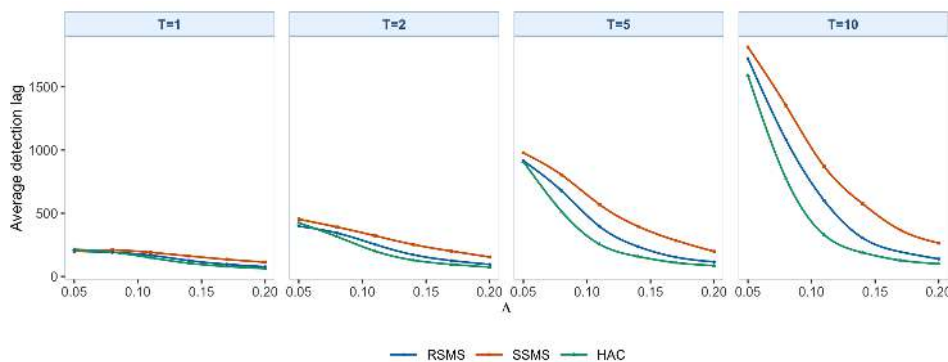
Method		Panel C: fMA(1) errors																	
		T = 1		T = 5		T = 10		T = 10		T = 10									
		0.1	0.4	0.7	1	1.3	1.6	0.1	0.4	0.7	1	1.3	1.6	0.1	0.4	0.7	1	1.3	1.6
RMS weighted CUSUM, $\gamma = 0$		200.1	190.3	167.1	125.6	96.0	76.2	397.2	343.6	252.9	171.3	125.0	94.9	914.8	678.1	395.0	236.7	151.9	114.9
RMS weighted CUSUM, $\gamma = 0.15$		199.3	208.7	190.0	161.7	134.4	112.8	452.3	390.6	321.5	252.2	200.0	158.7	978.0	805.7	568.2	396.4	284.1	197.1
HAC weighted CUSUM, $\gamma = 0$		175.8	176.8	163.3	132.3	100.7	75.6	366.0	343.6	277.6	194.1	137.0	94.6	921.7	759.7	484.2	295.1	169.6	119.2
HAC weighted CUSUM, $\gamma = 0.15$		156.6	169.2	172.7	159.0	134.8	111.4	371.6	373.2	314.2	271.4	216.8	162.4	876.1	836.2	665.9	483.7	340.8	240.3
RMS Page-CUSUM, $\gamma = 0$		241.9	228.0	197.7	159.7	127.7	106.4	507.2	433.3	305.6	222.7	175.5	140.6	1072.8	722.8	450.4	302.7	221.2	179.2
RMS Page-CUSUM, $\gamma = 0.15$		245.2	241.8	216.4	187.0	158.7	136.5	528.0	463.2	378.4	294.5	237.6	189.5	1189.5	885.1	625.2	441.5	333.2	239.8
HAC Page-CUSUM, $\gamma = 0$		226.9	212.4	184.0	143.8	111.9	91.5	469.1	394.7	279.4	197.4	151.0	118.5	1010.5	670.4	409.0	264.0	187.0	137.3
HAC Page-CUSUM, $\gamma = 0.15$		232.3	227.4	205.1	175.4	146.8	124.3	495.2	439.5	355.2	273.0	217.0	171.9	1085.3	847.0	597.5	417.3	304.8	224.6
RMS Multiscale MOSUM		163.0	160.7	158.6	128.2	114.2	98.7	391.3	360.1	328.2	288.3	246.1	211.6	1024.8	982.3	941.6	831.4	702.8	610.2
HAC Multiscale MOSUM		174.1	172.0	152.7	127.3	112.5	86.9	408.4	377.0	338.8	288.9	240.1	178.2	1122.4	1174.6	979.7	898.6	738.9	573.6



(a) BB errors; the four internal columns, from left to right, correspond to  $T = 1, 2, 5, 10$ .



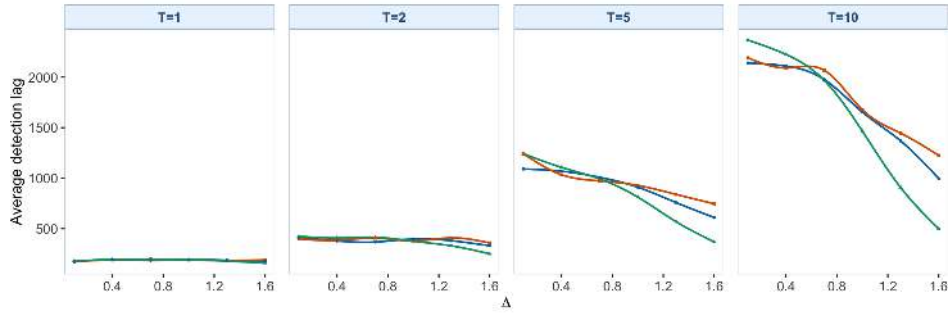
(b) IID errors; the four internal columns, from left to right, correspond to  $T = 1, 2, 5, 10$ .



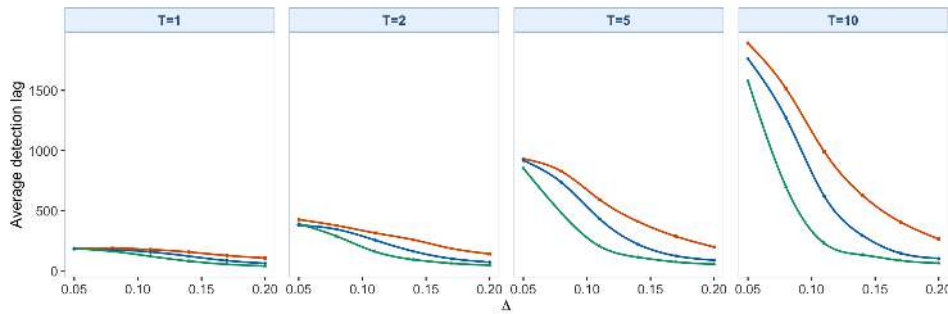
(c) fMA(1) errors; the four internal columns, from left to right, correspond to  $T = 1, 2, 5, 10$ .

Figure S4.41: ADD curves for weighted CUSUM,  $\gamma = 0$  under the localized-change setting. Each subfigure fixes one DGP, and the four internal columns correspond to  $T = 1, 2, 5, 10$ . The legend below the final subfigure identifies RSMS, SSMS, and HAC.

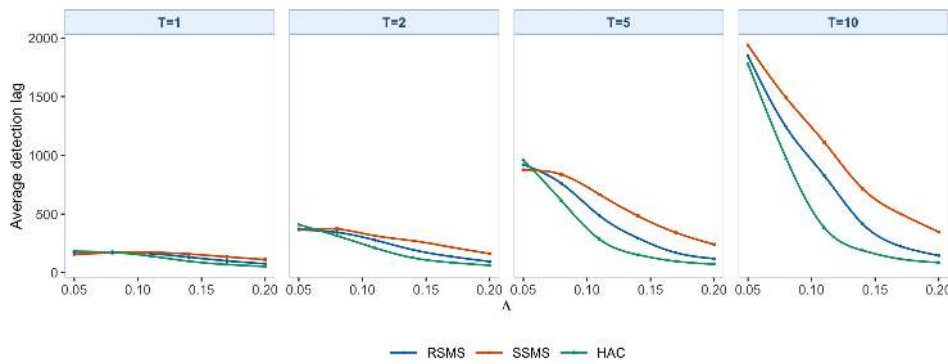
S4. SUPPLEMENTARY MONITORING STATISTICS



(a) BB errors; the four internal columns, from left to right, correspond to  $T = 1, 2, 5, 10$ .

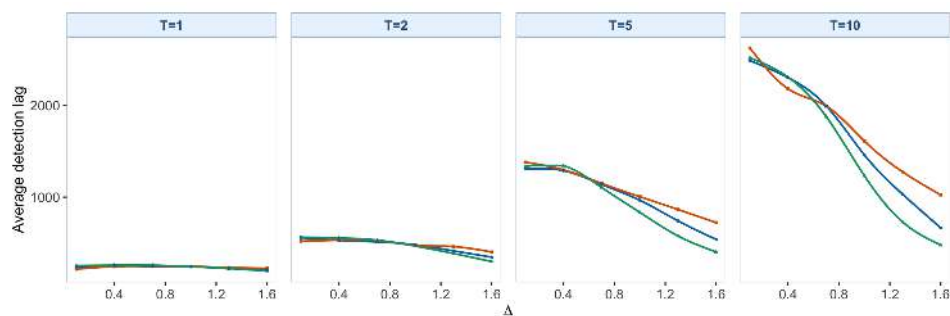


(b) IID errors; the four internal columns, from left to right, correspond to  $T = 1, 2, 5, 10$ .

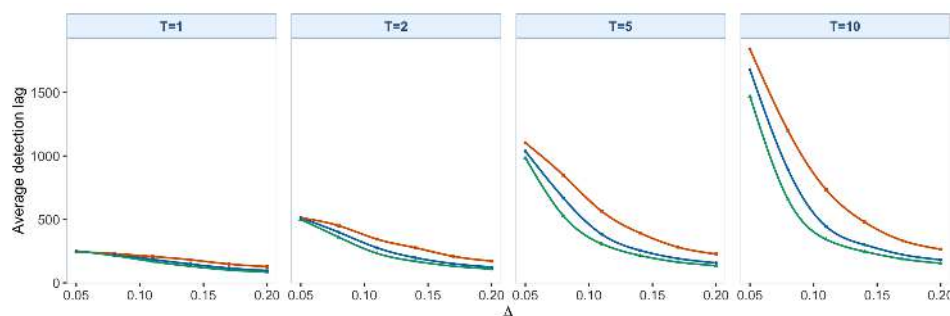


(c) fMA(1) errors; the four internal columns, from left to right, correspond to  $T = 1, 2, 5, 10$ .

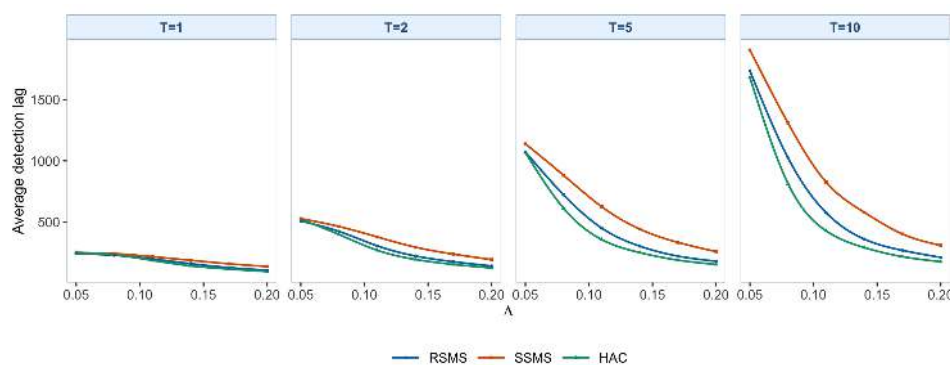
Figure S4.42: ADD curves for weighted CUSUM,  $\gamma = 0.15$  under the localized-change setting. Each subfigure fixes one DGP, and the four internal columns correspond to  $T = 1, 2, 5, 10$ . The legend below the final subfigure identifies RSMS, SSMS, and HAC.



(a) BB errors; the four internal columns, from left to right, correspond to  $T = 1, 2, 5, 10$ .



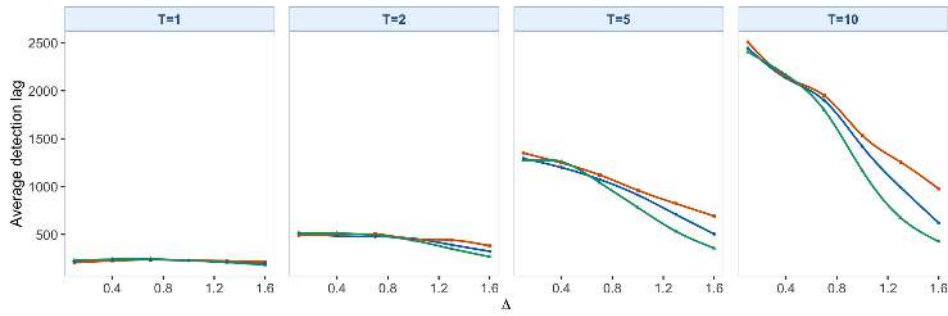
(b) IID errors; the four internal columns, from left to right, correspond to  $T = 1, 2, 5, 10$ .



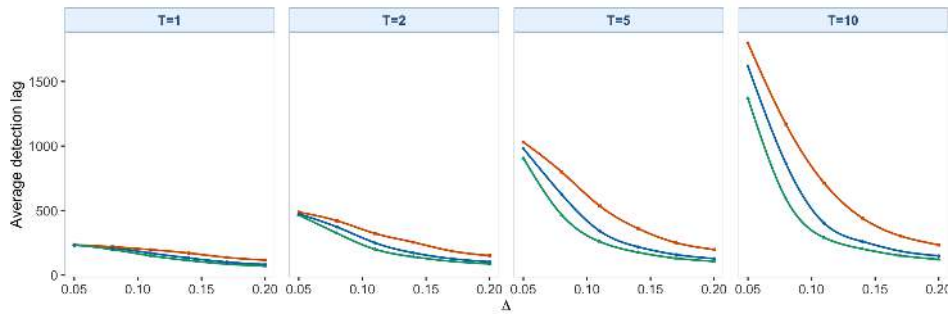
(c) fMA(1) errors; the four internal columns, from left to right, correspond to  $T = 1, 2, 5, 10$ .

Figure S4.43: ADD curves for Page-CUSUM,  $\gamma = 0$  under the localized-change setting. Each subfigure fixes one DGP, and the four internal columns correspond to  $T = 1, 2, 5, 10$ . The legend below the final subfigure identifies RSMS, SSMS, and HAC.

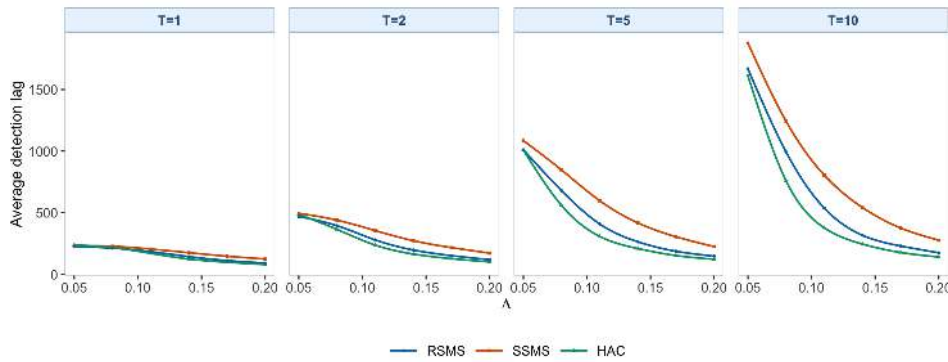
S4. SUPPLEMENTARY MONITORING STATISTICS



(a) BB errors; the four internal columns, from left to right, correspond to  $T = 1, 2, 5, 10$ .



(b) IID errors; the four internal columns, from left to right, correspond to  $T = 1, 2, 5, 10$ .



(c) fMA(1) errors; the four internal columns, from left to right, correspond to  $T = 1, 2, 5, 10$ .

Figure S4.44: ADD curves for Page-CUSUM,  $\gamma = 0.15$  under the localized-change setting. Each subfigure fixes one DGP, and the four internal columns correspond to  $T = 1, 2, 5, 10$ . The legend below the final subfigure identifies RSMS, SSMS, and HAC.

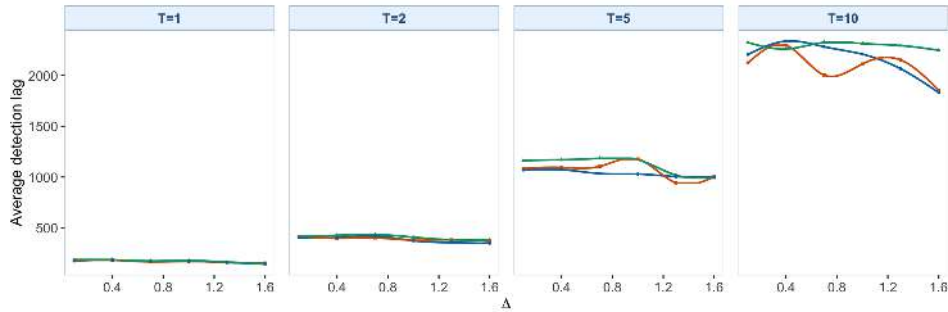
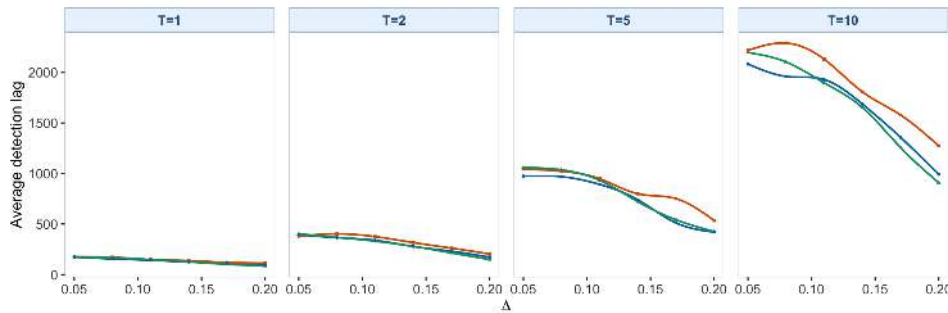
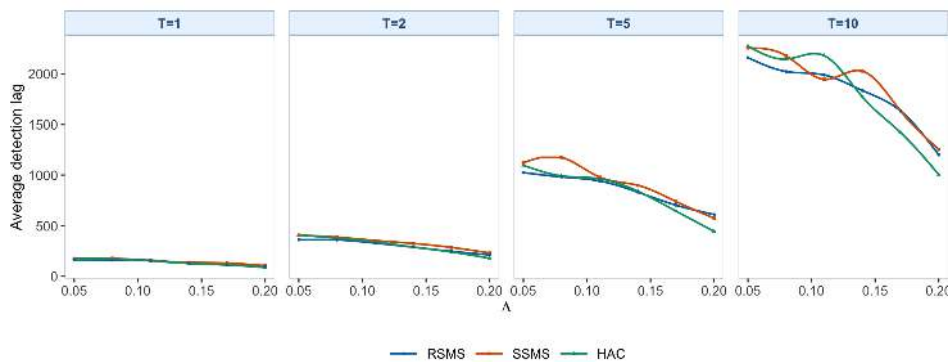
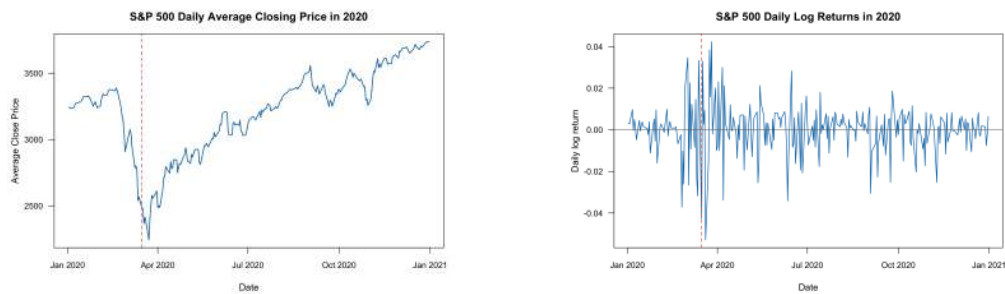
(a) BB errors; the four internal columns, from left to right, correspond to  $T = 1, 2, 5, 10$ .(b) IID errors; the four internal columns, from left to right, correspond to  $T = 1, 2, 5, 10$ .(c) fMA(1) errors; the four internal columns, from left to right, correspond to  $T = 1, 2, 5, 10$ .

Figure S4.45: ADD curves for Multiscale MOSUM with bandwidth set  $\mathcal{H} = \{0.05, 0.10, 0.20\}$  under the localized-change setting. Each subfigure fixes one DGP, and the four internal columns correspond to  $T = 1, 2, 5, 10$ . The legend below the final subfigure identifies RSMS, SSMS, and HAC.

## S5 Extended Empirical Analysis

### S5.1 Market background, intraday-curve regimes, and weighted-CvM results

This subsection collects material summarized in the main paper: the 2020 market background, the intraday return-curve regimes, the empirical weighted-CvM monitoring results, and the raw-magnitude diagnostics for the main KS decision windows.



(a) Daily average S&P 500 closing level in 2020. The dashed vertical line marks March 16, 2020.

(b) Daily log returns of the S&P 500 in 2020. The dashed vertical line marks March 16, 2020.

Figure S5.1: S&P 500 index level and return summaries in 2020.

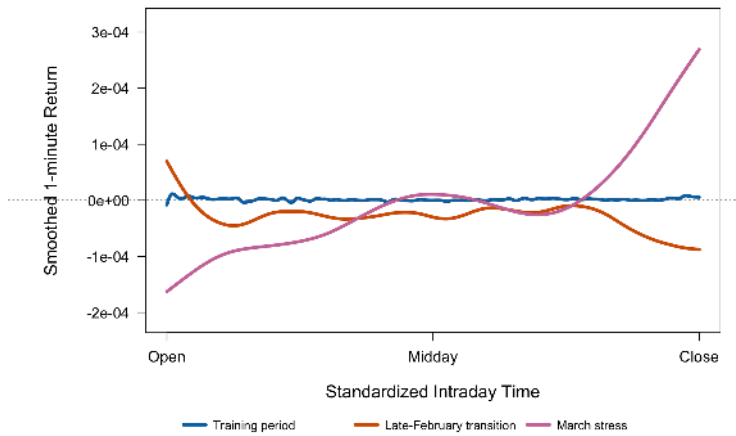


Figure S5.2: Average intraday return curves across three market states (training sample, late-February transition, March stress window). Each line is the mean smoothed 1-minute return profile evaluated on a common grid; the training-sample curve is nearly flat, whereas the transition and stress curves display pronounced opening and late-day shape changes and a more uneven middle segment.

S5. EXTENDED EMPIRICAL ANALYSIS

Table S5.1: Empirical weighted-CvM monitoring results for the S&P 500 intraday return curves.

Weight	Standardizer	Stat./CV	Reject?	First signal
<b>Panel A: <math>T = 1</math></b>				
Uniform	RSMS	0.93	No	No signal
Uniform	SSMS	0.03	No	No signal
Uniform	HAC	0.29	No	No signal
Early	RSMS	0.66	No	No signal
Early	SSMS	0.03	No	No signal
Early	HAC	0.22	No	No signal
Mid	RSMS	0.80	No	No signal
Mid	SSMS	0.03	No	No signal
Mid	HAC	0.23	No	No signal
Late	RSMS	1.05	Yes	Mar. 13, 2020
Late	SSMS	0.03	No	No signal
Late	HAC	0.33	No	No signal
<b>Panel B: <math>T = 2</math></b>				
Uniform	RSMS	2.10	Yes	Apr. 7, 2020
Uniform	SSMS	0.08	No	No signal
Uniform	HAC	0.73	No	No signal
Early	RSMS	1.71	Yes	Apr. 1, 2020
Early	SSMS	0.06	No	No signal
Early	HAC	0.61	No	No signal
Mid	RSMS	2.16	Yes	Apr. 1, 2020
Mid	SSMS	0.08	No	No signal
Mid	HAC	0.76	No	No signal
Late	RSMS	2.29	Yes	Apr. 13, 2020
Late	SSMS	0.08	No	No signal
Late	HAC	0.80	No	No signal
<b>Panel C: <math>T = 5</math></b>				
Uniform	RSMS	1.12	Yes	Oct. 14, 2020
Uniform	SSMS	0.05	No	No signal
Uniform	HAC	0.40	No	No signal
Early	RSMS	1.46	Yes	June 1, 2020
Early	SSMS	0.06	No	No signal
Early	HAC	0.51	No	No signal
Mid	RSMS	1.24	Yes	Aug. 10, 2020
Mid	SSMS	0.05	No	No signal
Mid	HAC	0.43	No	No signal
Late	RSMS	0.86	No	No signal
Late	SSMS	0.04	No	No signal
Late	HAC	0.32	No	No signal

Note: The four weight families are the finite-horizon Uniform, Early, Mid, and Late weights used in the simulation section. Stat./CV is the statistic divided by the matching 5% critical value.

Table S5.2: Raw intraday magnitude diagnostics for the main KS decision windows.

Window	Trading days	Avg. daily realized variation			
		Avg. $ r $ (basis points)	(RV) ( $\times 10^{-4}$ )	Rel. $ r $	Rel. RV
Training sample	50	1.13	0.12	1.0 $\times$	1.0 $\times$
Early 2020 pre-alarm period	38	1.91	0.36	1.7 $\times$	3.0 $\times$
RSMS( $T = 2$ ) to HAC( $T = 2$ )	25	12.11	11.47	10.7 $\times$	94.6 $\times$
RSMS( $T = 5$ ) to HAC( $T = 5$ )	15	13.15	13.32	11.6 $\times$	109.8 $\times$

Note: Computed from the raw 1-minute S&P 500 series. Average absolute returns are in basis points; daily realized variation is the within-day sum of squared 1-minute log returns scaled by  $10^{-4}$  (not annualized). Relative multiples use the unrounded values. The four windows are 2019-10-21 to 2019-12-31, 2020-01-02 to 2020-02-26, 2020-02-27 to 2020-04-01, and 2020-03-13 to 2020-04-02.

The empirical checks in this section use the same training sample, monitoring sample, retained score dimension, and smoothing choices as the paper’s empirical application. Only the monitoring statistic changes. The tables below report Page-CUSUM, weighted CUSUM, and multiscale MO-SUM signal dates as supplementary sensitivity checks for users who put more weight on earlier warning. The main paper complements these signal dates with raw intraday magnitude diagnostics over the decision windows left by the KS alarms.

The empirical application uses licensed 1-minute S&P 500 price data from TickData. The replication repository documents the required input fields and the processing scripts, but the raw TickData file is not redistributed because of licensing restrictions. In the empirical scripts, the intraday close price is used to form adjacent within-day log returns within each trading day. The first missing return created by within-day differencing is dropped, and the remaining timestamps define the intraday profiles used in the application. The training sample is October 21, 2019–December 31, 2019, followed by the 2020 monitoring sample. Each daily return profile is smoothed with cubic B-splines, evaluated on a 301-point grid, and projected onto the training-sample FPCA eigenfunctions.

## **S5.2 A 3D view of intraday return-curve movement before the alarm dates**

Figure S5.3 plots the smoothed intraday return surface from January 2 to April 2, 2020, and marks selected alarm dates from the main and supplementary monitoring statistics. The figure shows visible movement in the return surface before the later HAC alarm. By late January and especially late February, the opening and intraday return profiles have begun to move away from the late-2019 training sample, before the March 16 market-stress reference date. This visual check helps interpret why the supplementary statistics can signal earlier than HAC in the empirical application.

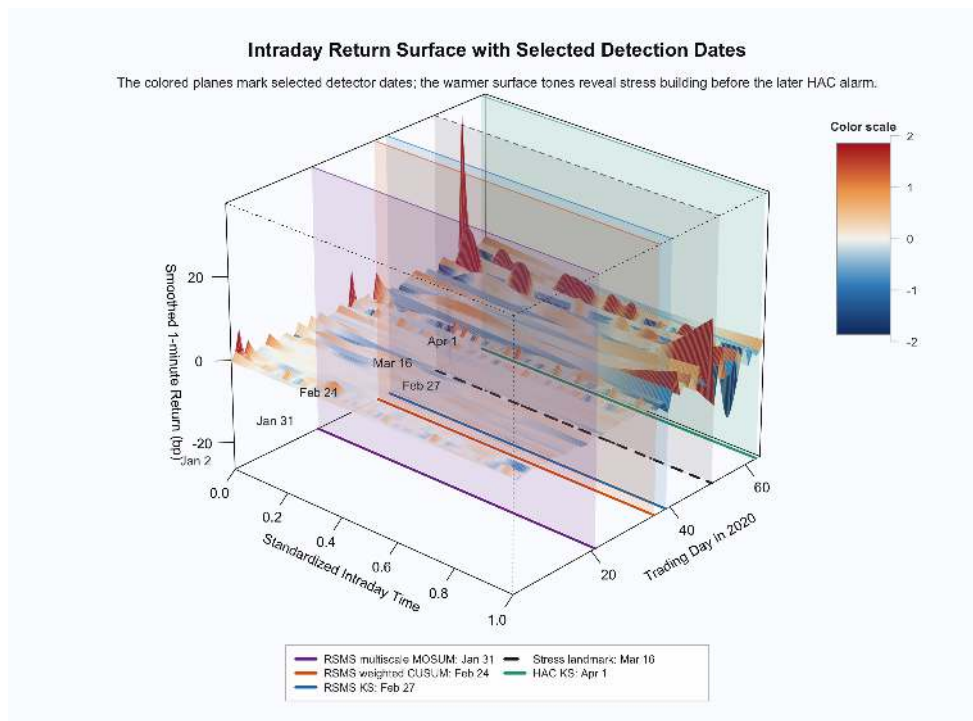


Figure S5.3: 3D view of the evolving intraday return surface in early 2020. The surface is built from daily smoothed 1-minute return curves. The purple, orange, blue, dashed charcoal, and green semi-transparent planes correspond to RSMS multiscale MOSUM (January 31), RSMS weighted CUSUM (February 24), RSMS KS (February 27), the March 16 market-stress reference date, and HAC KS (April 1), respectively. The figure is descriptive and complements the signal-date tables by showing that the intraday return surface is already moving away from the late-2019 training sample before the later HAC KS alarm.

### S5.3 Robustness of the main KS alarms to the choice of score dimension

Table S5.3 checks whether the main empirical KS ranking is sensitive to nearby choices of score dimension. The paper’s main choice remains  $K = 4$ . The neighboring  $K = 3$  and  $K = 5$  cases report how the signal dates change when the retained score dimension is moved in either direction.

Table S5.3: Robustness of the main empirical KS alarms to the choice of score dimension. Entries are first empirical alarm dates at the 5% level, with “No signal” indicating no threshold crossing over the finite monitoring horizon.

$K$	RSMS ( $T = 1$ )	RSMS ( $T = 2$ )	RSMS ( $T = 5$ )	HAC ( $T = 1$ )	HAC ( $T = 2$ )	HAC ( $T = 5$ )
<b>Panel A: <math>\gamma = 0</math></b>						
3	No signal	Mar. 17, 2020	Mar. 17, 2020	No signal	Mar. 31, 2020	Apr. 2, 2020
4	Feb. 26, 2020	Feb. 27, 2020	Mar. 13, 2020	No signal	Apr. 2, 2020	No signal
5	Feb. 26, 2020	Feb. 27, 2020	Mar. 10, 2020	No signal	Mar. 24, 2020	Mar. 25, 2020
<b>Panel B: <math>\gamma = 0.15</math></b>						
3	No signal	Mar. 17, 2020	Mar. 17, 2020	No signal	Mar. 31, 2020	Apr. 2, 2020
4	Feb. 26, 2020	Feb. 27, 2020	Mar. 13, 2020	No signal	Apr. 1, 2020	Apr. 2, 2020
5	Feb. 26, 2020	Feb. 27, 2020	Mar. 3, 2020	No signal	Mar. 24, 2020	Mar. 25, 2020

Note: The table recomputes the paper’s KS empirical alarms under the same training sample, smoothing choices, and 5% critical values, varying only the score dimension. SSMS remains below the 5% KS threshold for all score dimensions  $K \in \{3, 4, 5\}$  and horizons  $T \in \{1, 2, 5\}$ .

The signal dates are not identical across score dimensions. Lowering the score dimension to  $K = 3$  makes RSMS more conservative in the short horizon, eliminates the  $T = 1$  alarm, and delays the active alarms to mid-March, but RSMS still signals earlier than HAC at  $T = 2$  and  $T = 5$ . Returning to the main choice  $K = 4$  gives the late-February and mid-March RSMS dates reported in the paper. Raising the score dimension to  $K = 5$  preserves the same qualitative ordering and shifts the longer-horizon

RSMS alarm modestly earlier, while HAC also moves forward but remains later than RSMS.

#### S5.4 Alternative training-sample lengths

Table S5.4 gives a further robustness check in which the training-sample FPCA eigenfunctions are re-estimated from the last  $m = 75$  or  $m = 100$  pre-2020 trading days ending on December 31, 2019. The 80% FVE criterion retains  $K = 5$  in both checks. These alarm dates are not intended to replace the paper’s  $m = 50$ ,  $K = 4$  training-sample specification. They show that, when the training sample is lengthened, both RSMS and HAC detect the March return-curve movement, while SSMS remains below the threshold.

Table S5.4: Alternative training-sample robustness for the main empirical KS alarms.

$m$	$K$	$\gamma$	RSMS ( $T = 1$ )	RSMS ( $T = 2$ )	RSMS ( $T = 5$ )	HAC ( $T = 1$ )	HAC ( $T = 2$ )	HAC ( $T = 5$ )
75	5	0	Mar. 11, 2020	Mar. 13, 2020	Mar. 13, 2020	Mar. 13, 2020	Mar. 13, 2020	Mar. 13, 2020
75	5	0.15	Mar. 10, 2020	Mar. 11, 2020	Mar. 13, 2020	Mar. 13, 2020	Mar. 13, 2020	Mar. 13, 2020
100	5	0	Mar. 13, 2020	Mar. 13, 2020	Mar. 13, 2020	Mar. 13, 2020	Mar. 13, 2020	Mar. 17, 2020
100	5	0.15	Mar. 13, 2020	Mar. 13, 2020	Mar. 13, 2020	Mar. 13, 2020	Mar. 13, 2020	Mar. 13, 2020

Note: Each row re-estimates the training-sample FPCA eigenfunctions using the last  $m$  pre-2020 trading days ending on December 31, 2019, retains the number of components selected by the 80% FVE criterion, and reports first 5% KS alarm dates. SSMS remains below the threshold in all rows. The check is a robustness exercise for the empirical ranking, not a replacement for the  $m = 50$ ,  $K = 4$  training-sample specification used in the paper.

S5. EXTENDED EMPIRICAL ANALYSIS

Table S5.5: Empirical signal dates for selected CUSUM-style monitoring statistics after the common FPCA compression. Entries give statistic-to-critical-value ratios, rejection indicators, and first signal dates; the ratios are not percentages.

Detector	Standardizer	Tuning	Stat./CV	Reject?	First signal
<b>Panel A: <math>T = 1</math></b>					
Page-CUSUM	HAC	$\gamma = 0$	4.34	Yes	Mar. 2, 2020
Page-CUSUM	HAC	$\gamma = 0.15$	5.46	Yes	Mar. 2, 2020
Page-CUSUM	RSMS	$\gamma = 0$	14.92	Yes	Feb. 26, 2020
Page-CUSUM	RSMS	$\gamma = 0.15$	19.70	Yes	Feb. 26, 2020
Page-CUSUM	SSMS	$\gamma = 0$	0.34	No	No signal
Page-CUSUM	SSMS	$\gamma = 0.15$	0.41	No	No signal
Weighted CUSUM	HAC	$\gamma = 0$	7.98	Yes	Feb. 27, 2020
Weighted CUSUM	HAC	$\gamma = 0.15$	14.96	Yes	Feb. 27, 2020
Weighted CUSUM	RSMS	$\gamma = 0$	30.62	Yes	Feb. 24, 2020
Weighted CUSUM	RSMS	$\gamma = 0.15$	43.32	Yes	Feb. 24, 2020
Weighted CUSUM	SSMS	$\gamma = 0$	0.56	No	No signal
Weighted CUSUM	SSMS	$\gamma = 0.15$	0.93	No	No signal
<b>Panel B: <math>T = 2</math></b>					
Page-CUSUM	HAC	$\gamma = 0$	3.51	Yes	Mar. 2, 2020
Page-CUSUM	HAC	$\gamma = 0.15$	4.99	Yes	Mar. 2, 2020
Page-CUSUM	RSMS	$\gamma = 0$	10.80	Yes	Feb. 27, 2020
Page-CUSUM	RSMS	$\gamma = 0.15$	16.67	Yes	Feb. 26, 2020
Page-CUSUM	SSMS	$\gamma = 0$	0.35	No	No signal
Page-CUSUM	SSMS	$\gamma = 0.15$	0.50	No	No signal
Weighted CUSUM	HAC	$\gamma = 0$	9.51	Yes	Feb. 27, 2020
Weighted CUSUM	HAC	$\gamma = 0.15$	15.44	Yes	Feb. 27, 2020
Weighted CUSUM	RSMS	$\gamma = 0$	31.47	Yes	Feb. 26, 2020
Weighted CUSUM	RSMS	$\gamma = 0.15$	47.33	Yes	Feb. 24, 2020
Weighted CUSUM	SSMS	$\gamma = 0$	0.89	No	No signal
Weighted CUSUM	SSMS	$\gamma = 0.15$	1.28	Yes	Mar. 17, 2020
<b>Panel C: <math>T = 5</math></b>					
Page-CUSUM	HAC	$\gamma = 0$	2.72	Yes	Mar. 6, 2020
Page-CUSUM	HAC	$\gamma = 0.15$	4.07	Yes	Mar. 2, 2020
Page-CUSUM	RSMS	$\gamma = 0$	7.81	Yes	Feb. 27, 2020
Page-CUSUM	RSMS	$\gamma = 0.15$	12.93	Yes	Feb. 27, 2020
Page-CUSUM	SSMS	$\gamma = 0$	0.25	No	No signal
Page-CUSUM	SSMS	$\gamma = 0.15$	0.38	No	No signal
Weighted CUSUM	HAC	$\gamma = 0$	8.47	Yes	Feb. 28, 2020
Weighted CUSUM	HAC	$\gamma = 0.15$	14.40	Yes	Feb. 27, 2020
Weighted CUSUM	RSMS	$\gamma = 0$	26.86	Yes	Feb. 26, 2020
Weighted CUSUM	RSMS	$\gamma = 0.15$	43.07	Yes	Feb. 24, 2020
Weighted CUSUM	SSMS	$\gamma = 0$	0.76	No	No signal
Weighted CUSUM	SSMS	$\gamma = 0.15$	1.17	Yes	Mar. 17, 2020

Note: Weighted CUSUM uses the fixed weight  $\omega(\ell) = \ell^{-1/2}$ .

Table S5.6: Empirical signal dates for the multiscale MOSUM monitoring statistic after the common FPCA compression. Entries give statistic-to-critical-value ratios, rejection indicators, and first signal dates; the ratios are not percentages.

Detector	Standardizer	Tuning	Stat./CV	Reject?	First signal
<b>Panel A: <math>T = 1</math></b>					
Multiscale MOSUM	HAC	$\mathcal{H} = \{0.05, 0.10, 0.20\}$	7.51	Yes	Feb. 27, 2020
Multiscale MOSUM	RSMS	$\mathcal{H} = \{0.05, 0.10, 0.20\}$	22.67	Yes	Jan. 31, 2020
Multiscale MOSUM	SSMS	$\mathcal{H} = \{0.05, 0.10, 0.20\}$	0.47	No	No signal
<b>Panel B: <math>T = 2</math></b>					
Multiscale MOSUM	HAC	$\mathcal{H} = \{0.05, 0.10, 0.20\}$	18.09	Yes	Mar. 2, 2020
Multiscale MOSUM	RSMS	$\mathcal{H} = \{0.05, 0.10, 0.20\}$	74.07	Yes	Jan. 31, 2020
Multiscale MOSUM	SSMS	$\mathcal{H} = \{0.05, 0.10, 0.20\}$	1.28	Yes	Mar. 17, 2020
<b>Panel C: <math>T = 5</math></b>					
Multiscale MOSUM	HAC	$\mathcal{H} = \{0.05, 0.10, 0.20\}$	17.13	Yes	Mar. 2, 2020
Multiscale MOSUM	RSMS	$\mathcal{H} = \{0.05, 0.10, 0.20\}$	66.85	Yes	Jan. 31, 2020
Multiscale MOSUM	SSMS	$\mathcal{H} = \{0.05, 0.10, 0.20\}$	1.16	Yes	Mar. 17, 2020

Note: The reported MOSUM rows use the multiscale bandwidth set  $\mathcal{H} = \{0.05, 0.10, 0.20\}$ .

## S5.5 Supplementary monitoring statistics after the common FPCA compression

The supplementary CUSUM and MOSUM statistics can signal earlier than the main KS and weighted-CvM statistics. Among CUSUM-style statistics, RSMS weighted CUSUM signals on February 24, 2020 for all three horizons; RSMS Page-CUSUM also rejects early, but with smaller statistic-to-critical-value ratios. Among MOSUM-style statistics, RSMS multiscale MOSUM has the earliest reported local signal, January 31, 2020 at all three horizons. These dates should be interpreted with the simulation results in Appendix S4: in the reported simulation settings, multiscale MOSUM has lower SAP and is more sensitive to short local excursions than to the broader drift and accumulation patterns emphasized in the paper.

## REFERENCES

---

The SSMS rows are conservative, either not rejecting or crossing after the main RSMS alarms. The paper uses RSMS KS as the main statistic because, within the self-normalized class, it is less conservative than SSMS while avoiding HAC kernel and bandwidth choices across the simulation, contaminated-training, and empirical exercises.

### References

- Andrews, D. W. (1991). Heteroskedasticity and autocorrelation consistent covariance matrix estimation. *Econometrica* 59(3), 817–858.
- Andrews, D. W. and J. C. Monahan (1992). An improved heteroskedasticity and autocorrelation consistent covariance matrix estimator. *Econometrica* 60(4), 953–966.
- Aston, J. A. D. and C. Kirch (2012). Detecting and estimating changes in dependent functional data. *Journal of Multivariate Analysis* 109, 204–220.
- Aue, A., S. Hörmann, L. Horváth, and M. Hušková (2014). Dependent functional linear models with applications to monitoring structural change. *Statistica Sinica* 24(3), 1043–1073.
- Aue, A. and C. Kirch (2024). The state of cumulative sum sequential changepoint testing 70 years after page. *Biometrika* 111(2), 367–391.
- Aue, A., G. Rice, and O. Sönmez (2018). Detecting and dating structural breaks in functional data without dimension reduction. *Journal of the Royal Statistical Society Series B: Statistical Methodology* 80(3), 509–529.

- Bastian, P., R. Basu, and H. Dette (2024). Multiple change point detection in functional data with applications to biomechanical fatigue data. *The Annals of Applied Statistics* 18(4), 3109–3129.
- Berkes, I., R. Gabrys, L. Horváth, and P. Kokoszka (2009). Detecting changes in the mean of functional observations. *Journal of the Royal Statistical Society Series B: Statistical Methodology* 71(5), 927–946.
- Boniece, B. C., L. Horváth, and L. Trapani (2025). On changepoint detection in functional data using empirical energy distance. *Journal of Econometrics* 250, 106023.
- Cho, H. and C. Kirch (2022). Two-stage data segmentation permitting multiscale change points, heavy tails and dependence. *Annals of the Institute of Statistical Mathematics* 74(4), 653–684.
- Chu, C.-S. J., M. Stinchcombe, and H. White (1996). Monitoring structural change. *Econometrica* 64(5), 1045–1065.
- Den Haan, W. J. and A. T. Levin (1997). 12 a practitioner’s guide to robust covariance matrix estimation. *Handbook of statistics* 15, 299–342.
- Eichinger, B. and C. Kirch (2018). A MOSUM procedure for the estimation of multiple random change points. *Bernoulli* 24(1), 526–564.
- Hong, Y., O. Linton, B. McCabe, J. Sun, and S. Wang (2024). Kolmogorov–smirnov type testing for structural breaks: A new adjusted-range based self-normalization approach. *Journal of Econometrics* 238(2), 105603.

## REFERENCES

---

- Hörmann, S., L. Kidziński, and M. Hallin (2015). Dynamic functional principal components. *Journal of the Royal Statistical Society: Series B (Statistical Methodology)* 77(2), 319–348.
- Horváth, L., M. Hušková, and P. Kokoszka (2010). Testing the stability of the functional autoregressive process. *Journal of Multivariate Analysis* 101(2), 352–367.
- Kutta, T. and N. Dörnemann (2025). Monitoring time series with short detection delay. *Electronic Journal of Statistics* 19(1), 2239–2275.
- Kutta, T., A. Jach, and P. Kokoszka (2026). Monitoring panels of sparse functional data. *Journal of Time Series Analysis* 47(3), 660–674.
- Kutta, T. and P. Kokoszka (2025). Monitoring of functional time series. *Bernoulli* 31(4), 3356–3381.
- Müller, U. K. (2007). A theory of robust long-run variance estimation. *Journal of Econometrics* 141(2), 1331–1352.
- Shao, X. and X. Zhang (2010). Testing for change points in time series. *Journal of the American Statistical Association* 105(491), 1228–1240.
- Sharipov, O., J. Tewes, and M. Wendler (2016). Sequential block bootstrap in a hilbert space with application to change point analysis. *Canadian Journal of Statistics* 44(3), 300–322.
- Zhang, Y., C. Zhu, and X. Shao (2026). Change-point detection for object-valued time series. *Journal of Business & Economic Statistics* 44(1), 255–269.